Post-Eruptive Maturation of Dental Enamel: Development of an *in vitro* Model

Thesis Submitted in Accordance with the Requirements of the University of Liverpool

for the Degree of Doctor in Philosophy by Emma Jane Miles

UNIVERSITY OF LIVERPOOL

Department of Health Services Research

September 2016

Acknowledgements

Firstly, I would like to express my gratitude towards both the BBSRC and GlaxoSmithKline for providing the funding without which none of this work would have been possible. I would additionally like to thank the latter for the opportunity to experience your Weybridge site and make use of the equipment available.

I also need to express my extreme thanks to my supervisors, Professor Sue Higham, Dr Sabeel Valappil and Professor Richard Lynch. The three of you have offered me a wealth of advice, support and knowledge from both an academic and personal perspective and endless encouragement. I am eternally grateful for your patience and for always encouraging my enthusiasm.

So many people have helped me through this journey but I would like to extend particular thanks to Lee Cooper for his support both in and out of the lab and the countless techniques I would never have learnt without his guidance and patience. On a similar vein, I would like to thank Dr Gleb Komorov and Dr Elbert de Josselin de Jong for their aid, kindness and for sharing their expertise with me.

I would also like to extend thanks to Dr Stuart Kearns for conducting EPMA on some of my samples. Furthermore, I would like to thank Dr Shaz Khan and Dr Nasrine Mohammed for their patience and instruction during my visits to GSK.

I would like to thank all my colleagues in the Dental Research Wing, particularly, but not limited to, Jonathan Roberts, Gareth Owens, Khush Bahkt, James Hyde and Qian Wang for their friendship, kindness and taking the time to discuss my ideas. Also Chris Hope, Girvan Burnside, Gill Lloyd and Sophie Desmons for enriching this experience and expanding my general knowledge through regular testing.

I would like to express my gratitude to my friends, especially Richard Hague and Tom Park for helping ignite my interest in dental research. Also to my family for supporting me an always encouraging me. Especially my mum who is a constant inspiration and who always believes I can achieve anything. Last, but never least, I would like to thank Richard Wild for being there through the good and the tough, your support and encouragement knows no bounds and I owe you my deepest thanks.

Thank you

Declaration

This thesis is the result of my own work. The work presented in this thesis has not been presented, nor is currently being presented, either wholly or in part for any other degree or qualification.

Research works were carried out within the department of Health Services Research in the University of Liverpool.

Name: …… Signed: ……

Table of Contents

Index of Figures

Index of Tables

List of Abbreviations

AVG	Average
BMP	Bitmap File Format
CDFF	Constant-Depth Film Fermenter
Cyc	pH-cycled
d	Days
DS	Degree of Saturation
EDJ	Enamel-Dentine Junction
EDX	Energy-dispersive X-ray Spectroscopy
EPMA	Electron Microprobe Analysis
g	grams
g/cm³	Grams per Centimetre Cubes Volume
h	Hours
HAp	Hydroxyapatite
HMA	Hypomineralised Areas
KHN	Knoop Hardness
KSP	Solubility Product Constant
LD	Lesion Depth
ml	Millilitre
mm	Millimetre
MSI	Multispectral Imaging
Mth	Month
N	Newton
n	Sample Size

NC3Rs	National Centre for the Replacement Refinement and Reduction of Animals in Research
NCSP	Non-Contact Surface Profilometry
NHS	National Health Service
NIH	National Institute of Health
nm	Nanometre
PEM	Post-Eruptive Maturation
PF	Plaque Fluid
ppm	Parts Per Million
QLF-D	Quantitative Light-Induced Fluorescence Digital
R	Average Mineral Loss (ΔZ/LD)
Ra	Surface Roughness
s	Seconds
SE	Standard Error of the Mean
SEM	Scanning Electron Microscopy
SMH	Surface Microhardness
SPSS	Statistical Package for the Social Sciences
TIFF	Tagged Image File Format
TMR	Transverse Microradiography
WHO	World Health Organisation
WS	White-Spot
Yrs	Years
ΔF	Change in Fluorescence
ΔZ	Change in Mineral
µm	Micrometre
°	Degrees
%Vol	Percentage of Volume

Research Communications

Miles. E. J., Valappil. S. P., Lynch, R. J. M. and Higham, S. M. (2014) Effect of Exposure to Plaque-Fluid Representative pH-Cycling Conditions on Bovine Enamel Demineralisation. *61st Annual ORCA Congress, Greifswald, Germany*. 2-5 July 2014.

Miles. E. J., Valappil. S. P., Lynch, R. J. M. and Higham, S. M. (2014) Use of pH-Cycling Conditions to Model Post-Eruptive Maturation of Dental enamel *in vitro*. *11th International Medical Postgraduate Conference, Hradec Kralove, Czech Republic.* 27-28 November 2014.

Miles. E. J., Valappil. S. P., Lynch, R. J. M. and Higham, S. M. (2015) Use of Plaque-Fluid Representative pH-Cycling Conditions to Model Post-Eruptive Enamel Maturation *in vitro*. *62nd Annual ORCA Congress, Brussels, Belgium*. 1-4 July 2015.

Miles. E. J., Valappil. S. P., Lynch, R. J. M. and Higham, S. M. (2016) Effect of Strontium and Fluoride within a Plaque-Fluid-Representative pH-Cycling Model. *IADR General Session, Seoul, Republic of Korea*. 22-25 June 2016.

Miles. E. J., Valappil. S. P., Lynch, R. J. M. and Higham, S. M. (2016) Use of Zinc and Fluoride within an *in vitro* pH-Cycling Model of Post-Eruptive Enamel Maturation. *International Conference on QLF (ICQ), Seoul, Republic of Korea*. 26 June 2016.

Miles. E. J., Valappil. S. P., Lynch, R. J. M. and Higham, S. M. (2016) Use of Zinc and Fluoride within an *in vitro* pH-Cycling Model of Post-Eruptive Enamel Maturation. *63rd Annual ORCA Congress, Athens, Greece*. 6-9 July 2016.

Presentations without Proceedings

Miles. E. J., Valappil. S. P., Lynch, R. J. M. and Higham, S. M. (2013) Post-eruptive Maturation of Dental Enamel and its Effect on Susceptibility to Dental Caries. *GSK Science Symposium, Weybridge, UK*. 15 May 2013.

Miles. E. J., Valappil. S. P., Lynch, R. J. M. and Higham, S. M. (2013) Post-eruptive Maturation of Dental Enamel and its Effect on Susceptibility to Dental Caries. *IPHS PGR Student Conference, Liverpool, UK*. 14 June 2013.

Miles. E. J., Valappil. S. P., Lynch, R. J. M. and Higham, S. M. (2014) Post-Eruptive Maturation of Dental Enamel and its Effect on Dental Caries. *GSK Science Symposium, Weybridge, UK*. 29 May 2014.

Miles. E. J., Valappil. S. P., Lynch, R. J. M. and Higham, S. M. (2014) Use of pH-Cycling Conditions to Model Post-Eruptive Maturation of Dental Enamel *in vitro*. *IPHS PGR Student Conference, Liverpool, UK*. 13 June 2014.

Miles. E. J., Valappil. S. P., Lynch, R. J. M. and Higham, S. M. (2015) Development of a pH-cycling model of Post-Eruptive Maturation of Dental Enamel *in vitro*. *IPHS PGR Student Conference, Liverpool, UK*. 14 July 2015.

Miles. E. J., Valappil. S. P., Lynch, R. J. M. and Higham, S. M. (2015) Development of a pH-cycling model of Post-Eruptive Maturation of Dental Enamel *in vitro*. *GSK Science Symposium, Weybridge, UK*. 1 October 2015.

Miles. E. J., Valappil. S. P., Lynch, R. J. M. and Higham, S. M. (2015) Development of an *in vitro* pH-Cycling Model of Post-Eruptive Enamel Maturation. *Dental Research Seminar (University of Liverpool), Liverpool, UK*. 11 December 2015.

Abstract

Dental caries is a highly prevalent chronic disease, the treatment of which, forms a significant financial burden. Furthermore, due to the invasive nature and relatively high long-term failure rate of established treatments, focus has been placed on effective prevention strategies in order to instead circumvent the problem before it occurs. Prevalence of dental caries is particularly high in adolescents due to the increased susceptibility of newly erupted teeth to acid dissolution. A transient vulnerability that is gradually lost with time through a post-eruptive maturation process.

Post-eruptive maturation (PEM) refers to chemical and physical changes that occur in the outer enamel layers following exposure of newly erupted teeth to the oral environment. Whilst little is known about the underlying mechanism, it is believed to be a result of the natural fluctuation between de- and remineralising states within the oral cavity. To date, most literature regarding PEM places focus on measuring the outcomes of the process (Which include increased surface hardness, decreased porosity and a decrease in susceptibility to acid dissolution) as opposed to investigating the reasoning behind such changes. One reason for this focus is the difficulties faced when initially approaching the study of PEM, as there is currently no established model or protocol for recreating the process *in vitro.*

In order to address this problem, the current work outlines the development process of a proposed pH-cycling model for use in the study of PEM. The efficacy of the model was initially assessed though its ability to reduce acid dissolution and then also through its effect on surface microhardness. The often speculated role of repeated sub-clinical caries events as the basis to PEM was confirmed through the observation of significantly reduced mineral loss in enamel previously exposed to plaque-fluid-relevant pH-cycling conditions. Further to this, the ability of Fluoride, Zinc and Strontium to supplement this effect was demonstrated, in addition their ability to replicate the increased surface microhardness observed during PEM.

The 20-day, plaque-fluid-relevant, pH-cycling model proposed within this work has the potential to allow much greater insight into the underlying chemical mechanisms underpinning PEM, particularly the potential incorporation of ions such as F and Zn, in addition to allowing the testing and identification of agents to enhance the observed effects. As such, this work provides a much-needed springboard from which the clinical potential of PEM can be unlocked.

Chapter One: Background and Introduction

1.1 Dental caries

1.1.1 The Burden of Dental Caries

Dental caries is of the most pervasive diseases on the planet (Selwitz *et. al.* 2007, Vos *et. al.* 2015) and therefore forms a significant impediment to world health (Bedi *et. al.* 2016). Whilst it is not a threat to life, its high prevalence throughout the world and particularly within developed countries, where almost 100% of the population is affected to some degree, means that the financial burden of caries treatment is high. This can be illustrated best through referring to past statistics on caries treatment costs. Back in 2012 the World Health Organisation (WHO) placed dental caries as the 4th costliest disease within developed countries and as affecting 60-90% of schoolchildren worldwide (WHO Factsheet 318, 2012). Furthermore, in 2006, the NHS spent around £1977 million on dental interventions in England alone (NHS Report 2008). Whilst preventative measures have greatly improved over the past 60 years, the increased popularity and availability of fermentable carbohydrate-based foods, along with the increasing popularity of “little and often” diets have ensured dental caries remains a global problem. On a personal level, dental caries is painful and has a sizeable impact on speech, eating, confidence and other social behaviours (Locker 1992). As such, it can be highly detrimental to a patient’s quality of life (Low *et. al.* 1999, Gerritsen *et. al.* 2010).

Dental Caries can be defined as the demineralisation and eventual destruction of tooth mineral through acidic challenges generated by acid-producing bacteria in plaque. The process starts in the outer enamel, but if untreated can progress to the dentine, the pulp and, in some cases, the root of the tooth.

1.1.2 Caries Development

Caries is a complex multifactorial disease caused by the interaction of several local factors including the presence of acid-producing bacteria, the availability of fermentable carbohydrate, the composition of the saliva and the tooth itself. Additionally, there are a also a range of wider risk factors for caries development, including, but not limited to, income, hygiene levels, diet and socio-economic status (Figure 1.1).

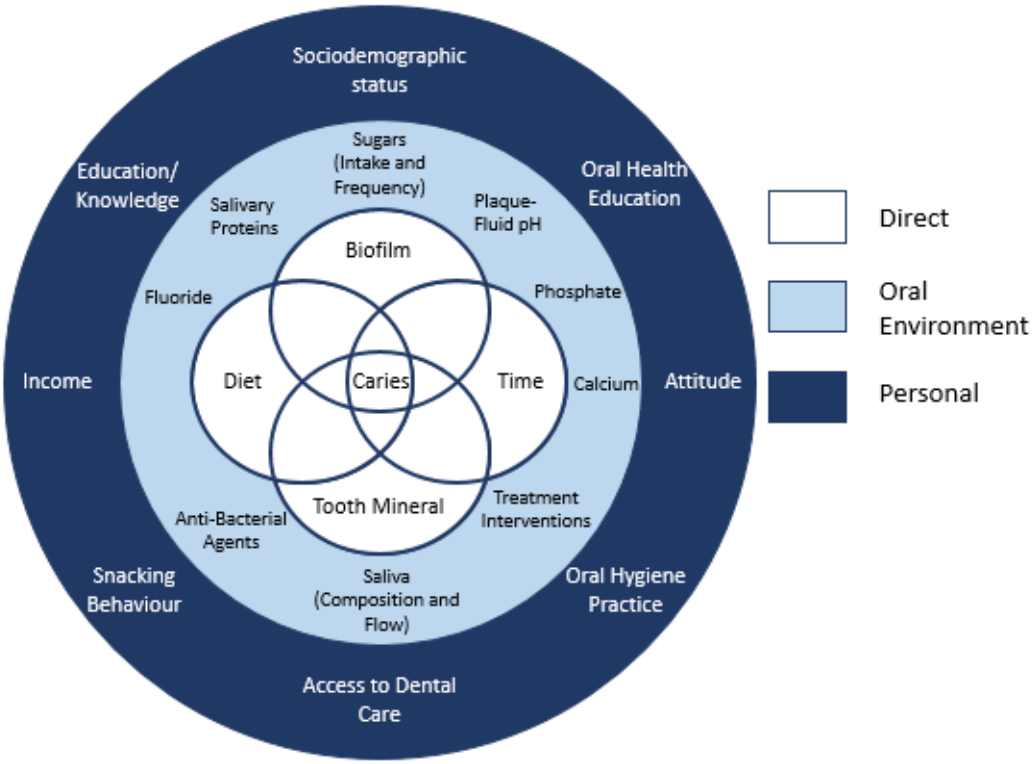

Figure 1.1: Factors Involved in Caries Development. *Diagram highlighting the multi-factorial nature of dental caries. Central Venn diagram contains direct causative factors, whilst outer circles represent the oral environment and wider personal influences. Adapted from Fejerskov and Manji (1990).*

During the caries development process, the enamel provides a surface upon which bacteria can colonise and eventually form into a mixed-species biofilm (Marsh 2004). A biofilm can be defined as a thin microbial layer, adhered to a structural surface alongside a secreted polymer matrix (Costerton *et. al.* 1999, Marsh 1992). Following biofilm formation, the conditions within the oral cavity provide a stable environment which serves to provide nutrients and encourage population growth (Marsh and Martin 1999). At this point the provision of fermentable carbohydrates from diet can cause this oral eco-system to promote acid-producing bacteria, which in turn lower the pH of the oral environment. This reduced pH leads to the dissolution of the underlying enamel surface and development of dental caries. It is important to note at this point that the oral environment is in a permanent state of flux between conditions that favour net de- and re-mineralisation and it is when the balance is tipped in favour of demineralisation that carious lesions are formed (Fejerskov *et. al.* 2008). This process was demonstrated in practice by Stephan (1940), who showed that within 2-4 minutes of exposure to glucose or sucrose, the pH of dental plaque dropped to 5, before restoring back to normal within 40 minutes. Whilst this observation forms a cornerstone of our understanding of the caries process, other authors have suggested that, whilst the same overall effect occurs, there is a much more significant drop in pH, which can take up to two hours to return to a resting, neutral pH (Graf and Muhlemann 1966, De Boever *et. al.* 1969). It is also important to appreciate that dental caries form over time and are the result of repeated exposure to acidic conditions over an extended period and not a single acidic event. It can therefore be considered the product of an overall net shift of the oral environment to favour demineralisation (Figure 1.2).

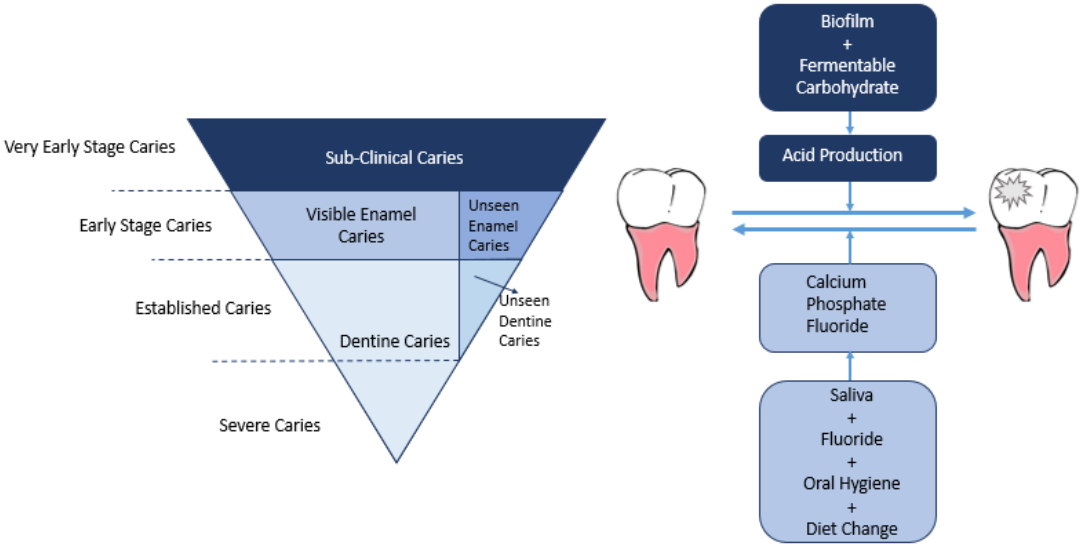

Figure 1.2: Schematic of Caries Development. *Left: Illustration demonstrating the stages of caries development through the different tooth layers. Adapted from Pitts (2004). Right: Schematic of the caries process highlighting the dynamic balance between de- and re-mineralising conditions. Adapted from Kidd and Joyston-Bechal (1997).*

1.1.3 Diagnosis and Treatment of Dental Caries

Dental caries can be diagnosed visually, providing a clean, dry-tooth surface and appropriate lighting are achieved, however such examination is difficult for the detection of early caries. Radiography is therefore the predominant method of clinical identification (Nyvad *et. al*. 2008, Mejare and Kidd 2008). Treatments for developed dental caries are invasive and subject to potential failure with time. It has therefore become a primary focus of both dental research and clinical care to focus first and foremost on prevention in a bid to circumvent the problem before it arises (Burt 1998). Classically, prevention focuses on a reduction in both the frequency and amount of sugar intake, combined with good oral hygiene practices (Ruxton *et. al.* 1999). Significant time and research has led to several novel and innovative active ingredients, being developed and implemented, the most notable of which being fluoride (Ripa 1991, Bratthal *et. al.* 1996, ten Cate 1997, Featherstone 1999). There is, however, still continuous time and effort dedicated to understanding the caries process

and natural resistance mechanisms with an aim of developing new and more appropriate ways to contribute to the caries decline.

1.2 Structure of Dental Enamel

Dental enamel is the hardest tissue in the human body (Bechtle *et. al.* 2010), with human teeth able to withstand forces over 700N during mastication (Hagberg 1987). It is also the most mineralised, showing higher crystallinity than dentine and bone when analysed by X-ray diffraction (LeGeros *et. al.* 1996). Composition-wise, it is acellular and made up of 95% carbonised apatite, 4-5% water and less than 1% organic matter (Angmar *et. al.* 1963, Robinson *et. al.* 1983, Elliot 1998, ten Cate 2007). When considered in terms of volume, enamel is 87% mineral, with the remaining 13% of space taken up by water and protein (LeGeros 1991). Structurally, enamel is formed of mineral rich prisms embedded in an organic sheath (Low *et. al.* 2008) (Figure 1.3). Each prism consists of many hexagonal carbonated-apatite crystals approximately 50x25nm and up to 1mm in length (Johansen 1965, Selvig and Halse 1972). The space between crystals is occupied by a mixed inorganic and organic matrix. Each prism is around 3-7µm in diameter (Gwinnett 1992, Cuy *et. al.* 2002) and extends from the dentine towards the surface (Johansen 1965). When viewed cross-sectionally, prisms appear keyhole- or fish scale-like and may fuse together along their length. Prisms can, in some cases, run along the full enamel depth (Daculsi *et. al.* 1984). At the interface between prisms there is an interprismatic space, containing water (11% Vol) and organic material (2% Vol), which is believed to be important for diffusion within the enamel tissue (Boyde 1989). At the enamel surface, there is an up to 100µm thick solid aprismatic layer, which is formed towards the end of the pre-eruptive maturation process (Boyde 1989, Gwinnett 1967, Kodaka 1989). The mineral content, and therefore porosity of dental enamel, is not uniform, with the prism density decreasing from the surface to the dentine (Robinson *et. al.* 2000). This is inverse to the porosity, organic material and fluid content, all of which increase from the surface to the enamel-

dentine junction (EDJ) (Hall *et. al.* 2000). The apatite crystal size is larger in the outer layers than the underlying enamel (LeGeros *et. al.* 1996).

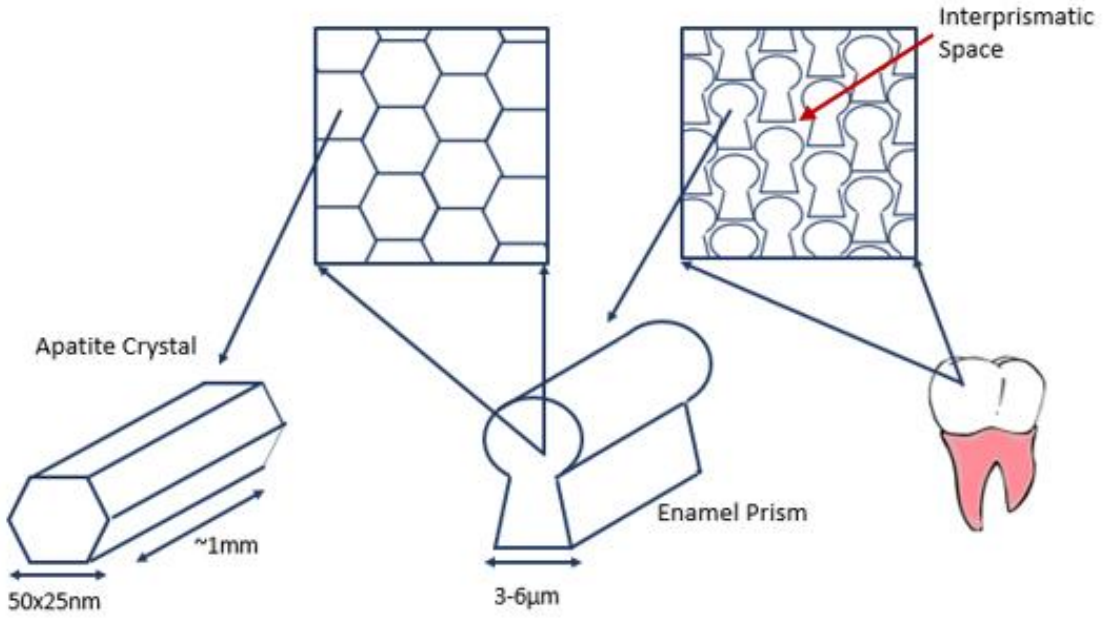

Figure 1.3: Structure of Dental Enamel. *Schematic of enamel structure. Keyhole-shaped prisms 3-6µm in diameter are arranged within interprismatic space. Each prism consists of tightly packed enamel crystals 50x25nm in size*. *Adapted from Fulmer* et. al. *(2014).*

Enamel is made up largely of carbonised apatite that contains several calcium substitutions. However, in order to fully understand its behaviour within the oral environment it is important to first consider the structure of stoichiometric hydroxyapatite (HAp), the formula of which is $Ca_{10}(PO_4)_6(OH)_2$ (Kay *et. al.* 1964). Within the hydroxyapatite, ions are arranged around a central hydroxyl column (Robinson *et. al.* 1995a). Each hydroxyl ion is surrounded by a triangle of calcium II ions, along with a triangle of phosphate ions at a 60° angle. These are then in turn surrounded by a hexagon of calcium I ions. These hexagonal plates stack on top of one another in the c-axis direction to form the crystal structure of the enamel (Figure 1.4). Therefore, by weight, enamel crystals are 37% Ca, 52% P and 3% OH.

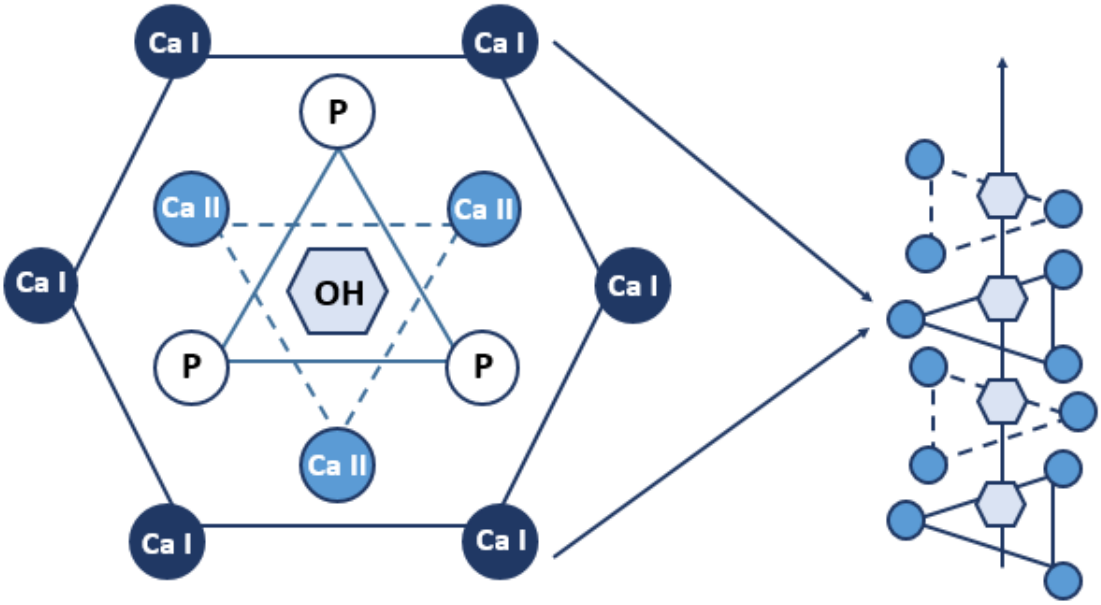

Figure 1.4 Crystal Structure of Hydroxyapatite. *HPA Crystal is formed of stacked hexagonal plates along a hydroxyl central column. Each plate consists of a central OH with calcium II and Phosphate triangles at 60º to one another. These are surrounded by a hexagon of calcium I ions. Adapted from Robinson et. al. (2000)*.

In reality the HAp in dental enamel varies from the stoichiometric structure described above. These changes take the form largely of missing or substituted calcium (Posner and Perloff 1957, Winand *et. al.* 1961) and hydroxyl (Myrberg 1968) groups. In fact, the hydroxyl content of enamel has been reported to be up to 30 percent lower than that of stoichiometric HAp (Young and Spooner 1969). Substituted ions within the HAp include carbonate, fluoride and magnesium amongst others and have a significant effect on the behaviour of the enamel when presented with an acid challenge (Robinson *et. al.* 1995a, Robinson *et. al.* 2000). This is illustrated by comparing the solubility product of stoichiometric HAp (3.04×10^{-5}) (Mc Dowell *et. al.* 1977) to those reported for enamel mineral (7.2×10^{-5} to 6.4×10^{-5}) (Patel and Brown 1975). Additionally, “pure” HAp has been shown to be both denser and harder than dental enamel (3.16 g/cm³ and 2.95 g/cm³, 430KHN and 370KHN respectively) (Bardow *et. al.* 2008). The hardness throughout the enamel is not uniform, with increased hardness in the outer layers

compared to areas near the EDJ (Roy and Basu 2008). Impurities within the apatite vary in their distribution through the enamel, with some, such as fluoride, zinc, tin and lead found in high concentrations at the surface as opposed to the underlying enamel (Robinson *et. al.* 1995b, Lindh and Tveit 2007). In contrast, others such as carbonate, magnesium and sodium show the reverse, with higher concentrations being found towards the EDJ (Little and Brudevold 1958, Robinson *et. al.* 2000, Watson *et. al.* 1967, Weatherell *et. al*. 1968, LeGeros *et. al.* 1996). Other ions, such as strontium and copper, exhibit a more even distribution across enamel depths (Larsen and Bruun 1994).

1.3 The Enamel and caries

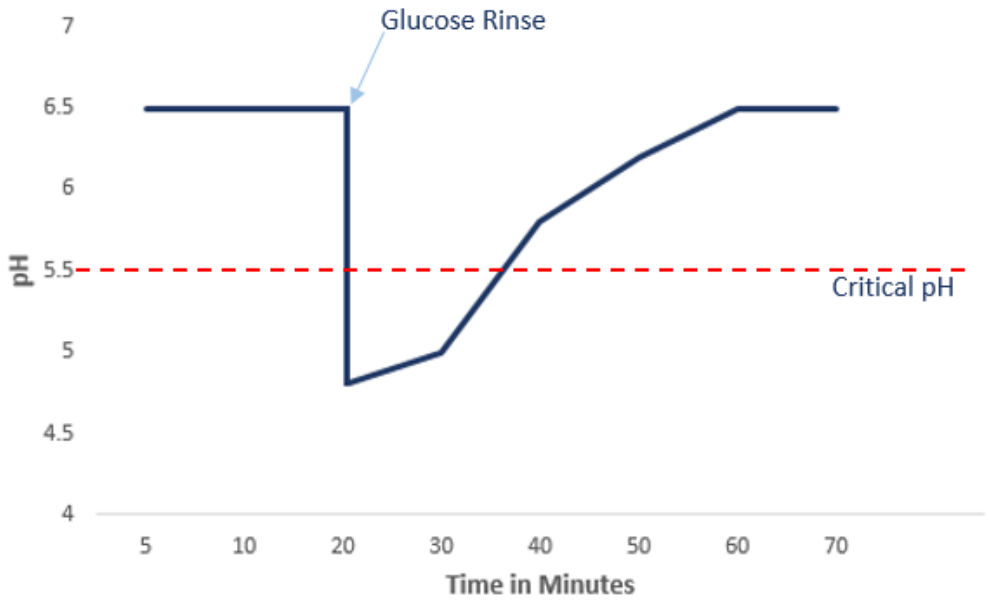

Figure 1.5 Stephan Curve. *Stephan Curve showing changes in pH following a glucose rinse. The "critical" pH threshold is also presented. Adapted from Stephan et. al. (1943).*

Due to the acellular nature of dental enamel, demineralisation can be considered as a chemical, as opposed to biological process. Fundamentally, it is caused by changes in

pH causing the oral fluids and interprismatic spaces to undergo a change in the degree of saturation (DS) with respect to Calcium and Phosphorous. When the fluids become under saturated with respect to Ca and P, dissolution of the enamel occurs. This is usually caused by a pH lower than the “critical” pH of 5.5 (Dawes 2003), above which remineralisation occurs. This is demonstrated in Figure 1.5 above. The DS is calculated by dividing the ionic activity product by the solubility product constant (KSP). For dental enamel this is not straightforward, as, although the KSP has been estimated (Fosdick and Stark 1939, Aoba 2004), substitutions that occur within the mineral can affect the value, making it hard to accurately predict (Francis 1965, Patel and Brown 1975, LeGeros 1981). During demineralisation more soluble aspects of the enamel, such as magnesium and carbonate, usually within the inner layers, are preferentially lost (LeGeros *et. al.* 1996, Robinson 2009) and then replaced during the subsequent remineralisation phase with alternative ions such as fluoride (Aoba *et. al*. 2003). This allows the mineral content to change with time and whether such changes are destructive is dependent on whether the oral environment is balanced towards dissolution or remineralisation (Kirkham *et. al.* 1994). There is evidence to suggest that *in vivo* both de- and remineralisation occur simultaneously (Robinson *et. al.* 2000).

Carious lesions characteristically form as an intact surface with an area of subsurface demineralisation (Silverstone 1968), this is distinct to erosive lesions, in which the mineral is lost from the surface itself (Larsen 1991). When viewed under polarising light, a caries lesion can be divided into four distinct zones, which are illustrated in Figure 1.6. The first, the translucent zone, is the found at the advancing edge of the lesion. It is the first recognised change in the mineral. Superficial to the translucent zone is the dark zone, which forms part of the advancing lesion. Whereas the translucent zone is only observed in some lesions, the dark zone occurs in 85-90% of lesions (Silverstone 1967). The body of the lesion is an area of enlarged pores where the most mineral has been lost. The body of the lesion lies under the surface zone,

which is an area of relatively unaffected enamel at the surface of the lesion usually 20-40µm in depth (Silverstone 1968). It is believed that this layer is a product of the dynamic nature of carious lesions and the alternating periods of de- and remineralisation.

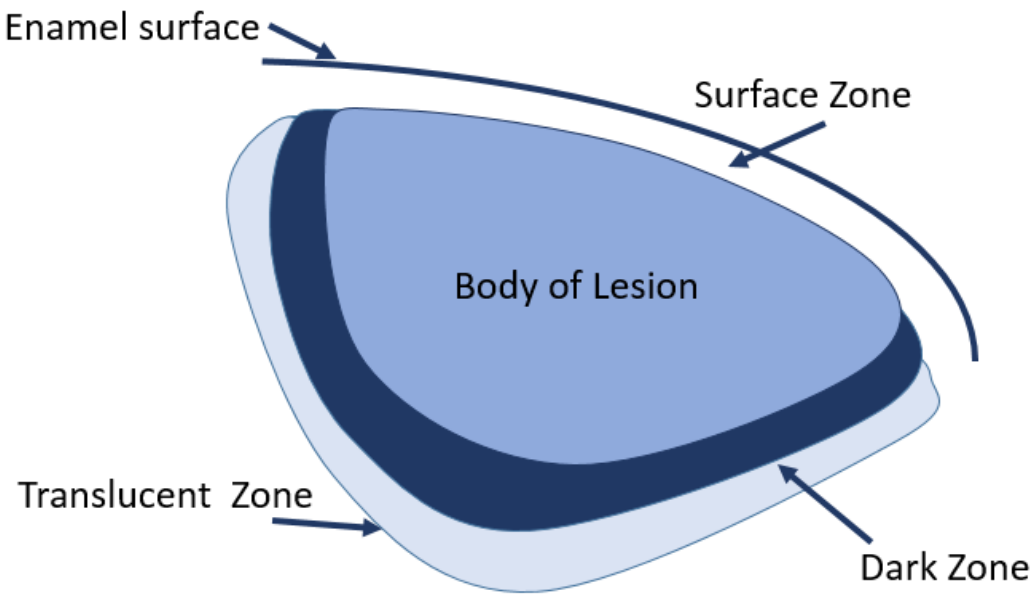

Figure 1.6: The Four Zones of a Caries Lesion. *Illustration depicting the four zones of a caries lesion. The translucent and dark zones form the advancing front of the lesion, whilst the body of the lesion contains the largest area of demineralisation. At the enamel surface there is a layer of relatively intact enamel known as the surface zone.*

1.4 Post-eruptive Maturation

Studies have shown that newly erupted teeth are more susceptible to acid challenges than those that have withstood the oral environment for a period of time, particularly those in the first 2-4 years post-eruption (Carlos and Gittelsohn 1965). It is believed this is due to the enamel undergoing a post-eruptive maturation process upon exposure to the oral environment.

Post-eruptive maturation (PEM) can be defined as the chemical and physical changes that occur in the outer layers of the dental enamel following the eruption of the tooth into the oral cavity (Crabb 1976, Woltgens *et. al.* 1981a). It is important to note that it is distinct from the pre-eruptive process of ameleogenesis, which is also commonly referred to as “maturation” within the literature. For the purposes of this thesis, it can be assumed that maturation is always used in reference to the post-eruptive process described above unless otherwise stated.

Early research into PEM was grounded on the observation that the molars of Sprague-Dawley rats that had not been fed a cariogenic diet possessed hypomineralised areas (HMA) which were indistinguishable from caries lesions when stained with silver nitrate (Francis and Briner 1966). However, when the rats were fed a regular lab diet for 70 days the number and severity of these areas decreased significantly. Whilst they suggested this could represent carious lesions formed 1-2 days from eruption, they noted that previous studies had reported that immature, un-erupted enamel stains in a similar manner. From this they concluded that newly-erupted enamel must undergo changes in mineralisation upon exposure to the oral environment.

Whilst the exact mechanism behind PEM is not known, it is believed that exposure to the constantly changing oral environment is the main driving force behind the process (Figure 1.7). The idea that the cyclic change from an acid challenge to remineralisation has the potential to change the structure of the enamel is supported by reports of the *in vivo* occurrence of laminated caries lesions, which possess areas of varying mineralisation within a single lesion (Lagerweij *et. al.* 2006).

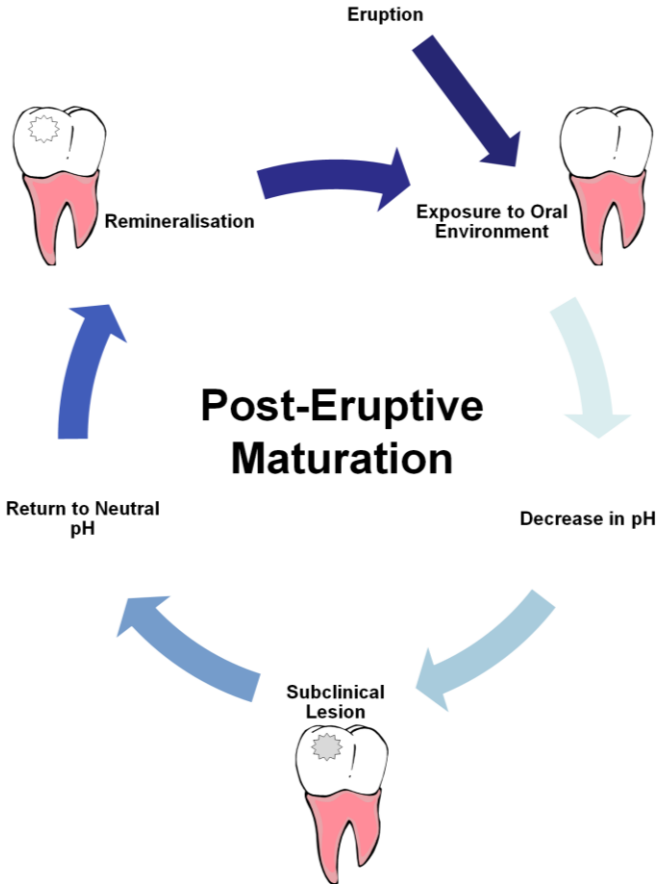

Figure 1.7: Schematic of the Proposed Mechanism Behind PEM. *Outline of the proposed cyclic exposure to sub-clinical caries events and remineralising conditions believed to form the basis for the PEM process.*

This idea is further demonstrated by *in vitro* studies that have shown arrested caries lesions to be less susceptible than sound enamel to an acid challenge (ten Cate and Duijsters 1982, Maltz *et. al*. 2006). Additionally, evidence has demonstrated that the surface layers of enamel are less susceptible to acid dissolution than the deeper layers (Brudevold 1948), which fits with the concept of outer surface remodelling during PEM. When enamel of two different post-eruptive ages (6mths/4yrs) was subjected to a lactic acid gel demineralisation, a significant difference in Ca and P loss was observed at a depth between 25 and 60µm, with the “younger” teeth demineralising at a greater rate (Woltgens *et. al.* 1981b). This supports the notion that acid vulnerability varies with eruptive exposure to the oral environment.

In situ studies that have compared the changes in mineralisation between white spot lesions (WS) and sound enamel have demonstrated that such lesions were less susceptible to acid challenges than sound enamel (Iijima and Takagi 2000). Additionally, whilst sound enamel formed a typical subsurface caries lesions, the WS lesions only lost mineral from below the surface. This makes sense, as the acid would bypass the difficult to demineralise surface areas, in favour of the more soluble area below the surface. This supports the idea that demineralisation followed by remineralisation is able to chemically and physically change the surface layers of enamel to be more resistant to acid challenges. This is further supported by additional *in situ* research that has created arrested carious lesions then subjected them to a further acid challenge (Maltz *et. al.* 2006), which found that the hardness of such lesions remained comparable to that of sound enamel subjected to the same challenge.

In terms of the ability for PEM to occur, the balance between the cyclic oral conditions appears to be of importance, as too severe an acid challenge would lead to carious lesion development, as opposed to the desired sub-clinical levels of demineralisation required (Fejerskov *et. al,* 1994). This was demonstrated in principle by the aforementioned animal studies (Francis and Briner 1966), where rats fed an un-supplemented cariogenic diet did not show the same reduction in HMA. They hypothesised that is was due to the extent of the acid challenge pushing the balance to a DS that favours net demineralisation.

To a certain extent, PEM has also been shown to also occur in the primary dentition, as changes in levels of trace elements within the enamel following eruption have been reported (Sabel *et. al.* 2009). This is supported by longitudinal studies that observed greater susceptibility to acid in newly erupted permanent teeth when compared to established deciduous ones, even though the primary enamel is historically more porous than its permanent counterpart (Gruythuysen *et. al.* 1991).

1.5 PEM Timeframe

Whilst some studies have suggested complete maturation can occur after 15 months (Schulte *et. al.* 1999), others have reported that the maturation process was not complete 66 months post-eruption (Kataoka *et. al.* 2007). Similarly, early electrical resistance studies found that a 36mth test period was not long enough to identify enamel as “matured”, suggesting that the actual time taken for enamel to fully mature might actually be much higher. This is demonstrated by research comparing enamel density between 18-24 year olds and 25-55 year olds, which determined that the enamel of the older group had a higher mineral density. This suggests that the enamel of 18-24 year olds is yet to reach full maturation (He *et. al.* 2011).

When hardness measurements are considered, significant changes have been reported within 2-3 yrs of eruption, however, it has been suggested that it may take over 10 years for enamel to reach its maximum level of hardness (Cardoso *et. al.* 2009, Palti *et. al.* 2008). Interestingly, it has also been noted that late eruption of a tooth does not have any effect in its ability to undergo PEM (Virtanen *et. al.* 1996). As such, it appears that the main indicative factor for PEM is the length of exposure of the enamel to the oral environment (Lynch 2013).

1.6 Physical changes within the enamel

1.6.1 Hardness

An increase in surface hardness following PEM has been reported for both animal models and human enamel. Such changes are believed to be due to increased crystal growth causing a decrease in intercrystalline space (Brudevold *et. al.* 1982, Briner *et. al.* 1971). It has been reported that enamel becomes significantly harder following 2-3 yrs exposure to the oral environment (Cardoso *et. al.* 2009), however it has been suggested that the much longer exposure is needed (Palti *et. al.* 2008). Such changes are believed to occur largely in the first 330µm of the enamel and be a product of

chemical changes such as the incorporation of fluoride. There is evidence that post-eruptive maturation serves to increase the crystallinity of enamel up to a depth of between 0.5 and 1mm (Brudevold *et. al.* 1982, Driessens *et. al.* 1982).

1.6.2 Porosity

The outer layer of enamel is highly porous at the time of tooth eruption and it has been shown that the PEM process has an effect on this porosity (Brudevold *et. al.* 1982). Unerupted teeth show higher permeability than those which have erupted (Silverstone and Johnson 1971) and, furthermore, teeth obtained 6-12 mths following eruption can have electrical resistance values inferring a level of porosity similar to that of carious enamel. Such studies have also shown that the electrical resistance increases and therefore porosity of first molars decreases with increasing post-eruptive age (Schulte *et. al.* 1999, Kataoka *et. al.* 2007).

1.7 Chemical Changes within the Enamel

1.7.1 Calcium and Phosphate

Ion exchange is constantly occurring at the enamel surface (Sognnaes 1975). Research has shown that the Ca and P content of human premolar enamel decreases from the surface towards the EDJ, before levelling off at a depth of around 60µm (Woltgens *et. al.* 1981a). Given the chemical composition of hydroxyapatite it is unsurprising that calcium and phosphate ions appear to be key to the maturation process, Briner *et. al.* (1971) even went as far as to define the entire maturation process as the accumulation of Ca and P by the enamel. Support for the post-eruptive effects of Ca and P can be found in animal studies in which hamsters were fed a bone meal supplemented diet. Researchers found that whilst supplemented dietary Ca and P had no pre-eruptive effect, it served to reduce subsequent caries when given post-eruptively (Gustafson *et. al.* 1968). It is, however, worth noting that this observation

may be a product of increased Ca and P availability changing the degree of saturation (DS) to reduce demineralisation as opposed to PEM-related incorporation.

He *et. al.* (2011) compared the Ca and P weight percent of younger (18-24yrs) and older (up to 55yrs) age groups and found that it was significantly higher in the older group. This difference was only present in the outer layers of the enamel, which is consistent with what would be expected during PEM. They also noted that there was a gradient of Ca and P from the surface to the dentine. Interestingly Woltgens *et. al.* (1981a) found the greatest post-eruptive differences were found at a depth of 25µm, where the Ca and P content decreased with age. It is possible that this is due, in part, to the substitution of calcium for other ions such as zinc.

Early studies by Francis and Briner (1966) using silver nitrate, demonstrated that Sprague-Dawley rats fed with a phosphate supplemented cariogenic diet possessed a significantly decreased incidence of HMA, similar to those fed a non-cariogenic diet. The authors suggested that this may be down to either the phosphate possessing an ability to inhibit lesion formation or to permit remineralisation.

1.7.2 Carbonate

Even before experimental evidence was obtained, it was speculated that carbonate was particularly susceptible to caries (Sobel 1962). This was supported by evidence that carbonate interferes with the crystal structure of HPA (Bachra and Trautz 1962) thorough replacement of either hydroxyl (Elliot *et. al.* 1985) or phosphate (LeGeros and Tung 1983) groups within the lattice. When incorporated into the HPA, carbonate is larger and therefore more difficult for the crystal to accommodate (Marshall and Lawless 1981). As such, the centres of the crystals become less ordered and therefore the stability of the mineral is reduced. This in turn leads to a higher KSP, leaving the enamel more susceptible to subsequent acid dissolution (Robinson *et. al.* 2000).

The incorporation of carbonate into the enamel occurs entirely pre-eruptively during enamel formation and a higher concentration is observed at the dentine than the surface (Robinson *et. al.* 2000, Watson *et. al.* 1967, Weatherell *et. al.* 1968, LeGeros *et. al.* 1996). This, along with the magnesium content, may serve to explain the smaller crystal dimensions and lower crystallinity observed in the inner layers of HPA (LeGeros *et. al.* 1996). Carbonate incorporation is believed to explain in part why newly erupted enamel is more soluble than matured enamel, as the loss or substitution of carbonate following eruption would serve to reduce the solubility product of the enamel. Evidence suggests that carbonate is preferentially lost during enamel demineralisation, as such, it makes sense that carbonate is lost at an early stage upon exposure of the enamel to the oral environment (Bachra and Trautz 1962, Woltgens *et. al.* 1981b).

1.7.3 Magnesium

Whilst magnesium is most commonly found on crystal surfaces or as a separate mineral phase, there is evidence that indicates to a certain extent it is also able to be incorporated into the HPA lattice in the place of calcium groups (Featherstone *et. al.* 1983). In such cases, the charge density of magnesium would cause a similar destabilising effect on the enamel to that observed with carbonate (LeGeros *et. al.* 1967, LeGeros 1984, Okazaki and LeGeros 1996, Robinson *et. al.* 2000). Beyond their similar effect on the solubility of dental enamel, it has also been suggested that magnesium and carbonate have a synergistic effect on one another's incorporation into HPA (LeGeros 1984, LeGeros *et. al.* 1996, Okazaki and LeGeros 1996). In addition to its effect on the structure of the HPA itself, Mg has been shown to inhibit crystal growth (Thiradilok and Feagin 1978, LeGeros *et. al.* 1996). Therefore, there is potential that Mg released during acid demineralisation could in turn inhibit the subsequent remineralisation process. The replacement of Mg during the PEM process would, therefore, also serve to reduce this occurrence during subsequent acid challenges.

Once again in a similar fashion to carbonate (Weatherell *et. al.* 1968), magnesium incorporation is believed to occur pre-eruptively during enamel formation (Robinson *et. al.* 2000) and is increased at higher temperatures, higher pH and in the presence of carbonate and fluoride (LeGeros *et. al.* 1996). A gradient from the dentine to the surface does to an extent seem to exist (Little and Brudevold 1958), but it is less defined than for carbonate and there are often pockets of high concentrations of Mg near the dentine (Robinson *et. al.* 1981). In a similar manner to carbonate, it makes sense to presume that the loss or replacement of magnesium from the HPA following eruption forms part of the chemical PEM process. In addition, magnesium, like carbonate, has been shown to be selectively removed during demineralisation (Hallsworth *et. al.* 1972), which is in keeping with the idea that it is lost as a part of the PEM process (Woltgens *et. al.* 1981b). Further to this, it has been hypothesised that in addition to the preferential loss of magnesium and carbonate, a preferential formation of apatite low in Carbonate and magnesium and high in fluoride is preferentially deposited during remineralisation, providing further support the proposed loss of Mg during PEM (LeGeros *et. al.* 1996).

In the case of magnesium, one further rationale for its preferential loss during carious attack is that the magnesium detected is actually bound to the enamel proteins as opposed to the mineral itself (Robinson *et. al.* 1981). This would explain the observed presence of concentrations higher than 0.1%, which would not be expected to be possible for hydroxyapatite formation (Boskey and Posner 1974). This notion is supported by the pattern of distribution of Mg which tends to be at higher in less dense areas and follows a similar pattern to that of enamel proteins (Robinson *et. al.* 1981). It would also serve to explain the preferential loss of Mg during dissolution, as protein and other organic material is more soluble than HPA mineral and would therefore be removed first.

1.7.4 Fluoride

Fluoride is commonly used in a wide range of preventative measures and treatments for dental caries. As such, it has been deemed responsible for a worldwide drop in caries incidence (Bratthall *et. al.* 1996). Whilst there is debate as to the need for systemic fluoride-based interventions such as water fluoridation, it is widely accepted that the majority of fluorides efficacy can be attributed to effects from topical application (Featherstone *et. al.* 1990, Ten Cate 1990). Whilst F is known to have anti-microbial effects, it is the chemical influences which will be focused upon here.

Given the well-established efficacy of fluoride as an aid to remineralisation, it makes sense to consider its potential within the maturation process. Early studies often mention the ability of fluoride to "enhance" the maturation process (Briner and Rosen 1967, 1968, Briner *et. al.* 1971), but as such research was carried out before the mechanisms of action of fluoride were fully understood, they fail to go into any further detail than observing a higher degree of mineralisation in its presence.

Further evidence for the role of fluoride within the maturation process is provided by the observation that fluoride is seen to accumulate in the surface layers of enamel shortly after eruption (Weatherell *et. al.* 1972). Research into fluoride uptake by enamel has demonstrated a much higher affinity to fluoride in newly-erupted as opposed to "matured" enamel (Mellberg and Nicholson 1968, Bruun 1973). In addition, topical fluoride studies have shown increased effects in teeth that erupt during the course of the investigation, than those already present (Wellock *et. al.* 1965, DePaola and Mellberg 1973). The increased uptake of fluoride by newly-erupted enamel may in part be due to the increased permeability of the newly erupted enamel, allowing greater diffusion (Brudevold *et. al.* 1982) A gradient of fluoride has been shown to exist within carious lesions from the surface towards the sound enamel underneath and fluoride has even been shown to be able to penetrate into the sound enamel beyond (Lagerweij

et. al. 2006). Importantly, fluoride has been shown to be able to penetrate not only carious, but also sound enamel up to depth of 100µm.

The incorporation of fluoride into the enamel structure is thought to occur through its replacement of hydroxyl ions (Young 1975, Aoba *et. al.* 2003). Once substituted, the symmetry and high charge density of the fluoride ion in comparison to the hydroxyl it replaces allows it to fit much tighter into the Ca II "triangles". In an opposite way to carbonate, this serves to reduce the solubility product (KSP) of the enamel through stabilising the crystal structure and leading to a more difficult to dissolve fluoridated crystal (Robinson *et. al.* 2000). Fluorapatite has a lower dissolving pH than HAp (4.5-5), so it makes sense to assume that HAp with fluoride incorporated would also have a lower dissolution pH than standard HAp. Fluoride concentrations as low as 0.05ppm have been shown to reduce solubility of the enamel HAp to that of stoichmetric HAp (Manly and Harrington 1959, Featherstone *et. al.* 1990). Furthermore, a logarithmic relationship between the amount of fluoride present and the decrease in solubility has been demonstrated (Featherstone *et. al.* 1990).

Fluorapatite forms is situations where acid is present along with fluoride at a concentration of approx. 50ppm. Alternatively, in situations where the F concentration at the enamel surface is greater than 100ppm a protective layer of calcium fluoride can also form on the enamel surface (Christofferson *et. al.* 1995).

Fluoride is believed to diffuse into the enamel from the plaque fluid at the same time as acid produced by plaque, upon which it binds to the enamel surface (Featherstone 1999). This affords some protection and acid will then selectively dissolve the non-fluoride bound apatite (Arends and Christofferson 1990). In addition to plaque-fluid fluoride levels, fluoride content of saliva, and particularly the balance between the two, has been shown to play an important role in fluoride action (Edgar and Higham 1995).

The cyclic change in environment proposed to be the driving force behind PEM fits within the idea of fluoride incorporation, as most post-eruptive incorporation of fluoride is believed to occur as part of de- and remineralisation events (Fejerskov *et. al.* 1994). Further to this, it has been shown that partially demineralised enamel is more susceptible to fluoride diffusion (Lynch and Smith 2012). In fact, the thermodynamic conditions at a neutral pH are unfavourable for passive diffusion of fluoride into the enamel (Lynch 2013).

Interestingly early research does highlight this, as germ-free rats treated topically with a 1% NaF solution showed no greater degree of "maturation" than regular rats treated with water (Briner and Rosen 1968), whereas regular rats with a 1% penicillin supplemented diet showed an increase. This highlights that both the acid challenge and the subsequent exposure to remineralisation are important and exposure to agents such a fluoride alone is not effective. The study mentioned hypothesised that oral bacteria must be important for fluoride action, and that it is the anti-microbial action of fluoride that is important. However, with advances in our understanding of the mechanism of fluoride it makes more sense to assume that is a combination of the oral biofilm increasing the availability of fluoride at the enamel surface and the remineralising action of fluoride within the enamel mineral, as opposed to an anti-bacterial effect that drives the maturation process observed (Watson *et. al.* 2005, Garcia-Godoy and Hicks 2008).

1.7.5 Zinc

Zinc is widely used in toothpastes as an anti-microbial agent, to reduce malodour and as an inhibitor of calculus crystal growth (Segreto *et. al.* 1991, Cummins and Creeth 1992, Young *et. al.* 2003). In terms of salivary clearance following product use, zinc exhibits similar bimodal clearance behaviour to fluoride (Cummins and Creeth 1992). Initial clearance over the first hour post-treatment is rapid, as loosely-bound zinc is cleared. Following this, clearance of the remaining, more tightly bound, zinc occurs

over several hours (Harrap *et. al.* 1984, Gilbert and Ingram 1988, Cummins and Creeth 1992). Clearance from plaque occurs in a similar fashion, with elevated levels detectable for up to 12 hours post-application. Additionally, plaque had been shown to demonstrate a build-up of zinc upon repeated application in a similar manner to fluoride (Afseth *et. al.* 1983, Hall *et. al.* 2003). Very little (1%) of zinc is found within the Plaque Fluid (PF) (Saxton *et. al.* 1986).

Zinc is present in both saliva and plaque (Menegario *et. al.* 2001, Burguera-Pascu *et. al.* 2007), with reported values ranging from 0.01-0.24ppm for saliva and 7.86-31.6ppm for plaque (Lynch 2011). It is also found naturally present in teeth (Brudevold *et. al.* 1963, Frank *et. al.* 1989), with most zinc deposition happening pre-eruptively, suggesting it has a use upon eruption (Brudevold *et. al.* 1963). Further to this zinc has also been shown to accumulate at the surface of the enamel following eruption, before being gradually lost over time (Brudevold *et. al.* 1963, Weatherell *et. al.* 1972). This suggests that it plays a role within the PEM process before being no longer needed and removed, possibly through deposition during sub-clinical caries events in a similar manner to other ions such as fluoride (Fejerskov *et. al.* 1994). The level of zinc in the surface areas of enamel varies between 430 and 2100 ppm dependent upon the placement of the tooth within the mouth. It is distributed within the enamel in the same manner as fluoride, but is deposited in a less regular fashion (Brudevold *et. al.* 1963).

An interesting feature of zinc is that whilst several studies have demonstrated its ability to reduce solubility of enamel (Brudevold *et. al.* 1963, Dedhiya *et. al.* 1973, Abdullah *et. al.* 2006), it has also been demonstrated as an inhibitor of crystal growth (LeGeros 1997). This ability to contribute to both the de- and remineralisation of enamel highlights its potential as a key player in the PEM process. Zinc has demonstrated potential to reduce dissolution of enamel to a similar degree as fluoride (Brudevold *et. al.* 1963). Furthermore, it is believed that in some conditions zinc is able to soften the surface of the enamel allowing fluoride to penetrate further into the surface layers of

the enamel, improving remineralisation (Lynch 2013). This would serve some explanation as to their similar distribution. Furthermore, animal studies in rats have shown that zinc-deficient rats presented more carious lesions than those fed a zinc-supplemented diet (Fang *et. al.* 1980). Studies using synthetic hydroxyapatite have shown that zinc is able to compete with calcium II ions to incorporate into the HPA lattice (Brudevold *et. al.* 1963, Mayer *et. al.* 1994, Terra *et. al.* 2002, Tang *et. al.* 2009), reducing solubility (Mayer and Featherstone 2000, Costa *et. al.* 2003). It is believed this occurs due to a reduction in crystal disorder, particularly when applied in combination with fluoride (Featherstone and Nelson 1980, Mayer and Featherstone 2000). Research studies using a HPA substrate have shown two potential interactions between enamel and zinc; incorporation into the lattice and adsorption onto the surface (Ingram *et. al.* 1992, Mayer *et. al.* 1994). This is supported by rat-based research that showed that when fed a zinc-supplemented diet, rats showed increased zinc and decreased skeletal calcium (Fang *et. al.* 1980). However experimental results reported for zinc are highly variable and often contradictory, with several studies reporting no effect of zinc on de- or remineralisation of enamel (Ingram *et. al.* 1984, Ripa *et. al.* 1990, ten Cate 1993, Laucello *et. al.* 2007). Furthermore, data relating to zinc incorporation to enamel within the mouth suggests very small concentrations, which would not be compatible with incorporation into the HPA lattice (Matsunaga *et. al.* 2009, Lynch *et. al.* 2011).

1.7.6 Other Ions

Given the nature of PEM, any component of the carbonated apatite may have an effect, however small. Several other trace elements, such as strontium, tin and copper have been shown to occur within the enamel, however the role they play, if any, within the structure is not entirely understood. Ions such as chlorine and tin, which are largely found in the surface layers of enamel are of particular interest, as this is where the majority of PEM changes are thought to occur (LeGeros *et. al.* 1996). Whilst not found

concentrated at the surface, the potential role of strontium (Sr) in PEM bears consideration. Studies have shown the ability of Sr to aid remineralisation (Thuy *et. al.* 2008) particularly when combined with fluoride, suggesting it may interact in a similar manner to zinc. Results of such studies, however, are highly variable and the exact mechanisms by which it exerts these effects are not fully understood (Lippert and Hara 2013).

1.7.7 Organic Components of Enamel

As 2% of dental enamel is formed of organic components, it makes sense to consider the role they may have in the PEM process (Boyde 1989). This is supported by the observation that the nitrogen content of enamel also seems to decrease with post-eruptive age (Savory and Brudevold 1959). Where enamel rods and inter-rod enamel meet, an area of inorganic matrix known as the enamel rod sheath is present and serves to connect rods to one another (ten Cate 1998). Rod sheath is comparatively less mineralised than other areas of the enamel and as such has a higher protein content. Rod sheath has been observed decrease with post-eruptive tooth age, particularly within the outer layers of the enamel (Miake *et. al.* 2016), or in unerupted enamel exposed to saliva (Nakajima *et. al.* 2003). This presumably occurs as the enamel becomes more mineralised due to PEM and it therefore follows that the protein content of matured enamel would be lower than that of immature, newly-erupted counterparts. The organic material found in the interprismatic regions of enamel has been shown to have raised solubility when subjected to acidic challenge than the rest of the enamel (Shellis 1996), supporting this idea, as it would therefore be preferentially lost.

This would, however, appear to be counter-intuitive to reducing the susceptibility of the enamel to caries, as several studies have demonstrated the role of proteins in reducing acid dissolution by decreasing acid penetration through the enamel and helping to maintain surface charge density (Epinosa *et. al.* 2010, Lubarsky *et. al.* 2012, 2014,

Baumann *et. al.* 2015). Whilst nanoindentation studies have found high protein-containing enamel to be softer (Xie, *et. al.* 2007), it has been argued that the small measurement area of a single prism employed by this technique does not represent the effect removing protein has on the interprismatic space (Baumann *et. al.* 2015). They go on to demonstrate that when Knoop surface microhardness over a larger area is conducted, surface softening is observed upon deprotonation.

Salivary proteins appear to play an important role in the PEM process (Brudevold *et. al.* 1982, Nakajima *et. al.* 2003), which is particularly highlighted by animal studies that have reported a reduction in observed levels of PEM following desalivation (Larson and Keyes 1967, Speirs 1967).

1.8 Approaches used for the Investigation of PEM

1.8.1 *In vivo*

Early studies into PEM focused on the use of *in vivo* animal models (Brudevold *et. al.* 1982). Whilst these are able to account for the entire *in vivo* process (White 1992), studies have shown that there is often variation between effects observed within such models and those observed within a clinical setting (Stookey *et. al.* 1985). One key variation that has been noted between rodent models in particular, is a naturally higher salivary pH than that reported for human saliva (Ericsson 1962). Additionally, reported calcium and phosphate content has also been shown to differ between rodent and human enamel (Murray 1936).From an experimental perspective, the ethical consideration of *in vivo* research must also be taken into account. Ethical approval and appropriate training can be lengthy and time-consuming and therefore it is generally better to use alternative approaches where suitable. This attitude falls in line with current government initiatives such as the National Centre for the 3 Rs (NC3Rs), which aim to reduce the levels of *in vivo* animal research where possible (Kilkenny *et. al.* 2010). Whilst some *in vivo* research has been conducted using human subjects, these have been

largely limited to superficial investigations recording changes in porosity over time using electrical resistance (Schulte et. al. 1999, Kataoka et. al. 2007).

1.8.2 *In vitro*

Whilst reductionist in nature (White 1995), it cannot be denied that *in vitro* microbe-free research, particularly demineralisation and remineralisation studies, has made a significant impact on our understanding of the caries process and of the structure of enamel itself (NIH 2001). One of the main advantages of such techniques is the ability to have tighter control over the parameters of an experiment, allowing specific criteria to be investigated (White 1995). De-/Remineralisation experiments are focused on the chemical basis of dental caries, and in principle involve the manipulation of the ionic environment to induce dissolution of deposition of mineral within an enamel substrate depending on what outcome is required. This approach has been used successfully within multiple studies to gain a better understanding of the chemical and physical changes that occur within dental enamel during both periods of acidic challenge (ten Cate and Duijsters 1983, Arends *et. al.* 1984) and remineralisation (Koulourides *et. al.* 1965, Reynolds 1997, Amaechi and Higham 2001). They have also been widely applied to the investigation of ion additions for potential therapeutic use, such as fluoride and zinc (Lippert *et. al.* 2012, Lynch 2011). The exclusion of additional variables and the biological variation naturally present *in vitro* makes such approaches effective at initial identification and investigation of such agents (White 1995, Valappil *et. al.* 2014), however secondary work beyond the limited *in vitro* environment is then required to validate the observed effects further (Lambrechts *et. al.* 2006).

Whilst the use of such approaches may raise concerns over the transferability of research conducted using “artificially-created” lesions to those which occur naturally *in vivo*, studies have shown that whilst there are some differences, lesions produced this way possess many similarities to those occurring *in vivo* (Arends and Christoffersen 1986).

Several approaches have been applied to demineralise enamel *in vitro* including the use of both chemically designed solutions (Larsen 1974, Moreno and Zahradnik 1974) as well as acidic gels (Silverstone and Johnson 1971, Groeneveld and Arends 1975).

1.8.2-1 pH-cycling

In principle, pH-cycling studies aim to re-create the changeable *in vivo* chemical environment of the mouth within a controlled *in vitro* setting. It is formed through exposure of substrate to several intermittent periods of both conditions favouring de- and re-mineralisation. They have been successfully applied to both sound enamel and pre-created lesions (ten Cate *et. al.* 1988, Demato *et. al.* 1990) and can be designed to provide a net result of both de- or re-mineralisation over the experimental time-frame (ten Cate and Duijsters 1982). Furthermore, they can be conducted entirely using inorganic solutions, or with the incorporation of saliva to account for the effects of salivary enzymes and other organic components (White 1987). The state of flux provided by the varied experimental solutions and ability to introduce saliva, make pH-cycling more representative than traditional de- and re-mineralisation counterparts.

As outlined generally for de- and remineralisation approaches above, pH-cycling has been used to test the effects of exposure to therapeutic agents both in solution (ten Cate *et. al.* 1988) and within novel materials, such as bio-reactive glasses (Valappil *et. al.* 2014) on both the de- and re-mineralisation processes. One of the main advantages of this type of approach is the wealth of analysis options afforded. Data can be collected both by assessing the changes in composition of the test solutions throughout the experimental period and by analysing the substrate both before and at its conclusion. The absence of a biological component also allows greater ability to halt the chemical process at intervals to allow data points to be taken longitudinally using a single specimen.

1.8.3 Biological Models: Constant Depth Film Fermenter (CDFF)

In an attempt to combat the reductionist nature of *in vitro* approaches, biological models have been developed that aim to apply key aspects from the *in vivo* situation into *in vitro* research (Arends 1995). Whilst they are less focused on the ionic basis of the caries process, they allow investigation of the microbial component within a much more standardised and relatively less variable environment than that present *in vivo* (Sissons *et. al.* 2007).

An example of one such biological model is the constant depth film fermenter (CDFF) (Coombe *et. al.* 1982), which is often regarded as one of the most advanced (Peters and Wimpenny 1988). The model is capable of supporting the production of oral biofilm upon the substrate, whilst still allowing control over most external variables (Kinniment *et. al.* 1996). This level of external control is one of the main advantages of this approach over those conducted on the *in vivo* environment. In comparison to other available biological models, the CDFF is also able to control the physical parameters during biofilm formation (Sissons 1997). In principle, the CDFF allows biofilm formation within a sealed and sterilised environment designed to allow gas exchange without contamination from the outside environment. Substrate is placed into pans that allow a recessed area for biofilm formation within a rotating turntable to ensure a constant thickness. It allows a range of external factors to be introduced over time such as growth media, sucrose and therapeutic agents such as fluoride using timed pumps.

In order to further reduce variability within the system, a dual-CDFF design has been created which allows a shared inoculum to be used between two units simultaneously (Hope *et. al*. 2012). This provides an inbuilt control condition to any introduced variables and helps to combat the issues associated with variability that arise from the use of microcosm inoculums (Sissons 1997). To date the CDFF model has been used

to create enamel lesions both in the absence and presence of fluoride (Owens 2013, Bahkt 2014).

1.8.4 *In situ*

In situ approaches aim to bridge the gap between the wider range of analysis options afforded by *in vitro* techniques and the representative *in vivo* environment. Within the dental field they usually involve the placement of a substrate into the mouth either attached to a fixed appliance or built into a removable one to observe the effects of the oral environment (Manning and Edgar 1992, West *et. al.* 2003, Amaechi and Higham 2001). The main advantage of such an approach is that it allows pre-treatment of the substrate, such as lesion creation, in addition to the use of destructive analysis techniques, whilst still allowing exposure to the *in vivo* environment. However, it is worth noting that some researchers have suggested that placement of an intra-oral appliance may actually cause change to the oral environment, moving away from a "true" *in vivo* situation (Brill *et. al.* 1977). Whilst they have largely been successfully used in the testing of novel therapeutic interventions (ten Cate 1994), they can also be used to investigate the effect of diet conditions on the enamel in greater detail (Komarov *et. al.* 2016). The greatest obstacles faced by this type of approach are based around the requirement for participants. This leads to issues surrounding both the ethical and financial considerations for such studies in addition to the need to subject compliance for accurate experimental results. Additionally, unlike *in vitro* based approaches, which are able to model the caries process over a much shorter period of time, *in situ* approaches require much longer experimental periods in order to achieve the same levels of demineralisation or remineralisation.

1.8.5 Enamel Substrates

Whilst human enamel is the ideal experimental substrate for use in research studies, sourcing intact, caries-free human teeth is becoming difficult and as such they are a

limited resource within the research environment. It therefore makes sense for researchers to explore alternative options where possible. The most common alternative enamel substrate used in such cases is bovine, although the use of other animal enamel substrates has also been explored (Featherstone and Mellberg 1981, Edmunds *et. al.* 1988).

Bovine and human enamel share a similar microstructure, however interprismatic spaces are larger in bovine enamel and contain fibril-like aggregations (Fonseca *et. al.* 2008). Bovine enamel is larger than its human counterpart, both in terms of overall and crystal size, with bovine enamel crystals usually being around 1.6 times larger (Arends and Jongebloed 1978). This difference in size means that there is potential to produce larger or even multiple samples from the same tooth, allowing same-tooth controls. Human incisors, in contrast, are much smaller and therefore do not afford this ability (Zero 1995). The reported calcium content by weight of bovine and human enamel when measured by electron microprobe shows similarity (37.9% and 36.8% respectively), although the distribution is more even throughout bovine enamel than human (Davidson *et. al.* 1973). Furthermore, the Ca/P ratio and hardness are comparable for both enamel types following exposure to a demineralisation event (Feagin *et. al.* 1969, Tantbirojn *et. al.* 2008).

When the protein of bovine and human enamel is considered, a similar molecular weight is observed. Bovine enamel protein, however, is deficient in alanine, resulting in bovine enamel being more porous than its human counterpart (Fincham *et. al.* 1982, Edmunds *et. al.* 1988, Arends *et. al.* 1989). This is highlighted by calcium release studies, which have shown significantly higher Ca ion release for bovine enamel when subjected to dissolution (Carmargo *et. al.* 2006).

In comparison to available human enamel, which is often only extracted due to caries or other defects, sound bovine enamel samples are relatively easy to obtain. Unlike sourcing human enamel, the age and source of bovine enamel can be defined and

controlled. Factors such as geographical location, gender and individual diet have been demonstrated to affect dental enamel composition (Lane and Peach 1997, Vernois *et. al.* 1989). Whilst some variation between bovine sources will still occur, sourcing bovine enamel allows much greater control over key parameters such as geographic location, diet and fluoride intake than is possible for human enamel (Zero 1995, Wright *et. al.* 2008).

In terms of experimental performance, the increased porosity of bovine enamel causes it to demineralise at a faster rate when exposed to an erosive challenge (White *et. al.* 2010, Amaechi *et. al.* 1999, Arends *et. al.* 1989). Microradiographically, lesions created in bovine enamel are deeper, with higher mineral loss. Observed differences, however, only seem to occur when exposure to acid is above a certain threshold, as erosion studies have shown no difference in microhardness between both enamel types when subjected to a short erosive challenge (up to 60 seconds in pH 3.2 citric acid) (White *et. al.* 2010). This suggests that the differences between bovine and human enamel are more pronounced within the enamel as opposed to at the outermost surface.

Interestingly, the age at which a bovine enamel specimen is obtained appears to affect its properties, most notably, surface microhardness (Fonseca *et. al.* 2008). When enamel obtained from younger (20-30 month) and older (>30 months) cattle were compared to enamel from 20-30-year-old humans, the older bovine enamel had a comparable surface hardness, whilst the younger enamel was significantly softer. From this the authors recommended the use of bovine enamel from older cattle, however the change in hardness suggests, in the context of this work, that bovine enamel may undergo, to a certain extent, a PEM process. As such, it would appear that in order to use bovine enamel as a substitute for human enamel in the study of PEM, it is advisable to try and use enamel obtained from sources younger than 30 months, as these may be “immature” and therefore more representative.

1.9 Analysis Techniques for the investigation of PEM

1.9.1 Hypomineralised Areas (HMA)

Early studies used silver nitrate staining to investigate the PEM process (Francis and Briner 1966). This technique was based on the fact that Hypomineralised areas (HMA) of enamel stain with silver nitrate in a similar way to carious lesions. They noted that newly erupted enamel possesses several HMA, which are gradually reduced after exposure to the oral environment. Whilst the significance of this method for providing the pioneering research into PEM cannot be denied, safer and more effective analysis methods have since been developed that are more appropriate to use.

1.9.2 Electrical Resistance

Electrical resistance can be used to measure porosity of enamel, as the more porous enamel is the more water and soluble electrolytes are present within the enamel. One of the main benefits of this method for the study of PEM is that it allows the porosity of a single tooth to be studied over time and due to its non-destructive and relatively non-invasive nature can be used *in vivo* (Schulte *et. al.* 1999). In the context of PEM, it has been particularly useful in estimating the amount of time taken for PEM to occur, as it allows the measurement of a single tooth from eruption through several time-points post-eruption. Porosity values of teeth vary *in vitro* to *in situ*, this highlights the importance of the surrounding environment for representative values (Tarbet and Fosdick 1971) and therefore make this approach more suitable for *in vivo* experiments.

1.9.3 Surface Microhardness (SMH)

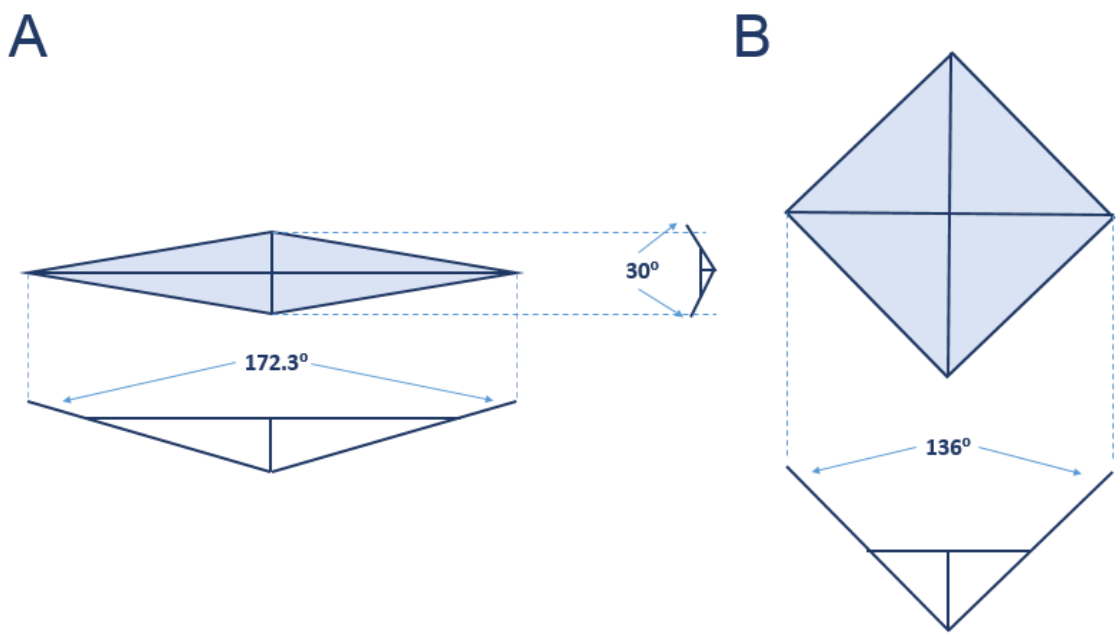

Figure 1.8: Illustration of Different Hardness Indenter Shapes. *Schematic showing the varying indenter geometry between Knoop (A) and Vickers (B) indenters.*

Hardness measurements based on the use of an indenter of known area that is driven into the surface of interest with a known force. The area of the resulting indentation is then used to calculate the hardness, as the softer the surface, the larger an indentation would be created. There are two main types of microhardness indenter used within dental research; these are Knoop and Vickers (Figure 1.8). Knoop microhardness is particularly commonly used for cross-sectional hardness, as it creates a relatively superficial indentation, making it suitable for thin or brittle materials. Knoop hardness values of between 272 and 440 have been reported for human enamel, with an increase in hardness observed towards the surface (Roy and Basu 2008, He *et. al.* 2010, Meredith *et. al.* 1996). Given the hardness of the HPA crystals from which enamel is formed, the deformation observed upon indentation appears to be caused by sliding within the interprismatic, protein-rich areas as opposed to the prisms themselves, which remain intact (He and Swain 2007).

Whilst microhardness works well when categorising materials with a planar-parallel surface, the calculation relies on the assumption that all surfaces of the indenter interact equally with the surface of interest (Brennecke and Radlanski 1995). This brings into question its suitability for use on enamel that has not been pre-prepared to be planar-parallel. This is supported by SEM measurements taken of Vickers indentations, which showed many lacked a clear square-shaped indent (Gutierrez-Salazar and Reyes-Gasga 2003). Measurement of surface hardness via indentation causes a permanent change to the enamel surface with each reading taken. This damage is important to take into account when combining SMH with further analysis techniques.

One important limitation of indentation-based hardness measurements is the requirement for the user to define the boundaries of the indentation created. Recorded data can be highly variable depending on the experience of the user and as such the accuracy of the results can be affected.

Recent advances in this technology have led to the development of nanoindentation-based hardness testing. Nanoindentation has been successfully applied to determine both the hardness and elastic modulus of enamel (Ge *et. al.* 2005, Low *et. al.* 2008). Nanoindentation works on the same principle as other Microhardness testers, but using a much smaller scale indenter. This allows the investigation of much smaller microstructures (several μm) in addition to reducing the damage to the surface caused by the indentation. However, Nanoindentation is even more affected by non-planar-parallel surfaces than traditional indentation methods, which has been reflected by the production of force curves in human enamel that demonstrate abnormal features due to load-dependant behaviour (He and Swain 2007).

1.9.4 Surface Profilometry

Surface profilometry involves taking scans across the surface of a sample in order to analyse the topography. Traditionally it involves a diamond-tipped stylus 1.5-2.5µm in size being drawn repeatedly across the surface (Stachowiak and Batchelor 2004) whilst the vertical movement is recorded. Whilst the constant contact of the stylus allows a relatively large vertical range (2-250µm), the diamond tip can cause damage to the surface. Additionally, the measurements can be confounded by external vibrations or movements.

Modern profilometry techniques have shifted to a non-contact approach, using a laser as opposed to a stylus to make measurements. In these approaches, a light spot less than 100µm in diameter is drawn across the surface and either the deflection of the beam or the confocal principle is used to determine the surface topography (Rodriguez *et. al.* 2008, McBride and Maul 2004). Whilst non-contact surface profilometry (NCSP) can overcome some of the issues of its stylus-based predecessor, it has been recognised that the results can be affected by the colour and transparency of the sample being measured. When surface roughness values are calculated, lighter and more transparent surfaces record a lower average roughness than darker, more opaque counterparts (Rodriguez *et. al.* 2008, McBride and Maul 2004).

1.9.5 Scanning Electron Microscopy (SEM)

Scanning electron microscopy (SEM) has been widely used within dental research to look at surface changes in enamel (Boyde and Lester 1967, Ferrazzano *et. al.* 2008). SEM is based on scattering electrons at the sample surface in order to evaluate the composition and topography. The technique has the potential to produce high resolution 3-D images with a large depth of field. Traditionally, SEM imaging requires the sample to be coated with a conductive material, usually gold, to prevent electrostatic charge accumulating on the surface. A large drawback of this is the

irreversible change to the images sample and therefore an inability to use it for further analysis. Modern SEM systems, however, have been developed to allow the imaging of uncoated samples using an environmental system, based within a pressurised container. This is advantageous over other, more traditional SEM systems, as it does not require alternation of the sample and following imaging the sample can be removed from the holder and used for further analysis.

1.10 Thesis Aims

One of the most reasonable explanations for the lack of understanding as to the underlying process behind post-eruptive enamel maturation is the absence of any appropriate methodology by which to approach such research. As such, the work contained within this thesis aimed to develop a suitable method by which the PEM process could be studied. The following objectives were therefore defined:

- To evaluate the ability of pH-cycling to simulate post-eruptive maturation of enamel
- To develop an *in vitro* model of post-eruptive maturation
- To assess of the ability of the proposed model to reduce susceptibility to an acid challenge
- To evaluate the ability of the proposed model to simulate the physical changes, such as increased surface microhardness, reported during PEM *in vitro*.
- Investigate the role of Zinc and Fluoride within the PEM process
- Assess the effect of strontium and fluoride-containing remineralisation solutions within the proposed model

Chapter Two: Materials and Methods

2.1 Basic Introduction to the Proposed Model

The model of PEM proposed within this work can be broken down into three stages. (Figure 2.1). Firstly, bovine enamel blocks are prepared and subjected to any pre-treatments. Blocks are then exposed to a pH-cycling regime and any additional treatments. Finally, the effect of the pH-cycling exposure is tested using a standard 72h demineralisation challenge. Whilst parameters pertaining to the specifics of the model may change between chapters, the basic structure outlined here will remain constant.

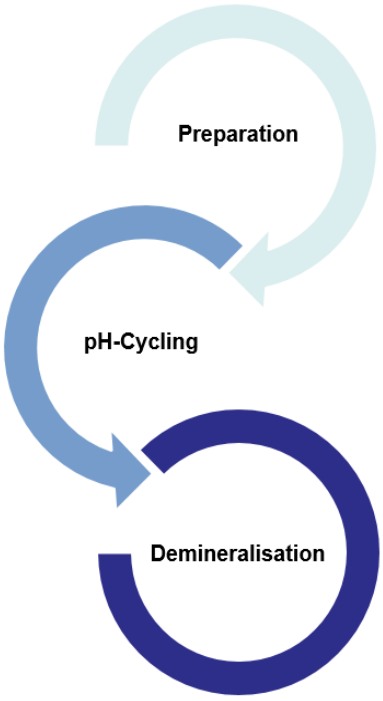

Figure 2.1: Outline of PEM Model. *The proposed model consists of three distinct stages, preparation, pH-cycling and a demineralisation challenge.*

2.2 Preparation of Bovine Enamel Blocks

Bovine incisors were collected from a local abattoir (Battlefield Road Abattoir, Harlescott, UK). Source cattle were no older than 36 months and had been exposed to non- fluoridated water sources. Teeth were stored refrigerated in a 1% w/v thymol/deionised water solution prior to use (BDH Laboratory Supplies, Poole, UK). Any remaining flesh and the root itself were removed prior to experimental use. Visual examination, quantitative light induced fluorescence (QLF-D) and multispectral imaging (MSI) were used to select teeth free from defects such as cracks and areas of demineralisation. Examples of excluded and accepted teeth are given in Figure 2.2.

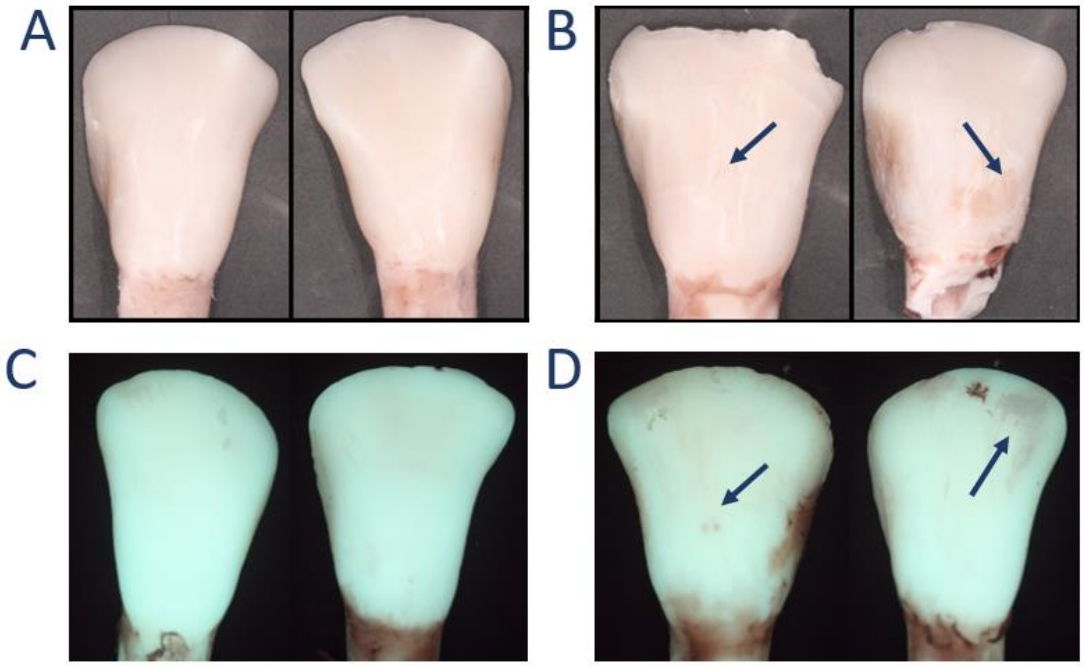

Figure 2.2: Tooth Selection Criteria. *White light and QLF-D images showing selected (A and C) and excluded (B and D) teeth. B: Arrows highlight surface defects such as deep grooves or damage. D: Arrows indicate dark patches representing either mineral loss or areas of over-abraded enamel.*

The surfaces of selected teeth were abraded with wet abrasive sheets from a rough (p240) to fine grade (p1500) to remove the outermost surface (Rhynowet Sheets, Insasa, Industria de Abrasivos, Spain). Care was taken to ensure teeth were kept

water-cooled to reduce any damage to the organic components of the enamel from the heat generated during the abrading process.

Prepared teeth were mounted onto a ceramic anvil using Green-Stick impression compound (Kerr Corporation, California, USA) and cut using a water-cooled precision diamond wire saw (Model 3241; Well Diamantdrahtsagen GmbH, Mannheim, Germany) to produce blocks approximately 10x4mm in size (Figure 2.3).

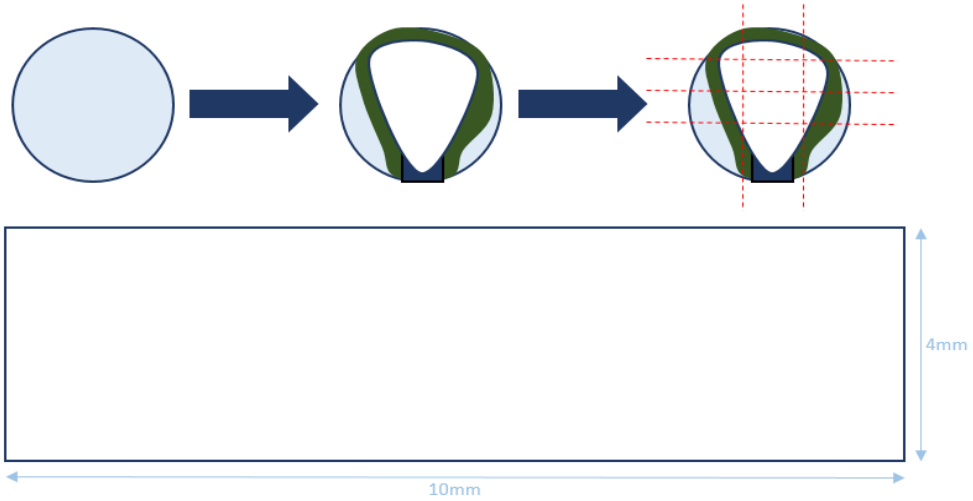

Figure 2.3: Creation of Bovine Enamel Blocks. *Illustration of mounting and sectioning process to produce 10x4mm bovine enamel blocks.*

The enamel surface of each block was polished with a pumice and deionised water slurry using a rotating brush attached to a motorised hand-piece. coated in clear acid resistant nail varnish (MaxFactor Nailfinity, Procter and Gamble, Weybridge, UK) to seal the edges and create a 9x3mm experimental window on the polished enamel surface, which can be seen illustrated in Figure 2.4.

Figure 2.4: Schematic of Prepared Experimental Block. *Illustration of fully prepared bovine enamel block with a 9x3mm experimental window on the polished surface.*

Blocks were mounted in threes with Green-Stick impression compound into 50ml disposable Sterilin containers (Sterilin Ltd. Newport, UK) using a glass rod placed through the lid as illustrated below (Figure 2.5).

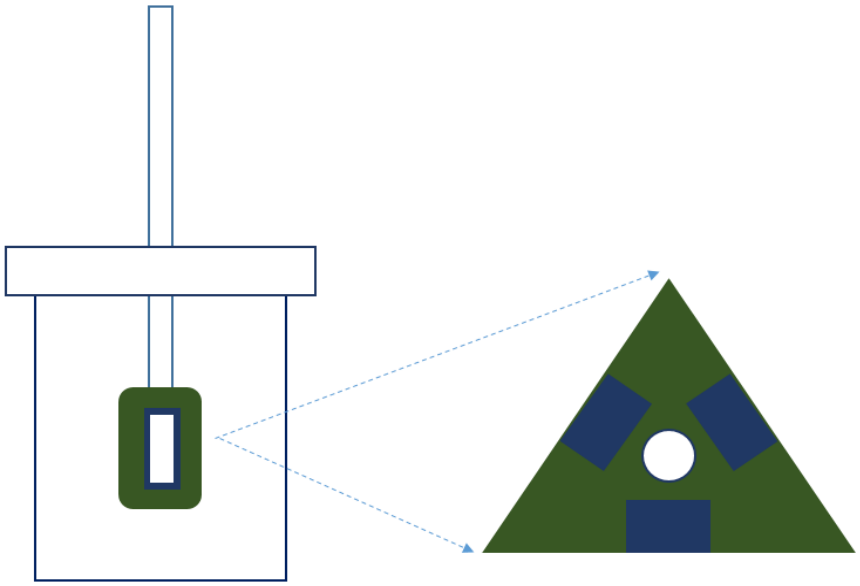

Figure 2.5: Mounting Process for Bovine Enamel Blocks. *Illustration depicting mounting of experimental blocks in groups of three within Sterilin containers.*

2.3 Design and Test of Demineralisation Solution

In order to address the chemical importance of PF composition within the model a demineralisation solution designed to represent ion concentrations and pH representative of plaque-fluid was devised for this work. Ion concentrations and pH values used during solution design were based on those obtained by Vogel *et. al.* (2000) for plaque fluid during an acid challenge. Values were calculated by taking the average of values obtained from upper and lower molar sites. The resulting solution can be seen in Table 2.1 below.

The pH-cycling model outlined below was designed not to produce clinically-detectable levels of demineralisation as a net result. In order to ensure this, three bovine enamel incisors were abraded and polished as previously described (Section 2.2) and an experimental window created using acid-resistant varnish. Teeth were subjected to 72h demineralisation and imaged using MSI at 1, 3, 6, 9, 24, and 72h. MSI was selected due previous findings from highlighting its ability to detect demineralisation at an earlier point than the QLF-D system (Adeyemi *et. al. 2013,* Desmons *et. al.* 2013). Additionally selection of a 72h total demineralisation time was informed by the aforementioned studies, which demonstrated production of clearly visible lesions when measured using MSI following this length of exposure to a standard demineralisation solution, such as the one illustrated in Table 2.2.

2.4 Exposure to Demineralisation Pre-treatment

Blocks were divided into 1-3 groups, and subjected to either 0, 1 or 3 hours demineralisation with agitation via a magnetic stirrer and flea using the solution outlined below (Table 2.1). Following exposure one third of the experimental window of each block was covered using acid-resistant nail varnish, as illustrated below (Figure 2.6), to provide a protected area for baseline values.

Figure 2.6: Preparation for Baseline Analysis. *In order to keep an area for baseline analysis, one third of the experimental window was covered.*

2.5 Exposure to pH-Cycling Regime

A pH-Cycling system designed for net remineralisation was used in order to expose the blocks to an acid challenge without creating detectable lesions. Blocks were subjected to a three 30min demineralisation-per-day pH-cycling regime for periods ranging from 0 to 20 days. A schematic of the pH-cycling process is presented below (Figure 2.7).

- **9am-9:30am** dH_2O Rinse/ Demineralising solution
- **9:30am-12:30pm** dH_2O Rinse / Remineralising solution
- **12:30pm-1pm** dH_2O Rinse / Demineralising solution
- **1pm-4pm** dH_2O Rinse / Remineralising solution
- **4pm-4:30pm** dH_2O Rinse / Demineralising solution
- **4:30pm-9am** dH_2O Rinse / Remineralising solution

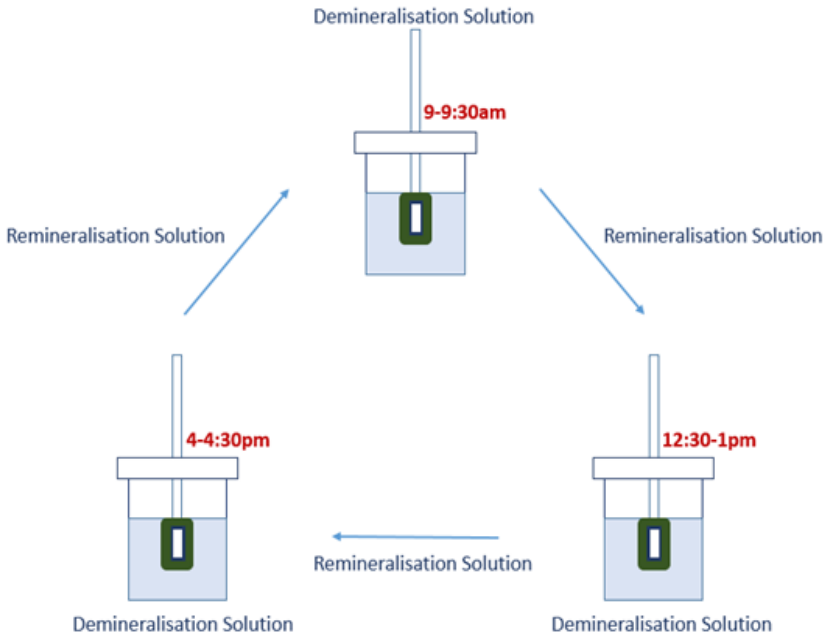

Figure 2.7: Outline of pH-cycling Regime. *Schematic of daily pH-cycling protocol observed for 0 to 20 days. Blocks are kept in remineralisation solution with the exception of three 30min demineralisation periods per day.*

As described previously, solutions were designed to have ion concentrations and pH representative of plaque-fluid. The demineralisation solution was devised as described previously (Section 2.3). The plaque-fluid-based remineralisation solution described by Lynch *et. al.* (2011) was used (Table 2.1), with the addition of 5.7µM Fluoride (From resting levels reported by Vogel *et. al.* (2000). Reagents used were obtained from BDH Laboratory Supplies (Poole, UK), with the exception of HEPES (Sigma-Aldrich Ltd., Dorset, UK).

Solutions were kept at room temperature under agitation with a magnetic stirrer and flea. Separate disposable Sterilin containers were used for each solution and blocks were rinsed in deionised water at each change. Solutions were refreshed at the start of each day.

Reagent	Demineralisation Solution	Remineralisation Solution
$CaCl_2$	2.25mM	1mM
KH_2PO_4	17.65mM	12.7mM
Lactic Acid	32.9mM	-
KCL	-	130mM
HEPES	-	20mM
NaF	4.25µM	5.7µM
pH	5.11	6.58

Table 2.1: Plaque-Fluid-Relevant (PF) Solutions. *Outline of chemical composition of demineralisation solution devised from PF measurements by Vogel* et. al*. 2000 and remineralisation solution described by Lynch et. al. 2007 with the addition of NaF.*

Following pH-cycling an additional third of the experimental window of each block was covered using acid-resistant nail varnish to protect it for analysis (Figure 2.8).

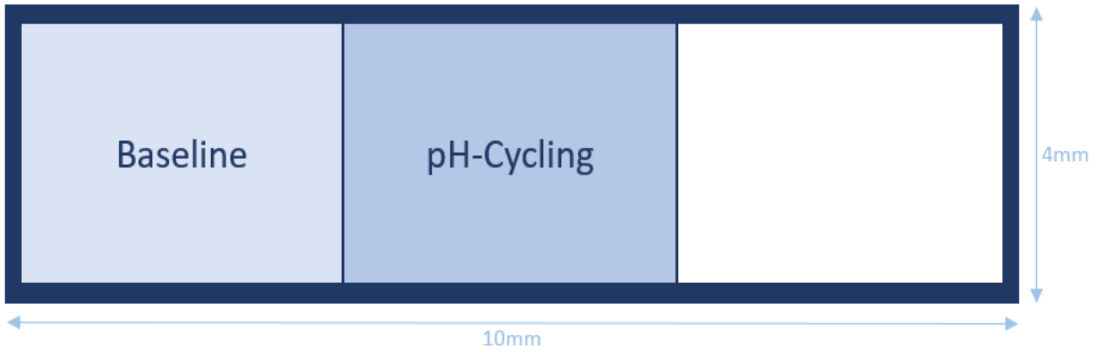

Figure 2.8: Allocation of pH-cycled enamel for analysis. *Following exposure to pH-cycling, the second third of the experimental window was covered to preserve area for analysis.*

2.6 Acid Challenge

Reagent	Concentration
$CaCl_2$	2.2mM
KH_2PO_4	2.2mM
Acetic Acid	50mM
NaF	0.05ppm
pH	4.5

Table 2.2: Standard Demineralisation Solution. *Chemical composition of standard acetic acid demineralisation solution.*

In order to test the effect of the pH-cycling regime on the acid susceptibility of the enamel, blocks were subjected to a 72-hour demineralisation challenge at room temperature, using a standard acetic acid-based solution, the contents of which are presented above (Table 2.2). Constant agitation was provided by a magnetic stirrer and flea. Following demineralisation, the final third of the enamel block was ready to be analysed (Figure 2.9).

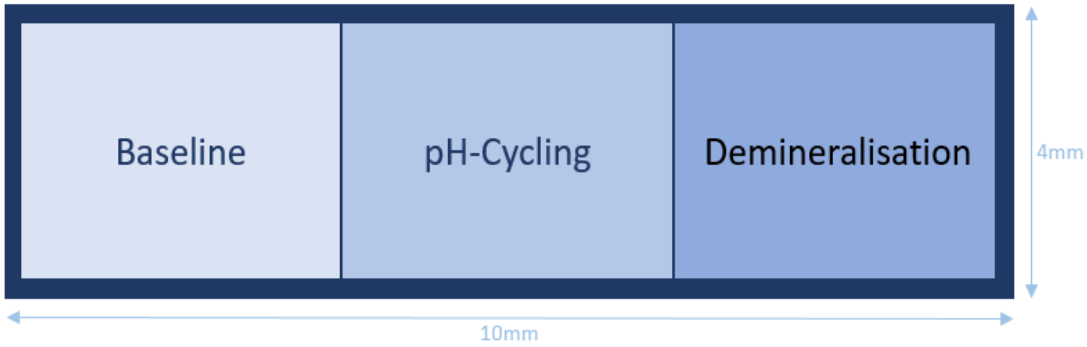

Figure 2.9: Bovine enamel blocks prepared for analysis. *Schematic of bovine enamel blocks with the experimental window divided into thirds to provide areas of baseline, pH-cycled and demineralised enamel for analysis.*

2.7 Non-Contact Surface Profilometry (NCSP)

Following the removal of all nail varnish using acetone, Non-contact surface profilometry (NCSP) (Proscan 2000, Scantron Industrial Products LTD) data was collected with an S5/03 scan-head (resolution 0.01µm, measuring range 0.3mm with a spot size of 4µm) at a sensor rate of 300 Hz with the averaging (Kalfman) filter set at 2. Each scan included the entire exposed window on the enamel surface. Mean surface roughness, Ra, was calculated by taking three measurements from each area. Data was stored in PRS file format and analysed using manufacturer provided software (Proscan 2000, Version 2.1.1.15). This process is illustrated in Figure 2.10.

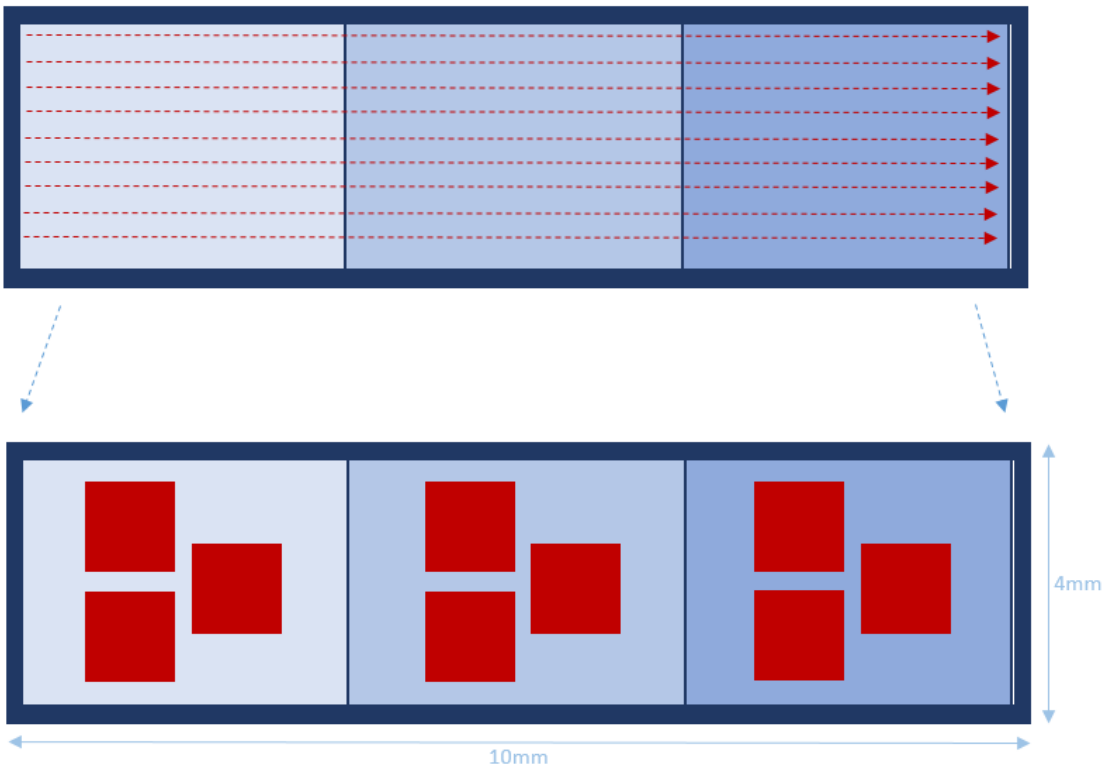

Figure 2.10: Outline of NCSP analysis process. *NCSP scans were taken across the entire experimental window. Surface roughness (Ra) measurements were taken three times for each analysis area.*

2.8 Quantitative Light-Induced Fluorescence (QLF)

Enamel blocks were allowed to air-dry before being imaged using the QLF-D system illustrated in Figure 2.11. In brief, the system consists of a tripod mounted digital SLR camera (Cannon EOS 450D; Cannon UK Ltd., Surrey, UK) with an attached QLF bio-illuminator with a working light emission wavelength of 405nm and a high pass 520nm filter (QLF-D; C3 Version 1.20.0.0; Inspektor Research Systems BV., Amsterdam). Images were taken at baseline, and at various time-points throughout the 72h demineralisation. Images were saved in BMP format and analysed using the accompanying QA2 software (QA2 Version 1.25.0.0; Inspektor Research Systems BV., Amsterdam). In brief, analysis is conducted by selecting an area of sound enamel encasing the lesion. The software then calculates a reconstruction of the sound surface and measured the difference between that and the actual image. This process is illustrated below in Figure 2.12.

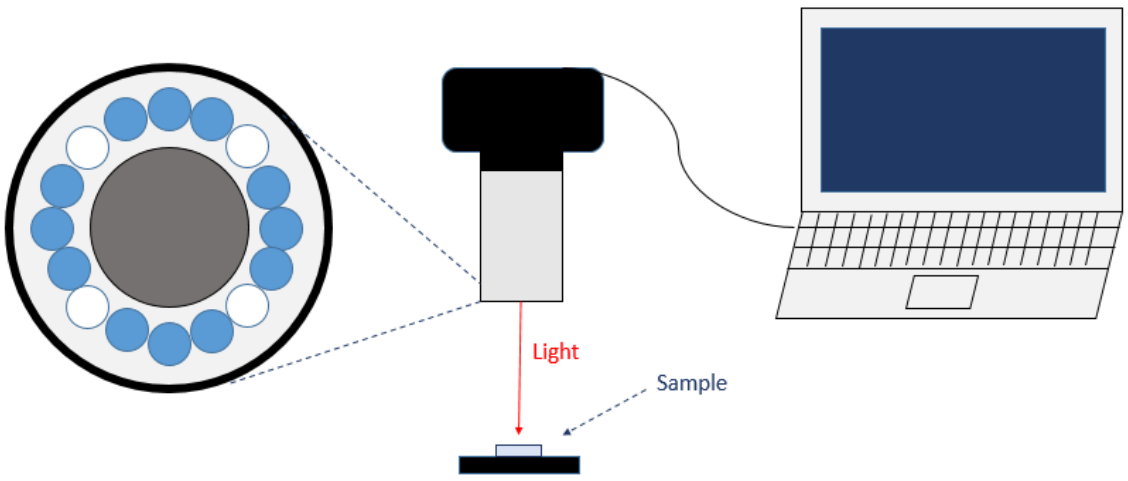

Figure 2.11: Illustration of QLF-D System. *QLF-D system. A Biluminator is connected to a tripod-mounted digital SLR camera with a 520nm high pass filter. A connected laptop is used to take both a white light and QLF (490nm blue light) image.*

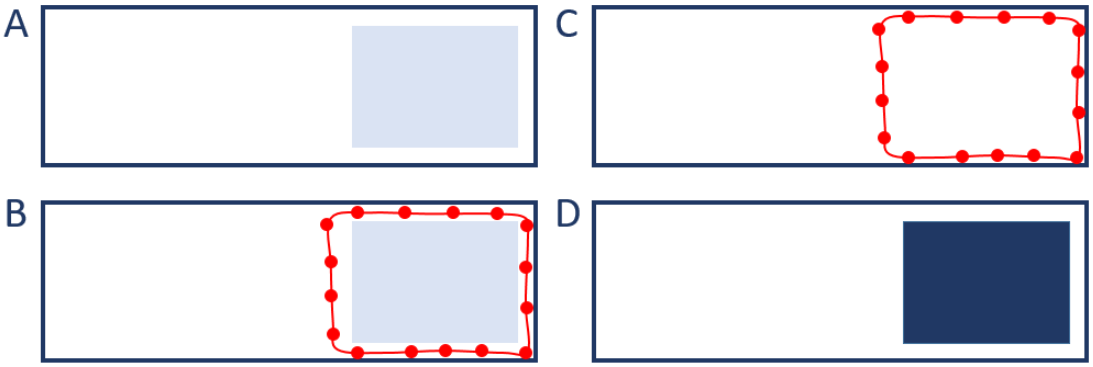

Figure 2.12: QLF-D Analysis Process. *Illustration depicting the basic process for quantifying fluorescence loss using the QA2 software. A: Example of block with lesion. B: A ring of sound enamel is selected around the area of interest. C: The software then creates a reconstructed sound surface. D: This is then used to calculate the change in fluorescence to give a numerical value.*

2.9 Multispectral Imaging (MSI)

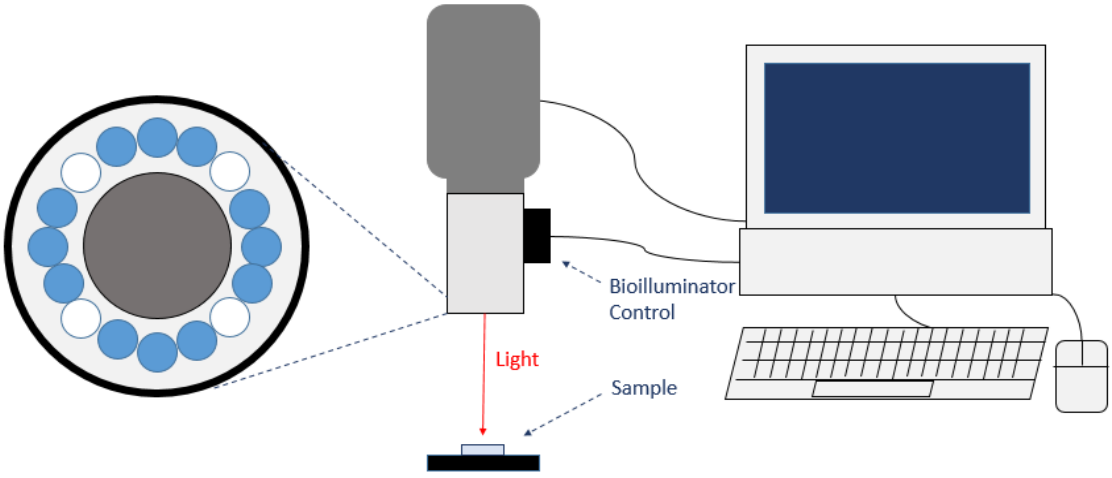

Figure 2.13: MSI System. *Illustration of the MSI system. A billuminator and 460nm filter is connected to a tripod-mounted multi-spectral camera. A connected PC is used to capture an image "cube".*

Enamel blocks were allowed to air-dry before being imaged using custom-built multispectral imaging system which is illustrated in Figure 2.13. The system consists of a tripod mounted multispectral camera (Nuance, CRi Inc. USA) with an attached QLF

bio-illuminator and a 460nm high-pass filter. Images were taken at baseline and at various points during the 72h exposure to demineralisation. Images were extracted at 520nm and saved in TIFF format. Images were then converted into BMP format and analysed using the QA2 software as described previously for QLF-D.

2.10 Transverse Microradiography (TMR)

An overview of the TMR preparation process is presented in Figure 2.14. Blocks were mounted onto ceramic anvils with Green-Stick Impression Compound and cut into transverse sections approximately 1.2mm in width using a precision diamond wire saw. Four sections from each were then mounted onto brass anvils using nail varnish and polished down to approximately 80µm in thickness using a diamond impregnated disc.

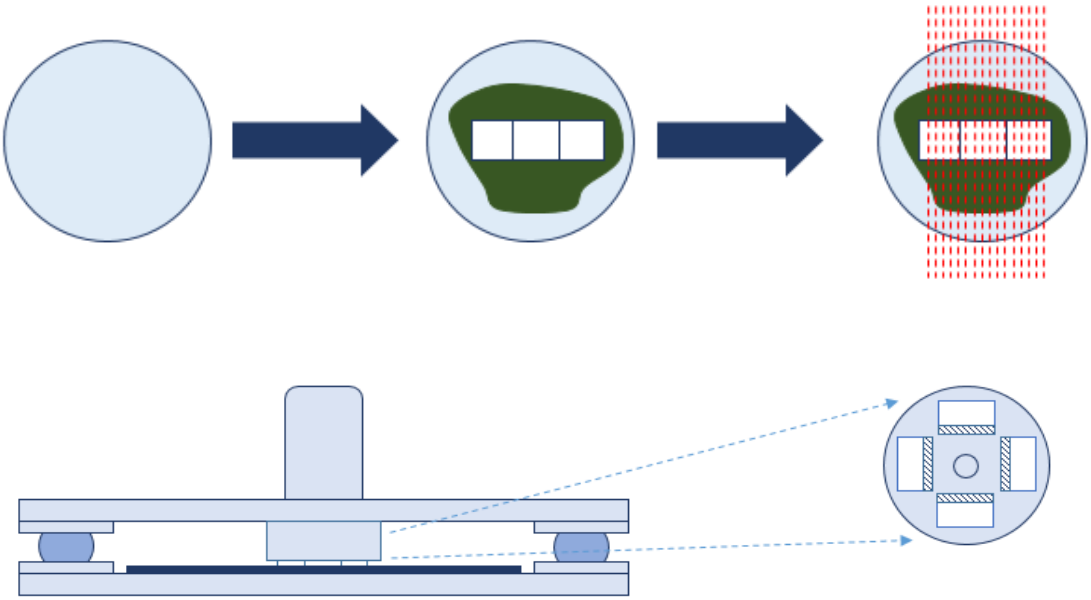

Figure 2.14: TMR Preparation Protocol. *Sections were mounted and cut into 1.2mm transverse sections across all three areas of interest. Four sections from each area were mounted on anvils and ground to 80µm in thickness.*

Sections were removed using acetone and mounted onto an acetate template using double sided tape and covered with a protective layer of clear film (3525 Ultralene Spex Sample Prep, New York, USA) as shown in Figure 2.15. Templates were

mounted with a 13-step aluminium step-wedge against a high-resolution x-ray film plate (Kodak type 1A High-Resolution Plates; Kodak, Rochester, USA). Plates were exposed to a CuKα X-ray source operating at 20mA and 20kV for 12 minutes at a distance of 57cm from the source. Radiographic plates were developed and fixed (Kodak D-19 Professional Developer; Kodak, Rochester, UK and Kodak Unifix; Kodak, Rochester, USA) for 10 minutes per stage and rinsed in water before being dried in an oven at 64˚C.

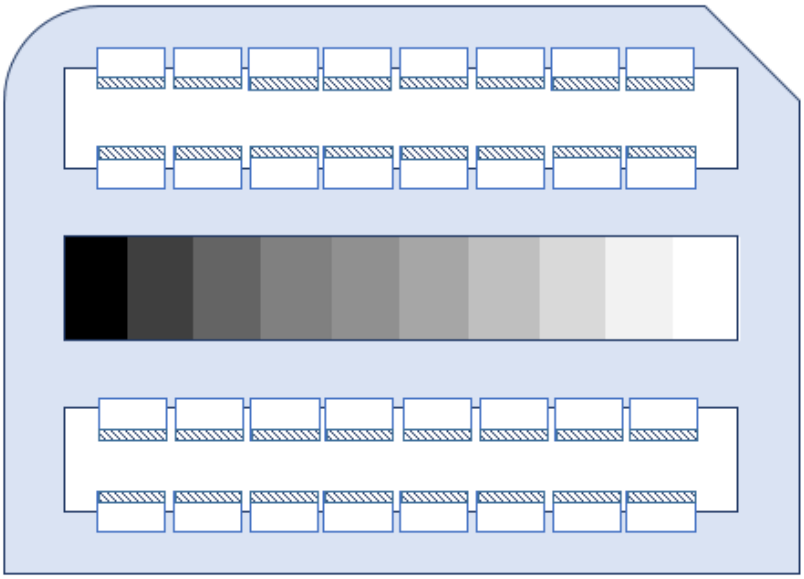

Figure 2.15: TMR Mounting Process. *Illustration of mounted transverse sections, with the enamel edge positioned over the windows. An aluminium step-wedge is mounted in the centre as a reference.*

An optical microscope with a CCD camera was used to calibrate the slide against the aluminium step-wedge and capture 4-5 images per section (magnification: 20x) using TMR 2000 software (Version 2.0.27.16; Inspektor Research Systems BV., Amsterdam). A correlation of no less than 0.9992 and an inhomogeneity value of below 1.5% were required to ensure that the radiograph was of adequate quality. TMR 2006 (Version 3.0.0.15; Inspektor Research Systems BV., Amsterdam) was then used to quantitatively determine the integrated mineral loss (ΔZ) and lesion depth (LD) and

average mineral loss (R, calculated as ΔZ/LD). In brief, this process involves selecting the area of interest, in addition to an area of underlying sound enamel and an area of the background as a “zero” reference. The software then uses the calibrated step-wedge to reconstruct the mineral content as a function of depth for the sample area. This process is illustrated below in Figure 2.16.

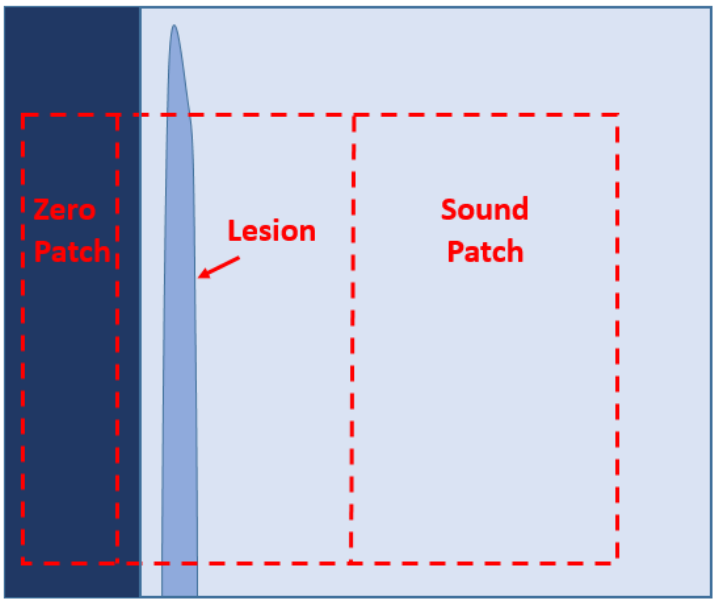

Figure 2.16: TMR Analysis Process. *Basic illustration of the TMR analysis process. Following calibration of the step-wedge and image capture, an area of interest is selected containing both an area of sound enamel and a “zero patch” outside of the section. This is used by the software to calculate lesion parameters of interest.*

2.11 Surface Microhardness (SMH)

Surface microhardness measurements were taken of baseline and pH-cycled enamel using a Vickers indenter with a load of 200g and a dwelling time of 15s (Buehler Micromet, Buelher, Illinois, USA). In brief the sample of interest was placed on the stage and the microscope used to focus on the surface. An indentation was then made on the surface with the Vickers indenter. The microscope was used to define the

outline of the indented area to allow the calculation of a Vickers hardness value. Six measurements were taken from each area of interest (Figure 2.17).

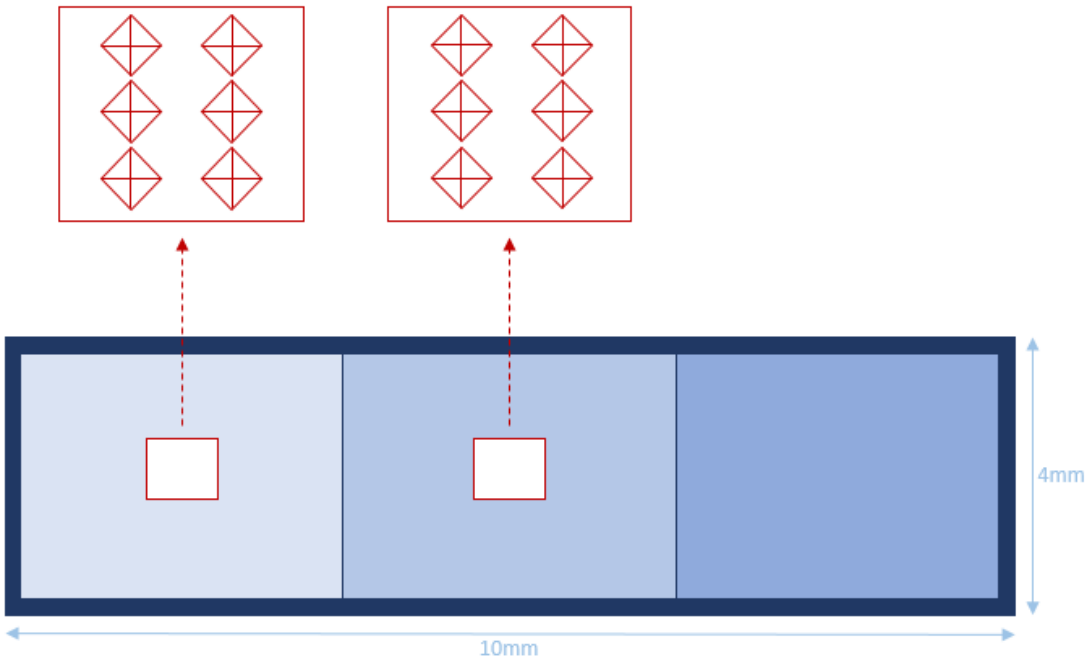

Figure 2.17: Schematic of SMH Measurement Process. *6 measurements were taken from each baseline and pH-Cycled area using a Vickers indenter*

2.12 Scanning Electron Microscopy (SEM)

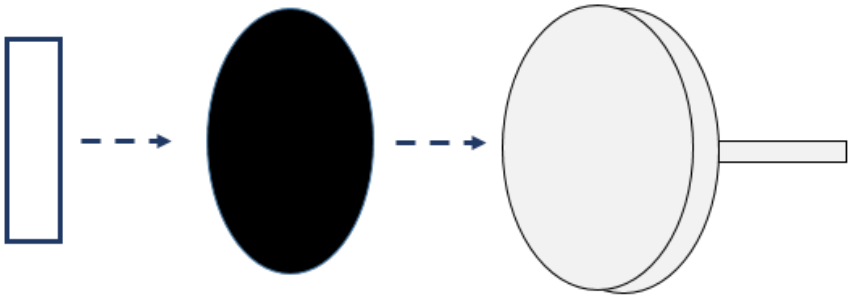

Figure 2.18: SEM Mounting Process. *Schematic of the preparation process for SEM analysis. Blocks are mounted onto metal holders using carbon discs.*

For the purposes of this work, samples were required for further analysis following SEM imaging. Therefore, a desktop SEM system compatible with non-coated samples was used (Phenom Pro, Phenom-World B.V. Netherlands). Samples were dried and

cleaned using acetone. Carbon discs were then used to mount each sample onto a metal holder, taking care to ensure it was secure (Figure 2.18). Mounted samples were cleaned using compressed air and mounted onto the desktop SEM sample holder for analysis using a desktop SEM system. Accompanying software was used for both image capture and EDX analysis (EID software package, Phenom-World B.V. Netherlands).

2.13 Electron Microprobe Analysis (EPMA)

One randomly selected section from each group was sent to Dr S. Kearns (University of Bristol), for electron microprobe analysis EMPA. The calcium, phosphorous, fluorine and zinc content of the enamel were measured to a depth of 100µm from the enamel surface.

2.14 Statistical Analysis

Data analysis was conducted using SPSS Statistics 22 (IBM UK Ltd., Portsmouth, UK) and Microsoft Excel 2013 (Microsoft Ltd., Berkshire, UK). Analysis was initially conducted un-blinded, but due to risk of bias blinding was introduced in later chapters (6 & 7). Means and standard error were calculated using Microsoft Excel 2013. Standard deviation measurements and Unpaired T-Test calculations were conducted using SPSS. Due to the increased introduction of error from repeated T-test calculations it is noted that an alternative approach, such as analysis of variance (ANOVA) should be applied to future work. For statistical tests a 95% confidence interval was applied ($P \leq 0.05$).

Chapter Three: Development of an *in vitro* pH-cycling Model of PEM

3.1. Background

3.1.1 Importance of Developing a PEM Model

One of the key barriers to the study of PEM highlighted upon review of the literature was the absence of a readily established investigation technique appropriate for the study of the PEM process itself, as many existing papers focus instead on describing the overall effects, such as decreased porosity and increased hardness (Kataoka *et. al.* 2007, Cardoso *et. al.* 2009). A large proportion of the supporting literature investigating PEM directly has been conducted either *in vivo* using a combination of animal models and non-invasive techniques such as electrical resistance (Schulte *et. al.* 1999, Kataoka *et. al.* 2007), or *in vitro* using extracted, sound, newly erupted molars (Palti *et. al.* 2008). For the purpose of this work, an *in vivo* approach was deemed unsuitable as, whilst it would provide an all-round more representative picture of the actual oral environment, they limit the use of destructive or invasive techniques and offer little ability to vary and control said environment. In a similar vein, whilst conducting *in vitro* studies on sound, newly-erupted extracted molars is in theory the perfect approach, the reality is they are not widely available. It is therefore crucial that the first stage of any investigation into PEM is to develop a suitable *in vitro* model with which it can be studied, making use of techniques and resources available.

3.1.2 Relevance of the Composition of Plaque-Fluid

Dental plaque is composed of 80-90% water, with the remaining dry weight made up of bacteria (70%) and a mixture of polysaccharides and glycoproteins (30%) (Marsh and Bradshaw 1995). Plaque-fluid (PF) can therefore be defined as the aqueous phase, of

which the composition is crucial to any chemical interactions at the enamel surface, due to its action as an ion reservoir. As discussed previously (Section 1.3), the degree of saturation of the PF with regards to Ca and P in relation to the enamel determines whether de- or remineralisation takes place at the enamel surface. The higher the DS in relation to enamel, the lower the probability that demineralisation will occur (Margolis and Moreno 1992). Furthermore, the availability of fluoride within the plaque fluid also affects both bacterial activity and, through its ability to diffuse into the enamel with bacteria-produced acid, the surface crystal structure (Featherstone 1999). Based on this principle, Margolis (1990), highlighted the importance of assessing the DS of ions within the plaque-fluid when assessing cariogenicity for research purposes. With this in mind, it is important that any attempt to model the complex *in vivo* chemical conditions required for PEM, cannot ignore the importance of PF composition. The current work therefore aimed to ensure that pH-cycling conditions were designed to be plaque-fluid relevant. Whilst several studies have categorised the contents of the PF (Moreno and Margolis 1988, Margolis and Moreno 1992, Gao *et. al.* 2001), the values obtained by Vogel *et. al.* (2000) were used for the purposes of this work.

3.2 Aims

This initial experiment aimed to determine whether exposure to plaque-fluid-relevant pH-cycling conditions could serve to reduce susceptibility of polished bovine enamel to a subsequent acid challenge. It also aimed to investigate the effect of a demineralisation pre-treatment on any such effect along with the length of exposure to the pH-cycling regime. In turn, this study aimed to determine whether this type pf pH-cycling regime could be used to form a suitable basis for the development of an *in vitro* bovine enamel model of post-eruptive maturation.

3.3 Materials and Methods

3.3.1 Outline of Proposed PEM Model

For the current chapter, the three-stage model outlined in the previous chapter (Section 2.1) was applied. Blocks were subjected to 0, 1 or 3h pre-treatment and a pH-cycling regime of either 0, 2, 4, 6, 8, 10, or 12 days. Assessment of the model was carried out in terms of a subsequent demineralisation, the extent of which was measured using QLF-D, MSI and TMR. In addition, NCSP analysis was conducted on all blocks. A summary of the current model protocol is illustrated in Figure 3.1 below.

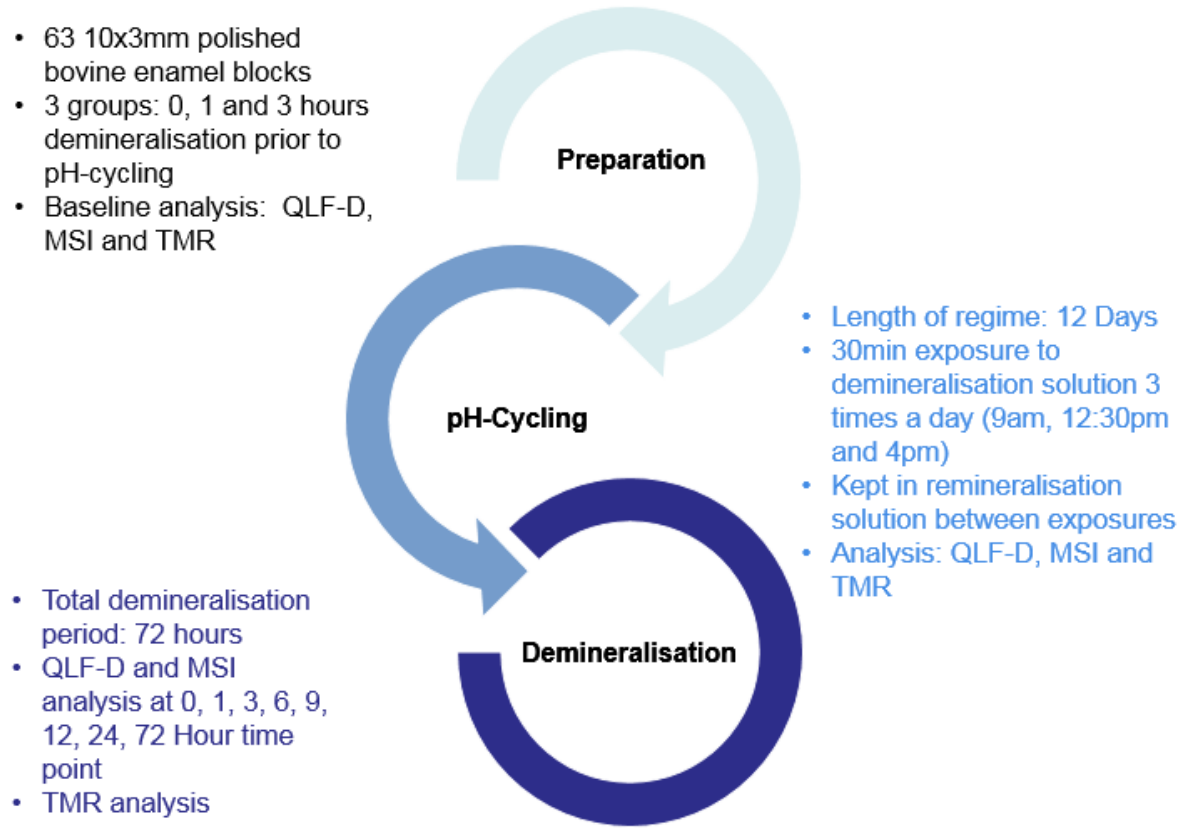

Figure 3.1: Summary of Current Model Protocol. *Outline of the current experimental procedure, broken down into the three stages of the proposed model.*

3.3.2 pH-Cycling Regime Specifics

The previously-described pH-Cycling system designed for net remineralisation was used in order to expose the blocks to an acid challenge without creating detectable lesions (Section 2.5). Blocks were subjected to a three 30min demineralisation-per-day pH-cycling regime for a total of 0, 2, 4, 6, 8, or 12 days. A schematic of the pH-cycling process is presented below (Figure 3.2).

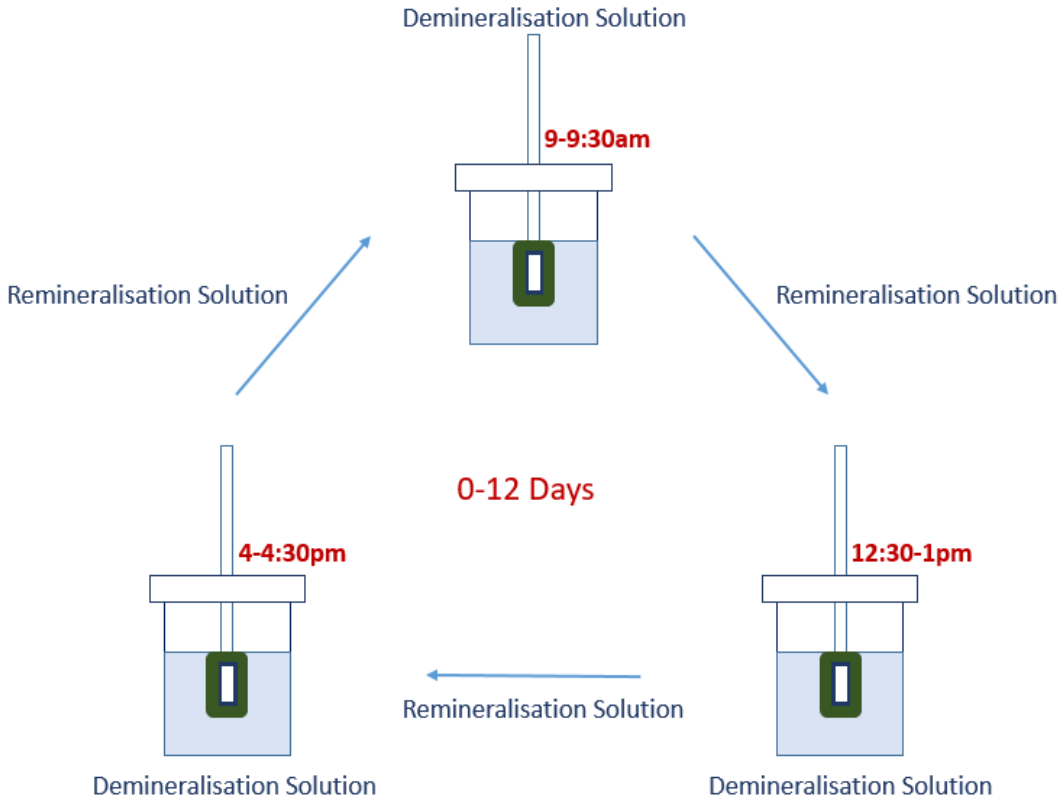

Figure 3.2: Outline of pH-cycling Regime. *Schematic of daily pH-cycling protocol observed for 0 to 12 days. Blocks are kept in remineralisation solution with the exception of three 30min demineralisation periods per day.*

3.3.3 Analysis Specifics

NCSP and TMR analysis was conducted for baseline, pH-cycled and demineralised enamel. QLF-D and MSI images were captured and analysed at baseline, following exposure to pH-cycling and at 0, 1, 3, 6, 9, 12, 24, 48 and 72h time points during the subsequent demineralisation challenge.

3.4 Results

3.4.1 Demineralisation Solution Test

Results from the PF demineralisation solution test demonstrated no detectable visual or quantitative changes in fluorescence loss and therefore mineral from baseline were observed. MSI images taken at baseline and following 72h solution exposure are presented in Figure 3.3 below.

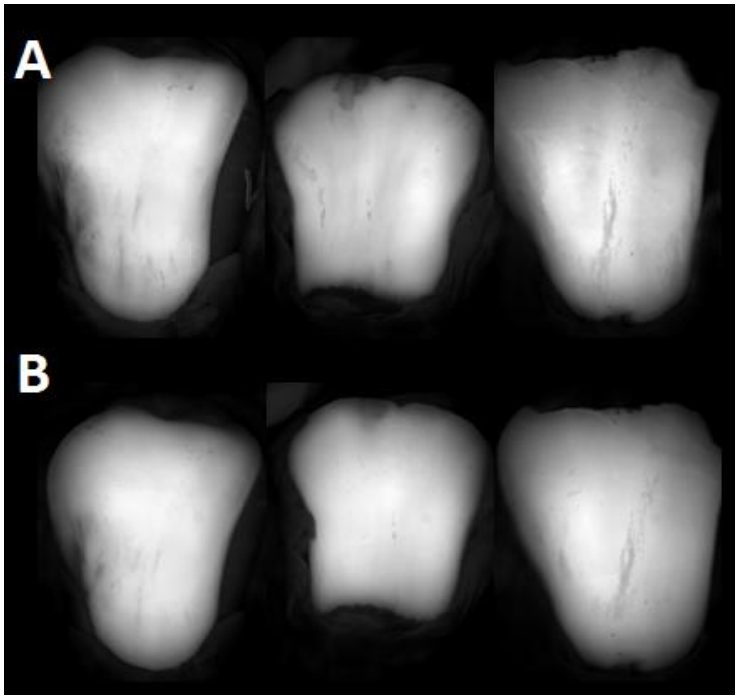

Figure 3.3: PF Demineralisation Solution Test Using MSI. *MSI images at baseline (A) and following 72h exposure to a plaque-fluid-relevant demineralisation solution (B).*

.

3.4.2 Analysis of pH-cycled Enamel

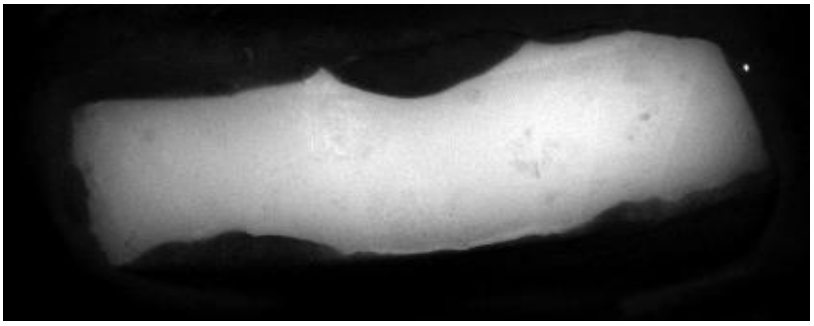

Figure 3.4: Change in Fluorescence Following 12 Days pH-cycling. *MSI image of bovine enamel block following exposure to a 12-day pH-cycling regime.*

Following exposure to the pH-cycling regime, no difference between baseline sound enamel and cycled enamel could be determined by either fluorescence-based techniques (Figure 3.4) or TMR (Figure 3.5), even for enamel exposed to the full 12-day pH-cycling regime. The presence or absence of a demineralisation pre-treatment had no effect on this outcome.

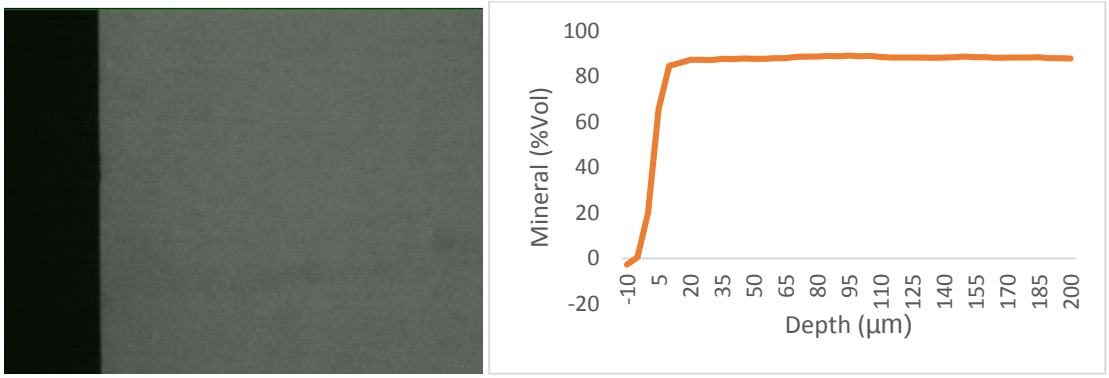

Figure 3.5: Change in Mineral Following 12 Days pH-cycling. *TMR Image and profile following 12-days exposure to pH-Cycling.*

3.4.3 Surface Roughness (Ra) of Enamel Following pH-cycling and Subsequent Demineralisation

Pre-Treatment		Sound ± SE	Cycled ± SE	Lesion ± SE
None	non cycled	2.66 ± 0.29	2.40 ± 0.20	1.99 ± 0.41
	pH-cycled	2.76 ± 0.61	2.65 ± 0.30	2.60 ± 0.08
1h	non cycled	2.30 ± 0.37	3.25 ± 0.91	3.75 ± 1.51
	pH-cycled	2.79 ± 0.22	2.46 ± 0.27	2.14 ± 0.42
3h	non cycled	1.78 ± 0.75	2.11 ± 1.30	2.47 ± 1.74
	pH-cycled	2.74 ± 1.24	3.29 ± 1.80	2.76 ± 1.06

Table 3.1: Effect of pH-cycling on Surface Roughness (Ra). *NCSP data representing surface roughness (Ra) of baseline (sound), pH-cycled and demineralised (Lesion) enamel for both cycled enamel and non-cycled controls subjected to 0, 1 or 3h demineralisation pre-treatment. Data presented along with the standard error of the mean. n=3.*

Production of non-contact surface profilometry (NCSP) scans proved difficult, due to the large size of the scan area and natural curvature of the enamel surface, however scans of the entire experimental window were achieved for each experimental block. Surface roughness (Ra) values obtained via NCSP for sound, pH-cycled and 72h demineralised enamel are presented in Table 3.1. NCSP found no relationship between exposure to 12d pH-cycling and surface roughness (Ra) of sound, cycled and demineralised enamel. Additionally, exposure to a demineralisation pre-treatment demonstrated no effect on Ra (Figure 3.6).

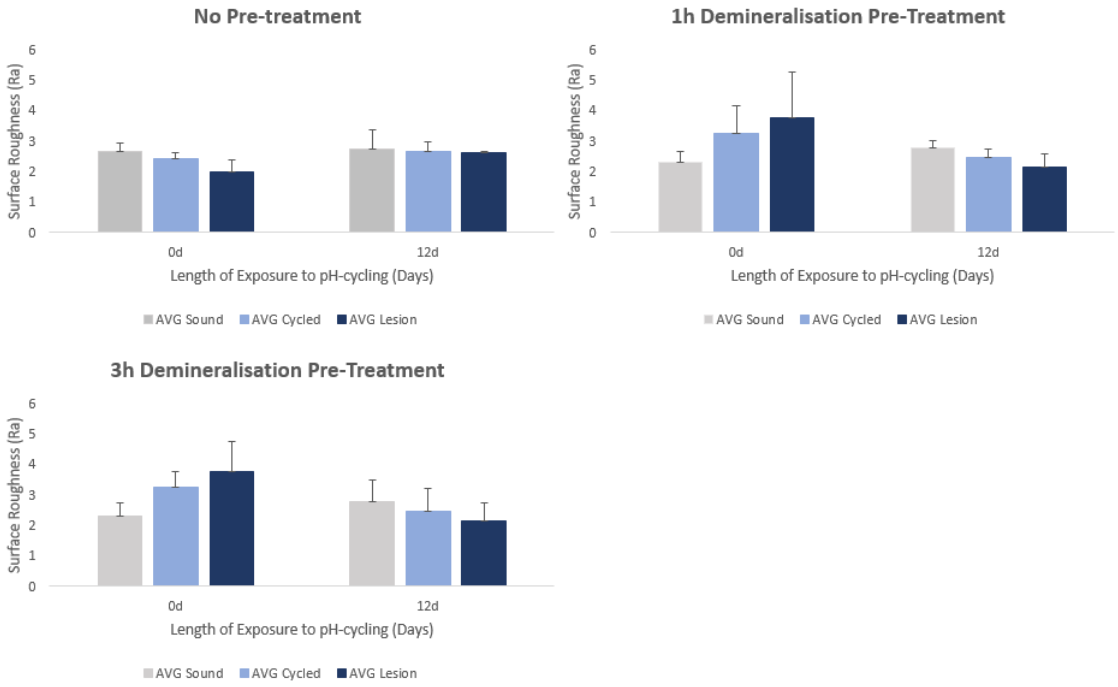

Figure 3.6: Graphical Representation of Changes in Ra. *Average (AVG) surface roughness (Ra) values for Sound, pH-cycled and demineralised enamel as measured using NCSP. Blocks were subjected to 0, 1 or 3h demineralisation pre-treatment. Error bars represent the standard error of the mean. n=3.*

3.4.4 Assessment of Demineralisation Using Quantitative Light Induced Fluorescence (QLF-D)

Total Fluorescence Loss: 0 Vs 12d Exposure

Fluorescence loss values (ΔF) measured using QLF-D for both enamel exposed to the full 12d pH-cycling regime and non-cycled controls are presented in Table 3.2 above. When the total fluorescence loss is compared, a significant decrease was observed for blocks exposed to a 1 or 3-hour demineralisation pre-treatment (P=0.042 and 0.036 respectively). For blocks not subjected to a demineralisation pre-treatment, a non-significant increase was observed for 12d pH-cycled enamel when considered against uncycled counterparts (Figure 3.7).

	0 Days ΔF ± SE	12 Days ΔF ± SE
None	6.53 ± 0.78	6.80 ± 0.94
1h	7.60 ± 0.31	1.90 ± 1.55
3h	7.13 ± 0.17	1.73 ± 1.42

Table 3.2: Total Fluorescence Loss 0 vs 12 Days Exposure to pH-cycling. *QLF-D data for demineralised bovine enamel blocks previously subjected to 0 or 12 days exposure to pH-cycling. Blocks were pre-treated for 0, 1 or 3h in demineralisation solution. Data is presented alongside the SE of the mean. n=3.*

Total Fluorescence Loss at Varying Lengths of pH-cycling Exposure

Images captured using the QLF-D system following 72h exposure to a demineralisation challenge are displayed below (Figure 3.8). When images of lesions produced in the no pre-treatment group are examined visually, no relationship between length of exposure to pH-cycling and lesion appearance can be established.

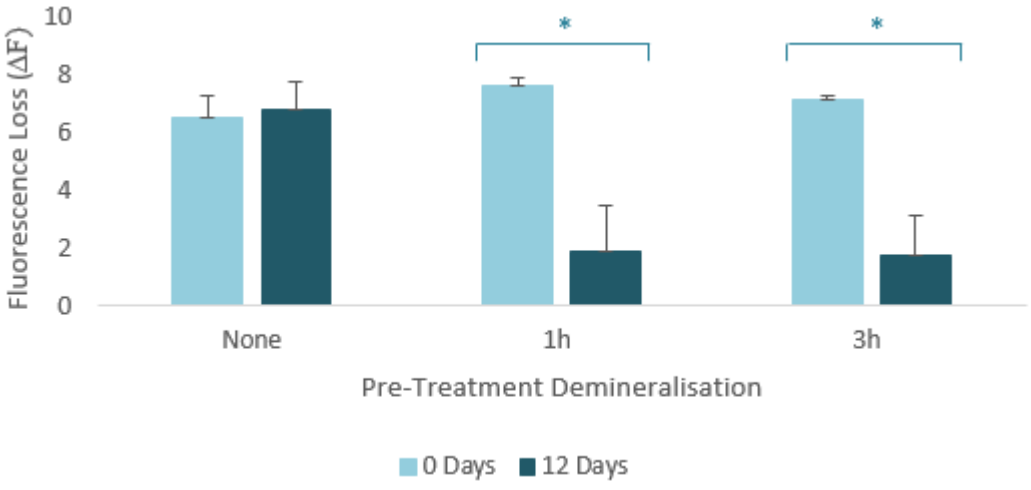

Figure 3.7: Fluorescence loss (ΔF) values following 72h demineralisation as measured using QLF-D. *Data comparing non-cycled blocks to those exposed to the full 12-day regime for enamel pre-treated for 0, 1 or 3h in demineralisation solution. Error Bars represent SE of the mean. *= P<0.05. n=3.*

In contrast, when lesions induced in enamel subjected to a 1h demineralisation pre-treatment are examined visually by QLF-D, lesions created in enamel subjected to 10 or 12 days pH-cycling appear lighter and more uneven that non-cycled counterparts. No discernible differences were observed for enamel subjected to shorter regimes and, in some cases (2 and 8 days), lesions appeared darker than those not subjected to a cycling regime.

Interestingly, when the same examination is conducted for enamel subjected to a 3h demineralisation pre-treatment, an inverse relationship between pH-cycling regime length fluorescence loss can be seen. In visual-terms, lesions created in enamel exposed to pH-cycling, present as lighter and less even in appearance than equivalent non-cycled controls.

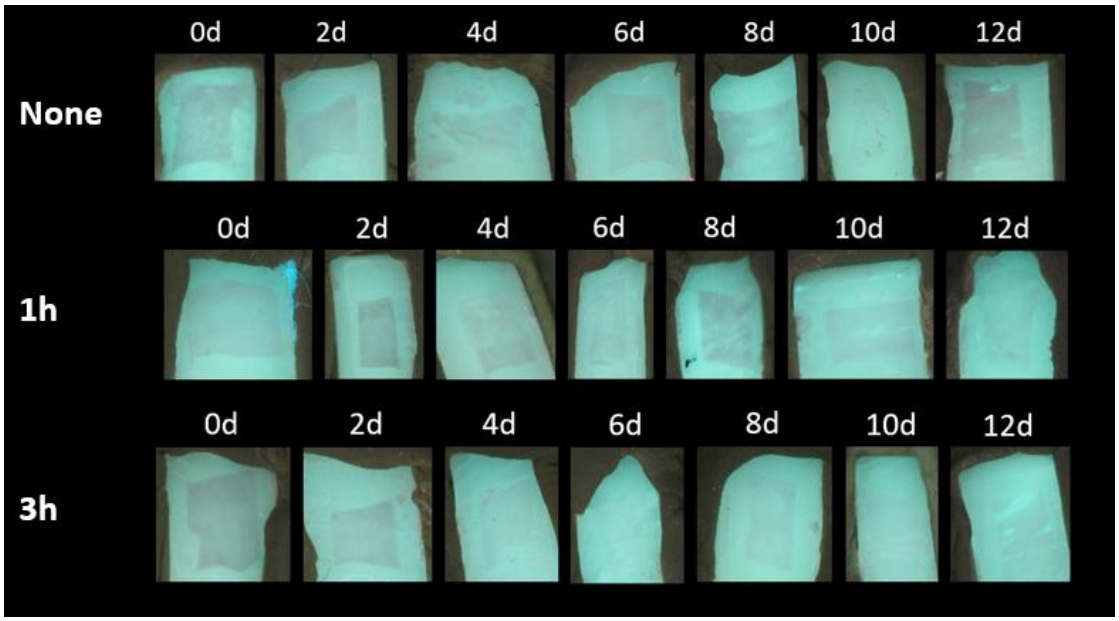

Figure 3.8: ***QLF-D Images Following 72h Demineralisation for Differing Lengths of pH-cycling Exposure.*** *QLF-D images visually comparing non-cycled enamel to that subjected to 0, 2, 4, 6, 8, 10, 12d pH-cycling for enamel pre-treated with 0, 1 or 3h exposure to demineralisation.*

The quantitative fluorescence loss values (ΔF) obtained for lesions created following a 72h demineralisation are presented in Table 3.3. For blocks not exposed to a demineralisation pre-treatment, no differences were observed between pH-cycled

blocks and non-cycled controls. In comparison a decrease in fluorescence loss was observed for all pH-cycled blocks exposed to a 1h demineralisation pre-treatment when compared to non-cycled controls. This observed decrease was significant for blocks pH-cycled for the full 12 days only (P=0.042).

Length of pH-cycling	No Demin ΔF ± SE	1h ΔF ± SE	3h ΔF ± SE
0 Days	6.53 ± 0.78	7.60 ± 0.31	7.13 ± 0.17
2 Days	4.23 ± 1.74	7.47 ± 0.38	8.10 ± 0.34
4 Days	1.90 ± 1.55	3.97 ± 1.63	4.40 ± 1.81
6 Days	6.07 ± 0.75	5.43 ± 2.59	3.87 ± 1.59
8 Days	6.47 ± 0.66	7.43 ± 1.05	5.70 ± 0.22
10 Days	5.10 ± 2.32	5.00 ± 2.33	4.50 ± 1.84
12 Days	6.80 ± 0.94	1.90 ± 1.55	1.73 ± 1.42

Table 3.3: ΔF following 72h demineralisation for enamel exposed to 0, 2, 4, 6, 8, 10 or 12 days pH-cycling. *Fluorescence loss values measured using QLF-D for 0, 1 or 3 demineralisation pre-treated enamel exposed to 0-12d pH-cycling following a subsequent 72h demineralisation challenge. Data is presented with the SE of the mean. n=3.*

For blocks subjected to a 3h demineralisation pre-treatment, a decrease in fluorescence loss was observed for all pH-cycled blocks when considered against non-cycled controls, with the exception of those subjected to a 2-day pH-cycling regime. Observed decreases were found to be significant for blocks subjected to 8 and 12 days of pH-cycling (P=0.013 and 0.036 respectively). However, a clear linear relationship between length of pH-cycling exposure and subsequent changes in fluorescence following demineralisation could not be established (Figure 3.9).

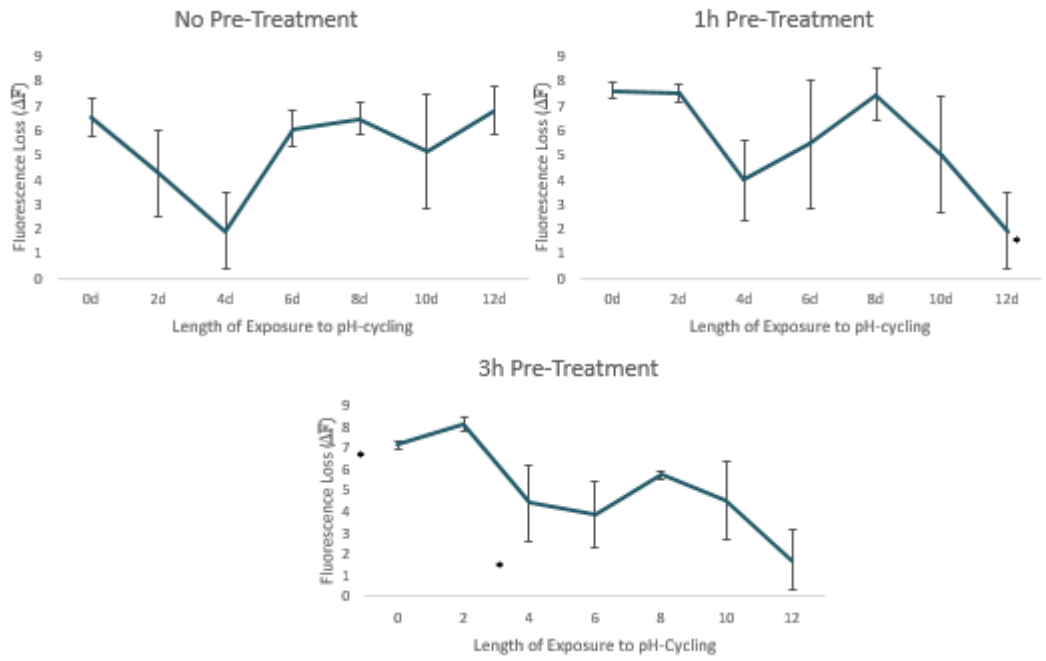

Figure 3.9: Graphical Representation of ΔF in relation to pH-cycling Exposure Length. *QLF-D fluorescence loss values for 0, 1 and 3h pre-treated enamel subjected to 0-12d pH-cycling and a subsequent 72h demineralisation. Error Bars Represent the SE of the mean. * = P<0.05. n=3.*

Progress of Fluorescence Loss over 72h Demineralisation

No Pre-Treatment:

When the progress of the lesions over the 72h demineralisation challenge is observed visually for enamel blocks in the no pre-treatment group, no patterns can be observed between the appearance of the lesions and the length of exposure of the blocks to pH-cycling. Additionally, no differences were observed for the initial time point at which lesions are first visible with relation to pH-cycling exposure.

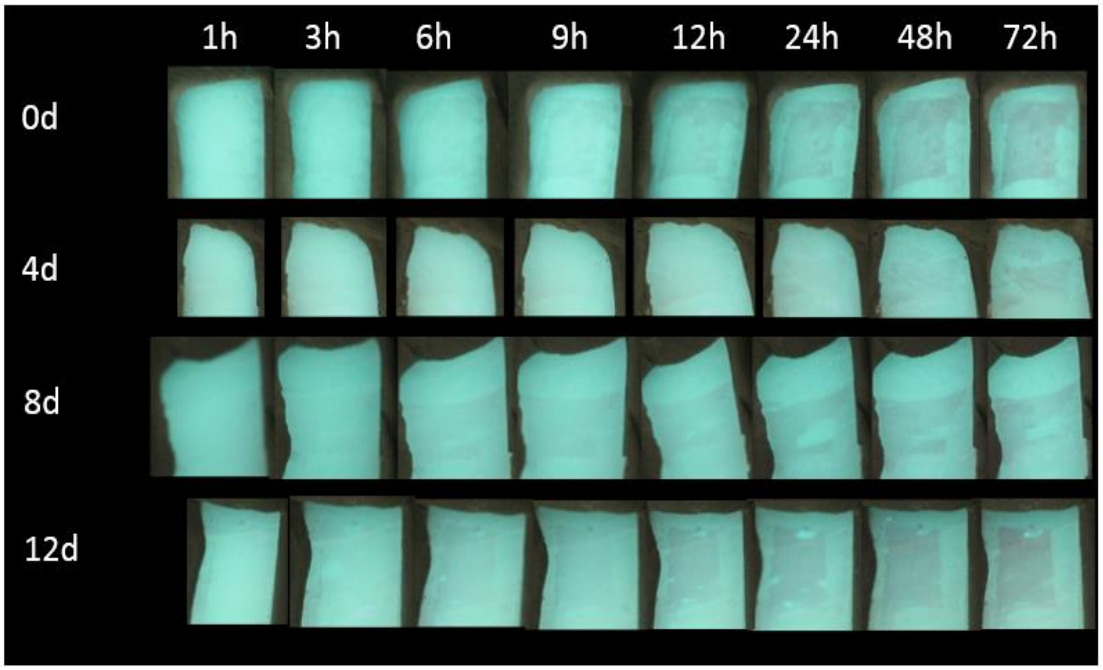

Figure 3.10: Visual QLF-D Lesion Progression in Non-Pre-Treated Enamel subjected to varying pH-cycling Regime Lengths. *Images captured using QLF-D demonstrating longitudinal lesion formation in non-pre-treated enamel subjected to varying pH-cycling exposures and a subsequent 72h demineralisation.*

When the numerical fluorescence loss (ΔF) values are considered, lesion progression was detected earlier for non-cycled enamel (9h) than that exposed to a pH-cycling regime. Additionally, enamel exposed to 4d pH-cycling demonstrated significantly lower ΔF values at 24 and 48h demineralisation than non-cycled controls (P=0.001 and 0.035 respectively). However, beyond that, no relationship between the length of pH-cycling regime the enamel was exposed to and the level of fluorescence loss could be established.

	n	0h ± SE	1h ± SE	3h ± SE	6h ± SE	9h ± SE	12h ± SE	24h ± SE	48h ± SE	72h ± SE
0d	3	0.00 ± 0.00	0.00 ± 0.00	0.00 ± 0.00	0.00 ± 0.00	1.77 ± 1.77	2.03 ± 2.03	4.77 ± 2.73	5.65 ± 0.88	6.53 ± 0.78
4d	3	0.00 ± 0.00	0.00 ± 0.00	0.00 ± 0.00	0.00 ± 0.00	0.00 ± 0.00	0.00 ± 0.00	0.00 ± 0.00	1.80 ± 2.20	1.90 ± 1.55
8d	3	0.00 ± 0.00	0.00 ± 0.00	0.00 ± 0.00	0.00 ± 0.00	0.00 ± 0.00	4.00 ± 1.94	4.40 ± 2.71	4.73 ± 2.91	6.47 ± 0.66
12d	3	0.00 ± 0.00	0.00 ± 0.00	0.00 ± 0.00	0.00 ± 0.00	0.00 ± 0.00	0.00 ± 0.00	2.03 ± 2.49	2.10 ± 2.57	6.80 ± 0.94

Table 3.4: Progression of Fluorescence Loss over 72h for non-pre-treated enamel subjected to 0-12d pH-cycling. *QLF-D-measured ΔF values at 0, 1, 3, 6, 9, 12, 24, 48 and 72h demineralisation time points for non-pre-treated enamel exposed to varying pH-cycling regime lengths. Data is presented with SE of the mean. n=3.*

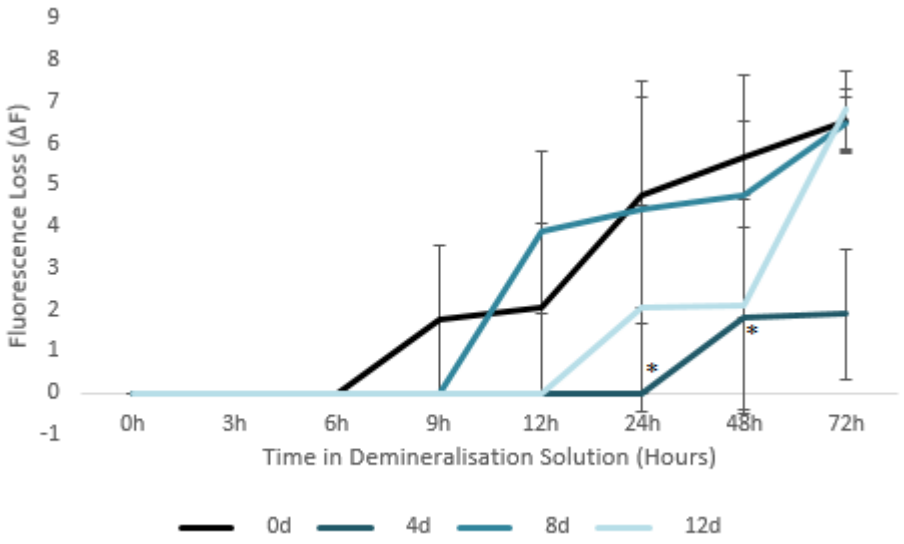

Figure 3.11: Graphical Representation of Demineralisation Progression over 72h for Varying pH-cycling Regime Lengths. *QLF-D data expressing ΔF changes over 72h exposure to demineralisation solution for non-pre-treated enamel subjected to 0-12d pH-cycling. Error Bars Represent the SE of the mean. *=P<0.05. n=3.*

1h Pre-treated Enamel:

When visual examination is conducted for enamel blocks exposed to a 1h demineralisation pre-treatment a similar situation to that demonstrated for the no treatment group was observed, as no clear relationship between the appearance of lesions exposed to differing extents of pH-cycling at equivalent time points is seen. QLF-D images are displayed in Figure 3.12 below.

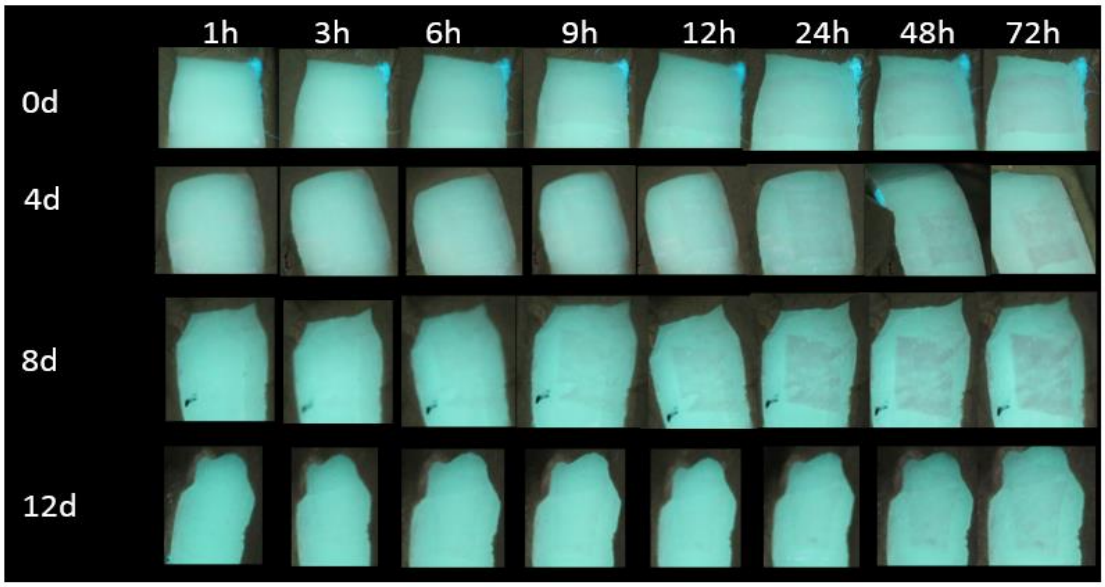

Figure 3.12: Visual QLF-D Lesion Progression in 1h Pre-treated Enamel subjected to varying pH-cycling Regime Lengths. *Images captured using QLF-D demonstrating longitudinal lesion formation in 1h pre-treated enamel subjected to varying pH-cycling exposures and a subsequent 72h demineralisation.*

When the numerical fluorescence loss values are taken into consideration (Table 3.5), enamel exposed to 0 or 8d pH-cycling behaved very similarly. In contrast, exposure to 4 or 12d pH-cycling resulted in lower fluorescence loss values at all comparable time points. Additionally, the lesions for these time points were first detected later than for those exposed to 0 or 8d pH-cycling. This is represented graphically in Figure 3.13 below.

	n	0h ± SE	1h ± SE	3h ± SE	6h ± SE	9h ± SE	12h ± SE	24h ± SE	48h ± SE	72h ± SE
0d	3	0.00 ± 0.00	0.00 ± 0.00	0.00 ± 0.00	0.00 ± 0.00	0.00 ± 0.00	0.00 ± 0.00	1.83 ± 2.25	6.20 ± 0.07	7.60 ± 0.31
4d	3	0.00 ± 0.00	0.00 ± 0.00	0.00 ± 0.00	0.00 ± 0.00	0.00 ± 0.00	0.00 ± 0.00	0.00 ± 0.00	1.73 ± 2.12	3.97 ± 1.63
8d	3	0.00 ± 0.00	0.00 ± 0.00	0.00 ± 0.00	0.00 ± 0.00	0.00 ± 0.00	0.00 ± 0.00	2.17 ± 2.65	6.10 ± 0.68	7.43 ± 1.05
12d	3	0.00 ± 0.00	0.00 ± 0.00	0.00 ± 0.00	0.00 ± 0.00	0.00 ± 0.00	0.00 ± 0.00	0.00 ± 0.00	0.95 ± 0.95	1.90 ± 1.55

Table 3.5: Progression of Fluorescence Loss over 72h for 1h pre-treated enamel subjected to 0-12d pH-cycling. *QLF-D-measured ΔF values at 0, 1, 3, 6, 9, 12, 24, 48 and 72h demineralisation time points for 1h pre-treated enamel exposed to varying pH-cycling regime lengths. Data is presented with SE of the mean. n=3.*

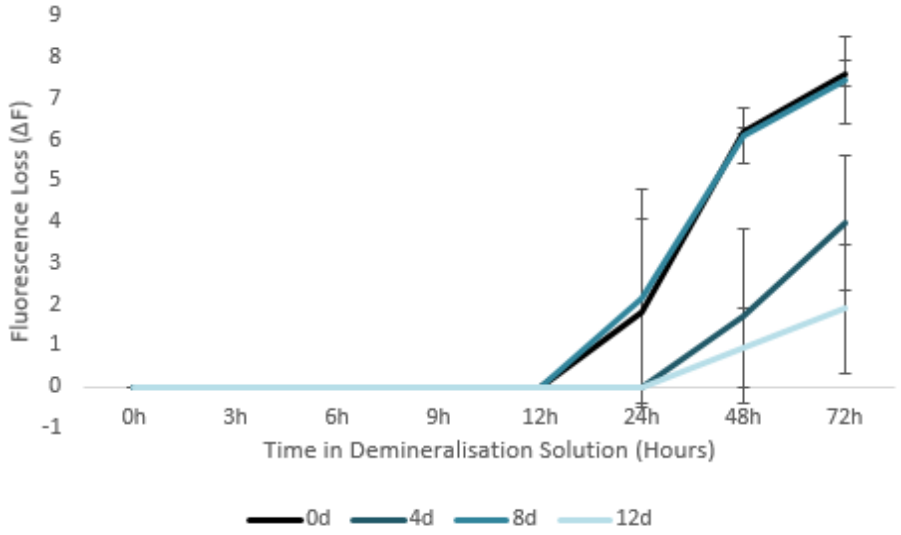

Figure 3.13: Graphical Representation of Demineralisation Progression over 72h for Varying pH-cycling Regime Lengths. *QLF-D data expressing ΔF changes over 72h exposure to demineralisation solution for 1h pre-treated enamel subjected to 0-12d pH-cycling. Error Bars Represent the SE of the mean. n=3.*

3h Pre-treated Enamel:

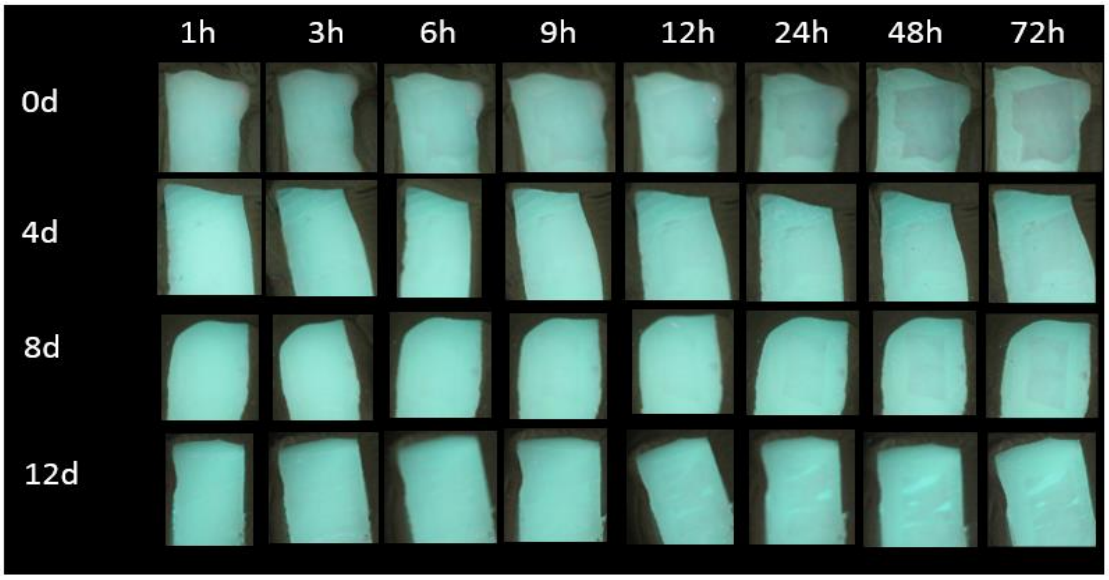

Figure 3.14: Visual QLF-D Lesion Progression in 3h Pre-treated Enamel subjected to varying pH-cycling Regime Lengths. *Images captured using QLF-D demonstrating longitudinal lesion formation in 3h pre-treated enamel subjected to varying pH-cycling exposures and a subsequent 72h demineralisation.*

Unlike the previous experimental groups, when blocks subjected to a 3h demineralisation pre-treatment are examined visually (Figure 3.14), a difference can be observed between non-cycled enamel and that subjected to a pH-cycling regime. Enamel exposed to pH-cycling regimes of all lengths demonstrated lesions lighter and less even in appearance than non-cycled controls at comparable time points. Additionally, lesions were visually detectable after less exposure to the acid solution for non-cycled enamel (9-12h), than that exposed to pH-cycling (6h).

Reported quantitative fluorescence loss values reflect the observations noted visually (Table 3.6), with first detection occurring at an earlier time point for non-cycled enamel blocks (24h vs 48/72h). Additionally, fluorescence loss values were lower for all lesions created in blocks exposed to a pH-cycling regime, when considered against non-cycled controls. This is presented graphically in Figure 3.15.

	n	0h ± SE	1h ± SE	3h ± SE	6h ± SE	9h ± SE	12h ± SE	24h ± SE	48h ± SE	72h ± SE
0d	3	0.00 ± 0.00	0.00 ± 0.00	0.00 ± 0.00	0.00 ± 0.00	0.00 ± 0.00	0.00 ± 0.00	3.93 ± 2.41	6.47 ± 0.22	7.13 ± 0.17
4d	3	0.00 ± 0.00	0.00 ± 0.00	0.00 ± 0.00	0.00 ± 0.00	0.00 ± 0.00	0.00 ± 0.00	0.00 ± 0.00	1.70 ± 2.08	4.40 ± 1.81
8d	3	0.00 ± 0.00	0.00 ± 0.00	0.00 ± 0.00	0.00 ± 0.00	0.00 ± 0.00	0.00 ± 0.00	0.00 ± 0.00	0.00 ± 0.00	5.70 ± 0.22
12d	3	0.00 ± 0.00	0.00 ± 0.00	0.00 ± 0.00	0.00 ± 0.00	0.00 ± 0.00	0.00 ± 0.00	0.00 ± 0.00	0.00 ± 0.00	1.73 ± 1.42

Table 3.6: Progression of Fluorescence Loss over 72h for 3h pre-treated enamel subjected to 0-12d pH-cycling. *QLF-D-measured ΔF values at 0, 1, 3, 6, 9, 12, 24, 48 and 72h demineralisation time points for 3h pre-treated enamel exposed to varying pH-cycling regime lengths. Data is presented with SE of the mean. n=3.*

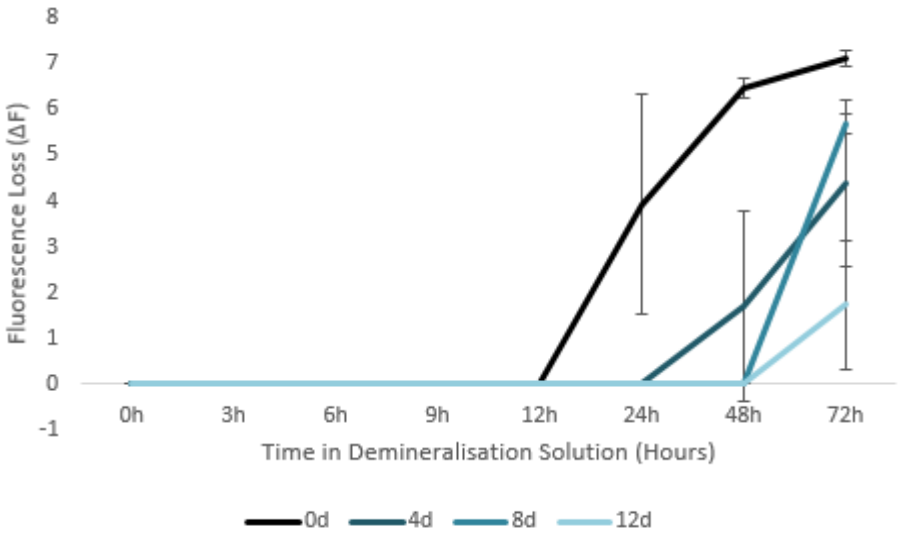

.

Figure 3.15: Graphical Representation of Demineralisation Progression over 72h for Varying pH-cycling Regime Lengths. *QLF-D data expressing ΔF changes over 72h exposure to demineralisation solution for 1h pre-treated enamel subjected to 0-12d pH-cycling. Error Bars Represent the SE of the mean. n=3.*

3.4.5 Multispectral Imaging (MSI) Analysis of Created Lesions

Total Fluorescence Loss: 0 Vs 12d pH-cycling Exposure

	0 Days ΔZ ± SE	12 Days ΔZ ± SE
None	13.00 ± 1.25	7.43 ± 1.86
1h	12.03 ± 1.39	6.50 ± 0.21
3h	9.73 ± 1.00	2.63 ± 2.15

Table 3.7: Total Fluorescence Loss 0 vs 12 Days Exposure to pH-cycling. *MSI data for demineralised bovine enamel blocks previously subjected to 0 or 12 days exposure to pH-cycling. Blocks were pre-treated for 0, 1 or 3h in demineralisation solution n=3.*

For lesions imaged using the MSI system, total fluorescence loss for non-cycled controls was higher than that for 12-day pH-cycled counterparts (Table 3.7). When analysed statistically, only the difference observed for blocks exposed to a 1h demineralisation pre-treatment was significant (p=0.032) (Figure 3.16).

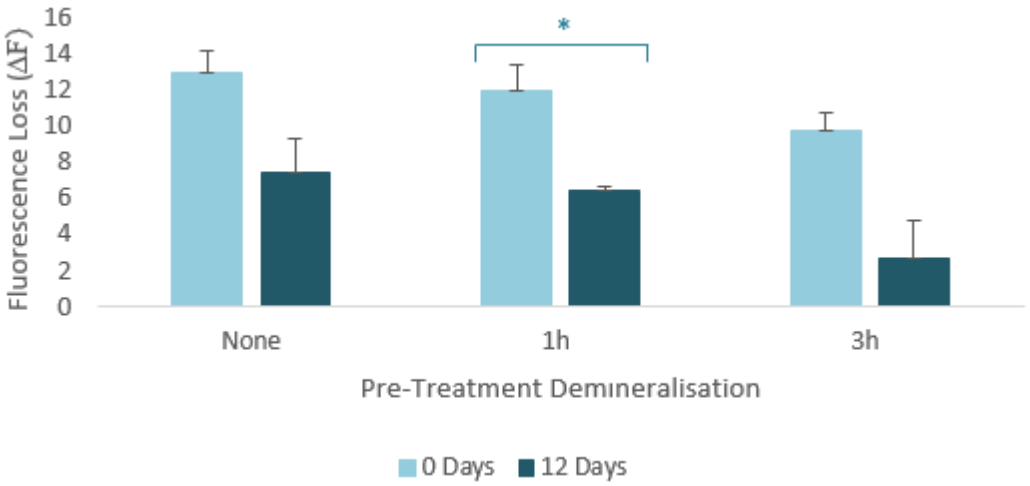

Figure 3.16: Fluorescence loss (ΔF) values following 72h demineralisation as measured using MSI. *Data comparing non-cycled blocks to those exposed to the full 12-day regime for enamel pre-treated for 0, 1 or 3h in demineralisation solution. Error Bars represent SE of the mean. *= P<0.05. n=3.*

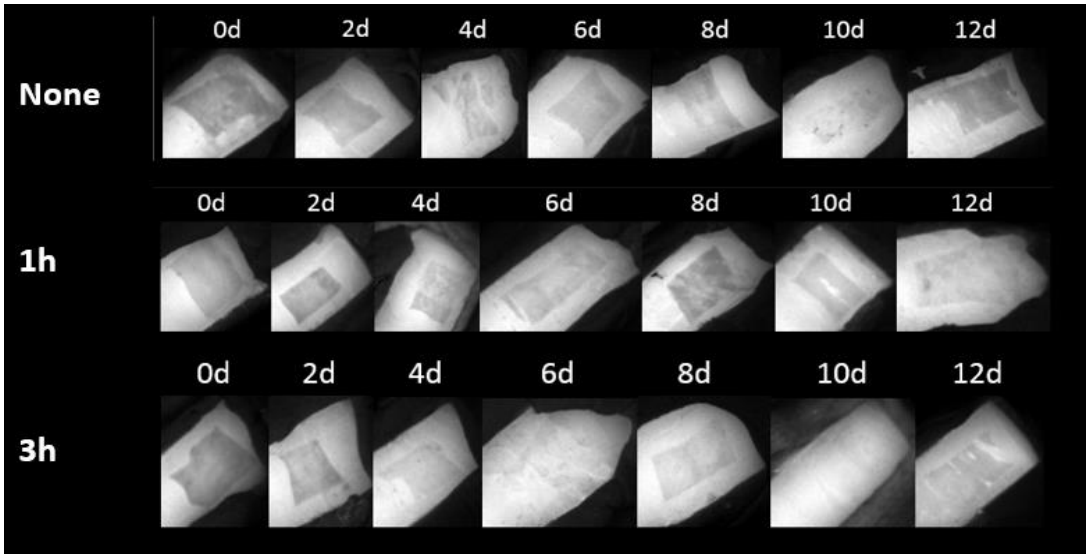

Figure 3.17: ***MSI Images Following 72h Demineralisation for Differing Lengths of pH-cycling Exposure.*** *MSI images visually comparing non-cycled enamel to that subjected to 0, 2, 4, 6, 8, 10, 12d pH-cycling for enamel pre-treated with 0, 1 or 3h demineralisation.*

Visual examination of images obtained using the MSI system for enamel in the no treatment group and that subjected to a 1h demineralisation pre-treatment showed a similar lack of relationship between lesion appearance and length of exposure to pH-cycling as reported above for those produced using QLF-D (Figure 3.17).

The MSI images obtained from 3h demineralisation pre-treated enamel also show consensus with those obtained via QLF-D when examined, demonstrating lesions that appear paler and less even for pH-cycled enamel when compared to non-cycled controls.

Length of pH-cycling	No Demin ΔF ± SE	1h ΔF ± SE	3h ΔF ± SE
0 Days	13.00 ± 1.25	12.03 ± 1.39	9.73 ± 1.00
2 Days	8.67 ± 2.26	11.33 ± 0.27	11.00 ± 0.47
4 Days	7.97 ± 0.98	8.93 ± 0.32	8.70 ± 0.57
6 Days	8.07 ± 1.28	10.50 ± 3.88	7.27 ± 0.98
8 Days	7.40 ± 2.28	10.50 ± 1.78	5.23 ± 2.17
10 Days	8.30 ± 7.94	10.40 ± 3.12	6.87 ± 2.82
12 Days	7.43 ± 1.86	6.50 ± 0.21	2.63 ± 2.15

Table 3.8: ΔF following 72h demineralisation for enamel exposed to 0, 2, 4, 6, 8, 10 or 12 days pH-cycling. *Fluorescence loss values measured using MSI for 0, 1 or 3 demineralisation pre-treated enamel exposed to 0-12d pH-cycling following a subsequent 72h demineralisation challenge. Data is presented with the SE of the mean. n=3.*

With the exception or 3h pre-treatment, 8 days, all blocks exposed to pH-cycling showed an observed decrease in fluorescence loss when considered in relation to non-cycled controls (Table 3.8). For the no pre-treatment group, this decrease was found to be significant in blocks exposed to 4, 6 and 8 days of pH-cycling (P=0.04, 0.05 and 0.022 respectively). For blocks subjected to a 1h demineralisation pre-treatment such observations were significant for blocks cycled for the total 12 days only (P=0.032). None of the observed decreases for 3h pre-treated blocks were found to be significant when analysed statistically (Figure 3.18).

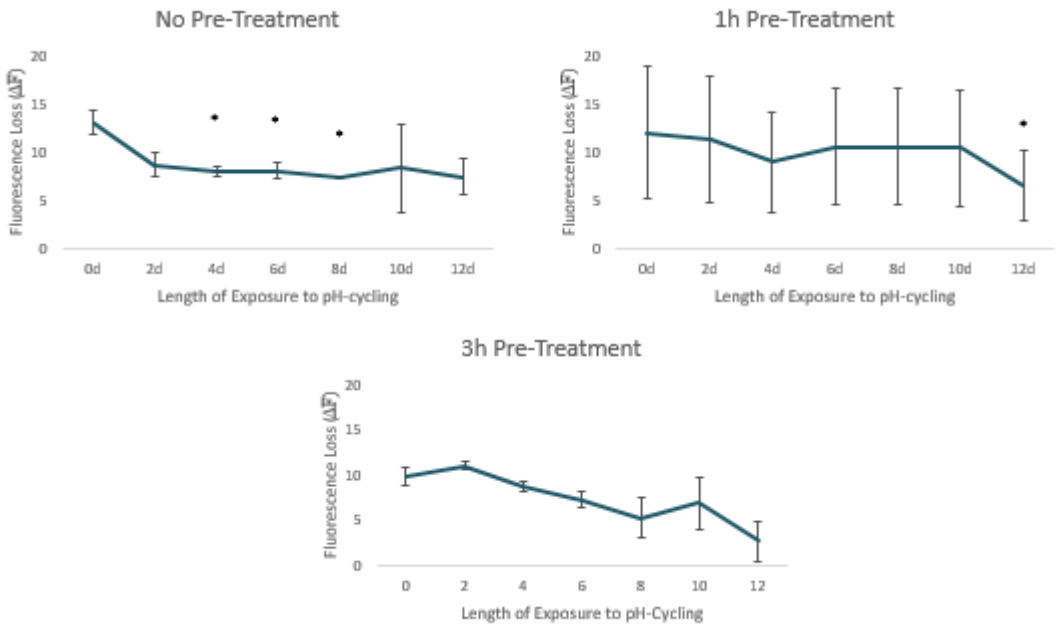

Figure 3.18: Graphical Representation of ΔF in relation to pH-cycling Exposure Length. *MSI fluorescence loss values for 0, 1 and 3h pre-treated enamel subjected to 0-12d pH-cycling and a subsequent 72h demineralisation. Error Bars Represent the SE of the mean. * = P<0.05. n=3.*

Progress of Fluorescence Loss over 72h Demineralisation

No Pre-Treatment:

When the progression of the lesions formed from non-pre-treated enamel is observed visually using MSI (Figure 3.19), unlike for QLF-D, a difference was observed between pH-cycled enamel and non-cycled controls. In a similar manner to QLF-D images obtained for 3h pre-treated enamel, lesions produced in pH-cycled enamel appeared lighter and less even than those produced in non-cycled controls.

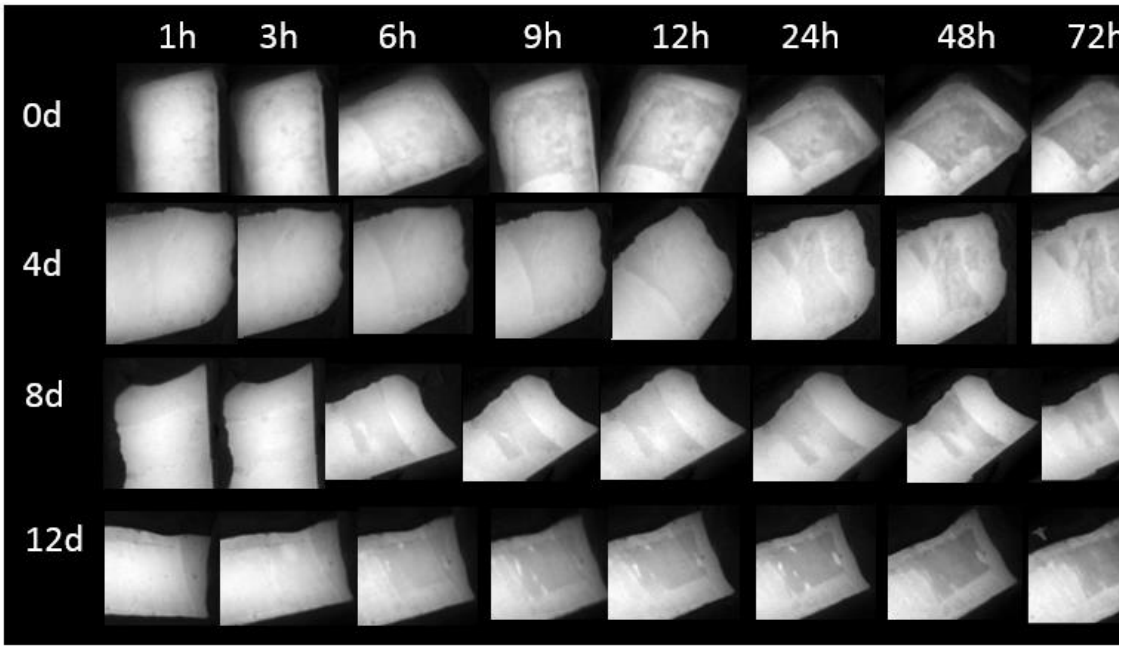

Figure 3.19: Visual MSI Lesion Progression in Non-Pre-Treated Enamel subjected to varying pH-cycling Regime Lengths. *Images captured using MSI demonstrating longitudinal lesion formation in non-pre-treated enamel subjected to varying pH-cycling exposures and a subsequent 72h demineralisation.*

The visual differences observed for MSI images when compared to QLF-D are supported by recorded numerical fluorescence loss values (Table 3.9). A decrease in fluorescence loss was observed for all pH-cycled blocks in comparison to non-cycled controls at all comparable time points. Additionally, lesions were numerically detectable at an earlier time point for non-cycled enamel than that subjected to a pH-cycling regime. There was, however, no clear relationship between the length of exposure to pH-cycling and subsequent fluorescence loss (Figure 3.20).

	n	0h ± SE	1h ± SE	3h ± SE	6h ± SE	9h ± SE	12h ± SE	24h ± SE	48h ± SE	72h ± SE
0d	3	0.00 ± 0.00	0.00 ± 0.00	1.97 ± 1.97	6.00 ± 0.35	6.87 ± 0.52	7.33 ± 0.84	7.47 ± 0.92	11.13 ± 0.87	13.00 ± 1.53
4d	3	0.00 ± 0.00	0.00 ± 0.00	0.00 ± 0.00	1.83 ± 1.83	1.90 ± 1.90	4.20 ± 2.11	4.53 ± 2.29	4.93 ± 2.47	7.97 ± 0.98
8d	3	0.00 ± 0.00	0.00 ± 0.00	0.00 ± 0.00	2.17 ± 2.17	3.97 ± 2.06	6.27 ± 2.18	6.90 ± 2.34	7.53 ± 4.24	7.40 ± 2.28
12d	3	0.00 ± 0.00	0.00 ± 0.00	0.00 ± 0.00	2.13 ± 2.13	4.10 ± 2.07	4.30 ± 2.18	4.60 ± 2.34	6.00 ± 4.24	7.43 ± 1.86

Table 3.9: Progression of Fluorescence Loss over 72h for non-pre-treated enamel subjected to 0-12d pH-cycling. *MSI-measured ΔF values at 0, 1, 3, 6, 9, 12, 24, 48 and 72h demineralisation time points for non-pre-treated enamel exposed to varying pH-cycling regime lengths. Data is presented with SE of the mean. n=3.*

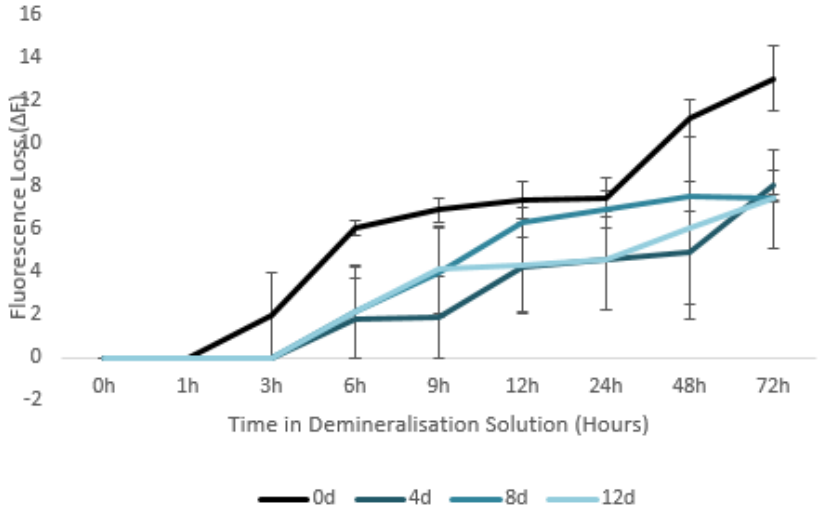

Figure 3.20: Graphical Representation of Demineralisation Progression over 72h for Varying pH-cycling Regime Lengths. *MSI data expressing ΔF changes over 72h exposure to demineralisation solution for non-pre-treated enamel subjected to 0-12d pH-cycling. Error Bars Represent the SE of the mean. n=3.*

1h Pre-treated Enamel:

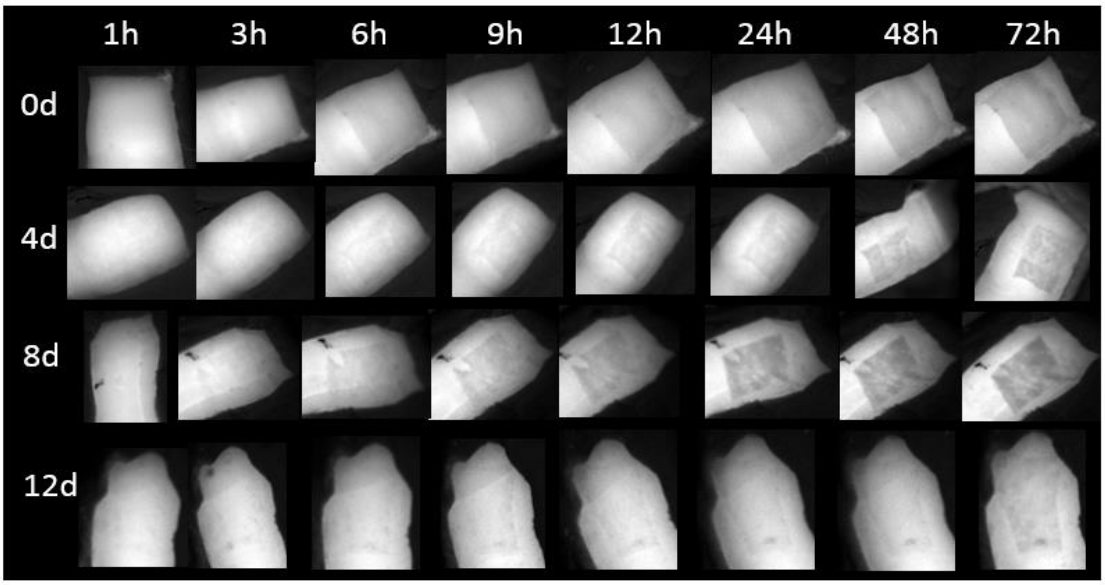

Figure 3.21: Visual MSI Lesion Progression in 1h Pre-treated Enamel subjected to varying pH-cycling Regime Lengths. *Images captured using MSI demonstrating longitudinal lesion formation in 1h pre-treated enamel subjected to varying pH-cycling exposures and a subsequent 72h demineralisation.*

MSI images obtained for 1h pre-treated enamel were mixed (Figure 3.21). Whilst lesions created in 4 and 12d pH-cycled enamel appear lighter at most time points in comparison to non-cycled controls, the differences are not clearly defined at the 72h time point. For 8h pH-cycled enamel, lesions actually appeared darker than non-cycled controls, however with more of an uneven appearance.

Numerically, the fluorescence loss values show a similar effect to the no pre-treatment group (Table 3.10). For any given time-point, a decrease in fluorescence loss was observed for pH-cycled enamel when considered against non-cycled controls. Additionally, fluorescence loss was detected at an earlier time point in non-cycled enamel in a similar manner to the previous results (Figure 3.22).

	n	0h ± SE	1h ± SE	3h ± SE	6h ± SE	9h ± SE	12h ± SE	24h ± SE	48h ± SE	72h ± SE
0d	3	0.00 ± 0.00	0.00 ± 0.00	3.67 ± 3.67	4.50 ± 2.27	6.30 ± 0.72	7.40 ± 0.40	8.20 ± 3.04	9.00 ± 0.50	12.03 ± 1.39
4d	3	0.00 ± 0.00	0.00 ± 0.00	0.00 ± 0.00	1.73 ± 1.73	2.03 ± 2.03	4.17 ± 2.10	5.40 ± 1.23	6.63 ± 0.57	8.93 ± 0.32
8d	3	0.00 ± 0.00	0.00 ± 0.00	0.00 ± 0.00	1.70 ± 1.70	4.27 ± 2.16	6.23 ± 0.52	7.23 ± 0.84	8.17 ± 1.43	10.50 ± 1.78
12d	3	0.00 ± 0.00	0.00 ± 0.00	0.00 ± 0.00	0.00 ± 0.00	0.00 ± 0.00	1.90 ± 1.90	4.20 ± 1.14	6.50 ± 0.65	6.50 ± 0.21

Table 3.10: Progression of Fluorescence Loss over 72h for 1h pre-treated enamel subjected to 0-12d pH-cycling. *MSI-measured ΔF values at 0, 1, 3, 6, 9, 12, 24, 48 and 72h demineralisation time points for 1h pre-treated enamel exposed to varying pH-cycling regime lengths. Data is presented with SE of the mean. n=3.*

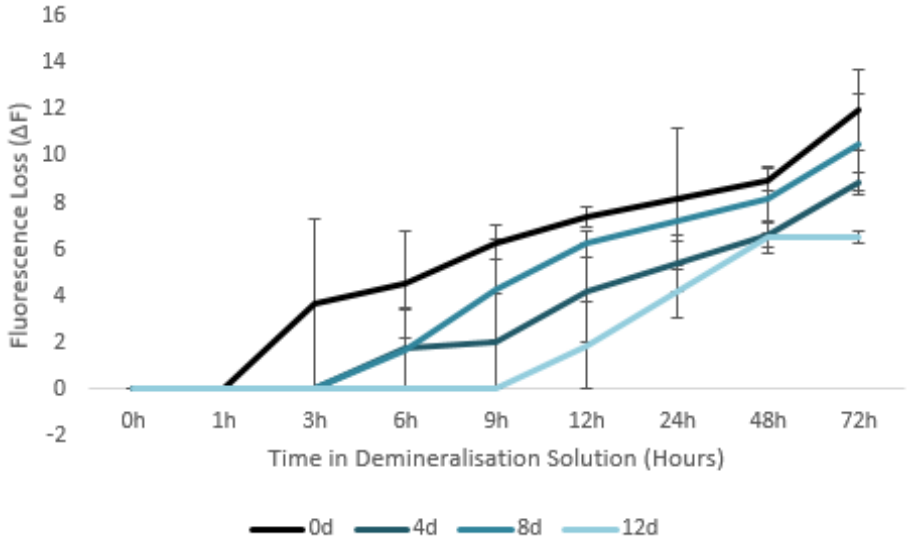

Figure 3.22: Graphical Representation of Demineralisation Progression over 72h for Varying pH-cycling Regime Lengths. *MSI data expressing ΔF changes over 72h exposure to demineralisation solution for 1h pre-treated enamel subjected to 0-12d pH-cycling. Error Bars Represent the SE of the mean. n=3.*

3h Pre-treated Enamel:

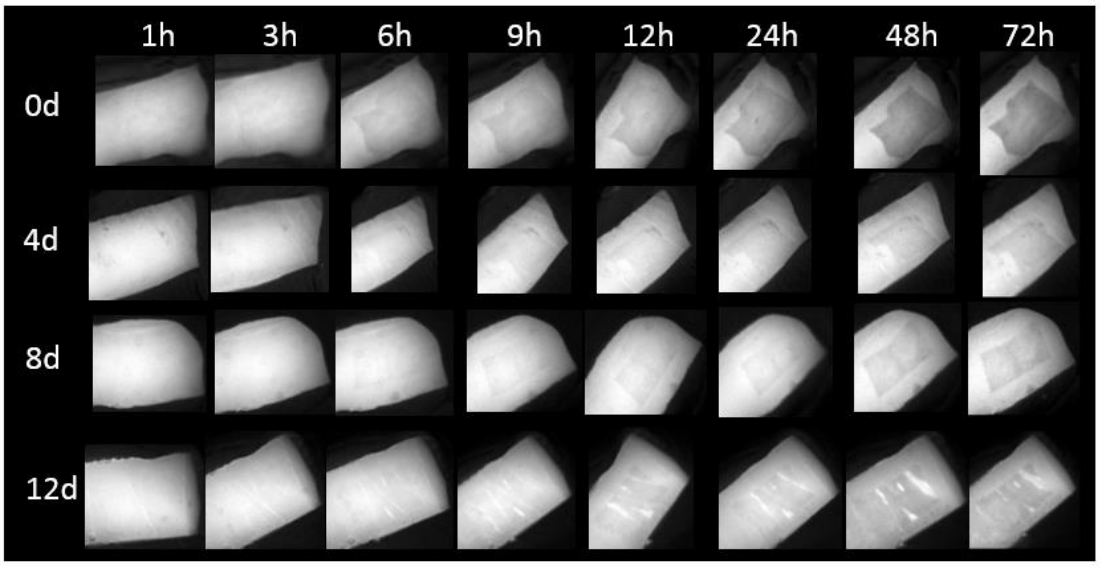

Figure 3.23: Visual MSI Lesion Progression in 3h Pre-treated Enamel subjected to varying pH-cycling Regime Lengths. *Images captured using MSI demonstrating longitudinal lesion formation in 3h pre-treated enamel subjected to varying pH-cycling exposures and a subsequent 72h demineralisation.*

Similar to the images obtained for QLF-D, 3h pre-treated enamel blocks showed reduced lesion visibility for pH-cycled enamel than that of non-cycled controls (Figure 3.23). In addition, lesions created in pH-cycled appeared less-even than those created in non-cycled enamel. Lesions were visually detectable at an earlier stage (3h) for non-cycled enamel than counterparts exposed to a pH-cycling regime (6h).

When numerical fluorescence loss values obtained by MSI are considered (Table 3.11), the visual difference observed for 4d pH-cycled enamel in comparison to non-cycled controls was less defined. A clear difference, however was observed for enamel subjected to 8 and 12d pH-cycling, where fluorescence loss values were lower than those for non-cycled controls at all comparable time points. Furthermore, lesions were first detectable 6-18h earlier when created using non-cycled controls (Figure 3.24).

	n	0h ± SE	1h ± SE	3h ± SE	6h ± SE	9h ± SE	12h ± SE	24h ± SE	48h ± SE	72h ± SE
0d	3	0.00 ± 0.00	0.00 ± 0.00	0.00 ± 0.00	2.00 ± 2.00	4.06 ± 2.13	4.43 ± 2.27	7.37 ± 1.04	7.87 ± 1.05	9.73 ± 1.00
4d	3	0.00 ± 0.00	0.00 ± 0.00	0.00 ± 0.00	1.67 ± 1.67	3.90 ± 1.96	4.07 ± 2.05	6.67 ± 0.57	7.00 ± 0.40	8.70 ± 0.57
8d	3	0.00 ± 0.00	0.00 ± 0.00	0.00 ± 0.00	0.00 ± 0.00	0.00 ± 0.00	0.00 ± 0.00	3.67 ± 1.84	4.73 ± 2.42	5.23 ± 2.17
12d	3	0.00 ± 0.00	0.00 ± 0.00	0.00 ± 0.00	0.00 ± 0.00	0.00 ± 0.00	1.97 ± 1.97	1.97 ± 1.97	2.20 ± 2.25	2.63 ± 2.15

Table 3.11: Progression of Fluorescence Loss over 72h for 3h pre-treated enamel subjected to 0-12d pH-cycling. *MSI-measured ΔF values at 0, 1, 3, 6, 9, 12, 24, 48 and 72h demineralisation time points for 3h pre-treated enamel exposed to varying pH-cycling regime lengths. Data is presented with SE of the mean. n=3.*

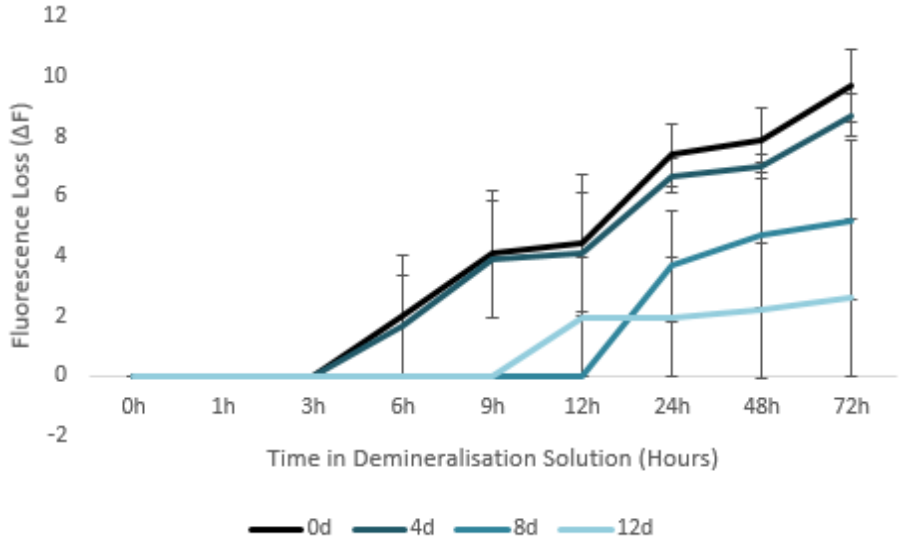

Figure 3.24: Graphical Representation of Demineralisation Progression over 72h for Varying pH-cycling Regime Lengths. *MSI data expressing ΔF changes over 72h exposure to demineralisation solution for 1h pre-treated enamel subjected to 0-12d pH-cycling. Error Bars Represent the SE of the mean. n=3.*

3.4.6 Transverse Microradiography (TMR) Measurement of Demineralised Enamel

Total Mineral Loss: 0 Vs 12d Exposure to pH-cycling

During preparation of the TMR sections, some sections were damaged during the grinding process. It was, however, ensured, through the grinding of additional sections, that at least three sections were radiographed per area of interest for analysis. Analysis was conducted by taking the mean mineral loss value for each section, before averaging obtained means to give a single value per block. Data reported below was then taken as the average of the three blocks for each condition.

	0 Days ∆Z ± SE	12 Days ∆Z ± SE
None	1891.42 ± 69.98	2161.67 ± 536.06
1h	1782.85 ± 304.99	895.31 ± 49.44
3h	1842.92 ± 448.99	793.15 ± 189.99

Table 3.12: Total Mineral Loss 0 vs 12 Days Exposure to pH-cycling. *TMR data for demineralised bovine enamel blocks previously subjected to 0 or 12 days exposure to pH-cycling. Blocks were pre-treated for 0, 1 or 3h in demineralisation solution. Data is presented with the SE of the mean. n=3.*

When the total mineral loss following 72h demineralisation was compared between non-cycled controls and samples exposed to the full 12 days pH-cycling (Table 3.12), a non-significant decrease in ∆Z was observed for blocks exposed to a 1 or 3-hour demineralisation pre-treatment. A non-significant increase in subsequent mineral loss was observed for enamel blocks not subjected to a pre-treatment. This is presented graphically in Figure 3.25 below.

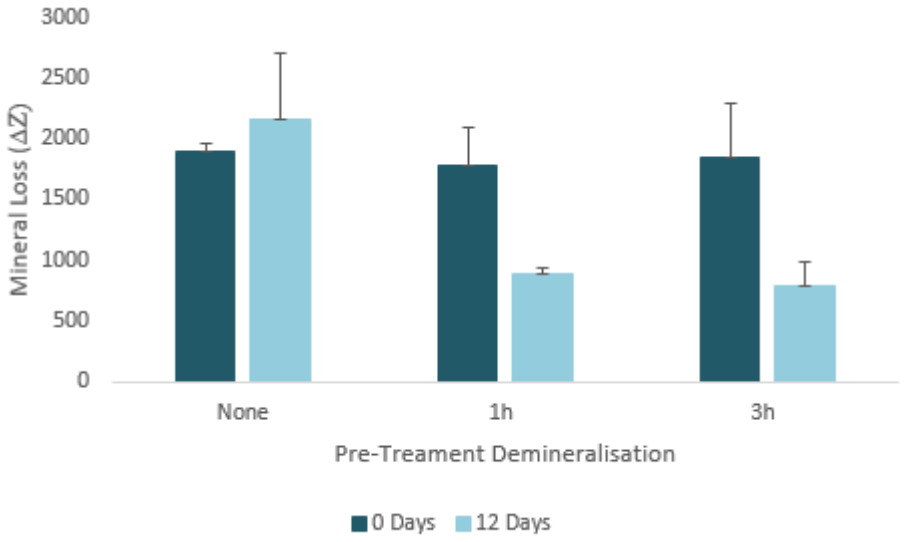

Figure 3.25: Mineral Loss (ΔZ) values following 72h demineralisation as measured using TMR. *Data comparing non-cycled blocks to those exposed to the full 12-day regime for enamel pre-treated for 0, 1 or 3h in demineralisation solution. Error Bars represent SE of the mean. n=3.*

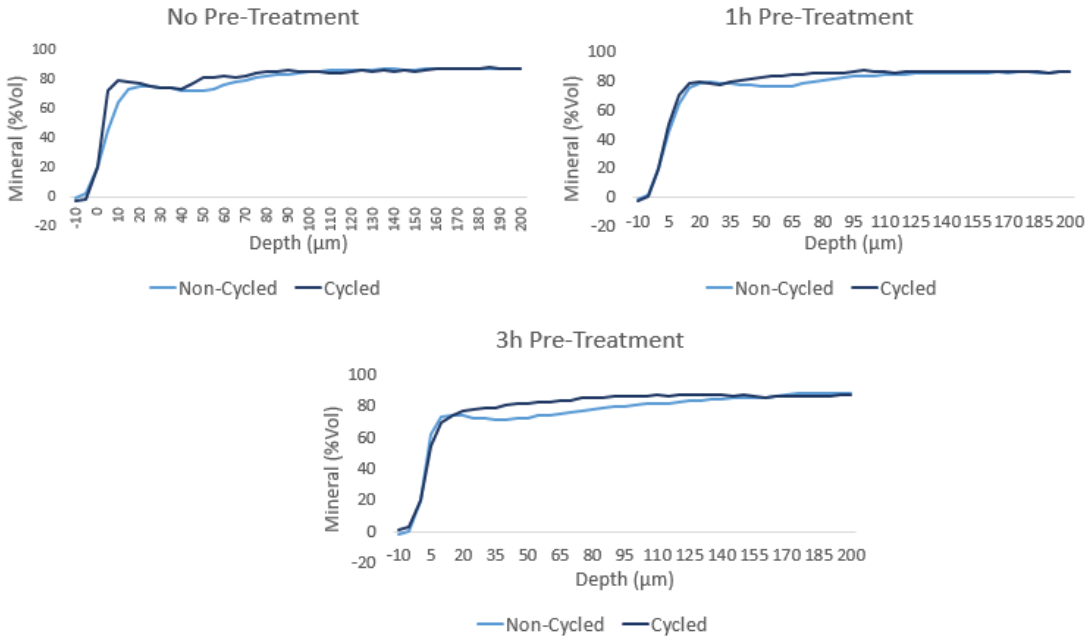

Figure 3.26: Mineral Loss as a Function of Depth. *Lesion profile created from TMR data for lesions created in 0, 1 and 3h demineralisation pre-treated enamel subjected to 0 or 12d pH-cycling.*

When the mineral loss is considered as a function of depth (Figure 3.26), the differences between enamel exposed to pH-cycling and relevant controls are subtle. For enamel not subjected to a demineralisation pre-treatment, observed lesions were similar, although a slightly more defined surface zone was present in enamel subjected to pH-cycling. In contrast, the profiles of lesions created in pre-demineralised enamel subjected to cycling demonstrated features much closer to that of sound enamel in contrast to the typical lesion features observed in comparable controls.

Mineral Loss in Enamel Subjected to Varying Lengths of pH-cycling Exposure

No Pre-Treatment:

pH-Cycling Length (Days)	Number of Blocks (n)	ΔZ ± SE	LD ± SE	R ± SE
0	3	1891.42 ± 69.98	98.56 ± 10.61	17.03 ± 1.20
2	3	890.56 ± 405.67	46.75 ± 25.04	21.72 ± 1.97
4	3	1247.72 ± 234.68	59.13 ± 5.21	22.72 ± 5.33
6	3	1785.41 ± 219.73	90.70 ± 6.90	19.70 ± 0.86
8	3	1514.72 ± 415.97	84.63 ± 16.70	22.04 ± 4.96
10	3	986.46 ± 69.79	71.64 ± 1.00	13.93 ± 1.24
12	3	2161.67 ± 536.06	110.93 ± 29.57	20.12 ± 4.54

Table 3.13: ΔZ, LD and R Values for Demineralised Enamel with Varying Lengths of pH-cycling Exposure. *TMR data for lesions created in non-pre-treated enamel subjected to 0-12d pH-cycling exposure. Data is presented with the SE of the mean. n=3.*

For blocks not subjected to any pre-treatment, no differences in mineral loss (ΔZ), lesion depth (LD) or R (%Vol) were observed between non-cycled enamel and that exposed to pH-cycling (Table 3.13). This is presented graphically in Figure 3.27 below.

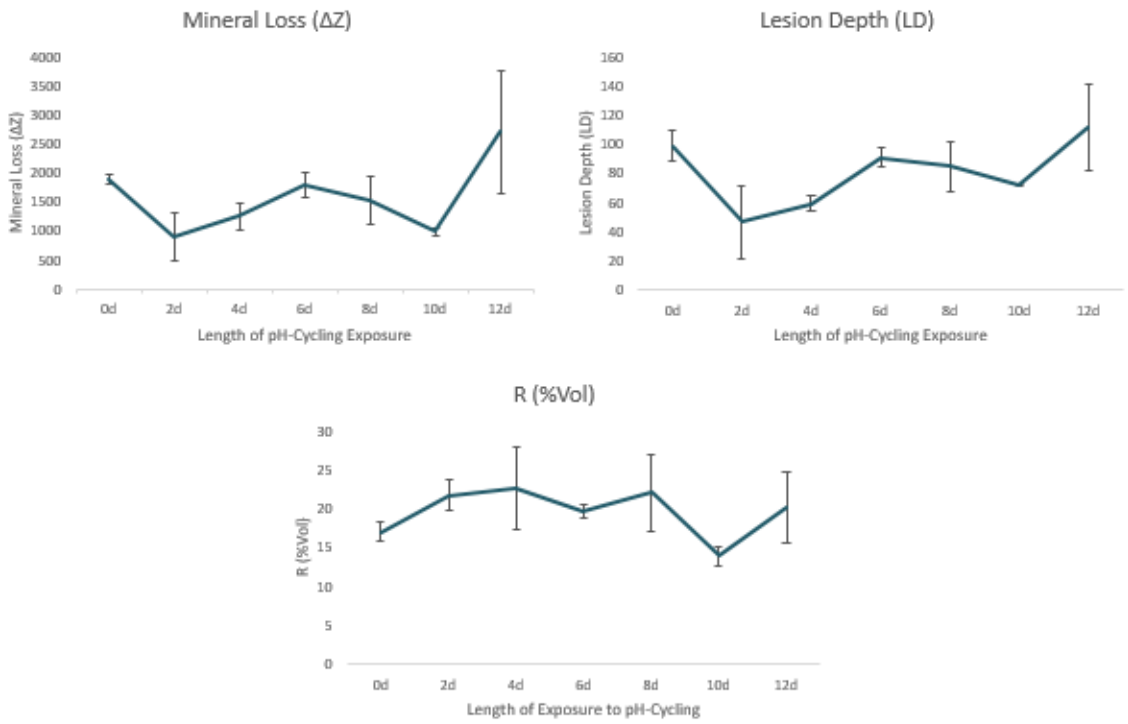

Figure 3.27: Graphical Representation of TMR Data for Demineralised Enamel with Varying Lengths of pH-cycling Exposure. *TMR data for lesions created in non-pre-treated enamel subjected to 0-12d pH-cycling exposure. Error bars represent the SE of the mean. n=3.*

1h Pre-treated Enamel:

For blocks subjected to a 1h pre-treatment, a decrease in both mineral loss and lesion depth was observed for all blocks exposed to pH-cycling when compared against non-cycled controls with the exception of those exposed to 2 days of cycling (Table 3.14). None of the observed decreases were found to be significant. No differences in R (%Vol) were observed between cycled and non-cycled enamel (Figure 3.28).

pH-Cycling Length (Days)	Number of Blocks (n)	ΔZ ± SE	LD ± SE	R ± SE
0	3	1782.85 ± 304.99	91.17 ± 18.32	19.59 ± 1.82
2	3	1776.83 ± 430.61	103.14 ± 16.97	18.32 ± 1.04
4	3	1680.08 ± 432.56	91.78 ± 14.20	17.28 ± 2.29
6	3	1151.57 ± 172.00	74.26 ± 13.84	16.18 ± 1.12
8	3	1256.83 ± 388.94	66.70 ± 20.49	22.83 ± 2.86
10	3	882.44 ± 328.24	47.39 ± 16.41	21.98 ± 1.17
12	3	895.31 ± 49.44	57.07 ± 5.90	18.32 ± 2.93

Table 3.14: ΔZ, LD and R Values for 1h Pre-treated Demineralised Enamel with Varying Lengths of pH-cycling Exposure. *TMR data for lesions created in 1h pre-treated enamel subjected to 0-12d pH-cycling exposure. Data is presented with the SE of the mean. n=3*

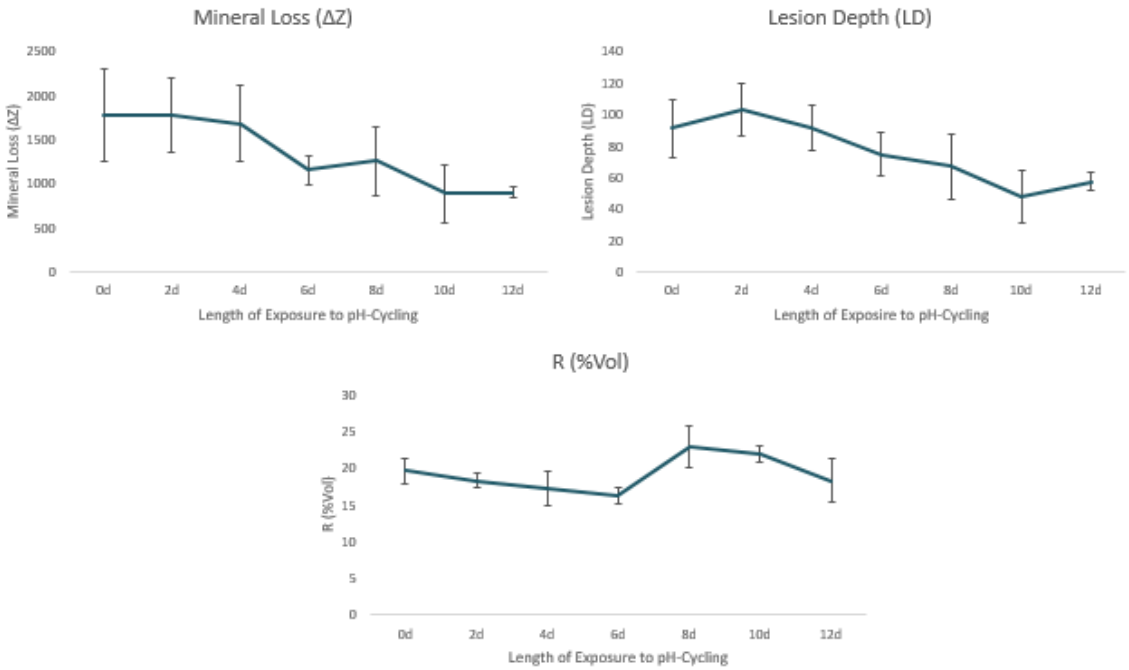

Figure 3.28: Graphical Representation of TMR Data for 1h Pre-treated Demineralised Enamel with Varying Lengths of pH-cycling Exposure. *TMR data for lesions created in 1h pre-treated enamel subjected to 0-12d pH-cycling exposure. Error bars represent the SE of the mean. n=3.*

3h Pre-treated Enamel

For blocks subjected to a 3h pre-treatment, a non-significant decrease in both mineral loss and lesion depth was observed for all blocks exposed to pH-cycling when related to values obtained for non-cycled controls with the exception of the 2d of cycling condition (Table 3.15). No differences in R (%Vol) were reported when pH-cycled and non-cycled enamel were contrasted (Figure 3.29).

pH-Cycling Length (Days)	Number of Blocks (n)	ΔZ ± SE	LD ± SE	R ± SE
0	3	1842.92 ± 448.99	89.15 ± 17.90	22.50 ± 2.12
2	3	3356.56 ± 1797.34	123.16 ± 43.07	25.39 ± 5.82
4	3	1175.90 ± 325.86	65.84 ± 18.77	19.49 ± 1.25
6	3	1132.91 ± 158.93	52.46 ± 7.60	23.97 ± 1.27
8	3	1722.08 ± 307.27	89.35 ± 8.23	18.98 ± 2.14
10	3	1314.58 ± 117.92	77.83 ± 1.91	18.10 ± 1.93
12	3	793.15 ± 189.99	42.20 ± 14.56	23.04 ± 2.74

Table 3.15: ΔZ, LD and R Values for 3h Pre-treated Demineralised Enamel with Varying Lengths of pH-cycling Exposure. *TMR data for lesions created in 3h pre-treated enamel subjected to 0-12d pH-cycling exposure. Data is presented with the SE of the mean. n=3*

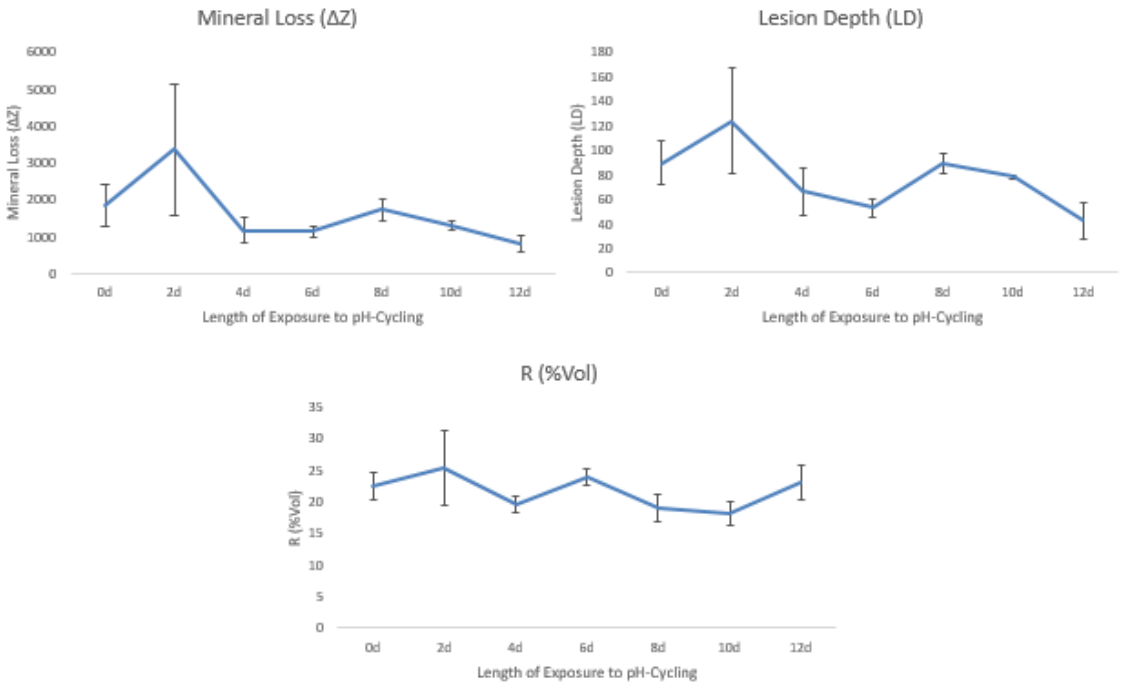

Figure 3.29: Graphical Representation of TMR Data for 3h Pre-treated Demineralised Enamel with Varying Lengths of pH-cycling Exposure. *TMR data for lesions created in 3h pre-treated enamel subjected to 0-12d pH-cycling exposure. Error bars represent the SE of the mean. n=3.*

3.4.7 Surface Chemical Changes in Produced Lesions Following Exposure to pH-cycling Measured by EPMA

Results from electron microprobe analysis were limited due to damage incurred to sections during both the polishing process and transportation. From the results obtained, it was, however, possible to draw comparisons between lesion samples created in enamel subjected to the full 12-day pH-cycling regime and non-cycled controls for enamel not subjected to a pre-treatment and those given the full 3h demineralisation pre-treatment. When the results for Ca and P content displayed graphically below (Figure 3.30) are considered, a decrease in both Ca and P at the surface can be observed for pH-cycled enamel in comparison to non-cycled controls regardless of pre-treatment conditions. For non-pre-treated enamel not subjected to a

cycling regime, a slight surface decrease in both Ca and P content can be observed, however the drop in P is more defined. Interestingly the surface decreases observed for pH-cycled counterparts are markedly more pronounced for Ca. This larger displacement of calcium at the surface for pH-cycled enamel is also reflected in 3h pre-treated enamel, however the Ca and P values for non-cycled controls are relatively even throughout the measured depth.

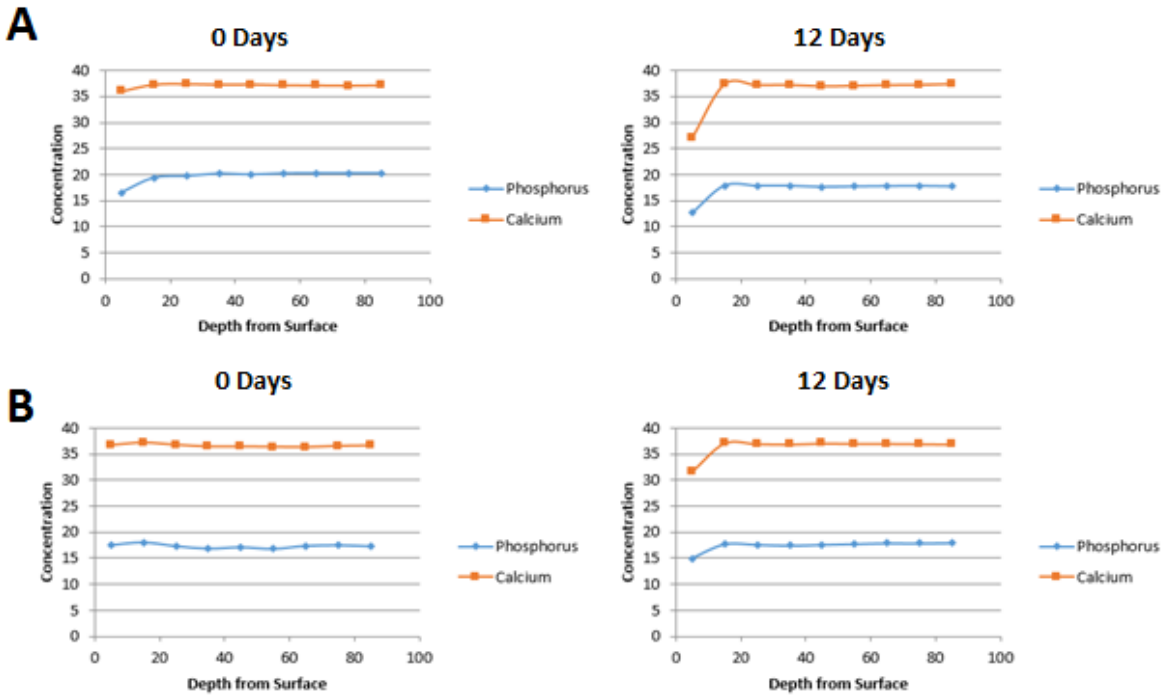

Figure 3.30: EMPA Analysis of Ca and P Content as a Function of Depth. *Ca and P content of lesions created in 0 (A) and 3h (B) pre-treated enamel subjected to 0 or 12d pH-cycling.*

EPMA analysis was also conducted for F and Zn content within the same samples and the results are presented graphically in Figure 3.31. For sound, non-pre-treated enamel, fluoride and zinc content decreased rapidly from the surface before levelling out at around 55nm. In comparison, enamel subjected to 12 days in PF-relevant pH-cycling conditions showed a lower concentration of zinc at the surface, but overall a similar pattern, with a sharp drop, before zinc levels reaching a plateau at around 15nm. For fluoride content, the results for pH-cycled enamel are more interesting.

Unlike sound enamel, where F content dropped sharply from the surface, F in cycled enamel stayed constant for the first 15µm, before following the same pattern of falling before levelling out.

For enamel subjected to a 3h demineralisation pre-treatment, F content follows a similar pattern to that's which was not subjected to a pre-treatment, however zinc levels were consistently low throughout the entire depth. The is in contrast to pH-cycled counterparts, which demonstrated higher levels of zinc at the surface in a similar manner to tested sound enamel. Fluoride content for 3h pre-treated cycled enamel presented similarly to that for non-treated, the exception being that fluoride content showed a slight increase over the initial 15nm.

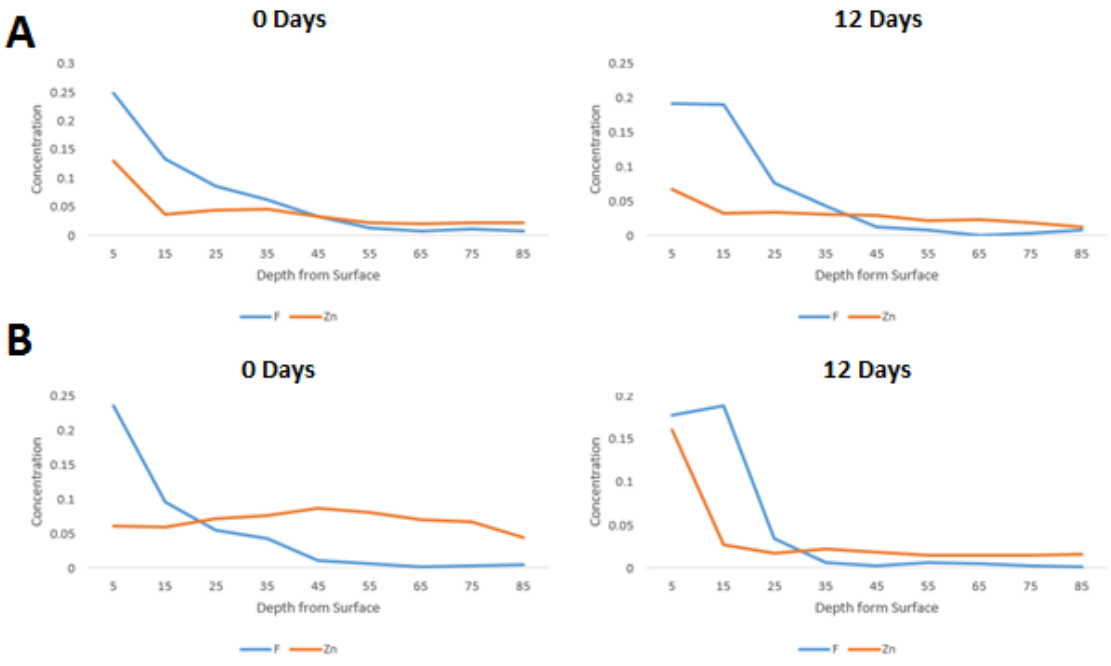

Figure 3.32: EMPA Analysis of F and Zn Content as a Function of Depth. *F and Zn content of lesions created in 0 (A) and 3h (B) pre-treated enamel subjected to 0 or 12d pH-cycling*

3.5 Discussion

Post-eruptive maturation is believed to be the result of exposure to subclinical caries events due to the cyclic nature of the oral environment (Lynch 2013). Therefore, the current study aimed to determine whether exposure to Plaque-fluid-relevant pH-cycling conditions could serve to reduce mineral loss during a subsequent acid challenge.

When total fluorescence loss values obtained by QLF-D were initially compared for enamel subjected to a full 12-day pH-cycling regime and non-cycled controls, the results appear promising. A significant decrease in fluorescence loss was observed for lesions created in pH-cycled enamel for both 1 and 3-hour pre-demineralised enamel. Similarly, the corresponding MSI images showed decreases for all three conditions, of which the 1h result was deemed significant. The TMR results also appear in consensus, however the situation is not as straightforward as it may appear from these results. When a wider range of pH-cycling regime lengths are taken into account, the situation appears to be much less clear-cut. It is for this reason that for the initial development of this model a range of regime lengths were used, to try and provide confirmation that observed relationships are a product of the pH-cycling as opposed to other factors. When these additional regime lengths are taken into account, there still does appear to be evidence that pre-treated enamel, particularly the longer 3h pre-treated enamel does appear to have the potential to demonstrate reduced fluorescence/mineral loss when exposed to pH-cycling conditions, however the relationship is not a strong as first perceived.

One of the main advantages of fluorescence-based detection methods is their ability to follow the progression of the created lesions over the 72h demineralisation period. When this is taken into consideration, whilst visually only blocks within the 3h pre-treatment condition appeared to demonstrate pH-cycling-related effects, lesions created in pH-cycled enamel, for the most part, developed at later time points than non-cycled counterparts. The combination of these findings provides support for the use of

pH-cycling, whilst also supporting the notion that enamel exposed to alternating periods of de- and re-mineralisation, demonstrates reduced mineral loss when subjected to a subsequent acid challenge (ten Cate and Duijsters 1982, Iijima and Takagi 2000, Maltz *et. al*. 2006)

When EPMA data is considered, the observation of a concentrated surface area of fluoride for both pH-cycled conditions that is not observed for non-cycled counterparts, particularly in conjunction with raised zinc for the 3h pre-treated condition hints at the synergistic behaviour occasionally reported in the literature (Lynch 2013). The EPMA results, however interesting, must be viewed with caution. When the rest of the collected data is considered, no differences in produced lesions were observed for blocks not previously exposed to a demineralisation pre-treatment. Furthermore, when the Ca and P data is also considered, very little loss is reported for lesions created in non-pH-cycled 3h pre-treated enamel, which does not match other reported findings within this study. One possible explanation for this would be that sections sent were on boundary of the lesion therefore were not representative of the lesion. In future, selection criteria should be applied to reduce further such occurrences.

The fact that reductions in fluorescence/mineral loss were observed more readily in enamel subjected to a 3h demineralisation pre-treatment makes sense when the changes that are theorised to occur during PEM are taken into account. It is believed that chemical changes, such as the incorporation of fluoride and other ions occur through their ability to replace particular aspects of the HPA lattice (Young 1975, Aoba *et. al.* 2003). Fluoride, in particular, has been shown to diffuse into the surface enamel simultaneously to bacterial acids (Featherstone 1999). This combined with the evidential support for slightly acidic dentifrices (Alves *et. al.* 2007, Brighenti *et. al.* 2013) suggests that the presence of the simultaneous dissolution and remineralising ions facilitates access to the enamel surface, making it easier for them to bind.

Additionally, TMR data shows whilst there was a perceived decrease in both mineral loss and lesion depth, the ratio data shows no difference in the characteristics of the lesion. This may be partially due to absence of the additional fluoride prophylaxis provided *in vivo* by daily brushing. Studies have shown that fluoride and other ions are capable of binding to the enamel surface, however for this to happen a high concentration is required, as opposed to the minimal values included in the PF solutions used here (Young 1975, Featherstone *et. al.* 1990).

When the results of NCSP are considered, reported values for surface roughness showed no discernible relationships between exposure to pH-cycling and surface roughness, even for 3-hour pre-treated enamel. Whilst this may also be a factor of the small sample sizes used in this initial experiment, it may also be due to several other possible factors. The first factor that may be causing a lack of observable differences between cycled and non-cycled enamel is the nature of caries lesions on comparison to other forms of mineral loss such as erosion. Whilst erosive lesions initially involve loss of the surface layers of enamel, allowing them to be readily detected by NCSP, caries lesions characteristically form with an intact surface area and an underlying subsurface area of demineralisation (Silverstone 1968, Larsen 1991). If the effects of the lesions are purely confined to below the surface, the surface-limited detection capability of NCSP would not detect any changes, as the roughness would not be affected. The second main limitation of the NCSP measurements taken here is the enamel blocks themselves and their effect on NCSP accuracy. NCSP measurements rely on detecting very slight changes in depth of a surface and are therefore confounded when the surface to be measured is itself not flat. Whilst the software is designed to account for some curvature, the relatively large size of the blocks used here result in the inclusion of the natural curve present in the bovine incisors from which they were made. This may be leading to reduction in the ability of the NCSP to detect subtle changes in surface roughness.

To summarise, whilst the initial results obtained from this study show promise, the small sample size used combined with the limited pH-cycling exposure times mean that it is difficult to confirm the observed effects without further work using longer exposure periods and larger sample sizes.

Chapter Four: Effect of Increased pH-cycling Exposure Time within an *in vitro* PEM Model

4.1 Background

4.1.1 Timescale of the PEM Process with Consideration to an *in vitro* Model

Previous research has failed to come to a consensus as to the required length of time for PEM to occur. Whilst some studies claim that full maturation was observed within 15 months (Schulte *et. al.* 1999), others claim it can take over 10 years for full maturation to be reached (Palti *et. al.* 2008). This failure to agree, may be, in part, due to a lack of understanding of the PEM process underlying the observed changes and therefore no clear parameters by which to define enamel as being "fully matured". This suggests that only the development of techniques to study the underlying process and improve our understanding will allow a clear idea of the actual timescale of PEM *in vivo*.

One of the main issues with the proposed model outline in the previous chapter is the pH-cycling times are not long enough to produce the same effects as years' worth of exposure to the oral environment. Whilst it would be naïve to think that such a process can be fully replicated within a relatively short *in vitro* system, the results from the previous chapter indicate that, with some modification and an extended exposure time, maturation to a certain extent could be observed. Whilst this will not serve to produce "fully matured" enamel, it may be able to recreate the process to enough of a degree for it to be studied and our understanding furthered. This concept is supported by studies that have shown that marked decreases in caries susceptibility can occur within

the first few years of eruption, regardless of whether the enamel has reached full maturation (Schulte *et. al.* 1999, Cardoso *et. al.* 2009).

4.1.2 Refinement of the Proposed *in vitro* PEM Model

Building on the work from the previous chapter, the current study aims to refine the proposed pH-cycling model primarily though the employment of a significantly longer length 20-day pH-cycling regime in comparison to the 12 day-regime used previously. Additionally, in order to streamline the model to make it easier to reproduce, only two demineralisation pre-treatment conditions, 0 and 3h will be used. In a similar vein, the intermittent regime lengths were also excluded, largely because including so many variations would make scaling up the sample-sizes at later stages unmanageable. The updated model outline can be seen in Figure 4.1 below.

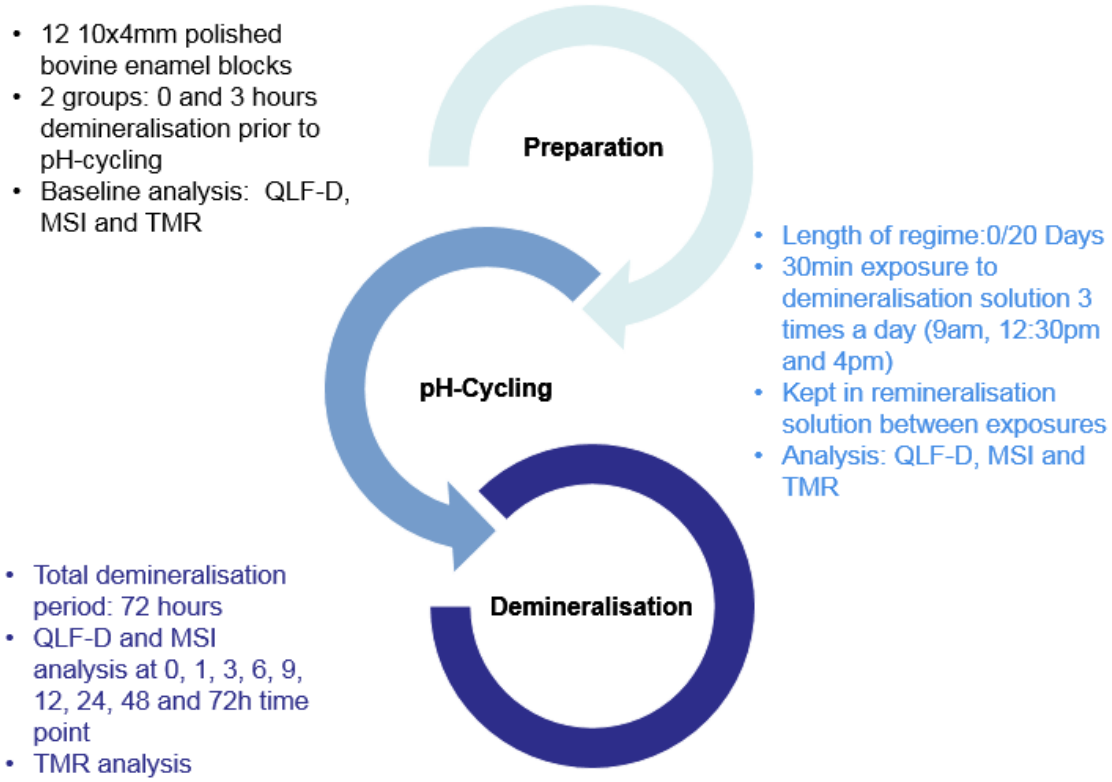

Figure 4.1: Summary of Current Model Protocol. *Outline of the current experimental procedure, broken down into the three stages of the proposed model*

4.2 Aims

The present study aimed to build upon the work described in the previous chapter by refining the proposed pH-cycling model of post-eruptive maturation. Secondly it also aimed to determine the effect of a longer exposure time to plaque-fluid-relevant pH-cycling conditions on the subsequent demineralisation of bovine enamel.

4.3 Materials and Methods

4.3.1 Selection and Preparation of Bovine Enamel Blocks

12 blocks prepared from bovine incisors and mounted as described previously (Section 2.2). Blocks were divided into two groups and subjected to either 0 or 3 hours demineralisation with agitation via a magnetic stirrer and flea. The PF demineralisation solution previously described was used (Section 2.3).

4.3.2 pH-Cycling Regime

The same pH-Cycling system designed for net remineralisation previously described (Section 2.5) was used with the length of exposure changed to a total of either 0 or 20 days (Figure 4.2).

4.3.3. Acid Challenge

In order to test the effect of the pH-cycling regime on the acid susceptibility of the enamel, blocks were subjected to a standard 72-hour acetic acid demineralisation challenge (Section 2.6).

4.3.4 Assessment of Demineralisation

Following the removal of all nail varnish using acetone, blocks were subjected to NCSP, QLF-D, MSI and TMR analysis (Section 2.7-2.10). MSI, QLF-D and TMR measurements were obtained at baseline, following pH-cycling and following 72h

demineralisation. Additionally, QLF-D and MSI images were taken at 0, 1, 3, 6, 9, 12, 24, 48h time points during the demineralisation challenge.

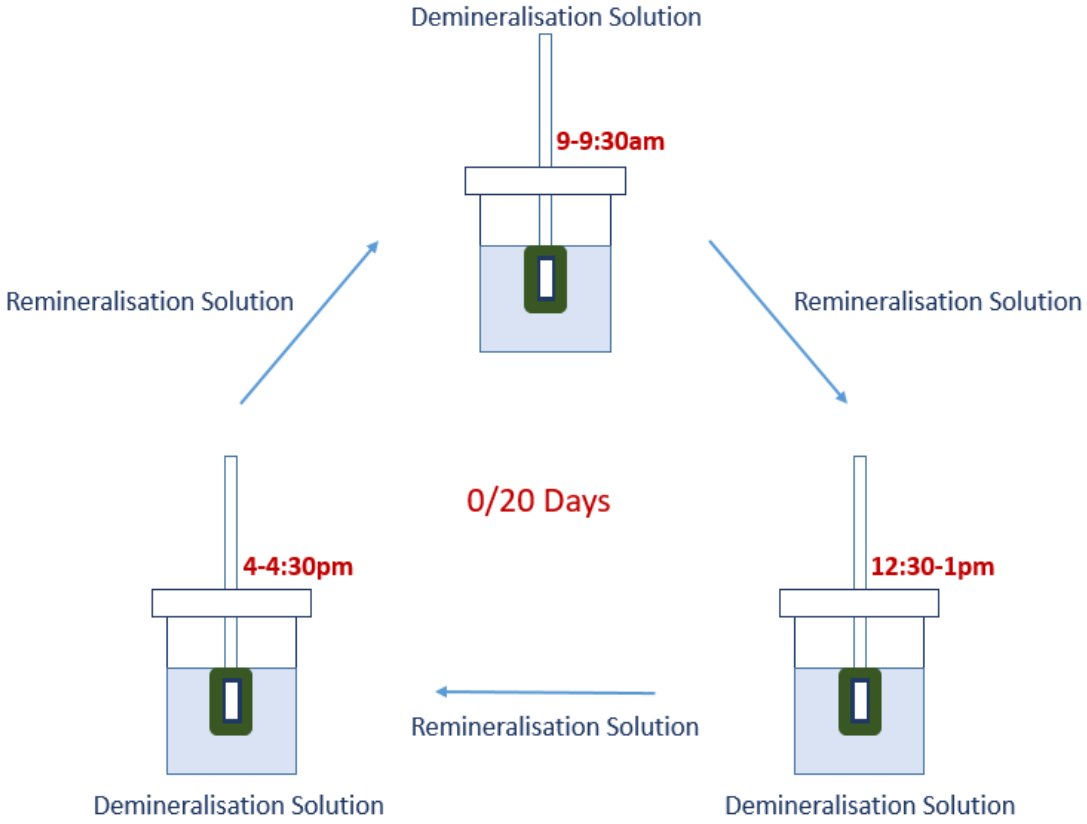

Figure 4.2: Outline of pH-cycling Regime. *Schematic of daily pH-cycling protocol observed for 0 to 20 days. Blocks are kept in remineralisation solution with the exception of three 30min demineralisation periods per day.*

4.4 Results

4.4.1 Effect of pH-cycling on Changes in Surface Roughness

For blocks in the no pre-treatment group, non-contact surface profilometry results were variable and no real pattern was observed between sound, pH-cycled and lesion areas for either cycled enamel or un-cycled controls (Table 4.1). For blocks subjected to a 3h demineralisation pre-treatment, NCSP results were similarly varied, although showed lower levels of variation than those not pre-treated. Once again no relationship between the different areas of enamel and surface roughness (Ra) was found (Figure 4.3).

Pre-Treatment		Sound	Cycled	Lesion
None	non cycled	0.70 ± 0.37	0.54 ± 0.21	0.49 ± 0.13
	pH-cycled	1.28 ± 0.74	0.98 ± 0.45	1.11 ± 0.62
3h	non cycled	0.52 ± 0.03	0.45 ± 0.03	0.96 ± 0.36
	pH-cycled	0.36 ± 0.07	0.35 ± 0.06	0.35 ± 0.04

Table 4.1: Effect of pH-cycling on Surface Roughness (Ra). *NCSP data representing surface roughness (Ra) of baseline (sound), pH-cycled and demineralised (Lesion) enamel for both 20d cycled enamel and non-cycled controls subjected to 0 or 3h demineralisation pre-treatment. Data presented along with the standard error of the mean. n=3.*

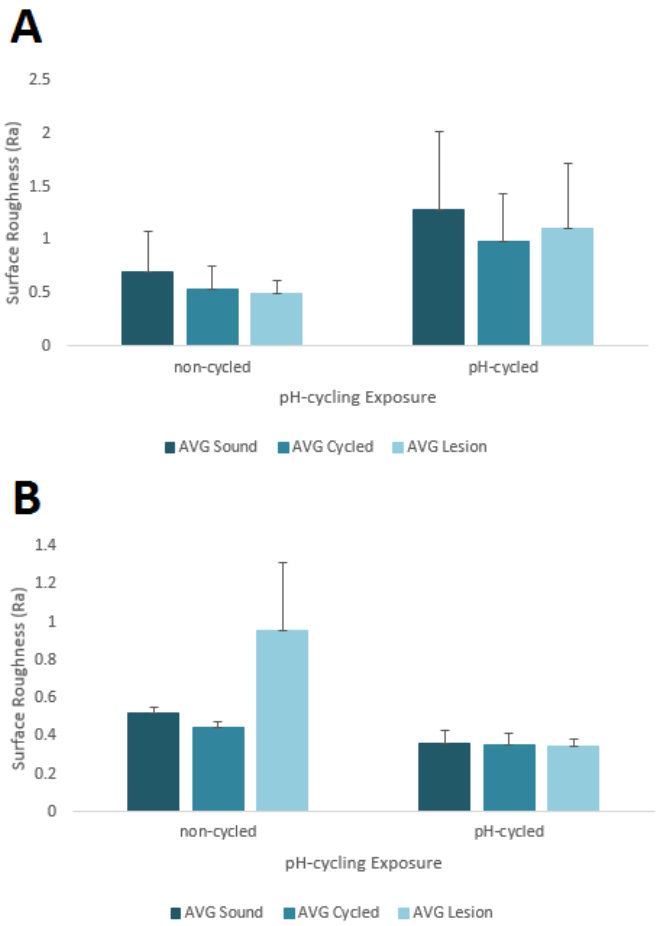

Figure 4.3: Graphical Representation of Changes in Ra. *Average (AVG) surface roughness (Ra) values for Sound, pH-cycled and demineralised enamel as measured using NCSP. Blocks were subjected to 0 (A) or 3h (B) demineralisation pre-treatment and 0 or 20d pH-cycling. Error bars represent the standard error of the mean. n=3.*

4.4.2 Assessment of Changes in Fluorescence Loss by QLF-D Following pH-cycling

Total Fluorescence Loss

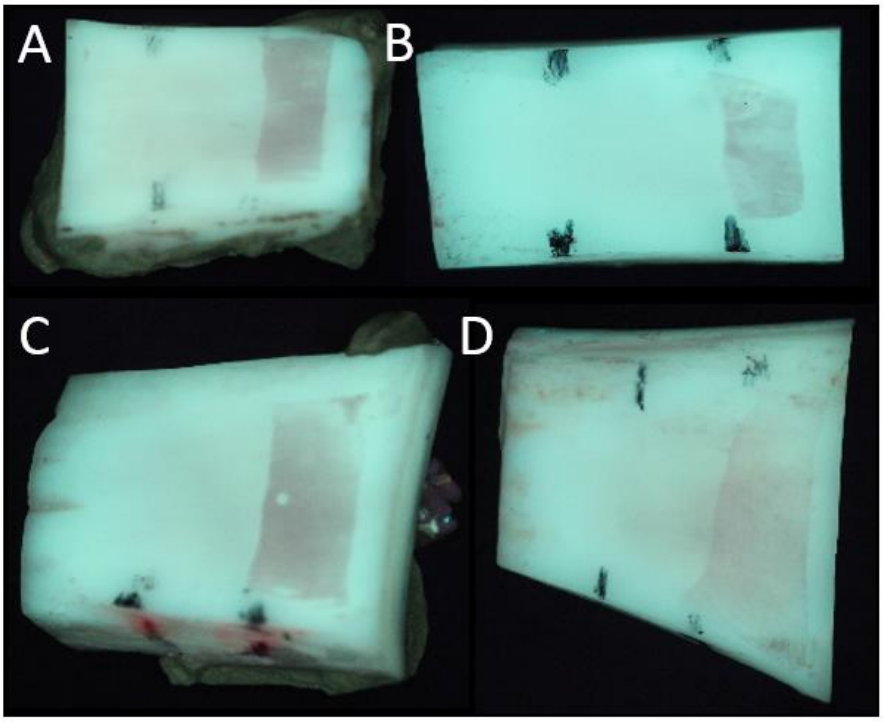

Figure 4.4: QLF-D Images Comparing Lesions Created in Cycled and Non-Cycled Enamel. *QLF-D images captured for lesions created in 0 (A/B) and 1h (C/D) pre-treated enamel subjected to 0 (A/C) or 20d (B/D) pH-cycling.*

When the QLF-D images were subjected to visual examination (Figure 4.4), lesions created on pH-cycled enamel appeared lighter in colour than those created on untreated, sound enamel. Additionally, such lesions appear to be less consistent in colour, patchy and uneven.

Pre-Treatment	Pre-Treatment	n	Non-Cycled ΔF ± SE	Cycled ΔF ± SE
None	None	3	13.00 ± 5.48	10.33 ± 2.67
3h	3h	3	13.23 ± 3.35	11.13 ± 2.87

Table 4.2: Total Fluorescence Loss Measured by QLF-D. *QLF-D data for demineralised bovine enamel blocks previously subjected to 0 or 20 days exposure to pH-cycling. Blocks were pre-treated for 0 or 3h in demineralisation solution n=3.*

For blocks not exposed to a demineralisation pre-treatment, a non-significant decrease in fluorescence loss was observed between pH-cycled blocks and non-cycled controls following a 72h demineralisation challenge (Table 4.2). Similarly, a non-significant decrease in fluorescence loss was observed for all pH-cycled blocks exposed to a 3h demineralisation pre-treatment in comparison to non-cycled controls. This is presented graphically in Figure 4.5 below.

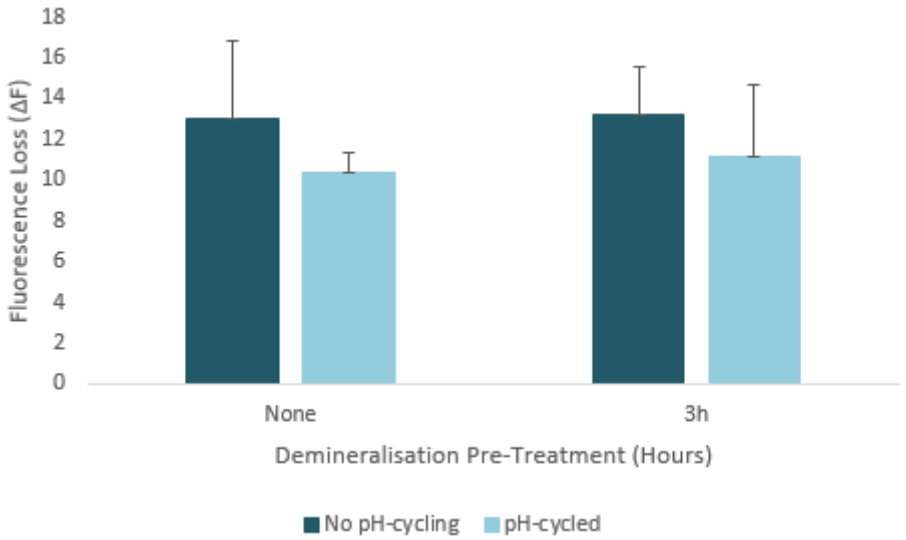

Figure 4.5: Fluorescence loss (ΔF) values following 72h demineralisation as measured using QLF-D. *Data comparing non-cycled blocks to those exposed to 20-day regime for enamel pre-treated for 0 or 3h in demineralisation solution. Error Bars represent SE of the mean. n=3.*

Progress of Fluorescence Loss over 72h Demineralisation

No Pre-Treatment:

Visual examination of lesion development over a 72h period via QLF-D imaging demonstrated that a dark area was first faintly visible at the 3h period for uncycled enamel and 9h for that exposed to pH-cycling for 20days (Figure 4.6). Similarly, a lesion was clearly visible from 6 days for un-cycled enamel in comparison to 12h for pH-cycled counterparts. All lesions observed for enamel subjected to the 20-day pH-

cycling regime appeared paler and more uneven in appearance when compared to non-cycled enamel exposed to the same amount of time in demineralisation solution.

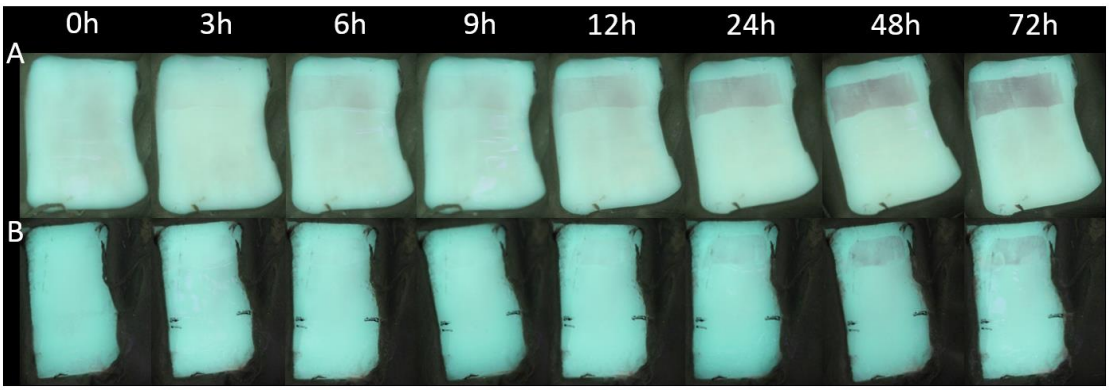

Figure 4.6: Visual QLF-D Lesion Progression in Non-Pre-Treated Enamel subjected to 0 or 20d pH-cycling. *Images captured using QLF-D demonstrating longitudinal lesion formation in non-pre-treated enamel subjected to pH-cycling for 0 (A) or 20d (B) and a subsequent 72h demineralisation.*

	n	0h ± SE	1h ± SE	3h ± SE	6h ± SE	9h ± SE	12h ± SE	24h ± SE	48h ± SE	72h ± SE
Non-Cyc	3	0.00 ± 0.00	0.00 ± 0.00	0.00 ± 0.00	6.10 ± 0.26	6.13 ± 0.26	6.93 ± 0.44	9.80 ± 1.42	11.87 ± 2.68	13.00 ± 5.48
Cyc	3	0.00 ± 0.00	0.00 ± 0.00	0.00 ± 0.00	0.00 ± 0.00	1.97 ± 1.97	2.30 ± 2.30	7.63 ± 0.55	10.17 ± 0.55	10.33 ± 2.67

Table 4.3: Progression of Fluorescence Loss over 72h for non-pre-treated enamel subjected to 0 or 20d pH-cycling. *QLF-D-measured ΔF values at 0, 1, 3, 6, 9, 12, 24, 48 and 72h demineralisation time points for non-pre-treated enamel exposed to varying pH-cycling regime lengths. Data is presented with SE of the mean. n=3.*

Whilst a dark area was visually detectable at 3h for non-cycled enamel, fluorescence loss was not detected by the QLF-D software until the 6h time point (Table 4.3). Numerically, fluorescence loss values were lower for pH-cycled enamel when related to

un-cycled controls at all comparable time points, however only the difference at 6h showed statistical significance (P=0.0001). Additionally, fluorescence loss values support the visual observation that lesions were detected at an earlier time point for non-cycled controls (6h) than enamel exposed to pH-cycling (9h). This is presented graphically in Figure 4.7 below.

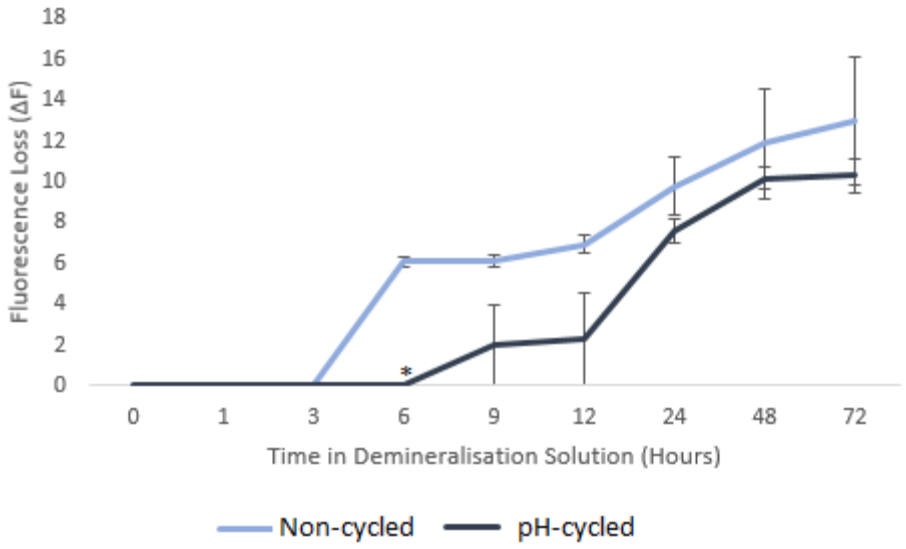

Figure 4.7: Graphical Representation of Demineralisation Progression over 72h for 0 and 20d pH-cycling Exposure. *QLF-D data expressing ΔF changes over 72h exposure to demineralisation solution for non-pre-treated enamel subjected to 0 or 20d pH-cycling. Error Bars Represent the SE of the mean. n=3.*

3h Pre-treated Enamel:

Visual examination of lesion development over a 72h period via QLF-D imaging demonstrated that a dark area was first observed at the 6h period for uncycled enamel and 9h for that exposed to pH-cycling for 20days (Figure 4.8). Additionally, a lesion was clearly visible from 9 days for un-cycled enamel as opposed to 12h for pH-cycled counterparts. All lesions observed for enamel subjected to the 20-day pH-cycling regime once again appeared paler and more uneven in appearance when related to non-cycled enamel exposed to the same amount of time in demineralisation solution.

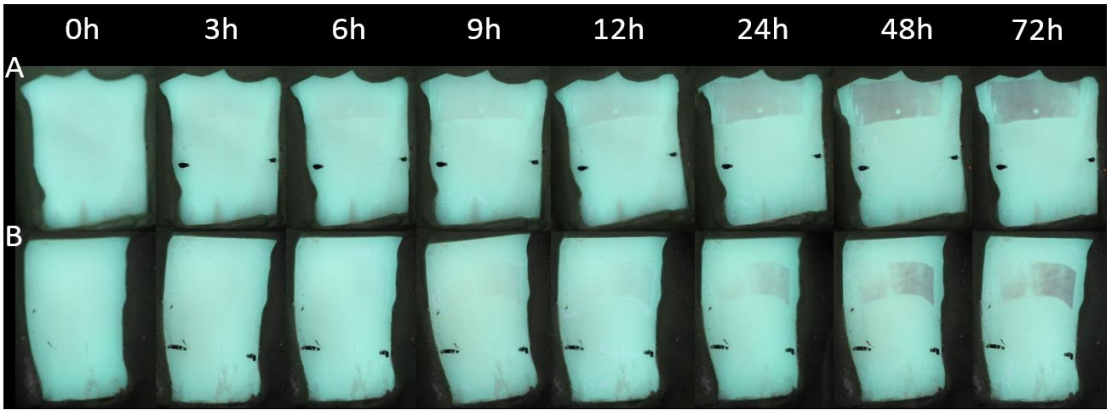

Figure 4.8: Visual QLF-D Lesion Progression in 3h Pre-treated Enamel subjected to 0 or 20d pH-cycling. *Images captured using QLF-D demonstrating longitudinal lesion formation in 3h pre-treated enamel subjected to pH-cycling for 0 (A) or 20d (B) and a subsequent 72h demineralisation.*

	n	0h ± SE	1h ± SE	3h ± SE	6h ± SE	9h ± SE	12h ± SE	24h ± SE	48h ± SE	72h ± SE
Non-Cyc	3	0.00 ± 0.00	0.00 ± 0.00	0.00 ± 0.00	0.00 ± 0.00	5.37 ± 0.03	5.60 ± 0.00	7.27 ± 0.18	11.60 ± 1,65	13.23 ± 3.35
Cyc	3	0.00 ± 0.00	0.00 ± 0.00	0.00 ± 0.00	0.00 ± 0.00	1.97 ± 1.97	4.07 ± 2.05	7.43 ± 1.13	9.47 ± 2.27	11.13 ± 2.87

Table 4.4: Progression of Fluorescence Loss over 72h for 3h pre-treated enamel subjected to 0 or 20d pH-cycling. *QLF-D-measured ΔF values at 0, 1, 3, 6, 9, 12, 24, 48 and 72h demineralisation time points for 3h pre-treated enamel exposed to varying pH-cycling regime lengths. Data is presented with SE of the mean. n=3.*

In a Similar manner to the non-treated group, dark areas were visually detectable for non-cycled enamel at earlier time points (6h) than were numerically detected by the QLF-D software (9h) (Table 4.4). Numerically, fluorescence loss values were lower for pH-cycled enamel than un-cycled counterparts at all time-points with the exception of 24h, where it was slightly higher (0.16 difference). Additionally, ΔF values do not

support the visual observation that lesions were detected at an earlier time point for non-cycled controls (6h) in comparison to enamel exposed to pH-cycling (9h) (Figure 4.9).

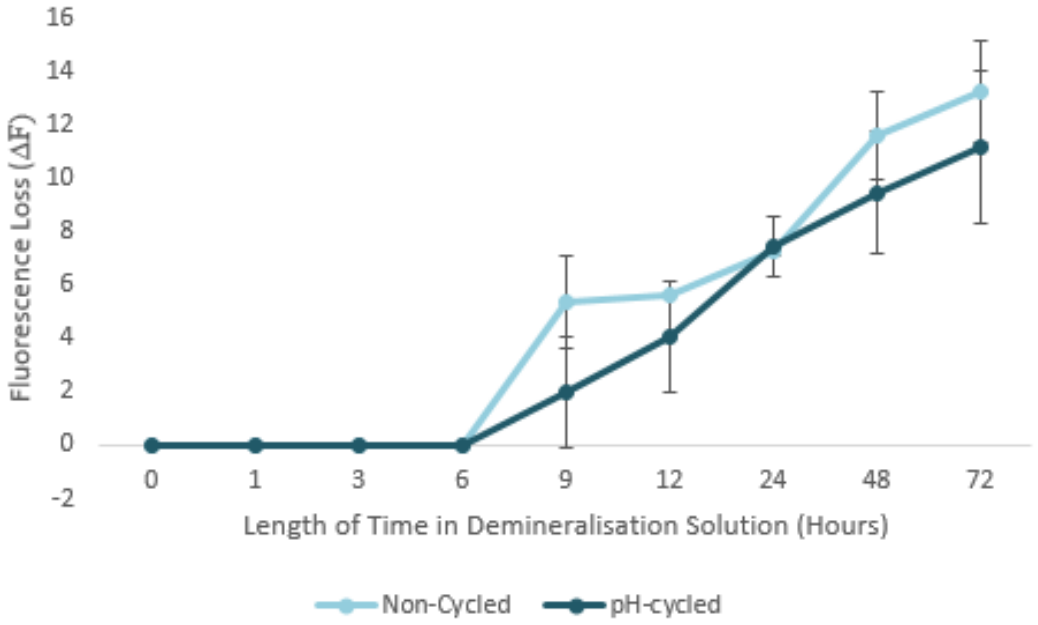

Figure 4.9: Graphical Representation of Demineralisation Progression over 72h for 0 and 20d pH-cycling Exposure. *QLF-D data expressing ΔF changes over 72h exposure to demineralisation solution for 3h pre-treated enamel subjected to 0 or 20d pH-cycling. Error Bars Represent the SE of the mean. n=3.*

4.4.3 Impact of pH-cycling on Fluorescence Loss Measured by MSI

Total Fluorescence Loss

When the MSI images of lesions created following 72h demineralisation are examined visually (Figure 4.20), those created on 20d pH-cycled enamel appear lighter in colour than those created on non-cycled, sound enamel controls. Additionally, such lesions appear to be uneven and variable in colour across the lesion area in a similar manner to that observed by QLF-D imaging above.

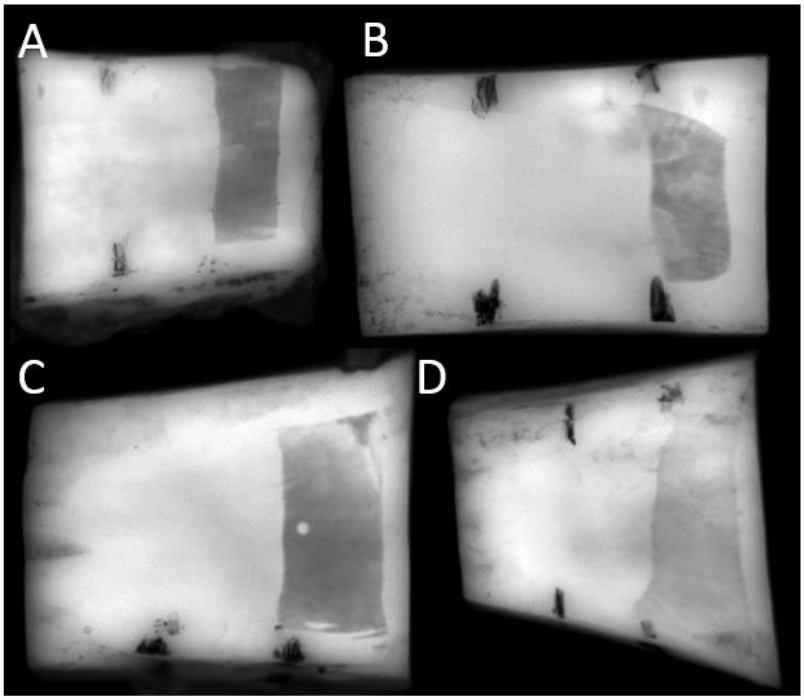

Figure 4.10: MSI Images Comparing Lesions Created in Cycled and Non-Cycled Enamel. *MSI images captured for lesions created in 0 (A/B) and 1h (C/D) pre-treated enamel subjected to 0 (A/C) or 20d (B/D) pH-cycling*.

Pre-Treatment	Pre-Treatment	n	Non-Cycled ΔF ± SE	Cycled ΔF ± SE
None	None	3	24.30 ± 6.17	21.37 ± 1.01
3h	3h	3	24.67 ± 0.77	17.97 ± 6.33

Table 4.5: Total Fluorescence Loss Measured by MSI. *MSI data for demineralised bovine enamel blocks previously subjected to 0 or 20 days exposure to pH-cycling. Blocks were pre-treated for 0 or 3h in demineralisation solution n=3.*

When quantitative analysis was conducted for non-pre-treated blocks subjected to a 72h demineralisation, a non-significant decrease in fluorescence loss was observed between pH-cycled blocks and non-cycled controls (Table 4.5). Additionally, a non-significant decrease in fluorescence loss was also observed for all pH-cycled blocks exposed to a 3h demineralisation pre-treatment in comparison to non-cycled controls. This is presented graphically in Figure 4.11 below.

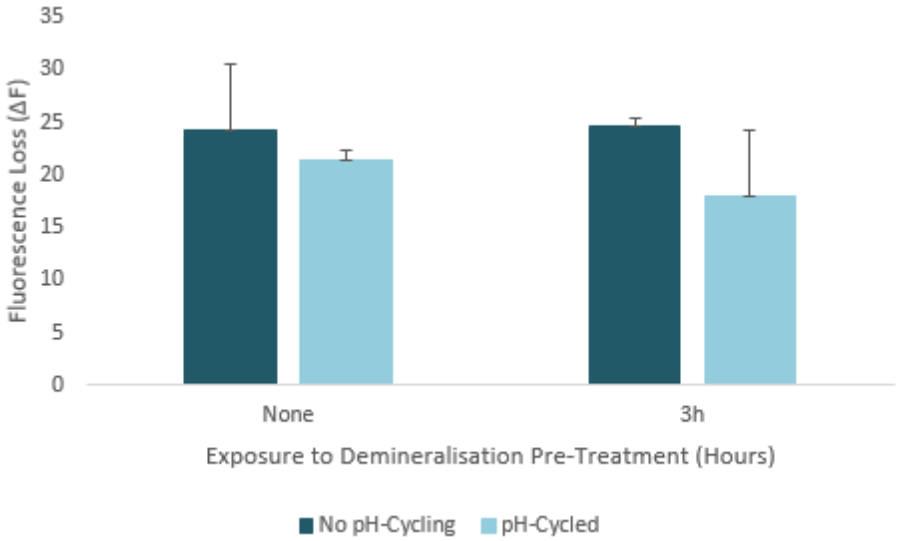

Figure 4.11: Fluorescence loss (ΔF) values following 72h demineralisation as measured using MSI. *Data comparing non-cycled blocks to those exposed to 20-day regime for enamel pre-treated for 0 or 3h in demineralisation solution. Error Bars represent SE of the mean. n=3.*

Progress of Fluorescence Loss over 72h Demineralisation

No Pre-Treatment:

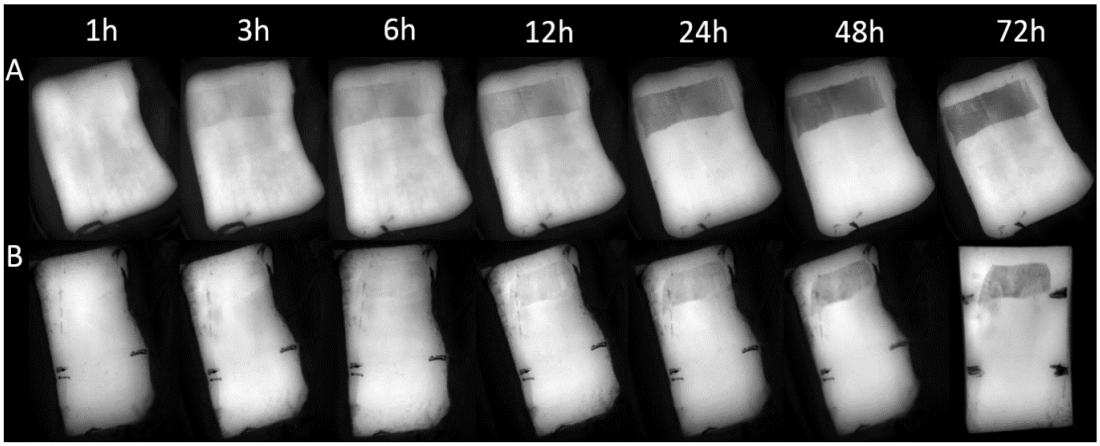

Figure 4.12: Visual MSI Lesion Progression in Non-Pre-Treated Enamel subjected to 0 or 20d pH-cycling. *Images captured using MSI demonstrating longitudinal lesion formation in non-pre-treated enamel subjected to pH-cycling for 0 (A) or 20d (B) and a subsequent 72h demineralisation.*

When MSI images of lesion progression over a 72h demineralisation period were examined, a dark area was first faintly visible at the 3h period for un-cycled enamel and 6h for that exposed to a 20-day pH-cycling regime (Figure 4.12). Furthermore, a lesion was clearly visible from 6 days for un-cycled enamel and 12h for pH-cycled counterparts. All observed lesions created on 20-day pH-cycled enamel appeared lighter and more variable in appearance when compared to non-cycled enamel controls subjected to the same demineralisation conditions.

Whilst MSI images showed a visually detectable lesion at 3h for non-cycled enamel, fluorescence loss was detected by the MSI software at the earlier 1h time point (Table 4.6). Similarly, the earliest fluorescence loss values for pH-cycled enamel were detected at 3h, as opposed to the 6h reported from visual examination. Numerically, fluorescence loss values were lower for pH-cycled enamel in comparison to un-cycled controls at all comparable time points, however none of the observed differences demonstrated statistical significance ($P<0.05$). Additionally, fluorescence loss values support the visual observation that lesions were detected at an earlier time point for non-cycled controls (1h) in comparison to enamel exposed to pH-cycling (3h) (Figure 4.13).

	n	0h ± SE	1h ± SE	3h ± SE	6h ± SE	12h ± SE	24h ± SE	48h ± SE	72h ± SE
Non-Cyc	3	0.00 ± 0.00	2.17 ± 2.17	7.87 ± 0.33	10.33 ± 1.02	12.67 ± 1.41	19.20 ± 3.74	22.53 ± 5.60	24.30 ± 6.17
Cyc	3	0.00 ± 0.00	0.00 ± 0.00	7.20 ± 0.36	7.60 ± 0.89	10.33 ± 1.39	12.23 ± 1.17	16.90 ± 1.46	21.37 ± 1.01

Table 4.6: Progression of Fluorescence Loss over 72h for non-pre-treated enamel subjected to 0 or 20d pH-cycling. *MSI-measured ΔF values at 0, 1, 3, 6, 9, 12, 24, 48 and 72h demineralisation time points for non-pre-treated enamel exposed to varying pH-cycling regime lengths. Data is presented with SE of the mean. n=3.*

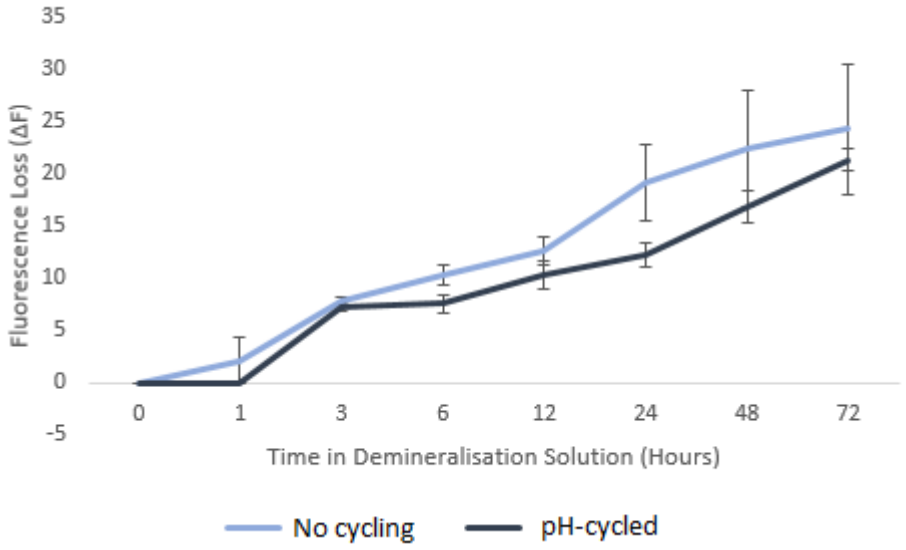

Figure 4.13: Graphical Representation of Demineralisation Progression over 72h for 0 and 20d pH-cycling Exposure. *MSI data expressing ΔF changes over 72h exposure to demineralisation solution for non-pre-treated enamel subjected to 0 or 20d pH-cycling. Error Bars Represent the SE of the mean. n=3.*

3h Pre-treated Enamel:

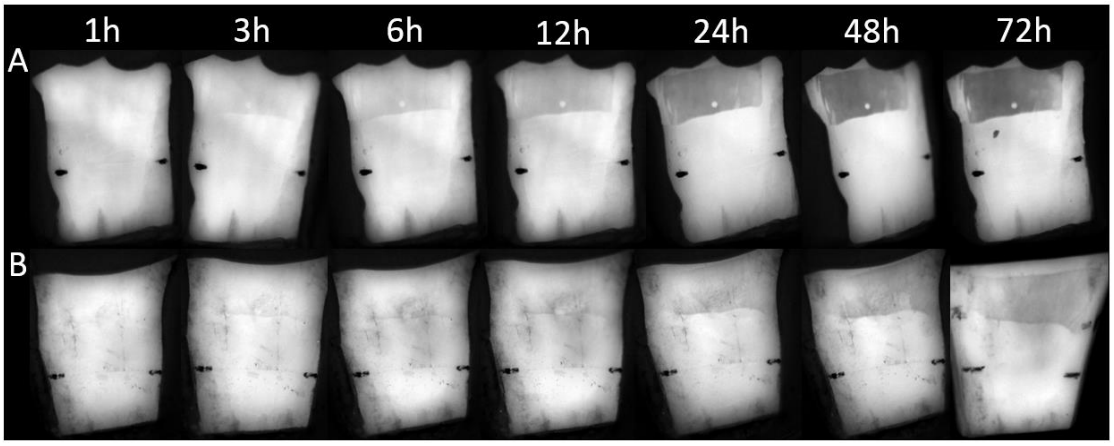

Figure 4.14: Visual MSI Lesion Progression in 3h Pre-treated Enamel subjected to 0 or 20d pH-cycling. *Images captured using MSI demonstrating longitudinal lesion formation in 3h pre-treated enamel subjected to pH-cycling for 0 (A) or 20d (B) and a subsequent 72h demineralisation.*

Visual examination of lesion development over a 72h period using MSI imaging demonstrated that a lesion was first visible by eye at the 3h period for uncycled enamel and 12h for that exposed to pH-cycling for 20days (Figure 4.14). The observed lesion was classed as clearly visible from 6 days for un-cycled enamel as opposed to 24h for pH-cycled counterparts. All lesions observed for enamel subjected to the 20-day pH-cycling regime appeared fainter and more uneven in appearance than those created using non-cycled enamel controls at the same time point during the demineralisation process.

	n	0h ± SE	1h ± SE	3h ± SE	6h ± SE	12h ± SE	24h ± SE	48h ± SE	72h ± SE
Non-Cyc	3	0.00 ± 0.00	2.00 ± 2.00	6.23 ± 0.20	7.30 ± 0.25	10.57 ± 0.91	15.23 ± 1.25	22.23 ± 1.09	24.67 ± 0.77
Cyc	3	0.00 ± 0.00	0.00 ± 0.00	2.33 ± 2.33	7.17 ± 1.17	9.03 ± 1.33	11.57 ± 2.67	15.80 ± 4.97	17.97 ± 6.33

Table 4.7: Progression of Fluorescence Loss over 72h for 3h pre-treated enamel subjected to 0 or 20d pH-cycling. *MSI-measured ΔF values at 0, 1, 3, 6, 9, 12, 24, 48 and 72h demineralisation time points for 3h pre-treated enamel exposed to varying pH-cycling regime lengths. Data is presented with SE of the mean. n=3*

Whilst a dark area was visually detectable at 3h for non-cycled enamel, fluorescence loss was once again detected by the MSI software from the earlier 1h time point (Table 4.7). Similarly, the earliest fluorescence loss values for pH-cycled enamel were detected at 3h, as opposed to the 12h reported from visual examination. Numerically, MSI fluorescence loss values were non-significantly lower for pH-cycled enamel than that not subjected to pH-cycling at all comparable time points ($P<0.05$). The fluorescence loss values obtained demonstrate that lesions were detectable at an earlier time point for non-cycled controls (1h) than enamel exposed to the 20-day pH-cycling regime (3h).

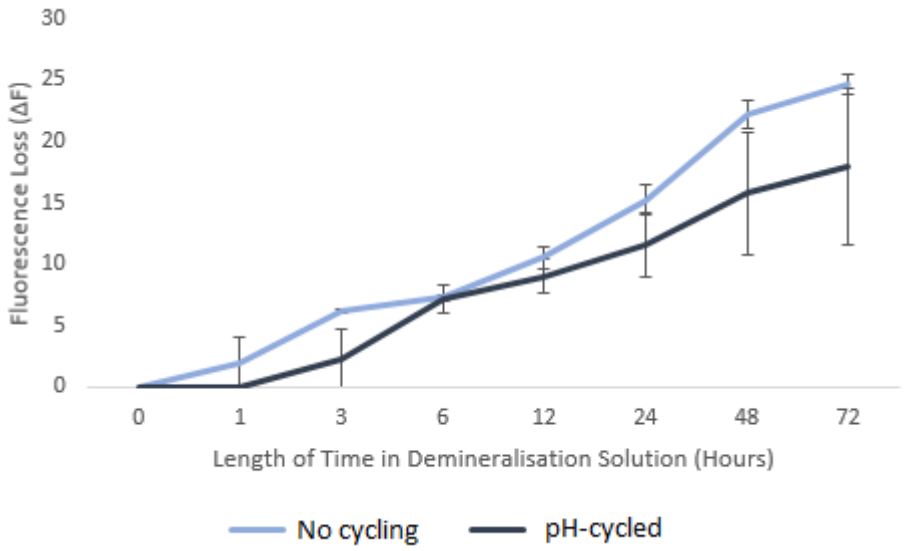

Figure 4.15: Graphical Representation of Demineralisation Progression over 72h for 0 and 20d pH-cycling Exposure. *MSI data expressing ΔF changes over 72h exposure to demineralisation solution for 3h pre-treated enamel subjected to 0 or 20d pH-cycling. Error Bars Represent the SE of the mean. n=3.*

4.4.4 TMR Evaluation of effect of pH-cycling Exposure on Subsequent Mineral Loss

	No pH-Cycling	pH-Cycled
ND	1143.33 ± 56.67	649.17 ± 125.29
3h	1966.12 ± 165.83	565.08 ± 252.58

Table 4.8: Total Mineral Loss 0 vs 20 Days Exposure to pH-cycling. *TMR data for demineralised bovine enamel blocks previously subjected to 0 or 20 days exposure to pH-cycling. Blocks were pre-treated for 0 or 3h in demineralisation solution. Data is presented with the SE of the mean. n=3.*

For enamel not subjected to a demineralisation pre-treatment, a non-significant decrease in mineral loss was observed for enamel subjected to a 20 day pH-cycling regime when considered in relation to non-cycled controls (Table 4.8). A similar

observation was also reported for enamel blocks subjected to a 3h demineralisation pre-treatment. This is presented graphically in Figure 4.16.

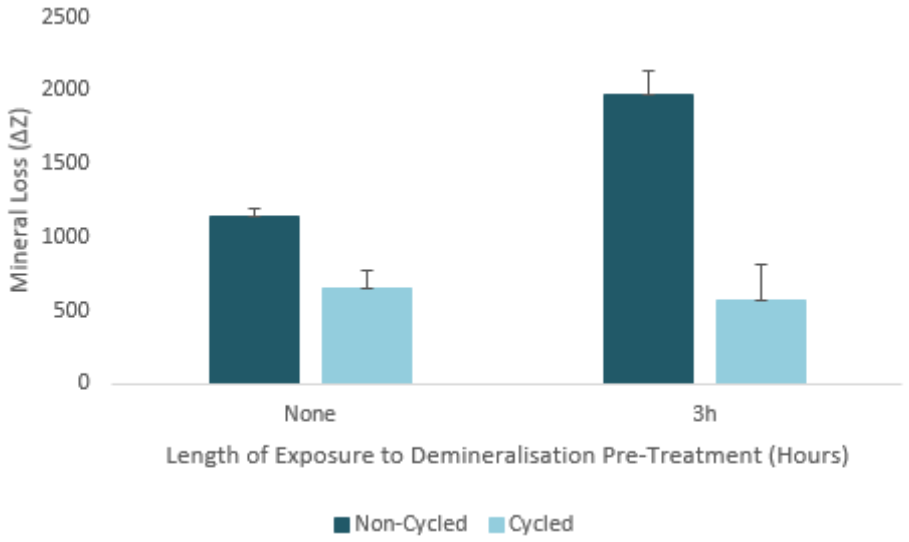

Figure 4.16: Mineral Loss (ΔZ) values following 72h demineralisation as measured using TMR. *Data comparing non-cycled blocks to those exposed to the full 12-day regime for enamel pre-treated for 0 or 3h in demineralisation solution. Error Bars represent SE of the mean. n=3*

In terms of changes in mineral over the depth of the lesion, no pre-treatment group demonstrated a similar profile for both non-cycled and pH-cycled enamel, although lesions created in pH-cycled enamel were smaller (Figure 4.17). In contrast, lesions created in pre-treated enamel had varying profiles depending on whether they were exposed to pH-cycling. Lesions created in non-cycled controls demonstrated a traditional lesion profile, with a defined surface layer, whereas pH-cycled enamel lesions had a much flatter profile, closer to that expected for sound enamel.

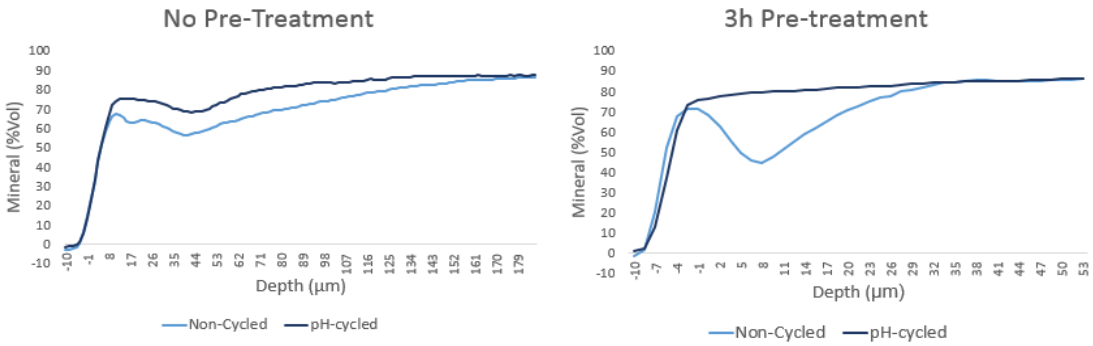

Figure 4.17: Mineral Loss as a Function of Depth. *Lesion profile created from TMR data for lesions created in 0 and 3h demineralisation pre-treated enamel subjected to 0 or 20d pH-cycling.*

4.5 Discussion

One of the limitations of the study presented in the previous chapter was the relatively short length of exposure of the enamel to the pH-cycling regime. It was optimistic to attempt to condense a process that has, in some cases, been reported to take over 10 years (Palti *et. al.* 2008) in to 12 days, however due to the limitations of a PhD project a balance must be found between what is desirable and what is feasible. As such the current work aimed to try and strike such a balance by increasing the length of the pH-cycling regime from 12 to 20 days. Whilst this may still seem a short time, it is worth noting that the effects of PEM have been observed after just 15 months following eruption (Schulte *et. al.* 1999). Additionally, in comparison to the *in vivo* situation, the *in vitro* model used here is simplified and reduced from the natural oral environment and, as such, should have a quicker effect than if an *in situ* or *in vivo* approach were used. It is also worth noting that most reported time frames focus on the point at which PEM is deemed to be complete (Schulte *et. al* 1999, Kataoka *et. al.* 2007, He *et. al.* 2011), as such it is possible that whilst the *in vitro* model outlined here may not succeed in producing “fully matured” enamel, it may still allow the ongoing process to occur and be observed in order to further our understanding.

The data collected appears to support this, as for both 3h demineralisation pre-treatment enamel and non-pre-treated sound enamel the desired decrease in demineralisation for pH-cycled enamel as opposed to non-cycled controls when demineralised was observed for both fluorescence and radiography based methods. Furthermore, enamel subjected to the pH-cycling regime showed detectable demineralisation at a later time point in comparison to controls when subjected to an acid challenge. This provides support for both the ability of the model to represent the PEM process, as well as previous research that has suggested that exposure to the oral environment, particularly acid challenges followed by remineralisation, is able to render the enamel less susceptible to a subsequent acid challenge (Iijima and Takagi 2000, Lagerweij and ten Cate 2006, Maltz *et. al*. 2006).

In the previous chapter, the desirable effects were only observed in enamel subjected to a demineralisation pre-treatment and not sound enamel. It was suggested that this was due to softening of the surface allowing the chemical changes to occur at the surface more easily and helping to compensate for the short length of the pH-cycling regime. Interestingly, the work described here demonstrated very similar effects for both 3h pre-treated and sound enamel when exposed to the 20-day pH-cycling regime. This is promising, as it not only provides support for the use of the longer regime for this model, but also suggested that the model is suitable for use to “mature” sound enamel specimens *in vitro*, which is more desirable for producing work that can be extended to *in vivo* research down the line.

Whilst the developments made to the model in this chapter show promise, there are still several limitations that still need to be addressed. Whilst the sample sizes used are appropriate for initial studies to determine what does and does not work, they are limiting and as such, most of the observed differences between cycled enamel and controls are not deemed to be statistically significant. As such, future studies with

larger samples are needed to verify the findings and to provide support and validation to the model.

Additionally, when reviewing the literature, a focus was placed on the key involvement of ions such as Calcium, Phosphate, Fluoride and Zinc (Brudevold *et. al.* 1963, Briner *et. al.* 1971, Bruun 1973, He *et. al.* 2011) within the PEM process, however the work up to this stage has largely overlooked this. Whilst care has been taken to create pH-cycling solutions representative of plaque-fluid, particularly with regards to Ca and P levels, as opposed to using standard solutions with the stoichemistry of hydroxyapatite, very little care has been taken to introduce F or Zn in to the system. Whilst there are low levels of F present in both the demineralisation and remineralisation solutions, this level is more representative of the base level of F in the plaque fluid and does not take into account the periodic higher levels of F provided by tooth brushing. Furthermore, there is no zinc available from either solution and, as all water used is deionised, there is no availability from the water source either. Reflecting on this it is important that the ongoing work takes into account the importance of such ions within the literature and aims to investigate their role and importance within an *in vitro* PEM model.

Chapter Five: Influence of Zn and F on PEM within an *in vitro* Model

5.1 Background

5.1.1 Zinc and Fluoride and Their Involvement in Caries

Both zinc and fluoride are common features of commercial toothpaste formulations, and have demonstrated anti-microbial properties (van Loveren 1990, Cummins and Creeth 1992). In terms of hard tissue, the protective effect of fluoride is widely established, with the recent caries decline heavily attributed to its use (Brathall *et.al.* 1996), however the role of zinc within caries chemistry is less defined. Data pertaining to the hard tissue effects of zinc is conflicting with it appearing to possess the ability to both enhance mineralisation and inhibit crystal growth dependant on the experimental parameters applied (Brudevold *et. al.* 1963, Dedhiya *et. al.* 1973, LeGeros 1997, Abdullah *et. al.* 2006). In terms of its interaction with fluoride, in certain conditions zinc has been shown to improve remineralisation by stopping the formation of a hypermineralised outer surface area. This may be due to the inhibition of crystal growth at the surface allowing deeper penetration of the fluoride into the lesion.

When this information is considered in the context of PEM, zinc may play a role in allowing fluoride to penetrate the enamel by softening the surface. This would explain why both ions appear to accumulate at the surface shortly after eruption before being gradually lost over time (Brudevold *et. al.* 1963, Weatherell *et. al.* 1972).

5.1.2 Incorporation of Zn and F within the Proposed PEM Model

Building on the work from the previous chapter, the current study aims to refine the proposed pH-cycling model primarily though the inclusion of additional zinc and fluoride

treatments during the pH-cycling regime. Beyond this, the 0 and 20d pH-cycling exposure times and 0 and 3h demineralisation pre-treatments will be continued. The updated model outline can be seen in Figure 5.1 below.

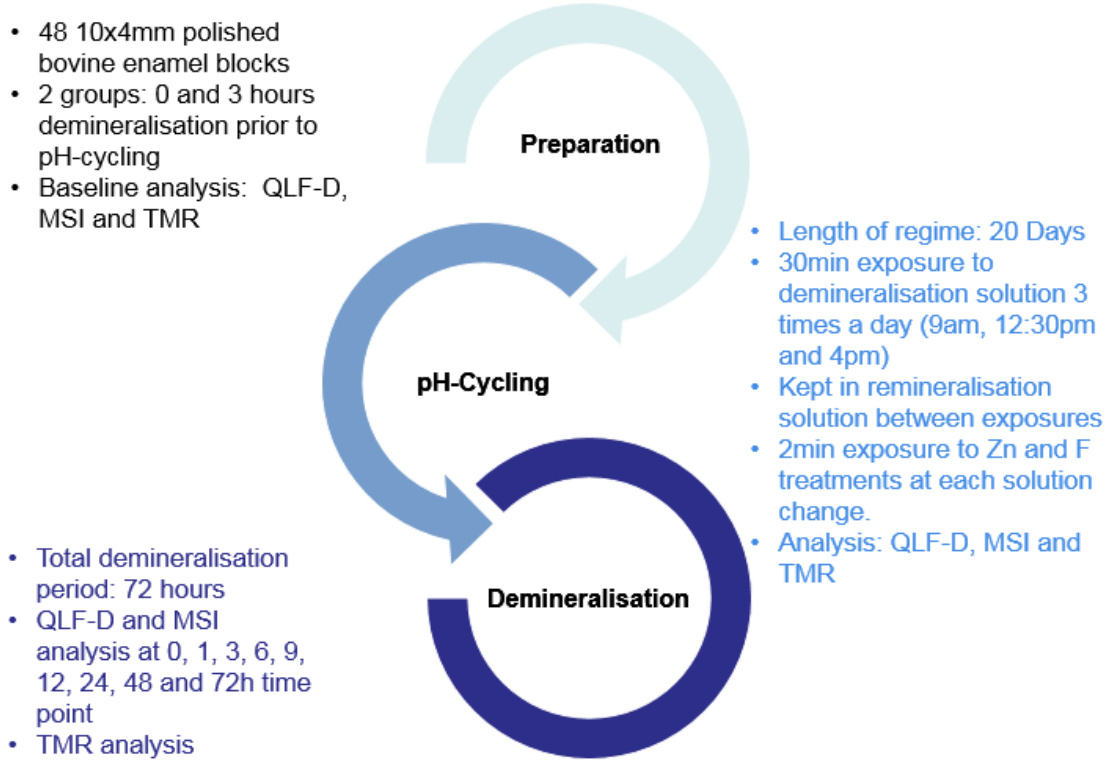

Figure 5.1: Summary of Current Model Protocol. *Outline of the current experimental procedure, broken down into the three stages of the proposed model*

5.2 Aims

The work within this chapter aimed to address some of the concerns about the developed PEM model outlines in the previous chapter, most notably, the lack of external ions such as fluoride and zinc. As such, it aimed to determine whether exposure to fluoride, zinc or a combination of the two served to reduce demineralisation during an acid challenge. Additionally, it aimed to investigate the effect of fluoride, zinc and a combination of the two on enamel exposed to plaque-fluid-relevant pH-cycling conditions.

5.3 Materials and Methods

5.3.1 Selection and Preparation of Bovine Enamel Blocks

48 blocks approximately 10x4mm in size were prepared and mounted from bovine incisors as described previously (Section 2.2). Blocks were subjected to 0 or 3h demineralisation pre-treatment using the PF demineralisation solution (Section 2.3)

5.3.2 pH-Cycling Regime

The pH-cycling regime outlined previously was applied for 0 or 20d (Section 2.5). The regime used in this chapter is presented in Figure 5.2 below:

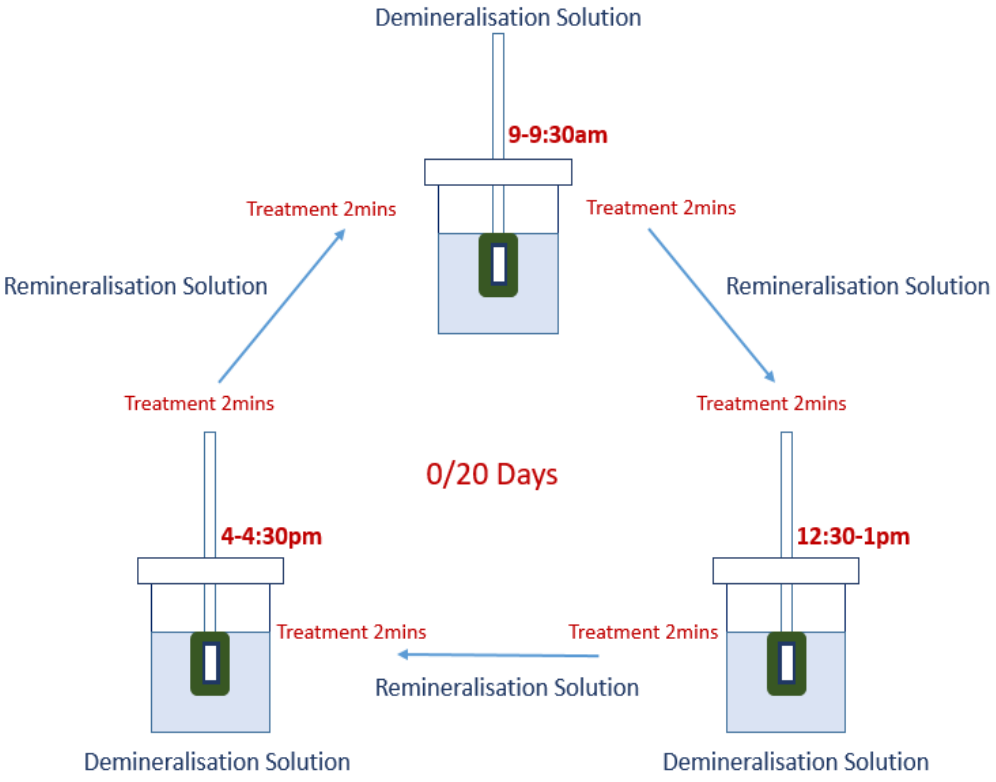

Figure 5.2: Outline of pH-cycling Regime. *Schematic of daily pH-cycling protocol observed for 0 to 20 days. Blocks are kept in remineralisation solution with the exception of three 30min demineralisation periods per day. 2min Zn and F treatments were conducted at each solution change.*

At each solution change blocks were either left as controls or treated for 2mins with either 231µm zinc Sulphate, 228ppm fluoride (as NaF) or a combination of the two. The zinc value was based on previous valued used by Lynch *et. al.* (2011), whilst the 228ppm fluoride was based on levels reported by Vogel *et. al.* (2000) for oral levels following dentifrice use.

5.3.3 Acid Challenge

To test the effect of pH-cycling a standard 72h demineralisation challenge was conducted at outline previously (Section 2.6).

5.3.4 Assessment of Demineralisation

Following demineralisation, blocks were subjected to NCSP, QLF-D, MSI and TMR analysis (Section 2.7-2.10). MSI, QLF-D and TMR measurements were obtained at baseline, following pH-cycling and following 72h demineralisation. In addition, QLF-D and MSI images were also taken at 0, 1, 3, 6, 9, 12, 24, 48h time points during the 72h demineralisation period.

5.4 Results

5.4.1 Effect of pH-cycling on Surface Roughness

No Pre-Treatment:

For blocks not exposed to a demineralisation pre-treatment, surface roughness values obtained by NCSP were highly variable (Table 5.1). As a result, no clear distinction between sound, treated and demineralised enamel could be identified. Data is presented graphically in Figure 5.3 below.

	No Treatment	pH-cycled	Fluoride	Fluoride Cycled	Zinc	Zinc Cycled	Zn/f	Zn/f Cycled
Sound	0.70 ± 0.37	1.28 ± 0.74	0.38 ± 0.04	0.64 ± 0.25	0.35 ± 0.05	0.32 ± 0.03	0.41 ± 0.08	0.54 ± 0.24
Treated	0.54 ± 0.21	0.98 ± 0.45	0.48 ± 0.08	0.53 ± 0.15	0.32 ± 0.04	0.37 ± 0.06	0.38 ± 0.04	0.48 ± 0.23
Lesion	0.49 ± 0.13	1.11 ± 0.62	0.46 ± 0.05	0.50 ± 0.12	0.38 ± 0.08	0.42 ± 0.08	0.66 ± 0.19	0.57 ± 0.31

Table 5.1: Effect of pH-cycling on Surface Roughness (Ra) for Non-pre-treated Enamel. *NCSP data representing surface roughness (Ra) of baseline (sound), pH-cycled and demineralised (Lesion) enamel for both 0 and 20d pH-cycled enamel not subjected to a demineralisation pre-treatment. Data presented along with the standard error of the mean. n=3.*

.

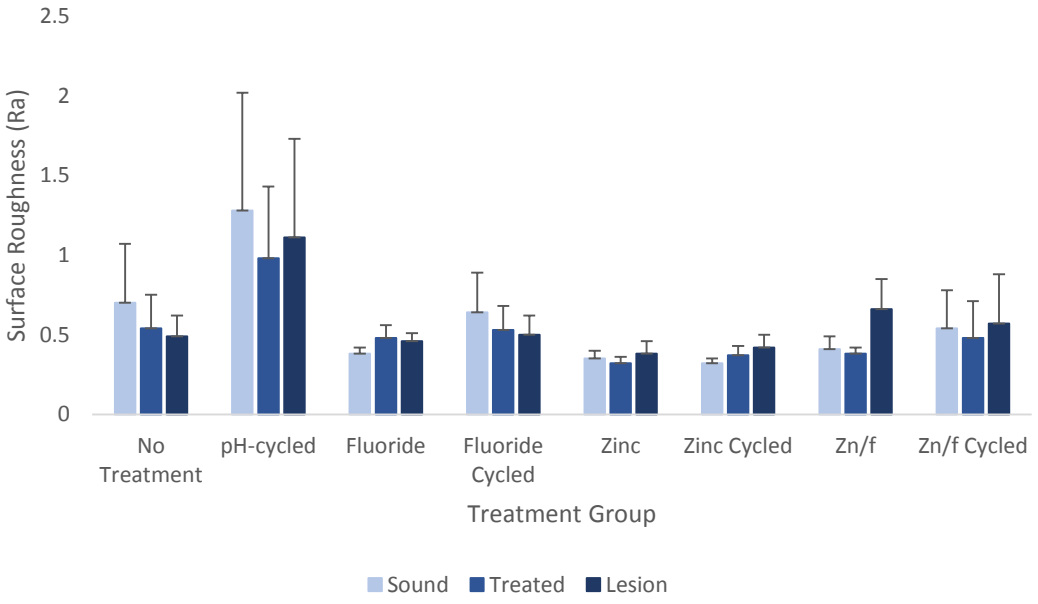

Figure 5.3: Graphical Representation of Changes in Ra. *Average (AVG) surface roughness (Ra) values for Sound, pH-cycled and demineralised enamel as measured using NCSP. Blocks were subjected to 0h demineralisation pre-treatment and 0 or 20d pH-cycling. n=3.*

3h Pre-treated Enamel:

Bovine enamel blocks subjected to a 3h demineralisation pre-treatment also showed highly variable surface roughness (Ra) values (Table 5.2). In a similar manner to untreated blocks, no relationship between surface roughness and the treatment conditions applied could be determined. Data is displayed graphically below in Figure 5.4.

	No Treatment	pH-cycled	Fluoride	Fluoride Cycled	Zinc	Zinc Cycled	Zn/f	Zn/f Cycled
Sound	0.52 ± 0.03	0.36 ± 0.07	0.52 ± 0.23	0.30 ± 0.04	0.86 ± 0.22	0.41 ± 0.02	0.45 ± 0.10	0.30 ± 0.02
Treated	0.45 ± 0.03	0.35 ± 0.06	0.55 ± 0.26	0.30 ± 0.04	0.75 ± 0.26	0.39 ± 0.02	0.44 ± 0.18	0.24 ± 0.02
Lesion	0.96 ± 0.36	0.35 ± 0.04	0.48 ± 0.14	0.32 ± 0.02	0.88 ± 0.14	0.47 ± 0.08	0.57 ± 0.26	0.27 ± 0.07

Table 5.2: Effect of pH-cycling on Surface Roughness (Ra) for 3h Pre-treated Enamel. *NCSP data representing surface roughness (Ra) of baseline (sound), pH-cycled and demineralised (Lesion) enamel for both 0 and 20d pH-cycled enamel subjected to a 3h demineralisation pre-treatment. Data presented along with the standard error of the mean. n=3.*

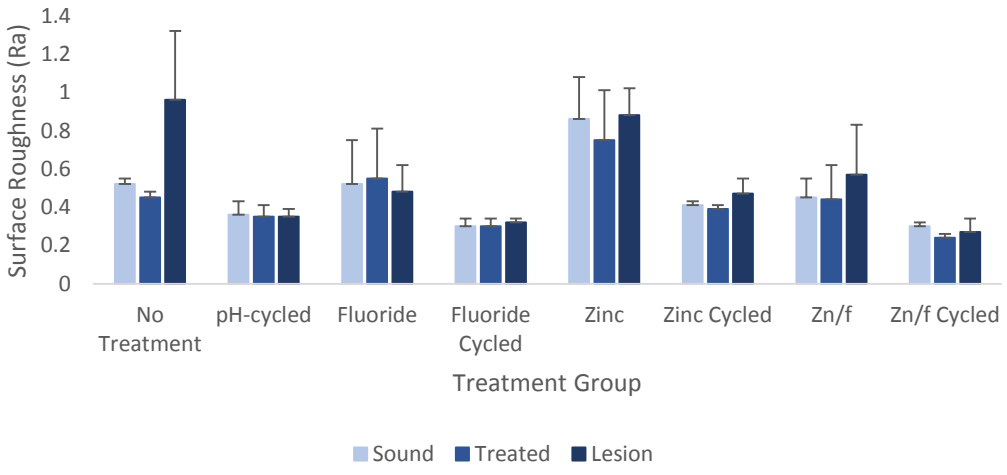

Figure 5.4: Graphical Representation of Changes in Ra. *Average (AVG) surface roughness (Ra) values for Sound, pH-cycled and demineralised enamel as measured using NCSP. Blocks were subjected to 3h demineralisation pre-treatment and 0 or 20d pH-cycling. n=3*

5.4.2 QLF-D Assessment of Fluorescence Loss

Total Fluorescence Loss

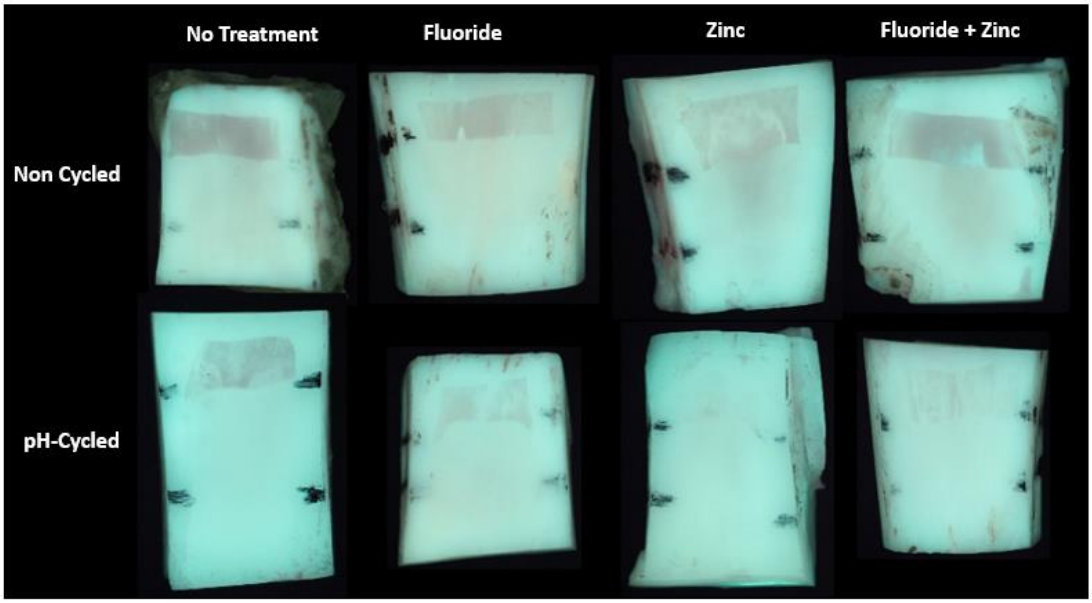

Figure 5.5: QLF-D Images Comparing Lesions Created in Non-pre-treated Cycled and Non-Cycled Enamel. *QLF-D images captured for lesions created in non-pre-treated enamel subjected to 0 or 20d pH-cycling in the presence of Zn and F.*

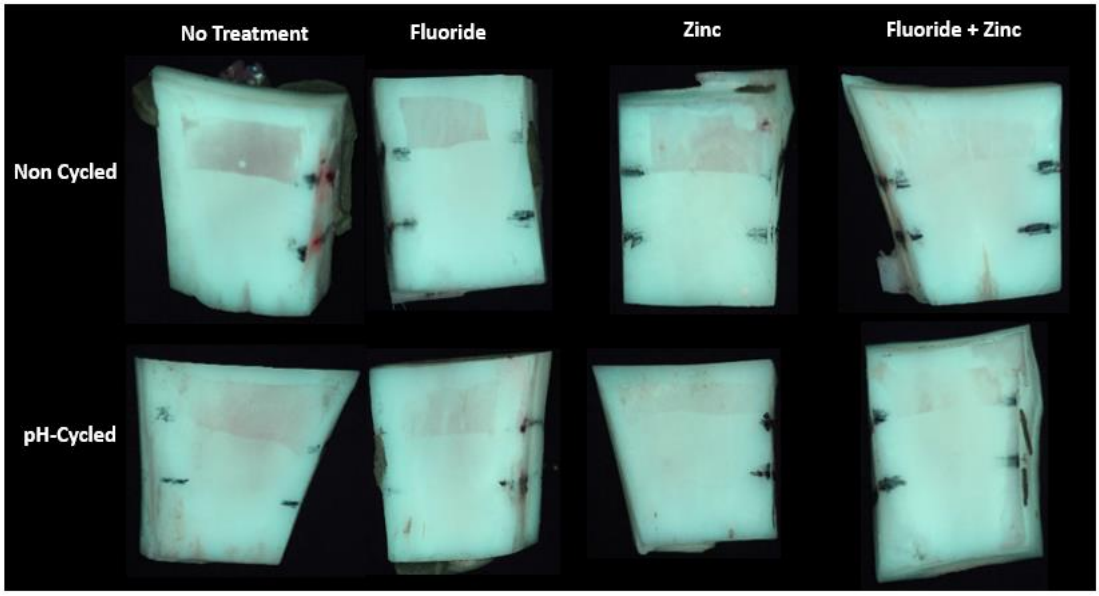

Figure 5.6: QLF-D Images Comparing Lesions Created in 3h Pre-treated Cycled and Non-Cycled Enamel. *QLF-D images captured for lesions created in 3h pre-treated enamel subjected to 0 or 20d pH-cycling in the presence of Zn and F.*

When acquired QLF-D images are examined visually (Figure 5.5), lesions created in non-cycled enamel appeared darker and more uniform than counterparts created in enamel subjected to a 20-day pH-cycling regime. Furthermore, the same effect was seen for lesions created in enamel exposed to fluoride and zinc treatments in conjunction with cycling regimes when contrasted to Zn and F treatments alone. Visual observations for 3h pre-treated enamel follow a similar pattern (Figure 5.6).

	Pre-Treatment	n	Non-Cycled ΔF ± SE	Cycled ΔF ± SE
Untreated	None	3	13.00 ± 5.48	10.33 ± 2.67
	3h	3	13.23 ± 3.35	8.47 ± 4.97
F	None	3	10.33 ± 2.17	8.47 ± 2.67
	3h	3	9.13 ± 0.12	8.47 ± 0.95
Zn	None	3	12.03 ± 4.33	8.7 ± 0.26
	3h	3	7.83 ± 1.56	7.8 ± 0.60
Zn +F	None	3	11.07 ± 4.45	7.37 ± 0.93
	3h	3	8.13 ± 1.17	8.37 ± 1.65

Table 5.3: Total Fluorescence Loss Measured by QLF-D. *QLF-D data for demineralised bovine enamel blocks previously subjected to 0 or 20 days exposure to pH-cycling. Blocks were pre-treated for 0 or 3h in demineralisation solution and assigned to Zn and F treatment groups. Data is presented with the SE of the mean. n=3.*

For enamel blocks in the no pre-treatment group, a non-significant decrease in fluorescence loss was observed for all blocks subjected to 20 days pH-cycling when compared with non-cycled controls (Table 5.3). The greatest difference in fluorescence loss (3.70) observed between cycled and non-cycled enamel was reported for blocks subjected to additional Zn/F treatments at each solution change (Figure 5.7). For blocks subjected to a 3h demineralisation pre-treatment a non-significant decrease in fluorescence loss was observed for cycled blocks that were not subjected to treatments and those treated with F only, when related to non-cycled controls. Very little to no

differences (<1) were observed between cycled and non-cycled enamel treated with Zn or Zn/F (Figure 5.8).

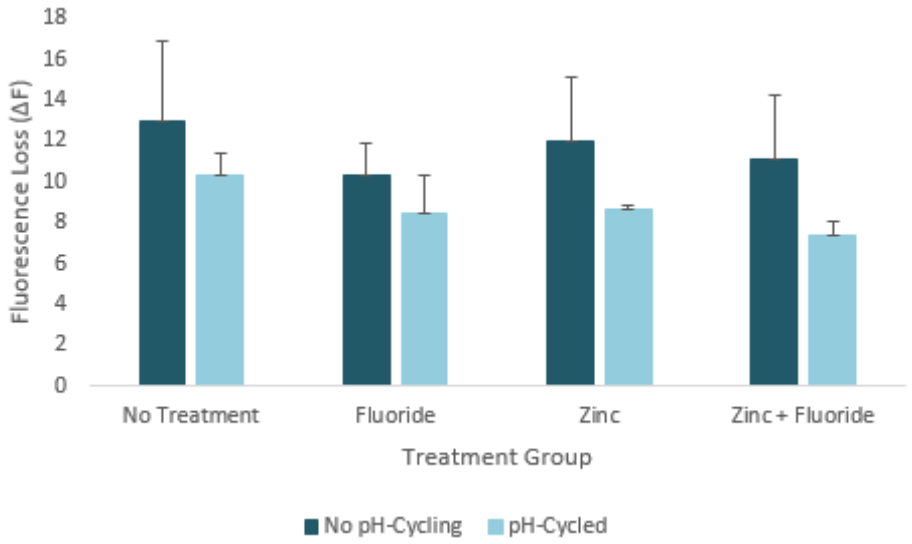

Figure 5.7: Fluorescence loss (ΔF) values following 72h demineralisation as measured using QLF-D for Non-pre-treated Enamel. *Data comparing non-cycled blocks to those exposed to 20-day regime in addition to Zn and F treatments for enamel pre-treated for 0h in demineralisation solution. Error Bars represent SE of the mean. n=3.*

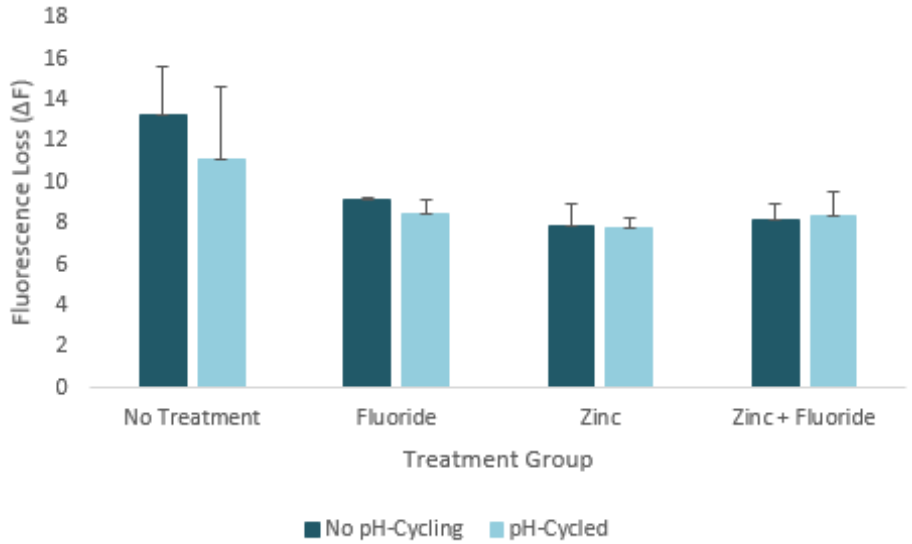

Figure 5.8: Fluorescence loss (ΔF) values following 72h demineralisation as measured using QLF-D for 3h Pre-treated Enamel. *Data comparing non-cycled blocks to those exposed to 20-day regime in addition to Zn and F treatments for enamel pre-treated for 3h in demineralisation solution. Error Bars represent SE of the mean. n=3.*

Progress of Fluorescence Loss over 72h Demineralisation Period

No Pre-Treatment:

When the progression of lesions formed in no pre-treatment group subjected to fluoride/zinc treatments are examined visually (Figures 5.9-5.11), created lesions can be detected at an earlier time point when created in non-cycled enamel in comparison to that subjected to a 20-day pH-cycling regime. Additionally, the lesions produced in pH-cycled enamel appear lighter and less even than non-cycled counterparts in a similar manner to the previous chapters.

The quantitative fluorescence loss values calculated using the QLF-D system support the observations made during visual analysis, with lesion progression occurring later in the 72h period and to a lesser extent for enamel subjected to pH-cycling in comparison to equivalent non-cycled controls (Table 5.4). Differences in ΔF between cycled enamel and non-cycled controls were significant for F: 6 and 9h (P=0.0001), Zn: 12h (P=0.0001) and Zn/F: 6h (P=0.0011). It was also noted that when presented graphically (Figure 5.12), lesion progression in blocks pH-cycled in conditions containing fluoride treatments occurred at a faster rate than for non-cycled controls.

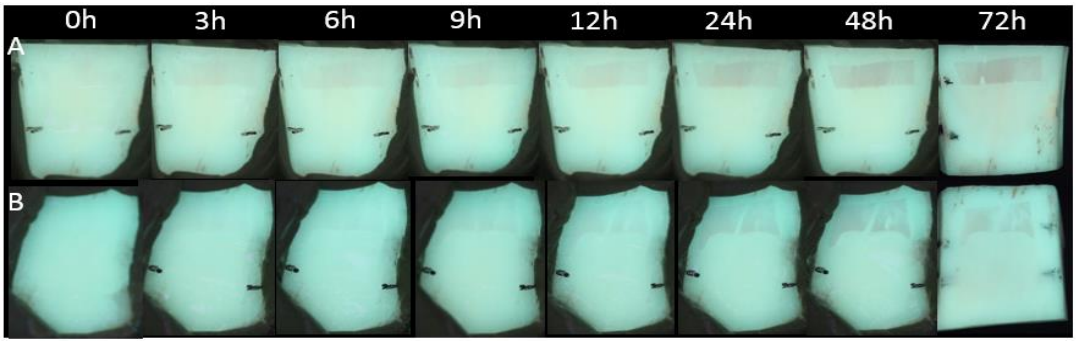

Figure 5.9: Visual QLF-D Lesion Progression in Non-Pre-Treated Enamel subjected to 0 or 20d pH-cycling and F Treatments. *Images captured using QLF-D demonstrating longitudinal lesion formation in non-pre-treated enamel subjected to pH-cycling for 0 (A) or 20d (B), 228ppm NaF Treatments, and a subsequent 72h demineralisation.*

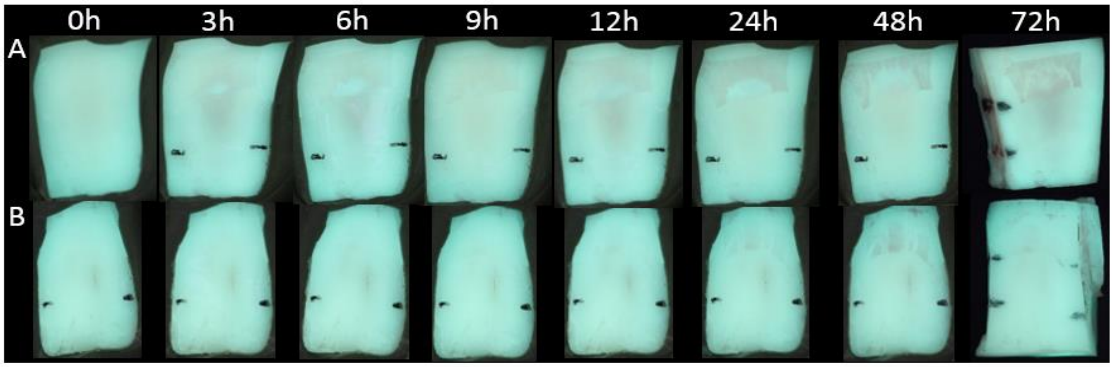

Figure 5.10: Visual QLF-D Lesion Progression in No-Pre-Treated Enamel subjected to 0 or 20d pH-cycling and Zn Treatments. *Images captured using QLF-D demonstrating longitudinal lesion formation in non-pre-treated enamel subjected to pH-cycling for 0 (A) or 20d (B), 231µm $ZnSO_4$ Treatments, and a subsequent 72h demineralisation.*

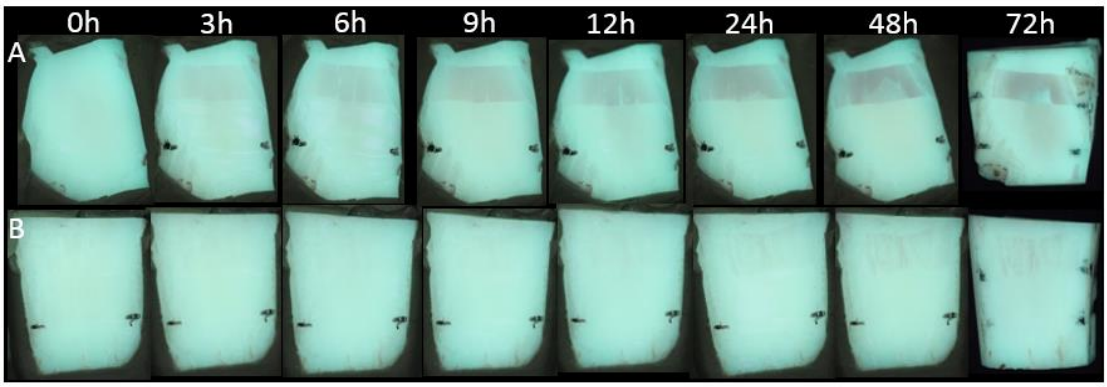

Figure 5.11: Visual QLF-D Lesion Progression in Non-Pre-Treated Enamel subjected to 0 or 20d pH-cycling and Zn/F Treatments. *Images captured using QLF-D demonstrating longitudinal lesion formation in non-pre-treated enamel subjected to pH-cycling for 0 (A) or 20d (B), 228ppm NaF and 231µm $ZnSO_4$ Treatments, and a subsequent 72h demineralisation.*

	n	0h ± SE	1h ± SE	3h ± SE	6h ± SE	9h ± SE	12h ± SE	24h ± SE	48h ± SE	72h ± SE
Non-Cyc	3	0.00 ± 0.00	0.00 ± 0.00	0.00 ± 0.00	6.10 ± 0.26	6.13 ± 0.26	6.93 ± 0.44	9.80 ± 1.42	11.87 ± 2.68	13.00 ± 5.48
Cyc	3	0.00 ± 0.00	0.00 ± 0.00	0.00 ± 0.00	0.00 ± 0.00	1.97 ± 1.97	2.30 ± 2.30	7.63 ± 0.55	10.17 ± 0.55	10.33 ± 2.67
F	3	0.00 ± 0.00	0.00 ± 0.00	0.00 ± 0.00	5.53 ± 0.09	5.70 ± 0.35	5.67 ± 0.15	8.07 ± 0.46	10.33 ± 0.93	10.33 ± 2.17
F Cyc	3	0.00 ± 0.00	0.00 ± 0.00	0.00 ± 0.00	0.00 ± 0.00	0.00 ± 0.00	1.90 ± 1.90	6.43 ± 0.54	8.57 ± 1.52	8.47 ± 2.67
Zn	3	0.00 ± 0.00	0.00 ± 0.00	0.00 ± 0.00	1.83 ± 1.83	4.47 ± 2.40	6.07 ± 0.09	8.73 ± 1.12	11.23 ± 2.52	12.03 ± 4.33
Zn Cyc	3	0.00 ± 0.00	0.00 ± 0.00	0.00 ± 0.00	0.00 ± 0.00	0.00 ± 0.00	0.00 ± 0.00	3.97 ± 2.01	5.07 ± 2.53	8.7 ± 0.26
Zn/F	3	0.00 ± 0.00	0.00 ± 0.00	0.00 ± 0.00	3.83 ± 1.95	3.87 ± 1.96	4.80 ± 2.66	8.83 ± 2.39	9.97 ± 2.38	11.07 ± 4.45
Zn/F Cyc	3	0.00 ± 0.00	0.00 ± 0.00	0.00 ± 0.00	0.00 ± 0.00	0.00 ± 0.00	0.00 ± 0.00	3.90 ± 1.96	6.77 ± 0.74	7.37 ± 0.93

Table 5.4: Progression of Fluorescence Loss over 72h for non-pre-treated enamel subjected to 0 or 20d pH-cycling with Zn and F Treatments. *QLF-D-measured ΔF values at 0, 1, 3, 6, 9, 12, 24, 48 and 72h demineralisation time points for non-pre-treated enamel exposed 0 and 20 pH-cycling (Cyc) in conjunction with Zn and F treatments. Data is presented with SE of the mean. n=3.*

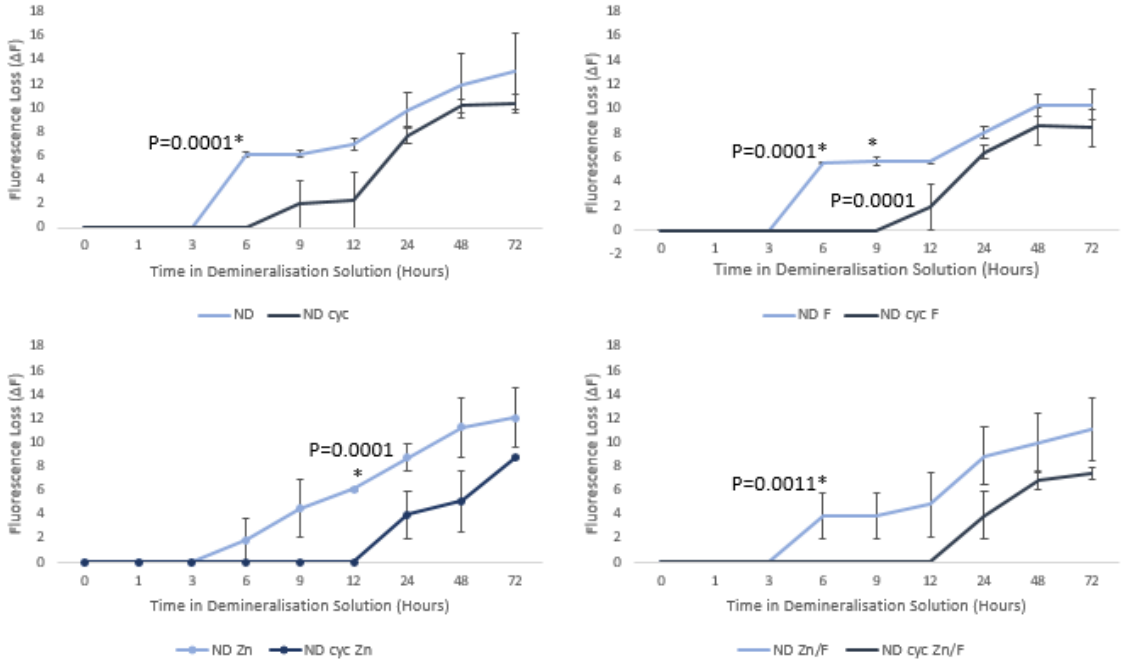

Figure 5.12: Graphical Representation of Demineralisation Progression over 72h for Zn and F Treated enamel with 0 and 20d pH-cycling Exposure. *QLF-D data expressing ΔF changes over 72h exposure to demineralisation solution for non-pre-treated enamel subjected to 0 or 20d pH-cycling in addition to Zn and F treatments. Error Bars Represent the SE of the mean. *= P<0.05. n=3.*

3h Pre-treated Enamel:

When the progression of lesions formed in 3h demineralisation pre-treated enamel treated with fluoride and zinc separately are subject to visual examination (Figure 5.13-5.15), lesions can be detected at an earlier time point for non-cycled enamel in comparison to that subjected to a 20-day pH-cycling regime in a similar manner to that observed for the no pre-treatment group above, however the differences are much less defined. Very little difference was observable between cycled and non-cycled enamel subjected to combined Zn + F treatments.

Numerical fluorescence loss values obtained for 3h pre-treated enamel subjected to both zinc treatment conditions show very similar patterns of lesions progression for both cycled and non-cycled enamel, with non-cycled blocks showing much slower

lesion progression than their non-zinc treated counterparts (Table 5.5). For fluoride-only treated enamel, results were more similar to those observed for non-pre-treated enamel previously, although the difference was less marked. ΔF values are presented in Figure 5.16.

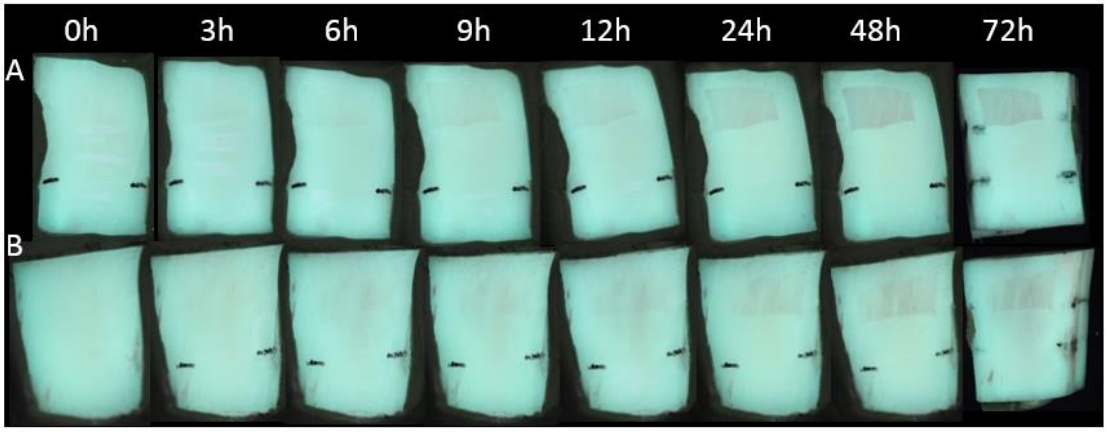

Figure 5.13: Visual QLF-D Lesion Progression in 3h Pre-treated Enamel subjected to 0 or 20d pH-cycling and F Treatments. *Images captured using QLF-D demonstrating longitudinal lesion formation in 3h pre-treated enamel subjected to pH-cycling for 0 (A) or 20d (B), 228ppm NaF Treatments, and a subsequent 72h demineralisation.*

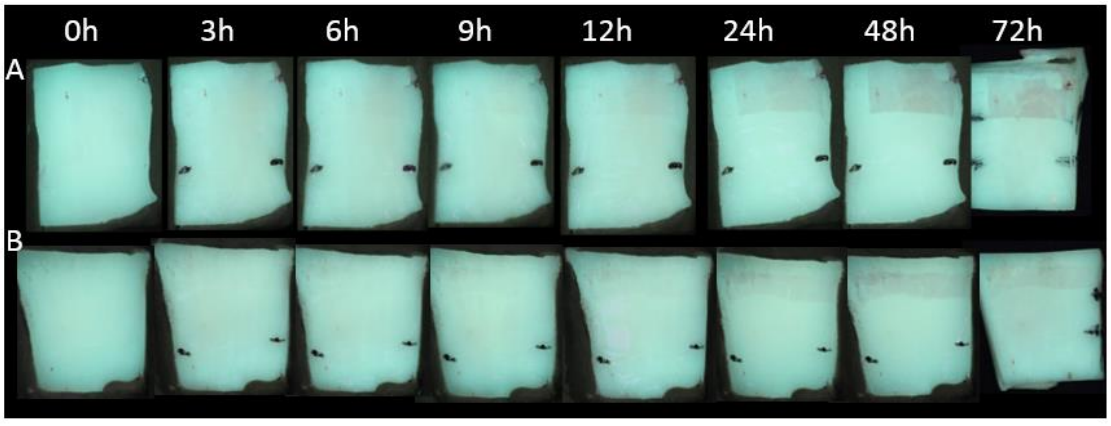

Figure 5.14: Visual QLF-D Lesion Progression in 3h Pre-treated Enamel subjected to 0 or 20d pH-cycling and Zn Treatments. *Images captured using QLF-D demonstrating longitudinal lesion formation in 3h pre-treated enamel subjected to pH-cycling for 0 (A) or 20d (B), 231µm $ZnSO_4$ Treatments, and a subsequent 72h demineralisation.*

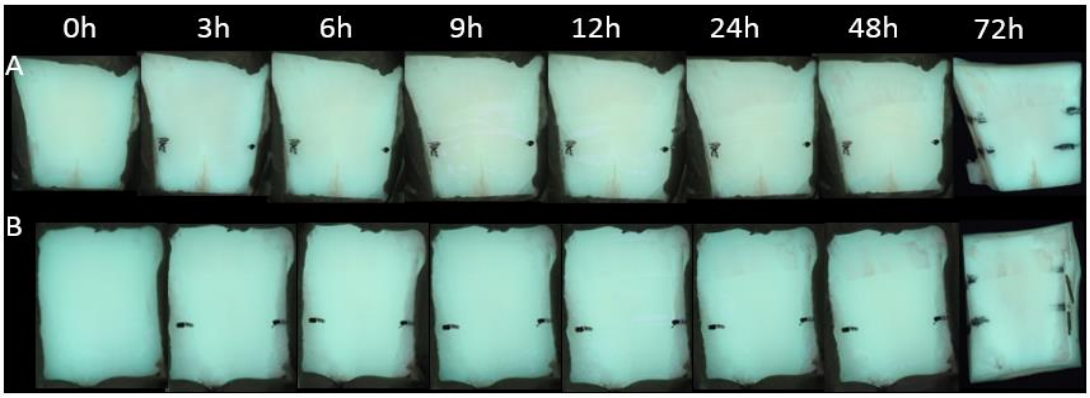

Figure 5.15: Visual QLF-D Lesion Progression in 3h Pre-treated Enamel subjected to 0 or 20d pH-cycling and Zn/F Treatments. *Images captured using QLF-D demonstrating longitudinal lesion formation in 3h pre-treated enamel subjected to pH-cycling for 0 (A) or 20d (B), 228ppm NaF and 231µm $ZnSO_4$ Treatments, and a subsequent 72h demineralisation.*

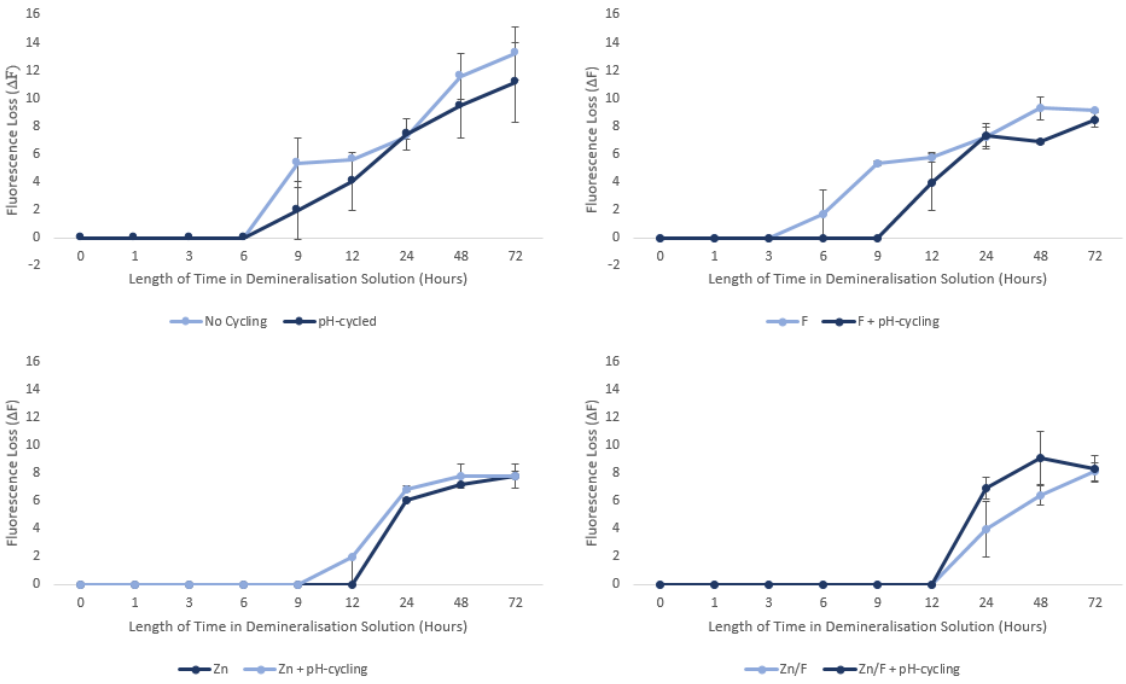

0Figure 5.16: Graphical Representation of Demineralisation Progression over 72h for Zn and F Treated enamel with 0 and 20d pH-cycling Exposure. *QLF-D data expressing ΔF changes over 72h exposure to demineralisation solution for 3h pre-treated enamel subjected to 0 or 20d pH-cycling in addition to Zn and F treatments. Error Bars Represent the SE of the mean. n=3.*

	n	0h ± SE	1h ± SE	3h ± SE	6h ± SE	9h ± SE	12h ± SE	24h ± SE	48h ± SE	72h ± SE
Non-Cyc	3	0.00 ± 0.00	0.00 ± 0.00	0.00 ± 0.00	0.00 ± 0.00	1.77 ± 1.77	5.60 ± 0.00	7.27 ± 0.18	11.60 ± 1,65	13.23 ± 3.35
Cyc	3	0.00 ± 0.00	0.00 ± 0.00	0.00 ± 0.00	0.00 ± 0.00	4.13 ± 2.07	4.07 ± 2.05	7.43 ± 1.13	9.47 ± 2.27	8.47 ± 4.97
F	3	0.00 ± 0.00	0.00 ± 0.00	0.00 ± 0.00	1.73 ± 1.73	5.37 ± 0.17	5.77 ± 0.32	7.27 ± 0.72	9.30 ± 0.85	9.13 ± 0.12
F Cyc	3	0.00 ± 0.00	0.00 ± 0.00	0.00 ± 0.00	0.00 ± 0.00	0.00 ± 0.00	4.00 ± 2.01	7.30 ± 0.87	6.90 ± 0.21	8.47 ± 0.95
Zn	3	0.00 ± 0.00	0.00 ± 0.00	0.00 ± 0.00	0.00 ± 0.00	0.00 ± 0.00	0.00 ± 0.00	6.03 ± 0.22	7.23 ± 0.91	7.83 ± 1.56
Zn Cyc	3	0.00 ± 0.00	0.00 ± 0.00	0.00 ± 0.00	0.00 ± 0.00	0.00 ± 0.00	2.00 ± 2.00	6.87 ± 0.22	7.80 ± 0.61	7.8 ± 0.60
Zn/F	3	0.00 ± 0.00	0.00 ± 0.00	0.00 ± 0.00	0.00 ± 0.00	0.00 ± 0.00	0.00 ± 0.00	3.97 ± 1.99	6.40 ± 0.70	8.13 ± 1.17
Zn/F Cyc	3	0.00 ± 0.00	0.00 ± 0.00	0.00 ± 0.00	0.00 ± 0.00	0.00 ± 0.00	0.00 ± 0.00	6.97 ± 0.78	9.10 ± 1.90	8.37 ± 1.65

Table 5.5: Progression of Fluorescence Loss over 72h for 3h pre-treated enamel subjected to 0 or 20d pH-cycling with Zn and F Treatments. *QLF-D-measured ΔF values at 0, 1, 3, 6, 9, 12, 24, 48 and 72h demineralisation time points for 3h pre-treated enamel exposed 0 and 20 pH-cycling in conjunction with Zn and F treatments. Data is presented with SE of the mean. n=3.*

5.4.3 Impact of Treatment Groups on Demineralisation measured via QLF-D

	n	Untreated ΔF ± SE	Treated ΔF ± SE
pH-Cycling	12	10.60 ± 0.74	8.83 ± 0.45
F	6	11.93 ± 0.71	9.09 ± 1.00
Zn	6	11.93 ± 0.71	9.10 ± 0.44
Zn +F	6	11.93 ± 0.71	8.73 ± 0.81

Table 5.6: Effect of Treatment Groups on ΔF as Measured using QLF-D.

Fluorescence loss values obtained via QLF-D for lesions created in enamel subjected to pH-cycling, F, Zn and Zn/F treatments and non-treated controls. Data is presented with the SE of the mean and n values.

In order to investigate the effects of the different treatments conditions, data was grouped into treated and untreated enamel based on the following criteria: pH-cycling, F, Zn and Zn/F (Table 5.6). A decrease in fluorescence loss was observed between treated and untreated blocks for each criterion, however only the difference between pH-cycled and non-cycled control blocks was significant (P=0.008). Values are presented graphically in Figure 5.17.

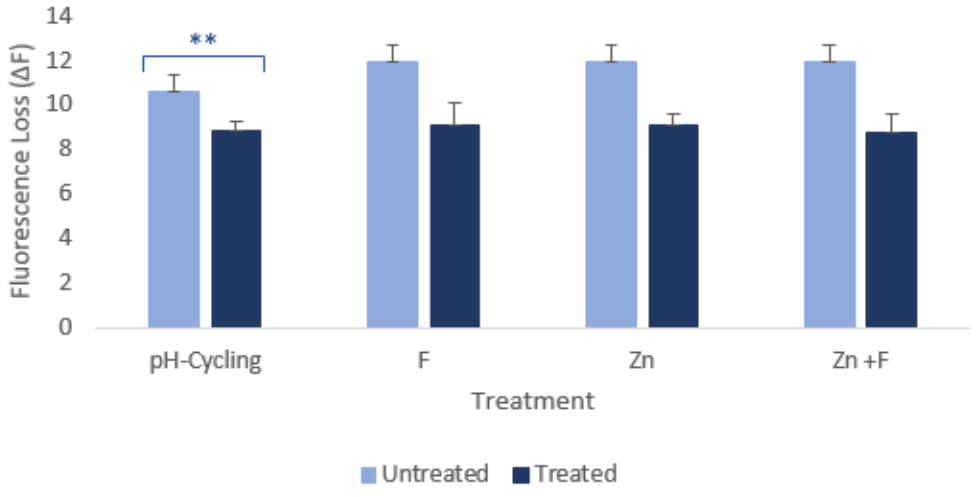

Figure 5.17: ΔF Measured using QLF-D for Varying Treatment Groups.

*Fluorescence loss values obtained via QLF-D for lesions created in enamel subjected to pH-cycling, F, Zn and Zn/F treatments and non-treated controls. Error bars represent the SE of the mean. **=P<0.01. n values are reported in Table 5.4.*

5.4.4 Effect of pH-cycling on demineralisation as measured via MSI

Total Fluorescence Loss

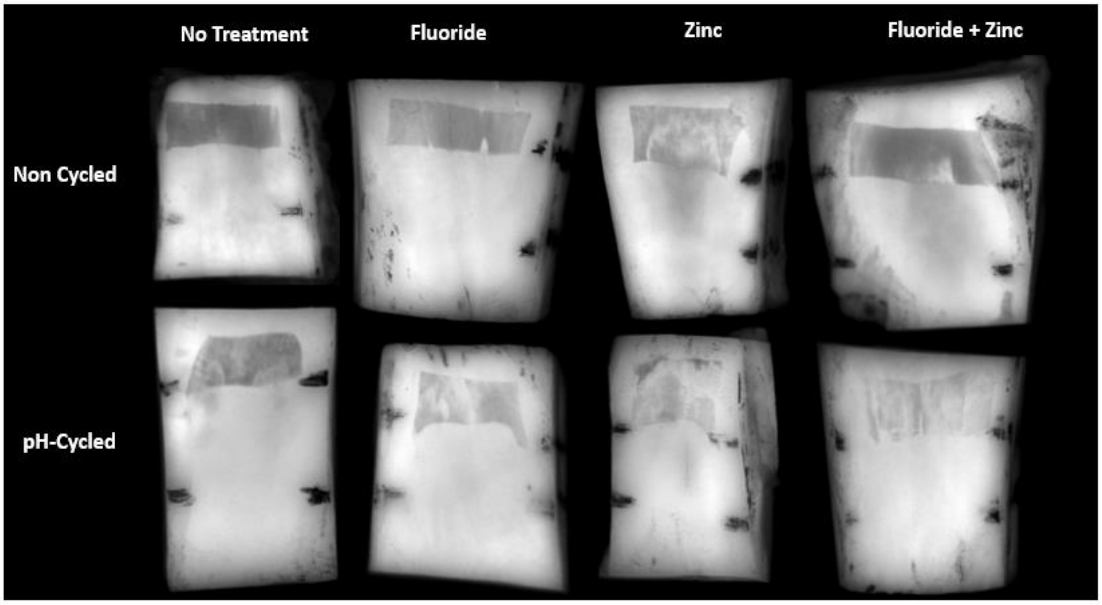

Figure 5.18: MSI Images Comparing Lesions Created in Non-pre-treated Cycled and Non-Cycled Enamel. *MSI images captured for lesions created in non-pre-treated enamel subjected to 0 or 20d pH-cycling in the presence of Zn and F.*

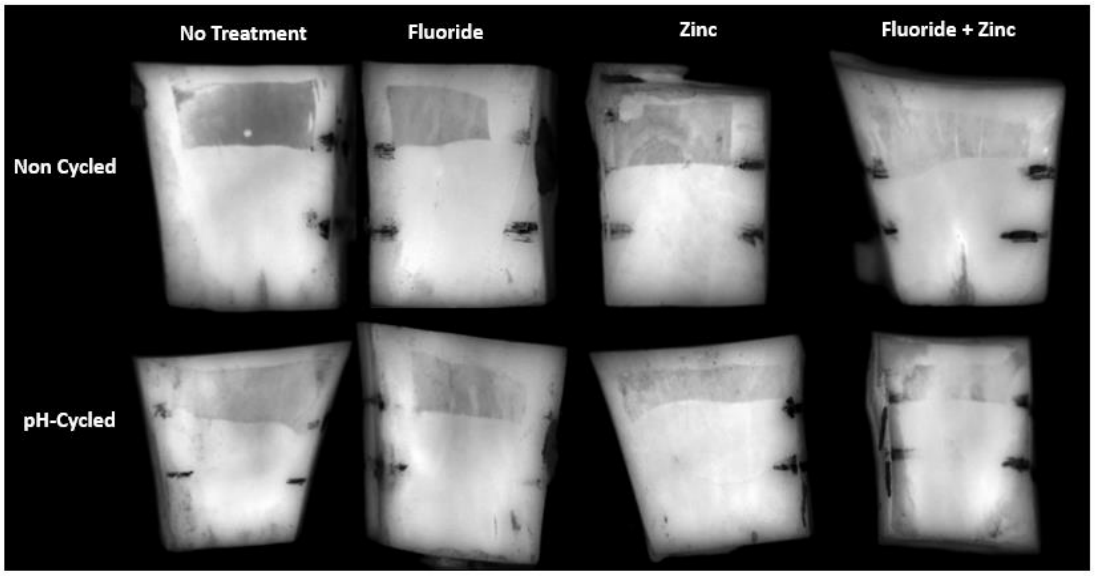

Figure 5.19: MSI Images Comparing Lesions Created in 3h pre-treated Cycled and Non-Cycled Enamel. *MSI images captured for lesions created in 3h pre-treated enamel subjected to 0 or 20d pH-cycling in the presence of Zn and F.*

Visual analysis of the progression of lesions formed in non-pre-treated enamel subjected to fluoride/zinc treatments demonstrate a visual change at an earlier time point for non-cycled enamel in comparison to that subjected to a 20-day pH-cycling regime (Figure 5.18). In a similar manner to previously observed, lesions produced in pH-cycled enamel appear lighter and less even than non-cycled counterparts. Visual observations for 3h demineralisation-pre-treated enamel display similar results (Figure 5.19), although little change in lesion appearance was observed for enamel treated with both Zn and F together.

	Pre-Treatment	n	Non-Cycled ΔF ± SE	Cycled ΔF ± SE
Untreated	None	3	24.30 ± 7.56	21.37 ± 1.24
	3h	3	24.67 ± 1.33	17.97 ± 10.96
F	None	3	20.83 ± 2.76	15.73 ± 5.24
	3h	3	20.60 ± 1.66	17.47 ± 4.67
Zn	None	3	20.93 ± 6.79	13.50 ± 1.90
	3h	3	16.53 ± 3.04	15.87 ± 0.95
Zn +F	None	3	23.17 ± 6.47	11.53 ± 2.79
	3h	3	15.40 ± 3.29	15.20 ± 4.28

Table 5.7: Total Fluorescence Loss Measured by MSI. *MSI data for demineralised bovine enamel blocks previously subjected to 0 or 20 days exposure to pH-cycling. Blocks were pre-treated for 0 or 3h in demineralisation solution and assigned to Zn and F treatment groups. Data is presented with the SE of the mean. n=3.*

For blocks in the no pre-treatment group, a non-significant decrease in fluorescence loss was observed for all blocks subjected to 20 days pH-cycling when compared with non-cycled controls (Table 5.7). The greatest difference in fluorescence loss (11.64) observed between cycled and non-cycled enamel was observed for blocks also subjected to additional Zn/F treatments at each change (Figure 5.20). For blocks subjected to a 3h demineralisation pre-treatment a non-significant decrease in

fluorescence loss was observed for cycled blocks that were not subjected to treatments and those treated with F only, when related to non-cycled controls. Very little to no differences (<1) were observed between cycled and non-cycled enamel treated with Zn or Zn/F (Figure 5.21).

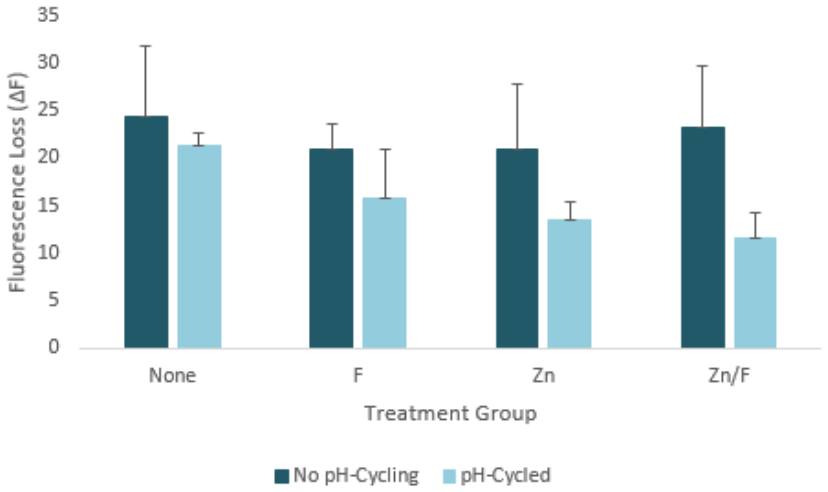

Figure 5.20: Fluorescence loss (ΔF) values following 72h demineralisation as measured using MSI for Non-pre-treated Enamel. *Data comparing non-cycled blocks to those exposed to 20-day regime in addition to Zn and F treatments for enamel pre-treated for 0h in demineralisation solution. Error Bars represent SE of the mean. n=3.*

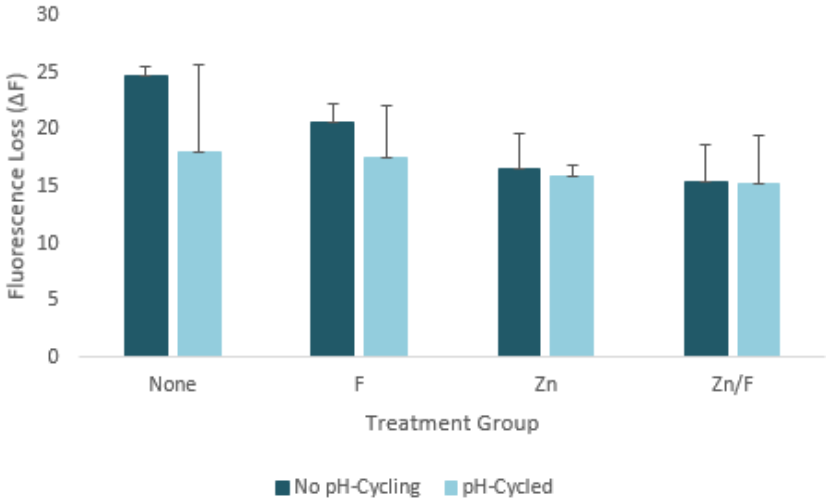

Figure 5.21: Fluorescence loss (ΔF) values following 72h demineralisation as measured using MSI for 3h Pre-treated Enamel. *Data comparing non-cycled blocks to those exposed to 20-day regime in addition to Zn and F treatments for enamel pre-treated for 3h in demineralisation solution. Error Bars represent SE of the mean. n=3.*

Progress of Fluorescence Loss over 72h Demineralisation

No Pre-Treatment:

When the progression of the lesion during the 72h acid-exposure is observed visually using MSI (Figures 5.22-5.24), lesions produced in enamel subjected to both pH-cycling and individual fluoride and zinc treatments appear less even than non-cycled counterparts. Whilst they also exhibit the slower progression and lighter appearance noted for images taken using the QLF-D system, the difference is less distinguishable. In contrast, a clear reduction in both progression time and lesion intensity was observed for pH-cycled enamel subjected to joint Zn + F treatments. Reported visual differences were mirrored by calculated numerical fluorescence loss values (Table 5.8), with lesion progression occurring later and to a reduced extent for enamel exposed to 20-days pH-cycling. Differences in ΔF between pH-cycled enamel and non-cycled controls were significant for the 6, 12 and 24h time-points for F-treated blocks (P=0.0045, 0.0117 and 0.0377 respectively) and 6h for those treated with Zn (P=0.0019). Data is presented graphically in Figure 5.25 below.

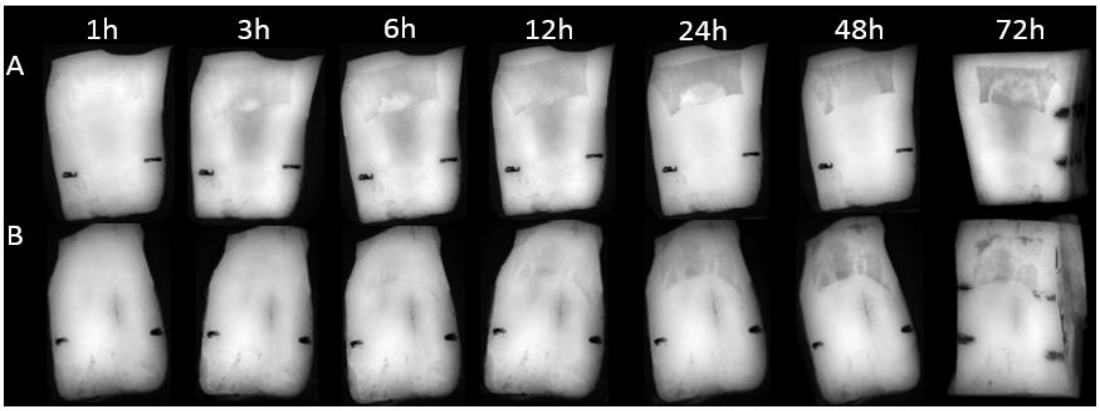

Figure 5.22: Visual MSI Lesion Progression in Non-Pre-Treated Enamel subjected to 0 or 20d pH-cycling and F Treatments. *Images captured using MSI demonstrating longitudinal lesion formation in non-pre-treated enamel subjected to pH-cycling for 0 (A) or 20d (B), 228ppm NaF Treatments, and a subsequent 72h demineralisation*

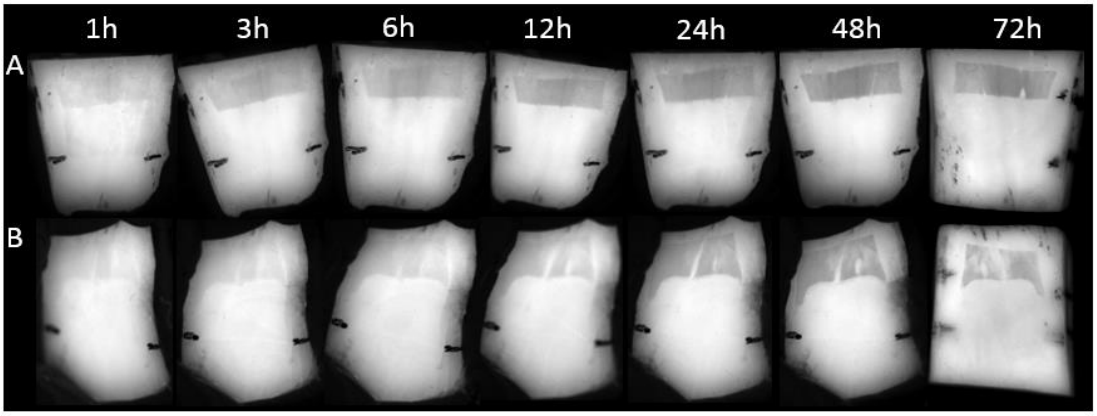

Figure 5.23: Visual MSI Lesion Progression in Non-Pre-Treated Enamel subjected to 0 or 20d pH-cycling and Zn Treatments. *Images captured using MSI demonstrating longitudinal lesion formation in non-pre-treated enamel subjected to pH-cycling for 0 (A) or 20d (B), 231µm $ZnSO_4$ Treatments, and a subsequent 72h demineralisation.*

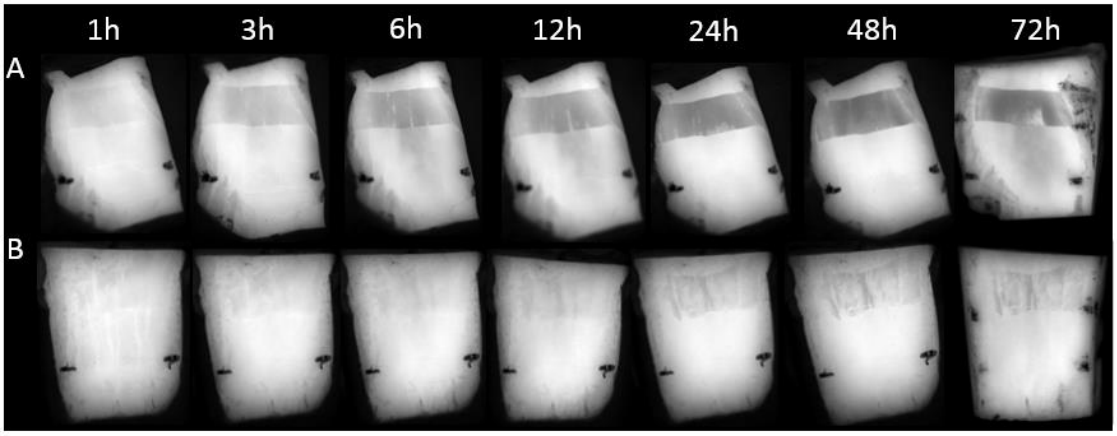

Figure 5.24: Visual MSI Lesion Progression in Non-Pre-Treated Enamel subjected to 0 or 20d pH-cycling and Zn/F Treatments. *Images captured using MSI demonstrating longitudinal lesion formation in non-pre-treated enamel subjected to pH-cycling for 0 (A) or 20d (B), 228ppm NaF and 231µm $ZnSO_4$ Treatments, and a subsequent 72h demineralisation.*

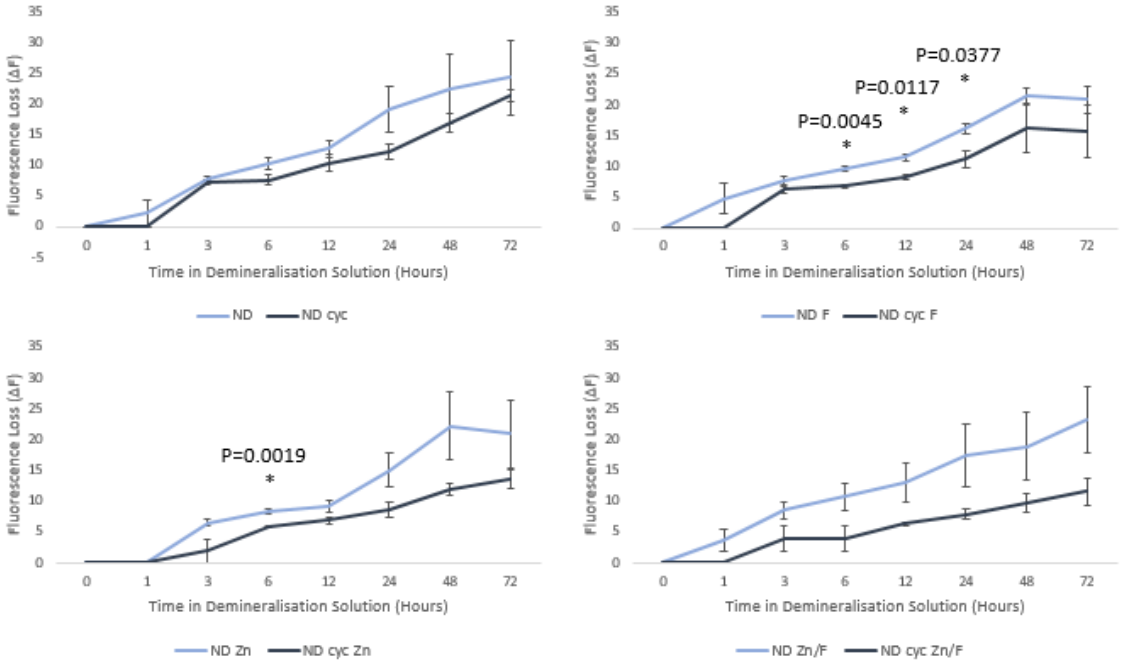

Figure 5.25: Graphical Representation of Demineralisation Progression over 72h for Zn and F Treated enamel with 0 and 20d pH-cycling Exposure. *MSI data expressing ΔF changes over 72h exposure to demineralisation solution for non-pre-treated enamel subjected to 0 or 20d pH-cycling in addition to Zn and F treatments. Error Bars Represent the SE of the mean. *= P<0.05. n=3.*

	n	0h ± SE	1h ± SE	3h ± SE	6h ± SE	12h ± SE	24h ± SE	48h ± SE	72h ± SE
Non-Cyc	3	0.00 ± 0.00	2.17 ± 2.17	7.87 ± 0.33	10.33 ± 1.02	12.67 ± 1.41	19.20 ± 3.74	22.53 ± 5.60	24.30 ± 7.56
Cyc	3	0.00 ± 0.00	0.00 ± 0.00	7.20 ± 0.36	7.60 ± 0.89	10.33 ± 1.39	12.23 ± 1.17	16.90 ± 1.46	21.37 ± 1.24
F	3	0.00 ± 0.00	4.77 ± 2.40	7.70 ± 0.78	9.67 ± 0.37	11.50 ± 0.60	16.20 ± 0.83	21.47 ± 1.23	20.83 ± 2.76
F Cyc	3	0.00 ± 0.00	0.00 ± 0.00	6.20 ± 0.56	6.77 ± 0.34	8.33 ± 0.39	11.17 ± 1.42	16.17 ± 3.88	15.73 ± 5.24
Zn	3	0.00 ± 0.00	0.00 ± 0.00	6.53 ± 0.54	8.37 ± 0.33	9.23 ± 0.92	15.07 ± 2.79	22.17 ± 5.58	20.93 ± 6.79
Zn Cyc	3	0.00 ± 0.00	0.00 ± 0.00	1.93 ± 1.93	5.77 ± 0.15	6.87 ± 0.60	8.53 ± 1.25	11.90 ± 0.92	13.50 ± 1.90
Zn/F	3	0.00 ± 0.00	3.70 ± 1.85	8.50 ± 1.30	10.67 ± 2.15	13.13 ± 3.17	17.40 ± 5.11	18.83 ± 5.49	23.17 ± 6.47
Zn/F Cyc	3	0.00 ± 0.00	0.00 ± 0.00	4.00 ± 2.03	3.90 ± 2.00	6.27 ± 0.27	7.87 ± 0.82	9.73 ± 1.62	11.53 ± 2.79

Table 5.8: Progression of Fluorescence Loss over 72h for non-pre-treated enamel subjected to 0 or 20d pH-cycling with Zn and F Treatments. *MSI-measured ΔF values at 0, 1, 3, 6, 12, 24, 48 and 72h demineralisation time points for non-pre-treated enamel exposed 0 and 20 pH-cycling in conjunction with Zn and F treatments. Data is presented with SE of the mean. n=3.*

3h Pre-Treatment:

When lesion progression is visually examined for lesions created in 3h demineralisation pre-treated enamel, the clear differences observed for the no pre-treatment group are not reflected (Figures 5.26-5.28). Lesions treated with Zn and F treatments appear less defined than untreated controls, but little difference is observed between their pH-cycled and non-cycled variants. Non-treated enamel subjected to pH-cycled shows a visual decrease in lesion appearance in comparison to non-cycled controls.

When considered in numerical terms (Table 5.9), non-treated and F-only treated blocks do appear to demonstrate a mild difference between pH-cycled and non-cycled blocks. Little difference in reported ΔF values was observed between pH-cycled enamel and non-cycled controls when blocks were also subjected to Zn or Zn/F treatments. This is represented graphically in Figure 5.29.

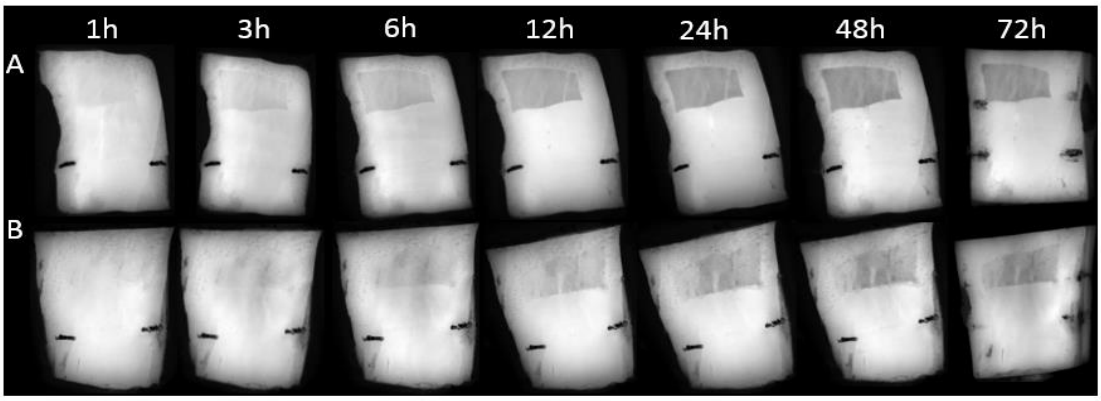

Figure 5.26: Visual MSI Lesion Progression in 3h Pre-treated Enamel subjected to 0 or 20d pH-cycling and F Treatments. *Images captured using MSI demonstrating longitudinal lesion formation in 3h pre-treated enamel subjected to pH-cycling for 0 (A) or 20d (B), 228ppm NaF Treatments, and a subsequent 72h demineralisation.*

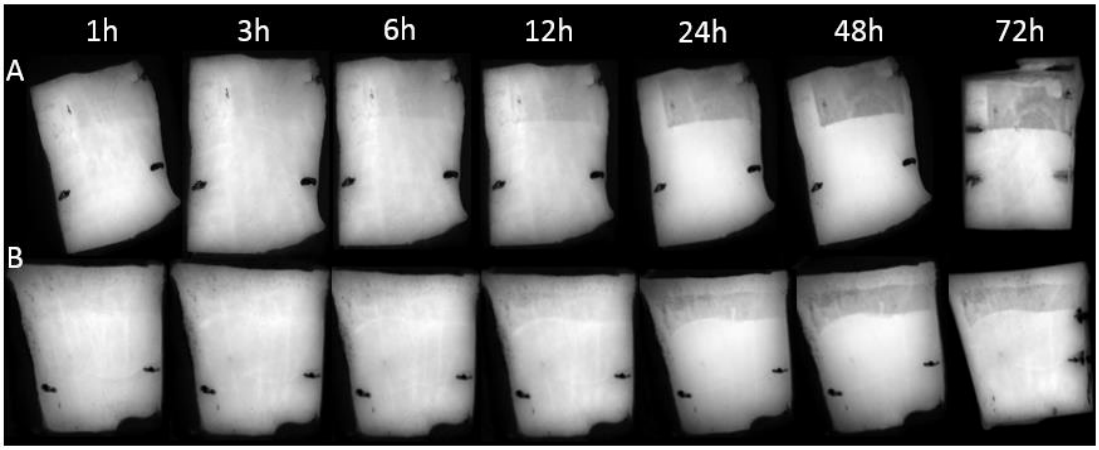

Figure 5.27: Visual MSI Lesion Progression in 3h Pre-treated Enamel subjected to 0 or 20d pH-cycling and Zn Treatments. *Images captured using MSI demonstrating longitudinal lesion formation in 3h pre-treated enamel subjected to pH-cycling for 0 (A) or 20d (B), 231µm $ZnSO_4$ Treatments, and a subsequent 72h demineralisation.*

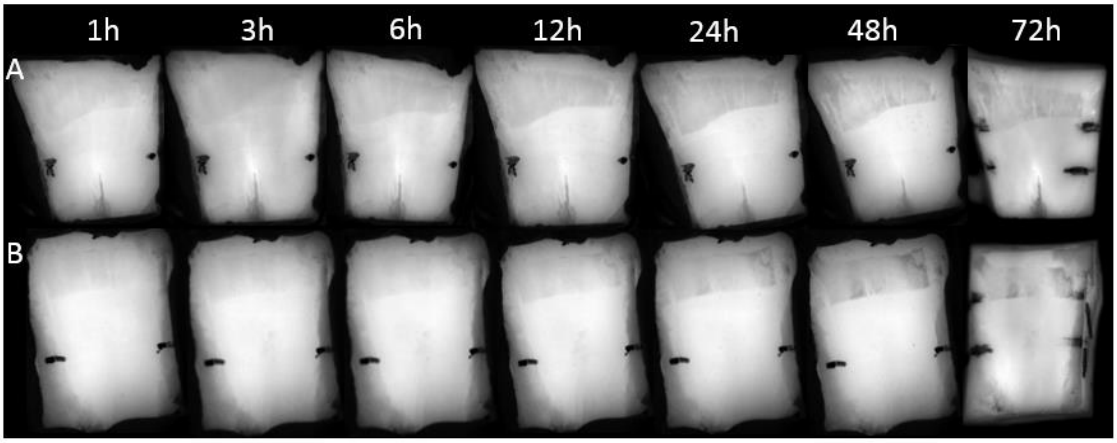

Figure 5.28: Visual MSI Lesion Progression in 3h Pre-treated Enamel subjected to 0 or 20d pH-cycling and Zn/F Treatments. *Images captured using MSI demonstrating longitudinal lesion formation in 3h pre-treated enamel subjected to pH-cycling for 0 (A) or 20d (B), 228ppm NaF and 231µm $ZnSO_4$ Treatments, and a subsequent 72h demineralisation.*

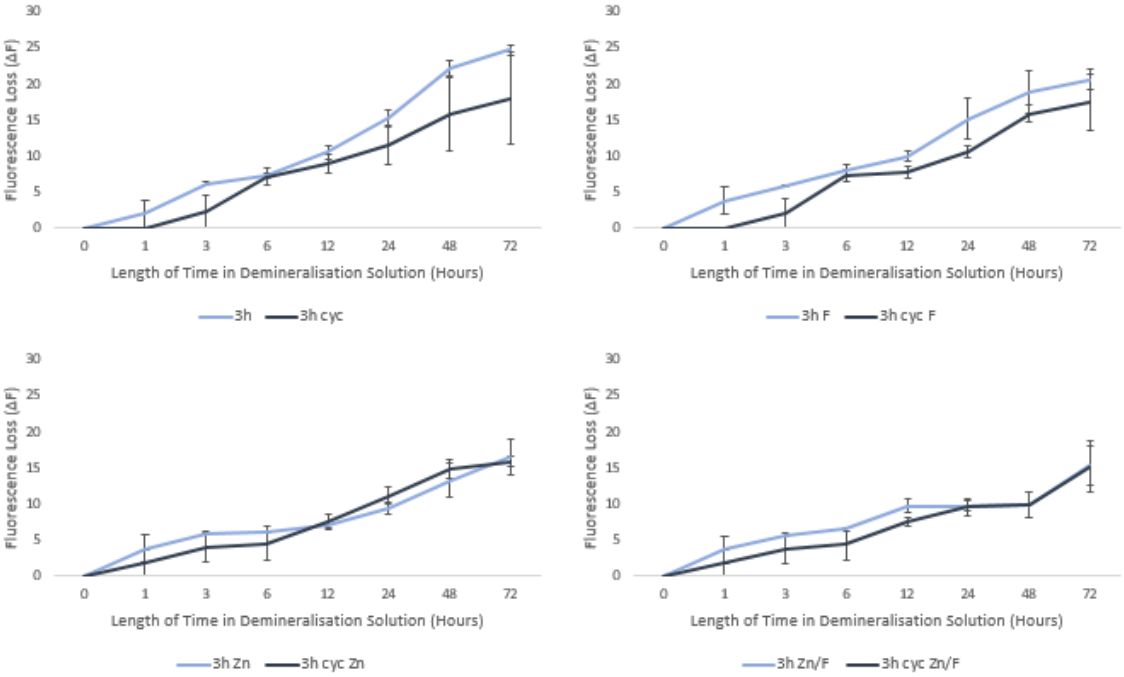

Figure 5.29: Graphical Representation of Demineralisation Progression over 72h for Zn and F Treated enamel with 0 and 20d pH-cycling Exposure. *MSI data expressing ΔF changes over 72h exposure to demineralisation solution for 3h pre-treated enamel subjected to 0 or 20d pH-cycling in addition to Zn and F treatments. Error Bars Represent the SE of the mean. n=3.*

	n	0h ± SE	1h ± SE	3h ± SE	6h ± SE	12h ± SE	24h ± SE	48h ± SE	72h ± SE
Non-Cyc	3	0.00 ± 0.00	2.00 ± 2.00	6.23 ± 0.20	7.30 ± 0.25	10.57 ± 0.91	15.23 ± 1.25	22.23 ± 1.09	24.67 ± 1.33
Cyc	3	0.00 ± 0.00	0.00 ± 0.00	2.33 ± 2.33	7.17 ± 1.17	9.03 ± 1.33	11.57 ± 2.67	15.80 ± 4.97	17.97 ± 10.96
F	3	0.00 ± 0.00	3.80 ± 1.90	5.93 ± 0.15	7.97 ± 0.82	9.97 ± 0.76	15.20 ± 2.81	18.80 ± 2.92	20.83 ± 2.76
F Cyc	3	0.00 ± 0.00	0.00 ± 0.00	2.03 ± 2.03	7.37 ± 0.79	7.87 ± 0.85	10.60 ± 0.91	15.90 ± 1.27	15.73 ± 5.24
Zn	3	0.00 ± 0.00	3.80 ± 1.90	5.80 ± 0.12	6.13 ± 0.12	7.00 ± 0.26	9.43 ± 0.87	13.27 ± 2.39	15.73 ± 5.24
Zn Cyc	3	0.00 ± 0.00	1.83 ± 1.83	4.07 ± 2.10	4.57 ± 2.32	7.57 ± 1.05	9.73 ± 1.18	9.87 ± 1.27	15.87 ± 0.95
Zn/F	3	0.00 ± 0.00	3.70 ± 1.85	5.77 ± 0.24	6.50 ± 0.23	9.73 ± 0.95	9.60 ± 1.12	9.87 ± 1.73	15.40 ± 3.29
Zn/F Cyc	3	0.00 ± 0.00	1.83 ± 1.83	3.67 ± 1.83	4.53 ± 2.29	7.57 ± 0.58	9.73 ± 0.67	9.87 ± 1.73	15.20 ± 4.28

Table 5.9: Progression of Fluorescence Loss over 72h for 3h pre-treated enamel subjected to 0 or 20d pH-cycling with Zn and F Treatments. *MSI-measured ΔF values at 0, 1, 3, 6, 12, 24, 48 and 72h demineralisation time points for 3h pre-treated enamel exposed 0 and 20 pH-cycling in conjunction with Zn and F treatments. Data is presented with SE of the mean. n=3.*

5.4.5 Impact of Treatment Groups on Demineralisation as Measured via MSI

	n	Untreated ΔF ± SE	Treated ΔF ± SE
pH-Cycling	12	24.30 ± 10.69	21.37 ± 1.76
F	6	20.83 ± 3.90	15.73 ± 7.41
Zn	6	20.93 ± 9.60	13.50 ± 2.69
Zn +F	6	23.17 ± 9.15	11.53 ± 3.95

Table 5.10: Effect of Treatment Groups on ΔF as Measured using MSI. *Fluorescence loss values obtained via MSI for lesions created in enamel subjected to pH-cycling, F, Zn and Zn/F treatments and non-treated controls. Data is presented with the SE of the mean and n values.*

When data was grouped into treated and untreated enamel based on the following criteria: pH-cycling, F, Zn and Zn/F (Table 5.10), a decrease in fluorescence loss was observed between treated and untreated blocks for each treatment condition. In terms of statistical significance, this was only displayed for ΔF values between pH-cycled and non-cycled controls (P=0.028). Values are presented graphically below (Figure 5.30).

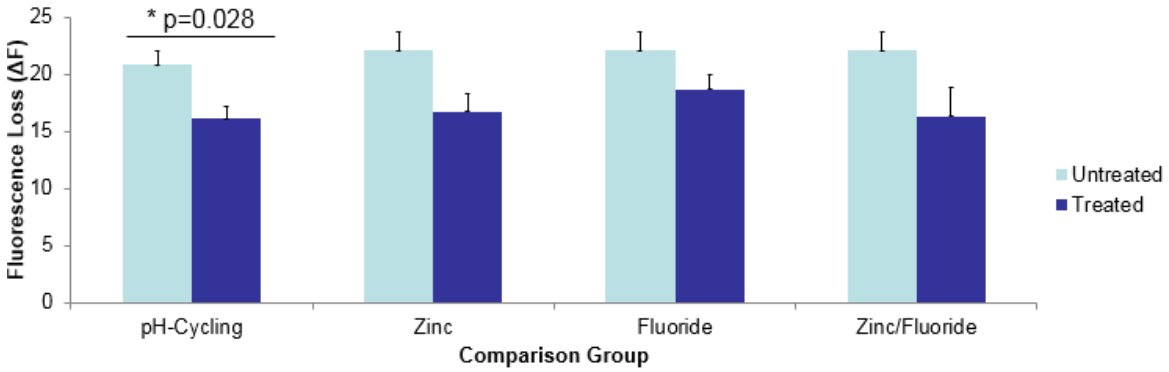

Figure 5.30: ΔF Measured using MSI for Varying Treatment Groups.

Fluorescence loss values obtained via MSI for lesions created in enamel subjected to pH-cycling, F, Zn and Zn/F treatments and non-treated controls. Error bars represent the SE of the mean. n values are reported in Table 5.4.

5.4.6 Effect of pH-cycling on Demineralisation as Measured via TMR

Mineral loss values reported for lesions created in blocks allocated to the no pre-treatment group demonstrated decreased mineral loss when enamel subjected to 20-day pH-cycling regimes when compared to those left un-cycled (Table 5.11). Similar differences were also observed for 3h pre-demineralised enamel, however with the exception of the untreated group, differences were less defined. No difference in mineral loss was observed for cycled and non-cycled 3h pre-treated enamel subjected to combined Zn + F treatments. This can be observed graphically in Figure 5.31/5.32.

	Pre-Treatment	n	Non-Cycled ΔZ ± SE	Cycled ΔZ ± SE
Untreated	None	3	1143.33 ± 56.67	649.17 ± 165.83
	3h	3	1966.12 ± 125.29	565.08 ± 252.58
F	None	3	900.69 ± 178.19	552.38 ± 247.62
	3h	3	948.28 ± 259.80	695.87 ± 401.64
Zn	None	3	857.48 ± 321.37	491.81 ± 85.69
	3h	3	619.03 ± 527.48	543.40 ± 141.21
Zn +F	None	3	558.78 ± 736.59	482.25 ± 132.75
	3h	3	532.88 ± 104.13	529.75 ± 29.75

Table 5.11: Total Mineral Loss Measured by TMR. *TMR data for demineralised bovine enamel blocks previously subjected to 0 or 20 days exposure to pH-cycling. Blocks were pre-treated for 0 or 3h in demineralisation solution and assigned to Zn and F treatment groups. Data is presented with the SE of the mean. n=3*

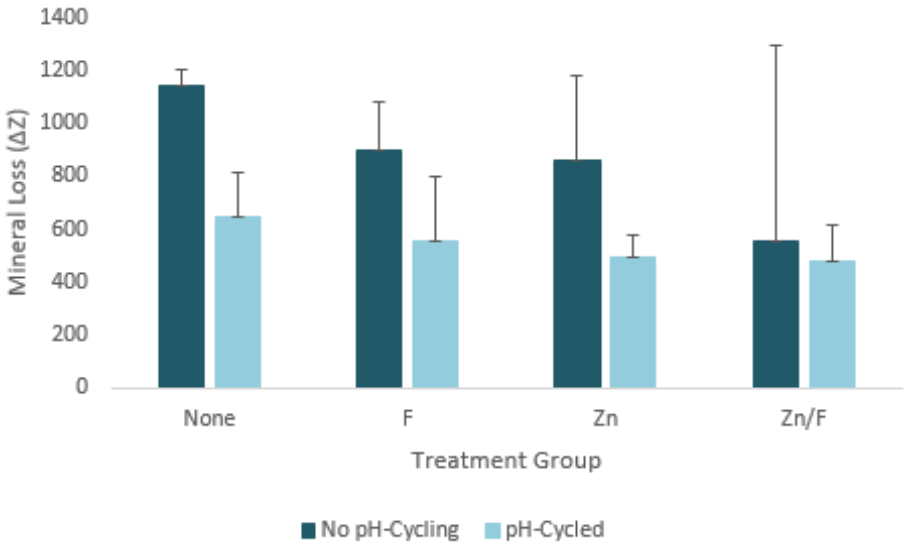

Figure 5.31: Mineral Loss (ΔZ) values following 72h demineralisation as measured using TMR for Non-pre-treated Enamel. *Data comparing non-cycled blocks to those exposed to a 20-day pH-cycling regime in conjunction with Zn and F treatments for non-pre-treated enamel. Error Bars represent SE of the mean. n=3.*

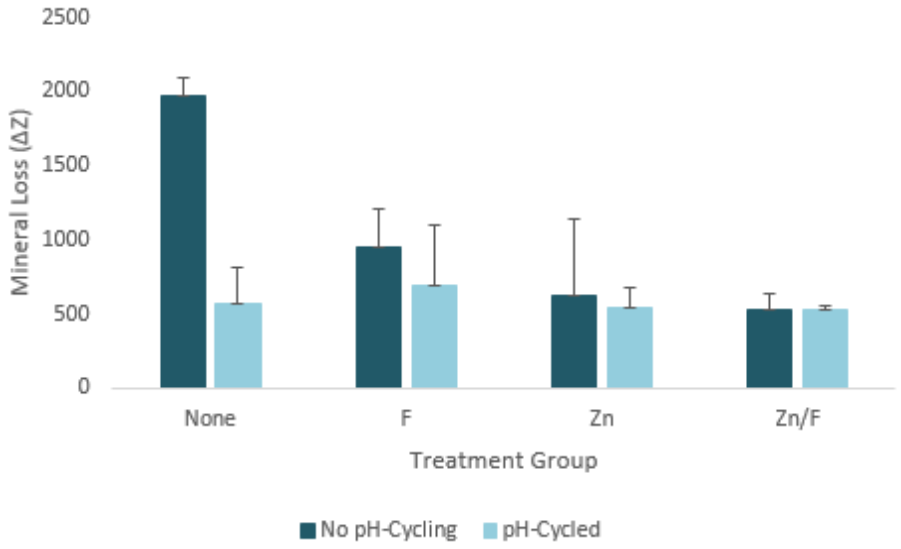

Figure 5.32: Mineral Loss (ΔZ) values following 72h demineralisation as measured using TMR for 3h Pre-treated Enamel. *Data comparing non-cycled blocks to those exposed to a 20-day pH-cycling regime in conjunction with Zn and F treatments for 3h pre-treated enamel. Error Bars represent SE of the mean. n=3.*

In terms of shape, lesions created in enamel subjected to fluoride treatments demonstrated the greatest difference between lesions formed in enamel subjected to pH-cycling and non-cycled controls, however a similar pattern to previous chapters was observed, with flatter, profiles close to those expected for sound enamel reported for lesions created in pH-cycled enamel subjected to all three treatments (Figure 5.33/5.34). Lesions created in non-cycled enamel displayed a more typical lesion shape, however were less defined than those observed in non-treated enamel. Enamel subjected to both zinc and fluoride demonstrated very little mineral loss, regardless of exposure to pH-cycling. Similar effects were observed regardless of pre-treatment group.

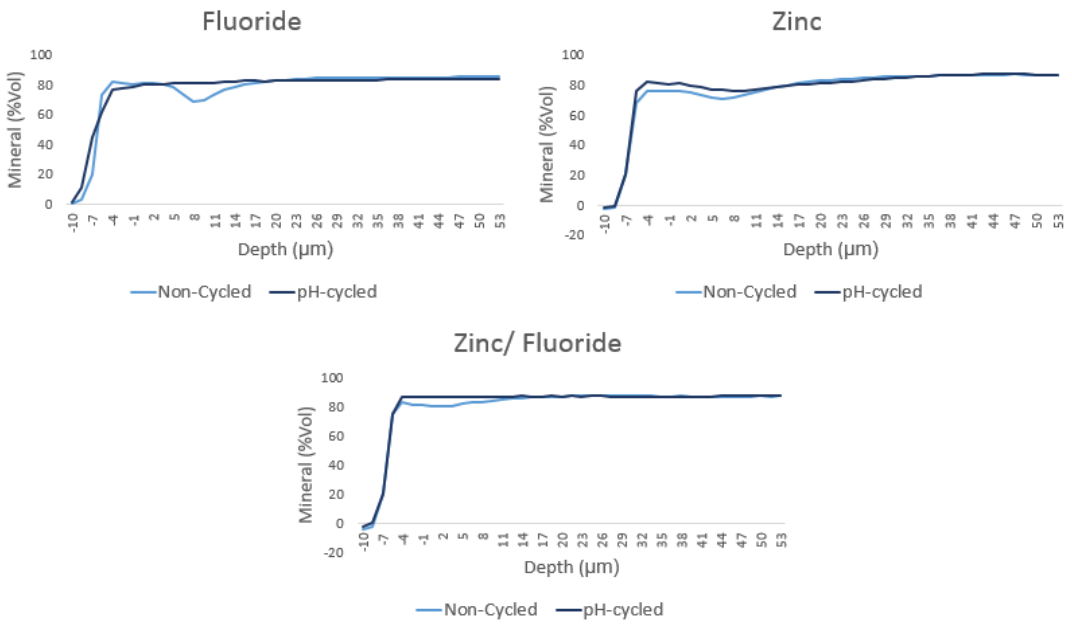

Figure 5.33: Mineral Loss as a Function of Depth for Non-pre-treated Enamel.

Lesion profile created from TMR data for lesions created in non-pre-treated enamel subjected to 0 or 20d pH-cycling in addition to Zn and F treatments.

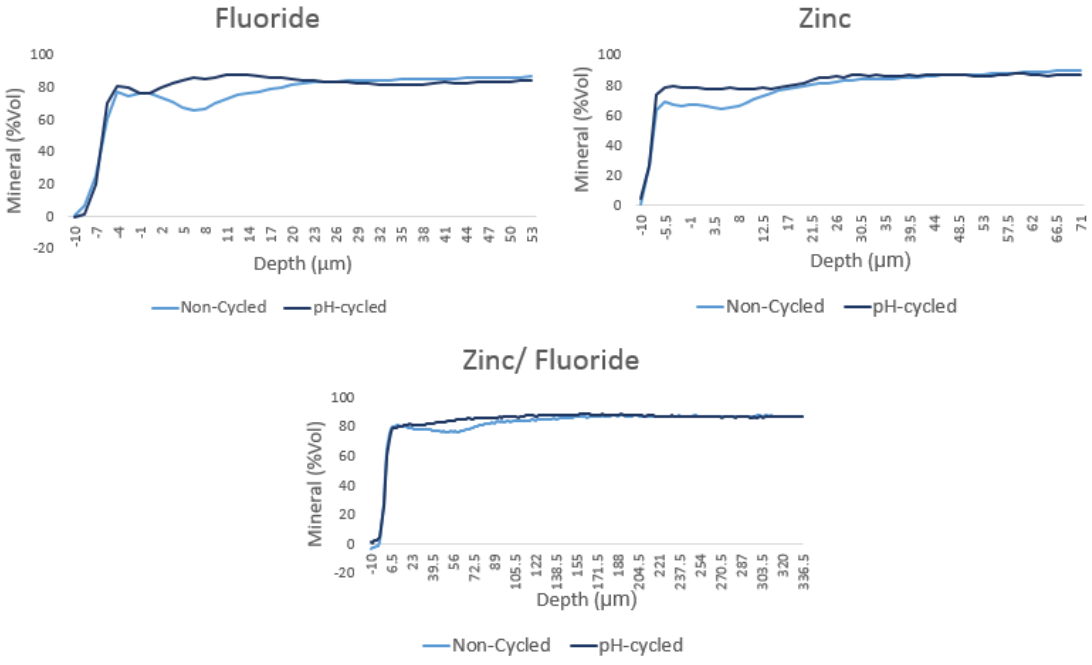

Figure 5.34: Mineral Loss as a Function of Depth for 3h pre-treated Enamel.

Lesion profile created from TMR data for lesions created in 3h pre-treated enamel subjected to 0 or 20d pH-cycling in addition to Zn and F treatments.

5.4.7 TMR Evaluation of the Impact of Treatment Groups on Demineralisation

When results are grouped to investigate the effects of the 4 treatment groups, a decrease between treated and untreated blocks can be observed for all groups. However only the difference observed for the effect of pH-cycling demonstrated statistical significance (p=0.021) (Figure 5.35).

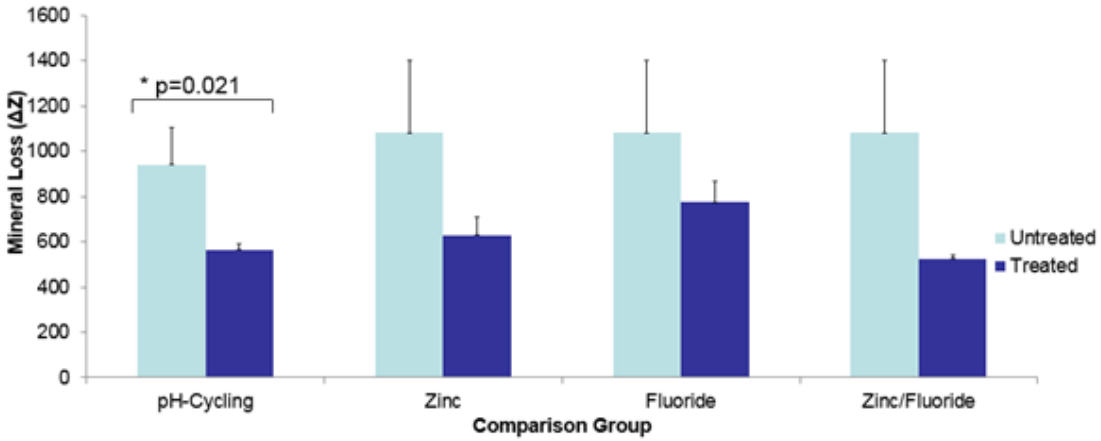

Figure 5.35: ΔZ Measured using TMR for Varying Treatment Groups. Mineral *loss values obtained via TMR for lesions created in enamel subjected to pH-cycling, F, Zn and Zn/F treatments and non-treated controls. Error bars represent the SE of the mean. pH-cycling: n=12 otherwise n=6.*

5.5 Discussion

Whilst the work outlined in the previous chapters has served to demonstrate the basis for the use of PF-relevant pH-cycling conditions to model the decreased susceptibility to acid dissolution observed during post-eruptive maturation, it has failed thus far to properly account for the importance of availability of ions such as zinc and fluoride for chemical changes to occur. Therefore, the present study aimed to observe the effects of regular Zn and F treatments within the model parameters previously outlined.

When lesions obtained from exposing non-pre-treated sound enamel to 20 days pH-cycling are compared visually to non-cycled controls, they appear lighter and less even in appearance for both the QLF-D and MSI imaging systems. Quantitative fluorescence loss data supports these observations, as a non-significant reduction in fluorescence loss was observed for all pH-cycled blocks in comparison to equivalent non-cycled controls. These results were also reflected for mineral loss, however TMR results were variable, largely due to the use of small sample sizes.

When development of the lesions is monitored by QLD-D and MSI, it can be seen that lesions created in pH-cycled enamel develop later than non-cycled counterparts and report lower ΔF values at any given time point. It is worth noting that these differences are more pronounced for the QLF-D imaging system in comparison to the MSI system, however this will be addressed at a later stage.

In contrast to the results obtained in chapter one, the differences observed above were not seen to the same extent for the 3h pre-treatment group. For this group differences between pH-cycled and non-cycled controls for groups exposed to zinc and fluoride treatments were less defined, particularly when both agents are provided. This is interesting as it implies that whilst in the absence of such treatments, a pre-demineralisation can serve to improve ion availability at the enamel surface, but when the ions are readily available, it has little effect. This makes sense in consideration of the literature, as F, in particular, has been shown to incorporate as part of the dynamic demineralisation process (Featherstone 1999, Fejerskov *et. al.* 1994, Lynch and Smith 2012), therefore a separate pre-demineralisation would have any influence on such conditions. Additionally, F has been reported to possess the ability to penetrate sound in addition to demineralising enamel (Lagerweij and ten Cate 2006).

Fluoride and Zinc have been shown to possess the ability to afford protective effects to enamel when faced with an acid challenge and to aid subsequent remineralisation

(Brudevold *et. al.* 1963, Dedhiya *et. al.* 1973, Abdullah *et. al.* 2006, Manly and Harrington 1959, Featherstone *et. al.* 1990). When the data recorded for lesions created in enamel not subjected to pH-cycled, but exposed to 2m F and Zn treatments 6 times a day for 20days (each pH-cycling solution change), a reduction in demineralisation can be observed that supports the established literature. Interestingly the protective effect appears to particularly pronounced in enamel subjected to combined Zn and F, which is in keeping with the suggestion that the two ions are able to have a synergistic effect of one another in terms of remineralisation and incorporation into the HPA (Lynch 2013). Another feature of the model worth noting when Zn and F treatments are included is that the protective effect of pH-cycling exposure reported in the previous chapter for non-treated enamel is reduced, presumably due to the already protective effect of the ions alone.

The observed differences in the behaviour of enamel subjected or not subjected to demineralisation pre-treatments, may, in part, also be due to the influence of the additional Zn and F, as, F in particular, has been shown to incorporate into HPa and aid remineralisation more effectively in enamel that is more porous (Brudevold *et. al.* 1982).

Similarly, to previous chapters, surface roughness values obtained from NSCP analysis were variable and did not provide any insight of note into the effects of the model. The rationale behind why the NCSP data is not providing any information of note have been addressed previously, and, as the situation has not varied, the decision as to whether to include the technique going forward needs to be addressed.

Overall the progress made in this chapter provides further support for the use of the pH-cycling conditions laid out in the previous chapter, but highlights the importance of ion availability for chemical changes to occur. However, the same limitations regarding the validation of thesis findings still need to be addressed. Going forward the work

presented here needs to be conducted on larger sample sizes and to consider parameters outside of lesion formation as an assessment.

Chapter Six: Refinement of the Proposed PEM Model

6.1 Background

6.1.1 Lesion Creation Methods

In order to study the demineralisation and remineralisation process *in vitro* several approaches have been devised in order to create artificial caries lesions. At their most simple, they involve the exposure of an enamel substrate to an acidic solution containing Ca and P designed to be under-saturated in comparison to HPA. Whilst more reductionist than some other lesion-creation methods, the relative ease makes it an effective way to mass produce lesions on order conduct remineralisation experiments. Further to this, the composition of the solution used can be altered to change the parameters of the created lesion to a certain extent.

One way in which this approach has been modified to make it more representative is to include alternating periods of remineralisation though pH-cycling. Described previously, this technique aims to simulate the cyclic conditions present *in vivo* and therefore to create more representative artificial lesions.

An alternate path which researchers have followed in an attempt to better re-create the *in vivo* conditions upon which carious lesions form is to try and change the texture of the dissolution media to be more representative. Such approaches involve the use of an acid-based hydroxyethylcellulose gel within which the substrate is submerged. This is designed to simulate plaque. In some cases, an additional top layer formed of an acid solution is also used.

6.1.2 Refinement of the Proposed *in vitro* PEM Model

Building on the work from the previous chapter, the current study aims to refine the proposed pH-cycling model primarily though the inclusion larger sample sizes. Beyond this, the 0 and 20d pH-cycling exposure times and Zn and F treatment groups will be continued. The Pre-treatment step has been removed, with only sound enamel being subjected to experimental conditions. The 72h demineralisation has been altered from an acetic acid solution to a lactic acid gel. Additionally, in order to investigate the physical changes in the enamel following pH-cycling exposure, surface microhardness measurements and SEM images will be taken. The updated model outline can be seen in Figure 6.1 below.

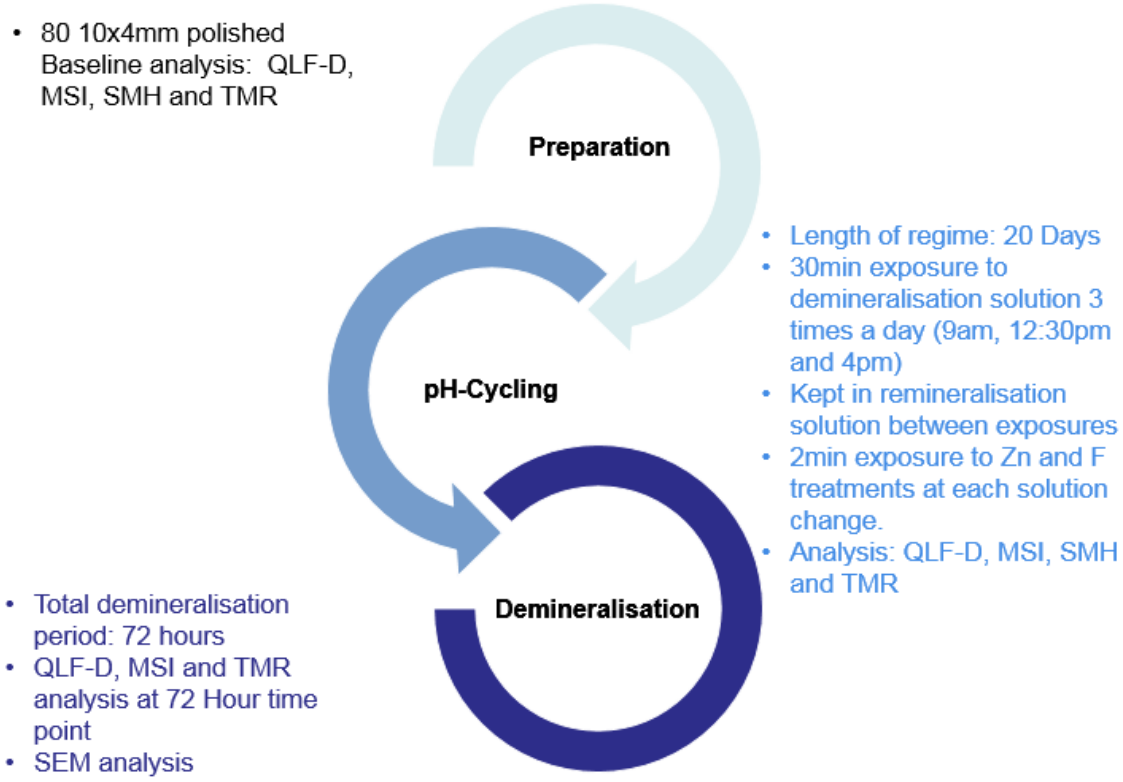

Figure 6.1: Summary of Current Model Protocol. *Outline of the current experimental procedure, broken down into the three stages of the proposed model*

6.2 Aims

The present study aimed to validate the findings of the previous chapter through the use of large sample sizes. Additionally, it aimed to improve upon the proposed model though the addition of a more-realistic demineralisation technique and the investigation of physical changes though the incorporation of surface micro hardness measurements.

6.3 Materials and Methods

6.3.1 Selection and Preparation of Bovine Enamel Blocks

80 blocks approximately 10x4mm in size were prepared from bovine incisors as described previously, but were subjected to an additional abrasion step using a weighted, water-cooled motorised polisher to make the blocks plane-parallel with respect to the enamel surface (EcoMet / AutoMet 250 & 300, Buelher, Illinois, USA).

Blocks were mounted in fives with Green-Stick impression compound into 50ml disposable Sterilin containers (Sterilin Ltd. Newport, UK) using a glass rod placed through the lid (Figure 6.2).

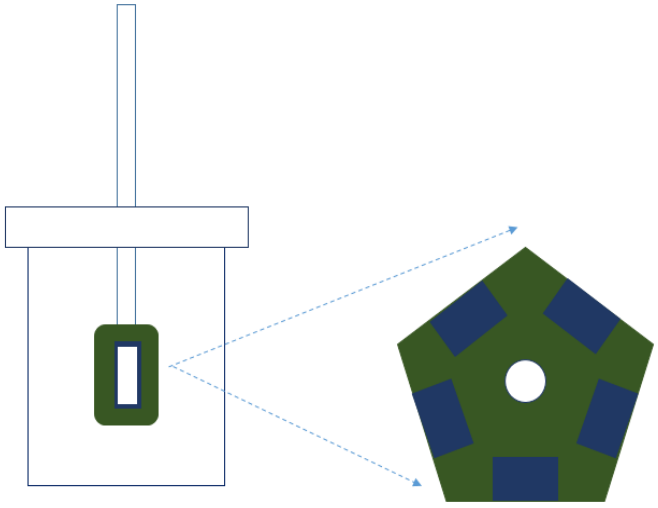

Figure 6.2: Schematic of Mounted Blocks. *Illustration depicting mounting of blocks in fives into Sterilin containers using Green Stick Impression Compound.*

6.3.2 pH-Cycling Regime

The previously described pH-cycling regime was followed for 0 or 20 days (Figure 5.2).

6.3.3 Acid Challenge

In order to test the effect of the pH-cycling regime on the acid susceptibility of the enamel, blocks were subjected to a 72-hour demineralisation challenge as before, but instead of an acetic acid solution, a lactic acid-containing hydroxyethylcellulose gel was used (pH 4.5, hydroxylethylcellulose: Sigma-Aldrich Ltd., Dorset, UK). Following Exposure to acid challenge, samples were blinded to reduce bias during analysis.

6.3.4 Assessment of Physical Changes

Blocks were subjected to Vickers's SMH analysis at baseline and following pH-cycling using the method described previously (Section 2.11). Selected blocks were also imaged using SEM (Section 2.12).

6.3.5 Assessment of Demineralisation

Enamel blocks were allowed to air-dry before being imaged and analysed as described previously using QLF-D and MSI. Images were taken at baseline, and following the 72h demineralisation challenge. TMR analysis was conducted outlined in Chapter 2 (Section 2.10).

6.4 Results

6.4.1 QLF-D Assessment of Fluorescence Loss

A significant decrease in fluorescence loss was observed for all cycled enamel blocks in comparison to non-cycled controls with the exception of those treated with Zn (No Treatment: P=0.0004, F: P=0.0001 and Zn/F: P=0.0001) (Table 6.1). The largest

decrease in fluorescence loss between non-cycled and cycled enamel was observed for non-treated enamel (14.96). Data is presented graphically in Figure 6.3 below.

	n	Non-Cycled ΔF ± SE	Cycled ΔF ± SE
Untreated	10	28.77 ± 3.40	13.81 ± 0.78
F	10	17.39 ± 1.01	12.01 ± 0.39
Zn	10	20.08 ± 1.37	16.33 ± 1.19
Zn +F	10	19.63 ± 1.60	11.29 ± 0.41

Table 6.1: Total Fluorescence Loss Measured by QLF-D. *QLF-D data for demineralised bovine enamel blocks previously subjected to 0 or 20 days exposure to pH-cycling. Blocks were assigned to Zn and F treatment groups. Data is presented with the SE of the mean. n=10.*

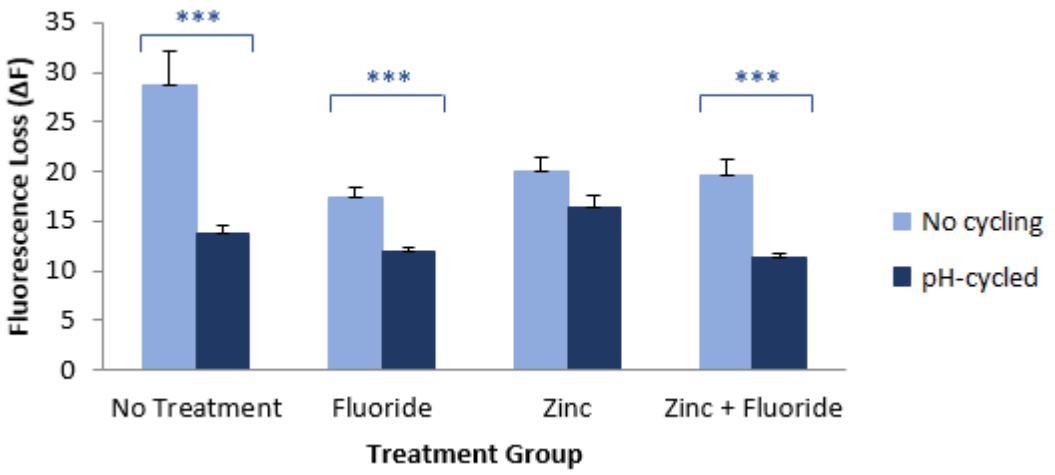

Figure 6.3: Fluorescence loss (ΔF) values following 72h demineralisation as measured using QLF-D. *Data comparing non-cycled blocks to those exposed to 20-day regime for enamel subjected to Zn and F treatments. Error Bars represent SE of the mean. ***= P<0.001. n=10.*

6.4.2 Fluorescence Loss Measured via MSI

	n	Non-Cycled ΔF ± SE	Cycled ΔF ± SE
Untreated	10	53.09 ± 4.97	31.39 ± 2.99
F	10	35.24 ± 1.40	22.68 ± 1.58
Zn	10	43.97 ± 3.37	32.63 ± 3.47
Zn+F	10	38.77 ± 1.22	24.58 ± 1.22

Table 6.2: Total Fluorescence Loss Measured by MSI. *MSI data for demineralised bovine enamel blocks previously subjected to 0 or 20 days exposure to pH-cycling. Blocks were assigned to Zn and F treatment groups. Data is presented with the SE of the mean. n=10.*

Fluorescence loss values recorded via MSI followed a similar pattern to results obtained using the QLF-D system: a significant decrease in fluorescence loss was observed for all lesions created in pH-cycled enamel blocks when compared to those created in non-cycled controls (No Treatment: P=0.0015, F: P=0.0001, Zn: P= 0.0308 and Zn/F: P=0.0001). The largest change in fluorescence loss between non-cycled and pH-cycled enamel lesions was observed for enamel not subjected to Zn and F treatments (21.70). ΔF values are presented graphically below (Figure 6.4).

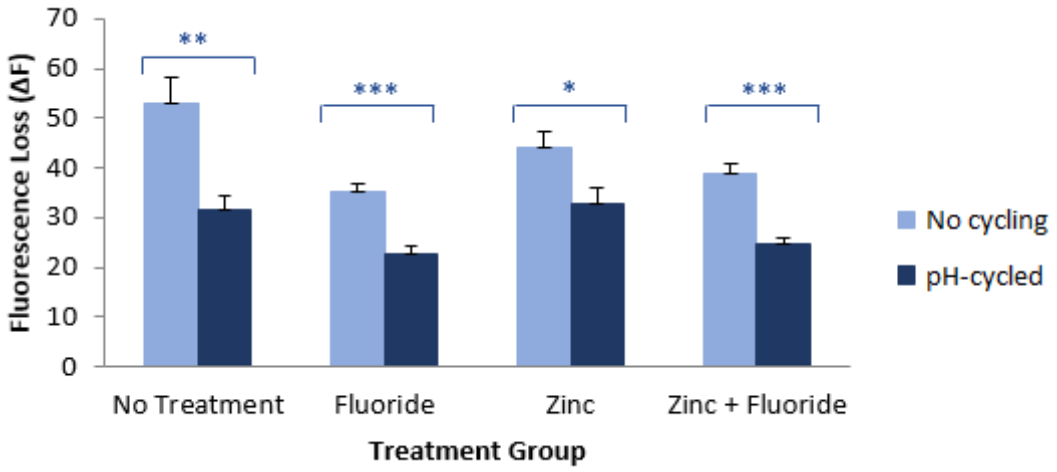

Figure 6.4: Fluorescence loss (ΔF) values following 72h demineralisation as measured using MSI. *Data comparing non-cycled blocks to those exposed to 20-day regime for enamel subjected to Zn and F treatments. Error Bars represent SE of the mean. ***= P<0.001, **=P<0.01, *=P<0.001. n=10.*

6.4.3 Effect of pH-cycling on Surface Microhardness

	Cycled?	n	Sound SMH ± SE	Cycled SMH ± SE
Untreated	N	10	348.33 ± 16.74	340.44 ± 35.07
	Y	10	351.00 ± 42.72	354.90 ± 38.30
F	N	10	359.20 ± 31.59	337.89 ± 32.22
	Y	5*	302.20 ± 46.39	337.80 ± 34.79
Zn	N	10	345.00 ± 35.67	343.80 ± 30.92
	Y	10	359.40 ± 24.49	347.40 ± 32.75
Zn + F	N	10	354.60 ± 15.29	365.80 ± 19.79
	Y	5*	349.80 ± 14.02	374.40 ± 7.57

Table 6.3: SMH for Sound and pH-cycled Enamel. Vickers *SMH measurements taken at baseline and following 0/20d exposure to pH-cycling and Zn and F treatments. Data is presented with the SE of the Mean. n=10 (* Some blocks were excluded due to soft surface deposits).*

Reported Vickers hardness values were variable, however an increase was observed for both cycled (24.60) and non-cycled (11.20) enamel subjected to Zn/F treatments. This increase was significant for the enamel also exposed to 20 days pH-cycling (P=0.0087). A non-significant decrease in SMH was observed for cycled enamel treated with zinc (12.00). From Table 6.3 it can be noted that the number of samples for both the pH-cycled group treated with F and that treated with combined Zn and F is reduced to 5. This was due to the presence of a soft deposit on the enamel surface that could not be removed and, as such, required them to be excluded from SMH analysis. Data is presented graphically in Figure 6.5.

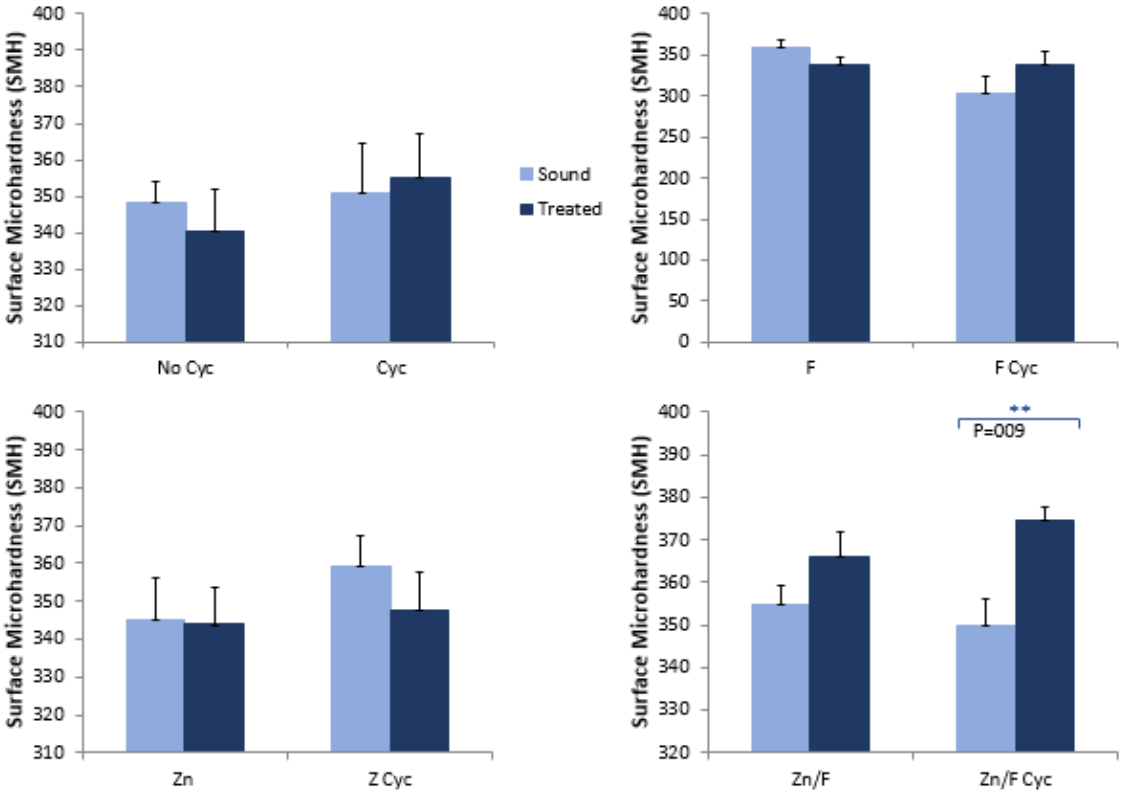

Figure 6.5: Vickers Surface Micro hardness (SMH) values comparing non-cycled areas to those exposed to 20 days of pH-cycling. *The standard error of the mean is displayed with each recorded value. ** represents significance at the P<0.01 level. n values are reported in Table 6.3.*

6.4.4 Scanning Electron Microscopy (SEM) Imaging

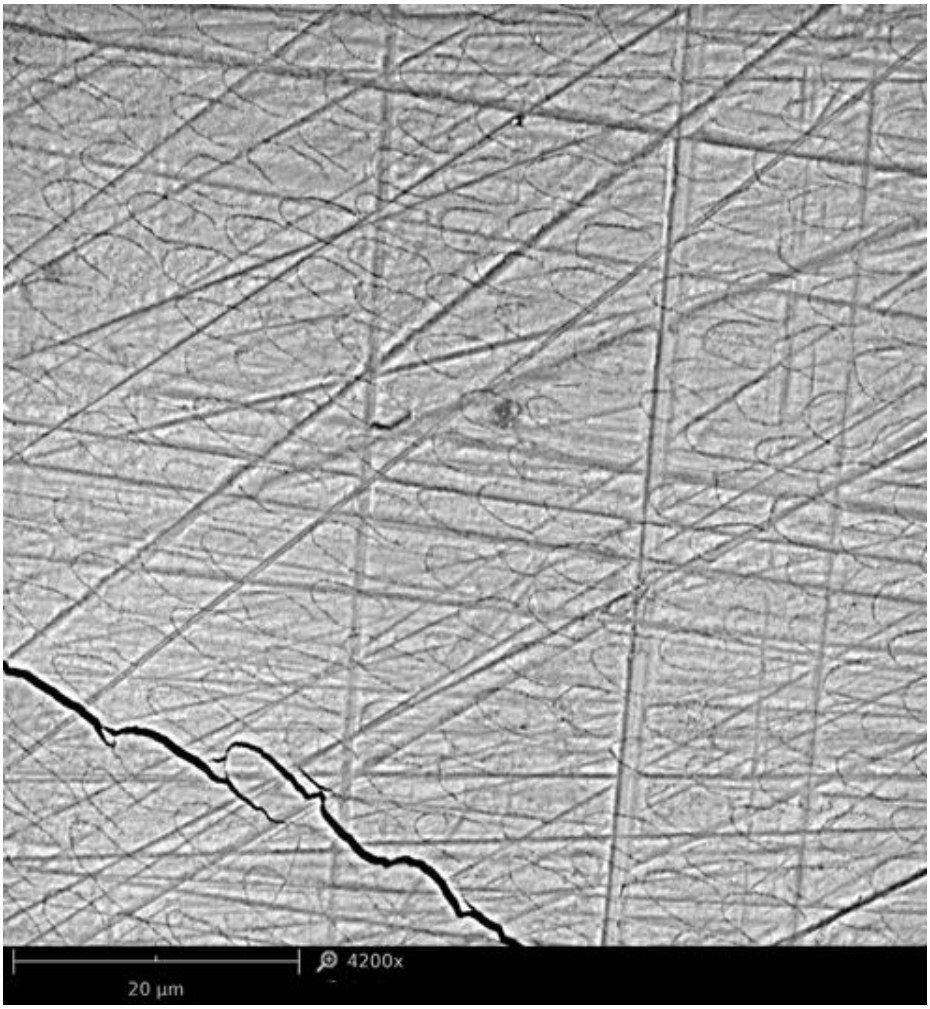

Figure 6.6: SEM image of Sound Enamel. *SEM image of sound enamel demonstrating the presence of enamel prisms. Damage sustained during the SEM process can also be observed.*

When SEM as used to image areas of sound enamel at a magnification of 4200x (Figure 6.6), striations from the polishing process during preparation can be seen along with areas of damage caused by the vacuum conditions required for imaging. In addition to induced-features, horseshoe-shaped marks can be seen across the surface indicating the boundaries of enamel prisms.

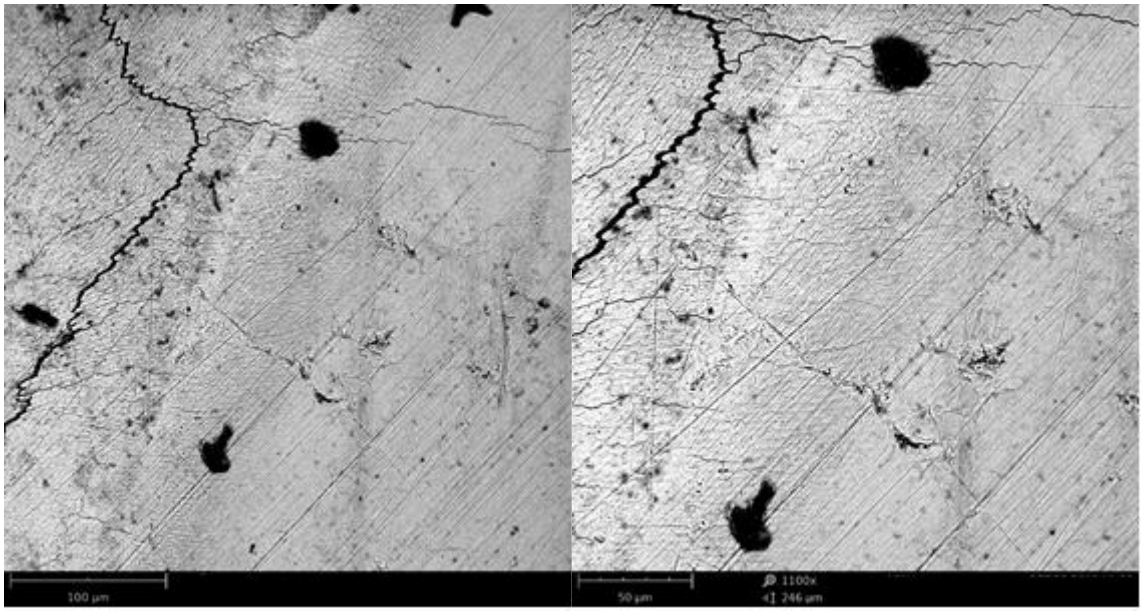

Figure 6.7: Lesion Boundary Imaged Using SEM for Sound Enamel. *SEM image demonstrating the gradual transition at the lesion boundary.*

When areas at lesion boundaries are viewed, the surface appearance between sound and demineralised enamel is distinct. Sound enamel appears even in colour and smooth aside from slight grooves created during polishing. In comparison, the lesion appears more textured, with the enamel prism structure clearly visible. When the magnification is increased, the boundary between the lesion and sound area can be seen to be not clearly defined and an intermediate area is visible between the two areas. Interestingly, when the lesion boundary is observed for pH-cycled enamel, the intermediate area is much smaller and the lesion is much more clearly defined from the surrounding enamel.

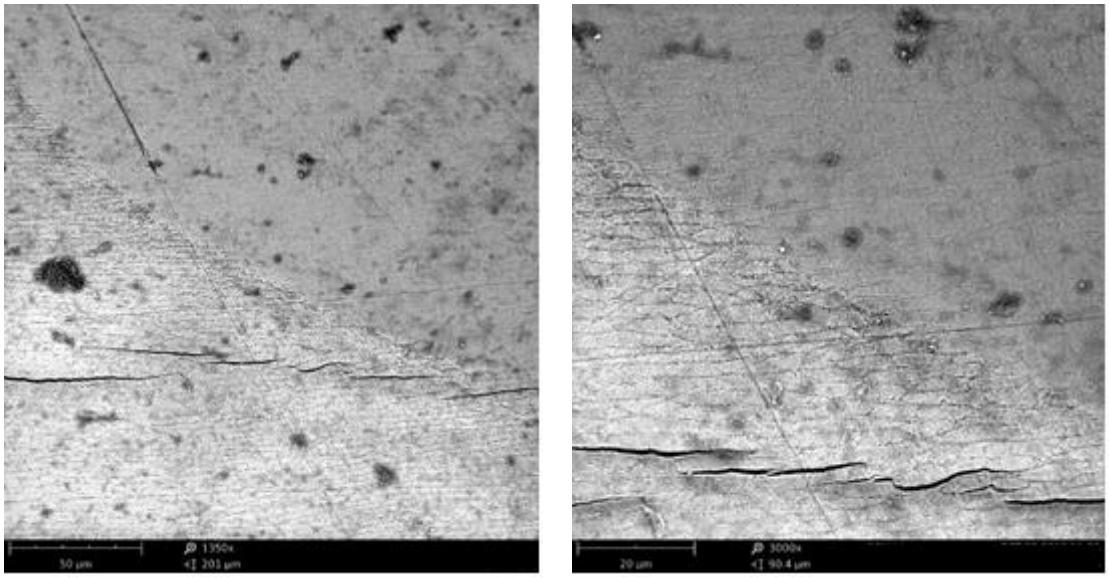

Figure 6.8: Lesion Boundary Imaged Using SEM for pH-cycled Enamel. *SEM image demonstrating the more defined lesion edge observed for pH-cycled enamel.*

6.4.5 Investigating surface deposits present in pH-cycled blocks exposed to F/Zn

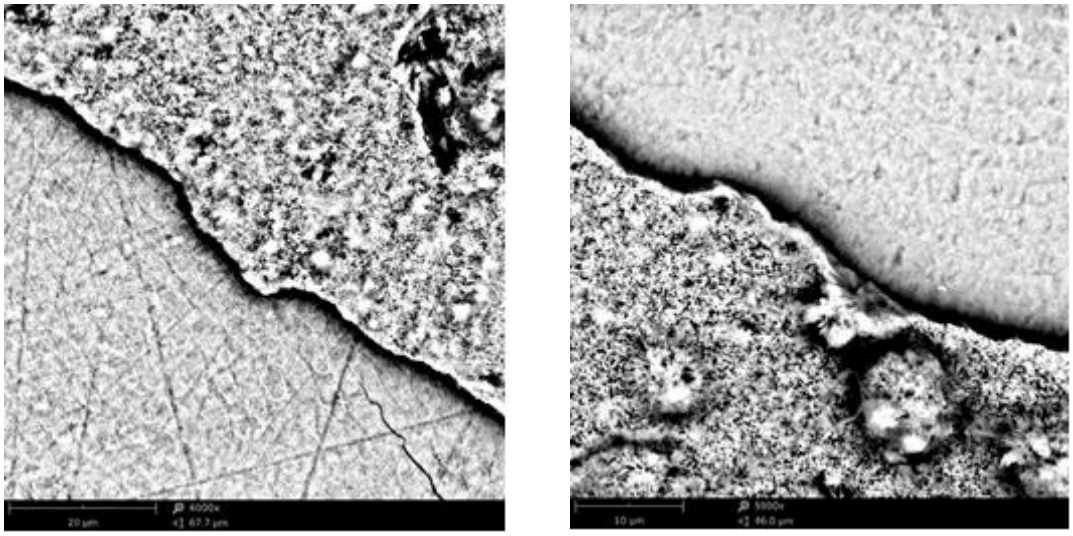

Figure 6.9: Surface Deposits Imaged Using SEM. *SEM image demonstrating the presence of a deposit on the enamel surface against demineralised (Left) and pH-cycled (Right) enamel.*

In order to try and better understand the surface deposit described in the previous section, scanning electron microscopy images were captured (Figure 6.9) and a basic EDX analysis conducted (Figure 6.10/6.11). The ability to use this technique was, however, limited as exposure to the vacuum caused damage to the enamel block, particularly in lesion areas. From the results displayed below, it can be seen that the deposits contain a higher ratio of fluorine in comparison to both underlying pH-cycled and lesion areas of enamel. In addition, deposits present a higher ratio of P to Ca than the underlying enamel areas. Interestingly, the pH-cycled area of underlying enamel demonstrated the presence of Zn, which was not observed in the other measurements taken.

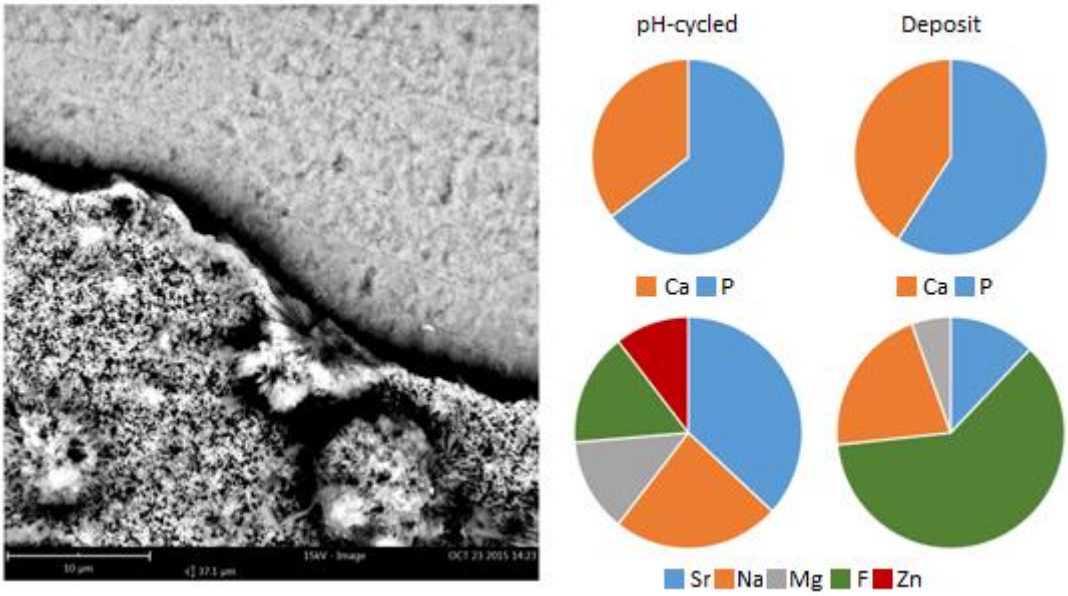

Figure 6.10: EDX Analysis for Surface Deposit and pH-cycled Enamel. *SEM image and basic EDX analysis demonstrating differences in the proportion of different elements such as Ca, P and F.*

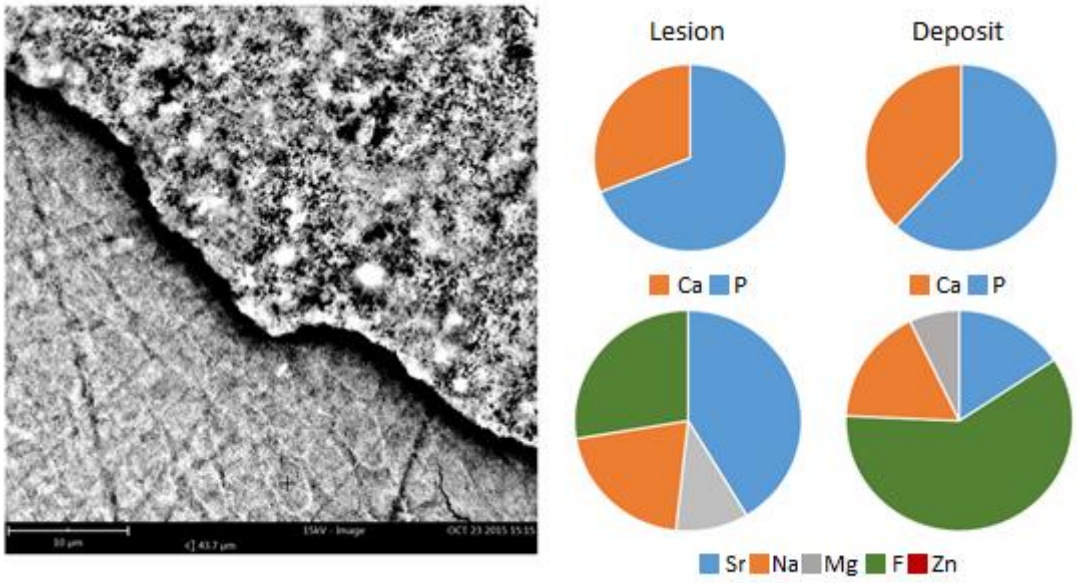

Figure 6.11: EDX Analysis for Surface Deposit and Lesion. *SEM image and basic EDX analysis demonstrating differences in the proportion of different elements such as Ca, P and F for surface deposit and underlying demineralised enamel.*

6.4.6 pH-cycling Dependent Changed in Mineral Loss Measured via TMR

	n	Non-Cycled ΔZ ± SE	Cycled ΔZ ± SE
Untreated	10	2244.43 ± 234.01	1155.15 ± 91.07
F	10	1520.67 ± 86.21	1191.17 ± 244.55
Zn	10	1701.02 ± 162.20	1549.63 ± 117.80
Zn +F	10	1476.10 ± 105.98	1476.10 ± 154.12

Table 6.4: Total Mineral Loss Measured by TMR. *TMR data for demineralised bovine enamel blocks previously subjected to 0 or 20 days exposure to pH-cycling. Blocks were assigned to Zn and F treatment groups. Data is presented with the SE of the mean. n=10.*

When mineral loss values obtained through TMR are observed (Table 6.4), a significant reduction in mineral loss following demineralisation was observed for lesions created in pH-cycled enamel in comparison to those created in non-cycled controls for untreated enamel (P=0.0004) and that subjected to combined zinc and fluoride treatments (P=0.0184). Additionally, a non-significant decrease was observed for pH-

cycled vs non-cycled enamel for the fluoride and zinc separate treatment groups. A decrease in mineral loss was also observed for non-cycled enamel exposed to all fluoride and zinc treatment groups in comparison to non-treated controls. Such differences were not observed for pH-cycled enamel. Data is presented graphically in Figure 6.12.

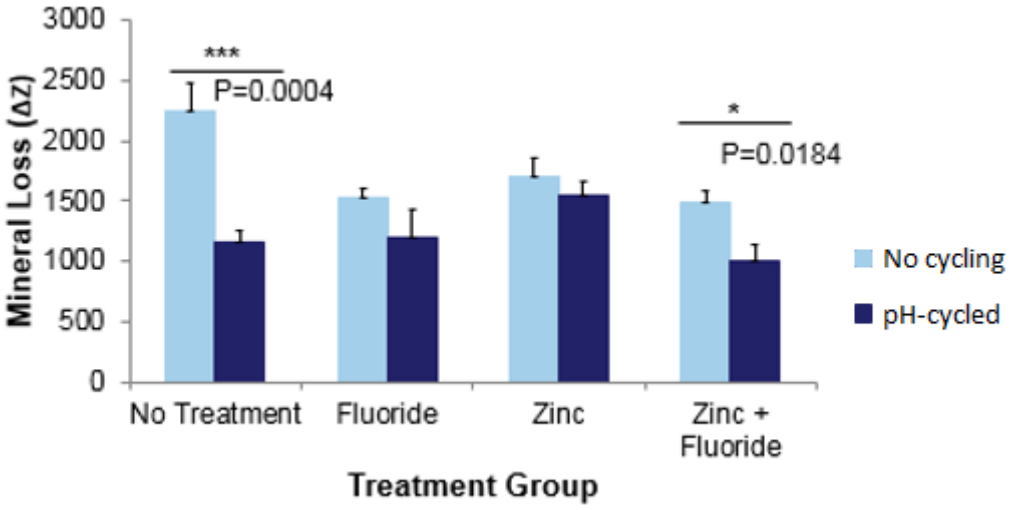

Figure 6.12: Mineral loss (ΔZ) values following 72h demineralisation as measured using TMR. *Data comparing non-cycled blocks to those exposed to 20-day regime for enamel subjected to Zn and F treatments. Error Bars represent SE of the mean. ***= P<0.001, * =P<0.05. n=10.*

When the effect of pH-cycling on parameters other than mineral loss are considered, a decrease in lesion depth was observed for lesions created in pH-cycled enamel when considered against non-cycled counterparts, with the exception of those in the fluoride treatment group. The ratio, or R, did not vary between lesions created on sound or pH-cycled enamel when a zinc-inclusive treatment was also administered, but was lower for cycled enamel than sound in the non-treated and F-treated conditions (Figure 6.13).

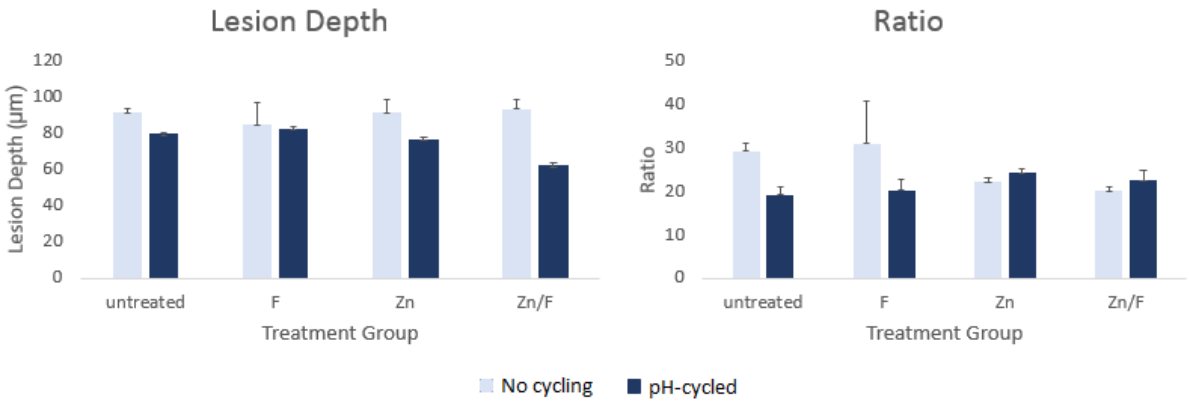

Figure 6.13: LD and R for Lesions Created in Sound and pH-cycled Enamel. *TMR data for LD and R for lesions created in sound enamel and that subjected to 20d pH-cycling. Zn and F treatments were also administered over 20d. Error bars represent the SE of the Mean. n=10.*

Upon further investigation of lesion characteristics, the profile of lesions varied depending on which treatment group they were allocated to (Figure 6.14). For non-treated enamel, lesions created in both cycled and non-cycled enamel demonstrated a classical lesion profile, with a shallower lesion with a larger surface area produced in pH-cycled blocks. In contrast, lesions created in sound blocks subjected to F treatments displayed lesions with a profile more comparable to an erosive than a carious lesion. Comparable pH-cycled blocks demonstrated a profile similar to that of sound enamel. Lesions created in blocks within the zinc treatment group formed a subsurface lesion, when created in sound enamel, but this area was much smaller and less defined when blocks were also subjected to pH-cycling. Blocks exposed to Zn/F treatments in combination with pH-cycling demonstrated very little demineralisation and a profile akin to that of sound enamel. When not combined with cycling, Zn/F treatments produced shallow lesions with a relatively undefined surface layer.

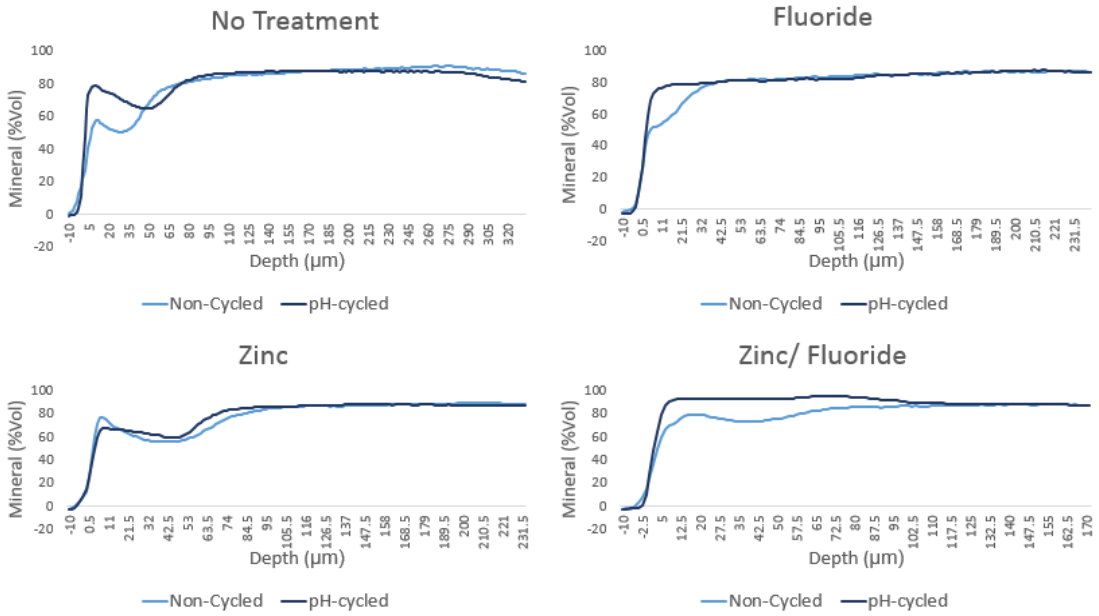

Figure 6.14: Mineral Loss as a Function of Depth. *Lesion profile created from TMR data for lesions created in sound enamel subjected to 0 or 20d pH-cycling in addition to Zn and F treatments.*

6.5 Discussion

The work within this chapter aimed to provide validation for the results obtained in previous chapters by using larger sample sizes and by including a means by which to assess the physical effect of the pH-cycling exposure on the enamel.

When the previously used parameter of reduced fluorescence/mineral loss as a marker for maturation is assessed, results show support for the model. A reduction in fluorescence loss was observed for all cycled groups when compared to non-cycled controls for both techniques. Additionally, the differences demonstrated statistical significance, with the exception of the zinc treatment group for QLF-D. These findings are further supported by the mineral loss values obtained by TMR, in which a decrease was also observed for each pH-cycled group in comparison to non-cycled counterparts, of which were significant for both the pH-cycling only and Zn + F treatment groups.

During the process of reviewing the literature a common theme within PEM research appears to be a tendency to define the process by its effects as opposed to the underlying process itself. This is largely due to a lack of understanding of both the mechanism behind the process itself as well as fundamental understanding we now have, such as the mechanisms and actions of fluoride. Regardless of the rationale behind this trend, it has led to the main parameters for the definition of PEM being a reduction in caries susceptibility, decreased porosity and increased surface micro hardness (Carlos and Gittelsohn 1965, Cardoso *et. al.* 2009, Kataoka *et. al.* 2007). Whilst the work to this point has primarily addressed the first parameter as a means of validating the presence of a maturation effect, the current chapter aimed to strengthen this by also taking into account the physical effects of the regime though the use of surface micro hardness.

For all treatment groups except zinc, an increase in SMH was observed for blocks subjected to pH-cycling, when compared to baseline. The effect was particularly pronounced for the combined zinc and fluoride treatment group. When referenced back to the literature, the observed hardness changes make sense. Fluoride has been shown, when present in high enough concentrations, to be able to bind to the surface enamel, particularly in the presence of acids (Christofferson *et. al.* 1995, Featherstone 1999). This is achieved through its ability to substitute in place of hydroxyl/phosphate groups, replacing lost carbonate within the HPA (Young 1975, Aoba *et. al.* 2003). Once bound the smaller fluoride ion is able to bind closer, reducing the porosity and strengthening the enamel. Whilst this explains the slight increase in SMH observed for the fluoride treatment group, it does not account for the markedly greater effect of the combined F and Zn group. To understand this difference, the role of the zinc must also be taken into account. Whilst fluoride has a proven track record as a catalyst to the remineralisation process, its effect has a tendency to be confined to the outer surface layers of the enamel. This can lead to the development of a hyper-mineralised surface,

with a large lesion underneath, as acids bypass the surface in favour of the more easily dissolved mineral. Zinc has been shown to possess the ability to increase the ability of fluoride to penetrate deeper into the enamel (Lynch *et. al.* 2011). This is believed to be due to the surface-softening action of zinc and as such also explains the reduction in SMH observed in the zinc-only treatment group.

For both fluoride-containing treatment groups, 50% of the pH-cycled blocks had to be excluded from SMH testing due to the presence of a deposit on the enamel surface that could not be removed through washing in water or acetone. Additionally, the deposit could not be removed though force when a small area was tested. In order to try and gain a better understanding of what may have caused it, scanning electron microscopy was used with a basic EDX analysis. Due to the unreliability of the EDX for estimating concentrations accurately, only the relative amounts of elements to one another were taken into account. When compared with the underlying pH-cycled enamel, the deposit contained a much larger proportion of fluoride. Whilst this may be due to some form of contamination, it may also suggest the potential for calcium fluoride deposits, which have been shown to form spherical globules with a crystalline structure on the enamel surface in the presence of surface fluoride availability greater than 100ppm (Christofferson *et. al.* 1995). If this was the case, it would be expected that the ratio of calcium would also be higher in the deposit than the underlying enamel, however, this is not the case here, where the ratio of Ca and P is actually lower. Whilst this does not completely exclude the possibility, as calcium fluoride forms mixed with phosphate, it would normally dissolve when formed *in vivo* due to the DS of the oral environment. The presence of calcium fluoride deposits would therefore suggest that the model is not effective at maintaining PF-relevant conditions and therefore actions, such as more frequent solution refreshes may need to be taken. The fact that only half the samples in each group were affected, suggests that the deposit may be a product of variation, during the pH-cycling process, as blocks were grouped into fives (n=10).

No conclusion could be drawn as to the true nature of the deposit without the employment of more detailed chemical analysis.

Overall, the findings of the chapter provide support for the previously proposed pH-cycling model, particularly when consideration is given to the fact that the Pre-demineralisation steps were completely removed and the observed changes were produced from sound enamel. Additionally, the SMH results also provide initial evidence that the model is also able to produce the physical changes reported to take place during PEM.

Chapter Seven: Effect of Strontium and Fluoride-Containing Remineralisation Solutions on PEM

7.1 Testing the Flexibility of the Proposed PEM Model

Building on the work from the previous chapter, the current study aimed to evaluate the ability to vary the parameters of the proposed model through the incorporation of varying remineralisation solutions in addition to exploring the effects of strontium on PEM. As such three Sr and F-containing remineralisation solutions were used. The updated model outline is presented in Figure 7.1 below.

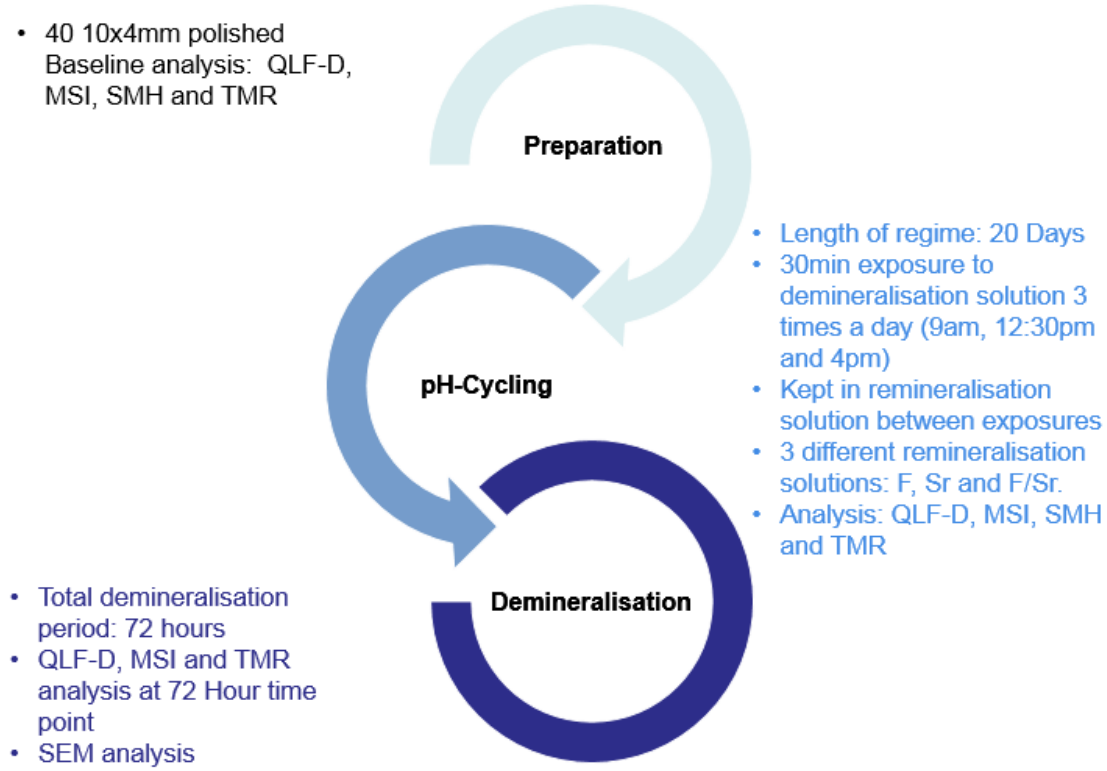

Figure 7.1: Summary of Current Model Protocol. *Outline of the current experimental procedure, broken down into the three stages of the proposed model*

7.2 Aims

The present work aimed to investigate the effect of remineralisation solutions containing varying combinations of strontium and fluoride within a plaque-fluid relevant pH-cycling model of PEM. It also aimed to determine the viability changing parameters of interest within the model on its ability to function as intended.

7.3 Materials and Methods

7.3.1 Selection and Preparation of Bovine Enamel Blocks

40 plane-parallel blocks approximately 10x4mm in size were prepared from bovine incisors and mounted in fives as described previously (Section 2.2/6.3.1).

7.3.2 pH-Cycling Regime

The base pH-cycling system previously described was used for a total of 0 or 20 days (Section 2.5) with changes made to the remineralisation solutions applied. The demineralisation solution described previously was used, but the remineralisation solution varied between groups to contain 5.7µM Fluoride (as NaF), 10ppm Strontium (as $SrCl_2$ (Sigma-Aldrich Ltd., Dorset, UK)) or a combination of the two (Table 7.1).

Reagent	F Remin Solution	Sr Remin Solution	Sr/F Remin Solution
KH_2PO_4	1mM	1mM	1mM
$CaCl_2$	12.7mM	12.7mM	12.7mM
KCL	130mM	130mM	130mM
HEPES	20mM	20mM	20mM
F (as NaF)	5.7µM	-	5.7µM
Sr (as $SrCl_2$)	-	10ppm	10ppm
pH	6.58	6.58	6.58

Table 7.1: Breakdown of varying remineralisation solutions used for pH-cycling. *Solutions were stored at room temperature and refreshed each day.*

7.3.3 Acid Challenge

In order to test the effect of the pH-cycling regime on the acid susceptibility of the enamel, blocks were subjected to a 72-hour demineralisation challenge using the lactic acid gel previously described (Section 6.3.3).

7.3.4 Assessment of Physical Changes

Blocks were subjected to Vickers's SMH analysis at baseline and following pH-cycling (Method: Section 2.11). Selected blocks were also imaged using SEM with EDX analysis (Method: Section 2.12/2.13).

7.3.5 Assessment of Demineralisation

Enamel blocks were allowed to air-dry before being imaged and using QLF-D and MSI. Images were taken at baseline, and following the 72h demineralisation challenge. TMR analysis was conducted outlined previously (Methods: Sections 2.8-2.10).

7.4 Results

7.4.1 Impact of Sr and F on demineralisation as measured via QLF-D

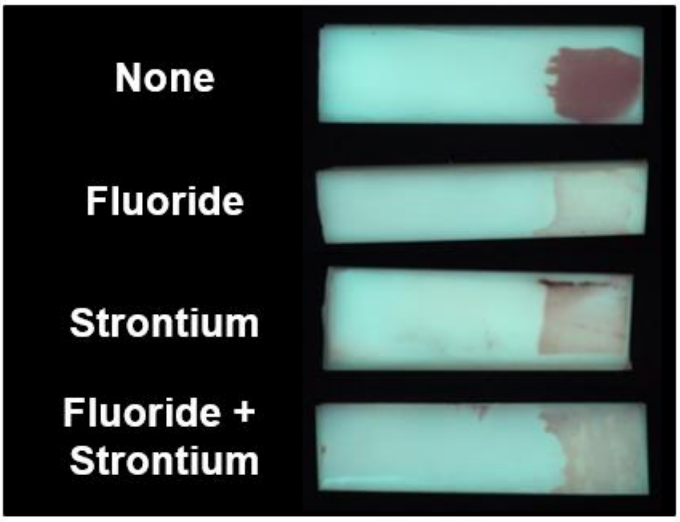

Figure 7.2: QLF-D Images Following 72h Demineralisation. *QLF-D images for lesions created in sound enamel exposed to 0 or 20d pH-cycling in the presence of F and Sr containing remineralisation solutions.*

When QLF-D images of lesions created in sound enamel and that exposed to 20d pH-cycling in F, Sr and Sr/F remineralisation solutions are considered, those created in pH-cycled enamel appear lighter in colour (Figure 7.2). Numerically, a significant decrease in fluorescence loss was reported for all lesions created in pH-cycled enamel in comparison to non-cycled controls (F: P=0.0004, Sr: P=0.0132 and Sr/F: P=0.0341) (Table 7.2). The largest difference was observed for blocks pH-cycled with the Fluoride only containing remineralisation solution (14.96). Data is presented graphically in Figure 7.3.

	n	ΔF ± SE
Untreated	10	28.77 ± 3.40
F	10	13.81 ± 0.78
Sr	10	15.24 ± 3.56
Sr + F	10	20.03 ± 1.71

Table 7.2: ΔF Values Following 72h Demineralisation. *QLF-D data for lesions created in sound enamel exposed to 0 or 20d pH-cycling in the presence of F and Sr containing remineralisation solutions. Data is presented with the SE of the mean. n=10.*

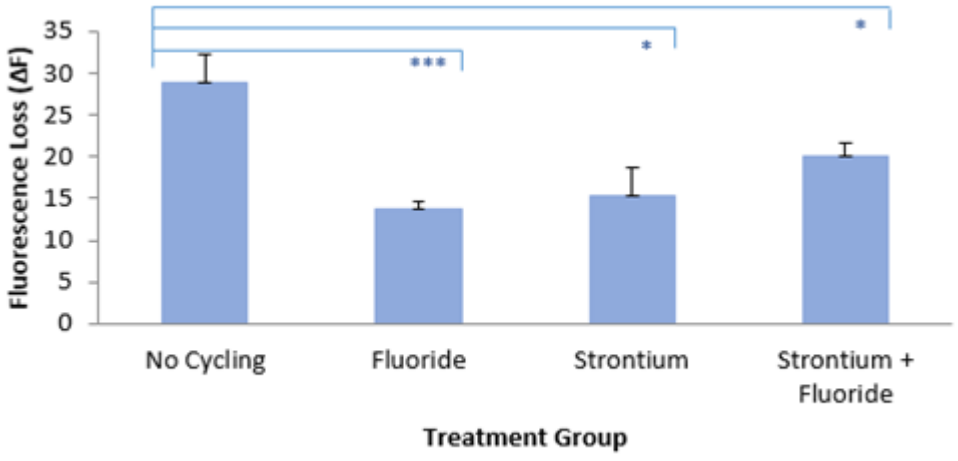

Figure 7.3: ΔF Values Following 72h Demineralisation Obtained by QLF-D. *QLF-D data for lesions created in sound enamel exposed to 0 or 20d pH-cycling in the presence of F and Sr containing remineralisation solutions. Error bars represent the SE of the mean. ***= P<0.001, *= P<0.05. n=10.*

7.4.2 MSI Assessment of the Effect of Varying Remineralisation Conditions on Fluorescence Loss

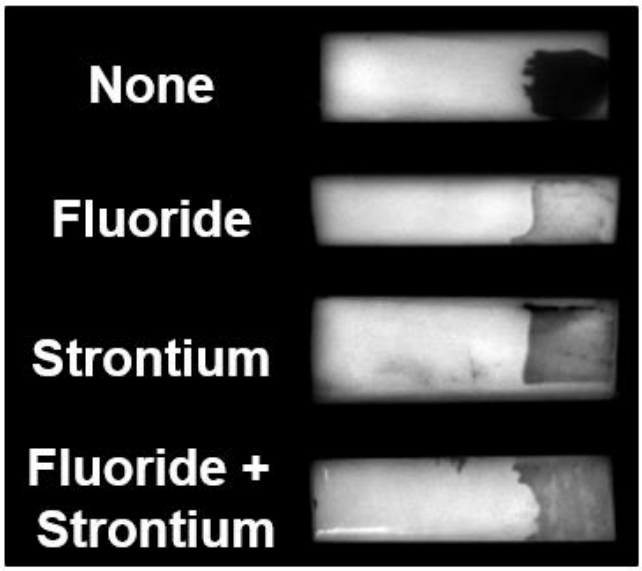

Figure 7.4: MSI Images Following 72h Demineralisation. *MSI images for lesions created in sound enamel exposed to 0 or 20d pH-cycling in the presence of F and Sr containing remineralisation solutions.*

When MSI images are visually analysed, lesions produced in pH-cycled enamel appear less pronounced than those created in sound enamel (Figure 7.4), however the observed difference is reduced in comparison to the previously reported QLF-D images. Lesions produced in blocks subjected to pH-cycling in the F-only solution group demonstrated the most marked visual difference in lesion appearance. A Significant decrease in fluorescence loss was reported for lesions created in enamel pH-cycled with remineralisation solutions containing F and Sr individually when related to non-cycled controls (F: P=0.0015 and Sr: P=0.0070) (Table 7.3). A non-significant decrease was observed lesions created in blocks cycled for 20 days with a remineralisation solution containing both Sr and F (6.04). The largest decrease was observed for blocks pH-cycled with the Fluoride only containing remineralisation solution (21.70). Data is represented graphically below (Figure 7.5).

	n	ΔF ± SE
Untreated	10	53.09 ± 4.97
F	10	31.39 ± 2.99
Sr	10	32.40 ± 4.63
Sr + F	10	47.05 ± 3.08

Table 7.3: ΔF Values Following 72h Demineralisation Obtained via MSI. *MSI data for lesions created in sound enamel exposed to 0 or 20d pH-cycling in the presence of F and Sr containing remineralisation solutions. Data is presented with the SE of the mean. n=10.*

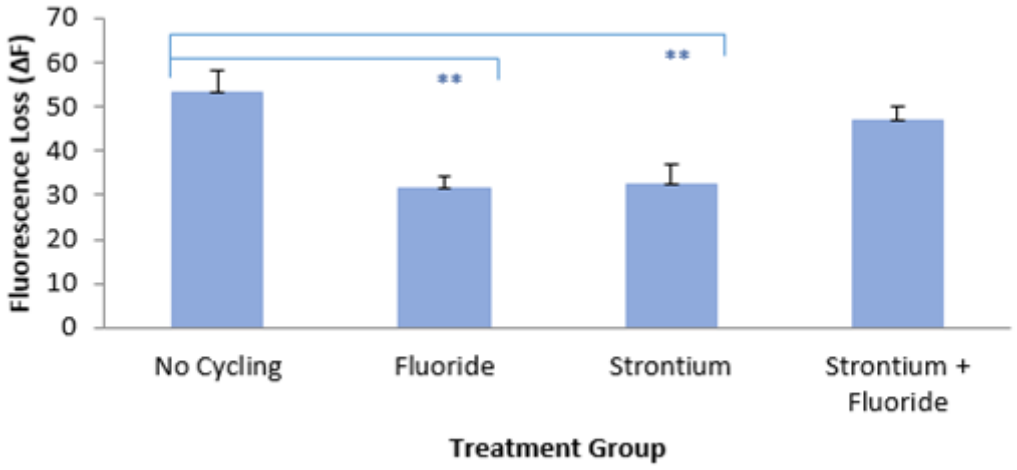

Figure 7.5: Fluorescence loss following 72h demineralisation as measured by MSI. *Data comparing non-cycled blocks to those exposed to 20 days of pH-cycling with remineralisation solutions containing F, Sr or Sr/F. Error bars represent the standard error of the mean (SE). ** and * Indicate significance at the P<0.01 and 0.05 levels respectively. n=10.*

7.4.3 Surface Microhardness Analysis of Sound and pH-cycled Enamel

	n	Sound SMH ± SE	Cycled SMH ± SE
Untreated	10	348.33 ± 16.74	340.44 ± 35.07
F	10	351.00 ± 42.72	354.90 ± 38.30
Sr	10	364.50 ± 8.86	385.70 ± 18.96
Sr + F	10	347.40 ± 18.47	376.70 ± 15.57

Table 7.4: SMH at Baseline and Following pH-cycling. *Vickers Surface Microhardness (SMH) values comparing non-cycled areas to those exposed to 20 days of pH-cycling with remineralisation solutions containing F, Sr and Sr/F. The standard error of the mean is displayed with each recorded value. n =10.*

Microhardness readings for the non-cycled controls and fluoride only groups were variable (Table 7.4), but a significant increase in micro hardness was observed from baseline in blocks subjected to remineralisation solutions containing Sr and Sr and F combined (P=0.0049 and 0.0012 respectively). SMH values are represented graphically in Figure 7.6.

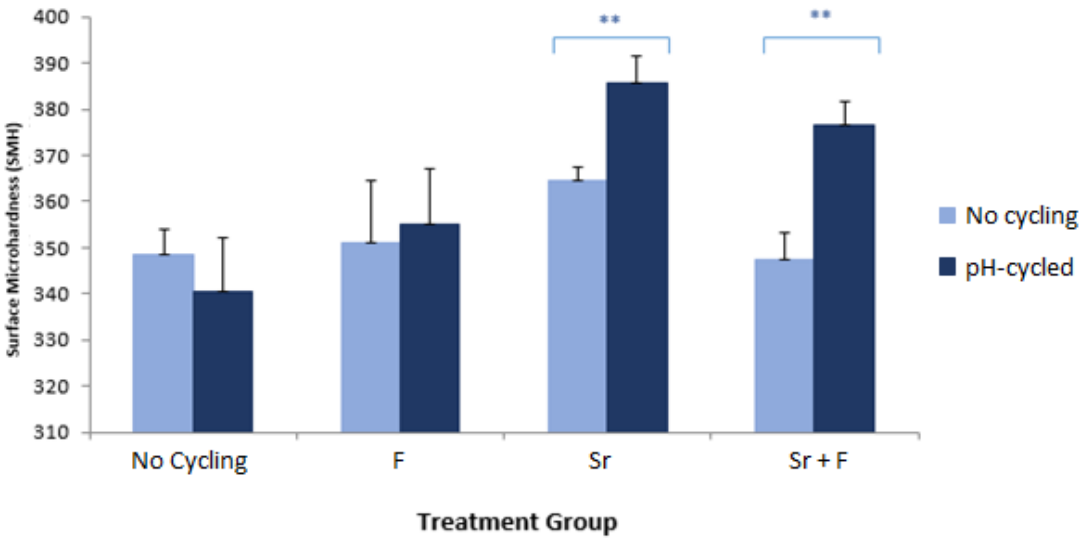

Figure 7.6: Vickers Surface Microhardness (SMH) Values. *Data comparing non-cycled areas to those exposed to 20 days of pH-cycling with remineralisation solutions containing F, Sr and Sr/F. The standard error of the mean is displayed with each recorded value. ** represents significance at the P<0.01 level. n=10.*

7.4.4 TMR Assessment of Changes in Mineral Loss

	n	ΔZ ± SE
Untreated	10	2244.43 ± 234.01
F	10	1155.15 ± 91.07
Sr	10	1433.62 ± 221.91
Sr + F	10	1817.65 ± 245.15

Table 7.5: ΔZ Values Following 72h Demineralisation Obtained via TMR. *TMR data for lesions created in sound enamel exposed to 0 or 20d pH-cycling in the presence of F and Sr containing remineralisation solutions. Data is presented with the SE of the mean. n=10.*

When mineral loss values obtained by TMR are considered (Table7.5), a significant decrease was observed for lesions created in enamel exposed to 20d pH-cycling with remineralising solutions containing Fluoride (P=0.0004) and strontium (P=0.0217) separately. Additionally, a non-significant decrease was observed for lesion created in enamel blocks subjected to a 20-day pH-cycling regime using a remineralising solution containing both fluoride and strontium when compared against those created in non-cycled controls (Figure 7.7).

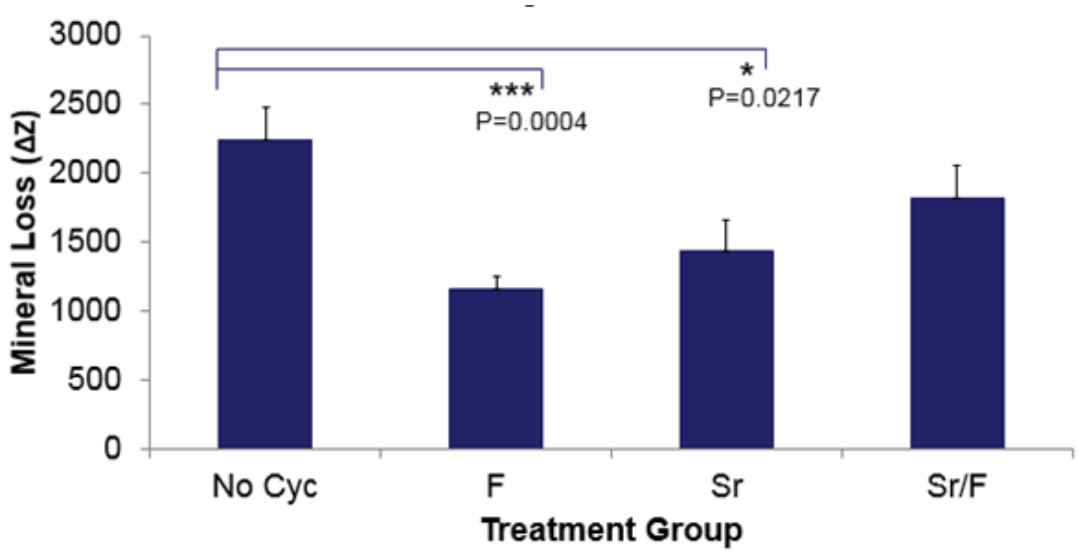

Figure 7.7: Mineral loss following 72h demineralisation as measured by TMR. *Data comparing non-cycled blocks to those exposed to 20 days of pH-cycling (cyc) with remineralisation solutions containing F, Sr or Sr/F. Error bars represent the standard error of the mean (SE). *** and * Indicate significance at the P<0.001 and 0.05 levels respectively. n=10.*

When the shape and characteristics of created lesions are considered, a decrease in both lesion depth and the ratio, R, can be seen for all pH-cycled conditions when considered against non-cycled controls (Figure 7.8). in terms of lesion profile, created lesions followed a typical caries lesion shape, with the exception of the Sr-only group, which formed a lesion with a small, less defined surface area (Figure 7.9). The surface area in lesions produced in both fluoride containing groups demonstrated a larger surface area than non-cycled counterparts.

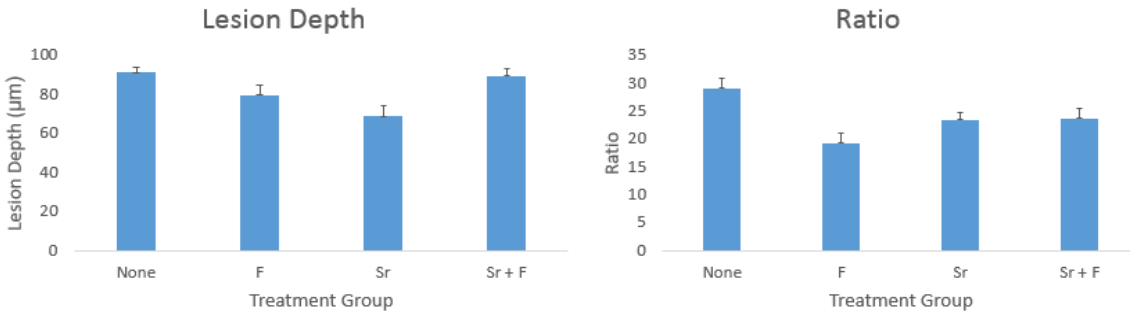

Figure 7.8: LD and R for Lesions Created in Sound and pH-cycled Enamel. *TMR data for LD and R for lesions created in sound enamel and that subjected to 0/20d pH-cycling with Sr and F containing remineralisation solutions. Error bars represent the SE of the Mean. n=10.*

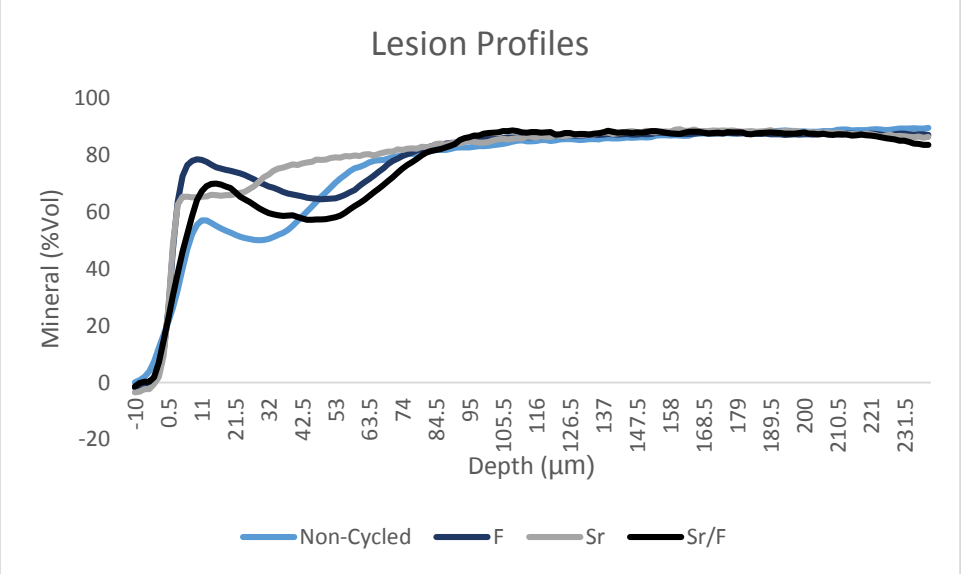

Figure 7.9: Lesion Profiles for Lesions Created in Sound and pH-cycled Enamel. *Lesion profiles created from TMR data for lesions created in sound enamel and that subjected to 0/20d pH-cycling with Sr and F containing remineralisation solutions.*

7.4.5 Effect of Sr on Enamel as Viewed using SEM

When scanning electron microscopy was used, vacuum conditions caused damage to the enamel surface which can be observed as visible cracks in the below SEM images (Figure 7.10). However, from the data that was collected, basic EDX analysis suggests

a higher Sr content (as related to other elements) for enamel pH-cycled with a Sr-only containing remineralisation solution when compared to sound enamel.

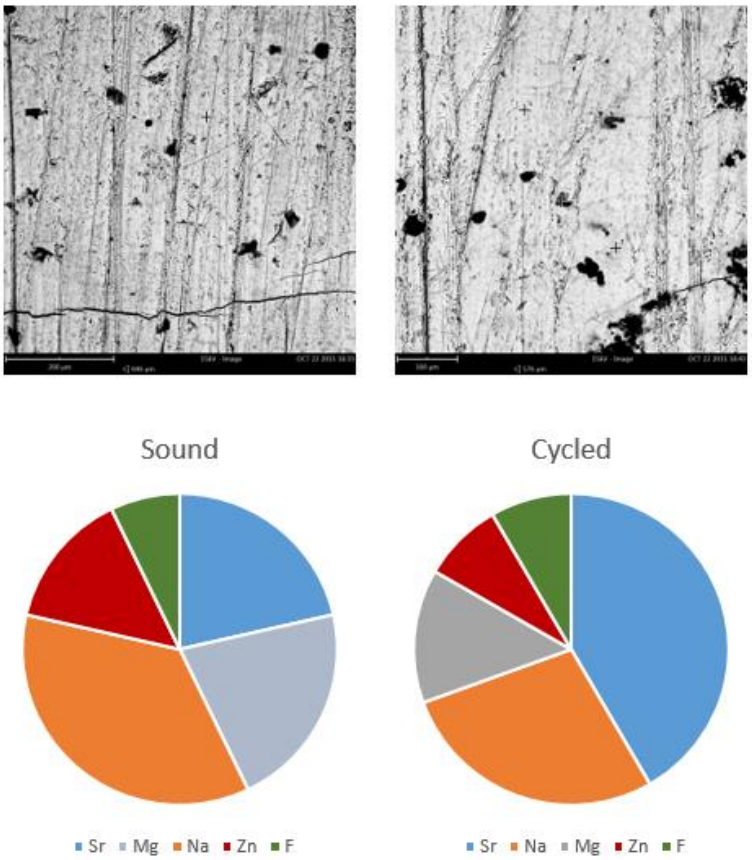

Figure 7.10: EDX Analysis for Sound and pH-cycled Enamel. *SEM image and basic EDX analysis demonstrating differences in the proportion of different elements such as Zn, Sr and F following exposure to 20d pH-cycling with Sr.*

7.5 Discussion

Following on from the findings of the experiments reported in the previous chapter, to further test and validate the proposed pH-cycling model, the current chapter aimed to determine the suitability for the model to still function when the parameters are altered. This is an important feature, as in order for it to be used to gain an understanding of the PEM process, it must be able to demonstrate the effects of different solution and treatment combinations.

Due to the varied findings on the potential remineralising capabilities of Sr reported in the literature (Lippert and Hara 2013), it was difficult to predict how it would behave when substituted into the PEM model. Whilst a reduction in fluorescence/mineral loss was observed for all pH-cycled blocks in comparison to the non-cycled controls, regardless of remineralisation solution, the standard F-only remineralising solution was still the most effective. Most evidence for Sr as a remineralisation agent is formed around its dual administration with F in the concentrations used for this work (Thuy *et. al.* 2008). This is hypothesised to potentially occur through a similar mechanism to zinc, where surface softening affords F better access to the lesion and therefore a larger surface area to bind. The results obtained in this study do not provide support for this idea, as, whilst effective compared to non-cycled controls, the Sr + F group was the least effective. The reduced performance of the combined Sr and F Solution when compared to F alone, suggests that the simultaneous application may actually be inhibiting the effect of the F to a certain degree. Even more interesting, is the fact that the Sr-only solution was more effective. The reason behind this is not apparently clear, but it is worth noting at this point that the Sr-only groups were still exposed to F, as whilst the remineralising solution was F-free, the demineralisation solution contained 4.25µm F, as NaF. This raises the possibility that the timing of dual Sr and F administrations is a factor, and that alternating, not simultaneous, administration is more effective.

When an SEM-EDX combination is used to give an estimate of relative content of the sound and pH-cycled enamel for the Sr-only group, a second possible explanation for the varying Sr behaviour is highlighted. Cycled enamel showed elevated strontium in comparison with other elements. This suggests potential for the Sr to be binding to the enamel at the surface and therefore it may be the case that the dual application of Sr +F is leading to competition in some aspect of the process, reducing the action of both substances.

When the physical effects of the different solutions are taken into account, the impact of Sr is markedly different. Whilst a slight increase was reported in SMH for F-only enamel following pH-cycling, there was no strong evidence for an increase in hardness. In comparison, a marked increase in SMH, similar to that observed for blocks treated with Zn +F (Section 6.4.3) was observed for both the Sr containing groups. However, to determine the underlying mechanism by which these changes occur requires repetition with more in depth chemical characterisation of both sound and cycled enamel.

One of the aims set out at the beginning of this development process was that the proposed model should be amenable to the substitution and incorporation of differing experimental variables, whilst maintaining its intended function. The data reported in this chapter provides support for the ability of the current model to meet such expectations, as the substitution of external 2m treatments for varying remineralisation solution compositions was still able to produce pH-cycled enamel that demonstrated key features of PEM such as reduced susceptibility to acid and increased SMH.

In summary, the current study, in addition to providing further support for the general basis for the model, demonstrates its ability to be applied as a tool to investigate the ability of different conditions on the ability to replicate the effects of PEM *in vitro*.

Chapter Eight: Validation of Fluorescence-Based Methods for Detecting Demineralisation

8.1 Background

Whilst there is no currently defined indicator of the occurrence of PEM, studies have reported a decrease in caries susceptibility following exposure of enamel to the oral environment (Carlos and Gittelsohn 1965). In addition, the other two most commonly reported effects of the process are in increase in surface hardness and a decrease in porosity, both of which would contribute to the observed increased resistance to demineralisation for matured enamel. It therefore made sense to test the ability of the current model to "mature" enamel *in vitro* through an acid challenge and assessment the level of demineralisation between matured and control enamel. It is therefore important that reliable and validated quantitative methods for the detection of demineralisation, particularly at relatively low levels are used.

8.1.1 TMR

First described by Angmar *et. al.* (1963), Transverse Microradiography (TMR) is widely regarded as the gold standard for assessing mineral changes within the dental field. The technique is based on the production of a radiograph of a transverse section of enamel and comparing the x-ray adsorption to a step-wedge standard exposed simultaneously (ten Bosch and Angmar-Mansson 1991). This allows the calculation of a volume percentage of mineral (%Vol) as a function of depth from the enamel surface (µm) and has a proven track record for detecting changes in mineral due to de- and re-mineralisation (Arends *et. al.* 1983a, 1983b). In order to automate the process, dedicated software has been developed to allow quantification and analysis of such changes (de Josselin de Jong *et. al.* 1987). However, the main drawback of TMR is the

destructive nature of the preparation process. This means that TMR is not suitable for *in vivo* use and when used *in vitro,* samples only have limited further use. Further to this, the preparation process can result in damage to or loss of samples, which can affect subsequent results (Anderson *et. al.* 1998).

8.1.2 QLF-D

Quantitative light induced florescence is a caries detection system based on assessing changes in fluorescence of dental hard tissues following demineralisation. It is based on the established auto-fluorescence properties of dental enamel which were first demonstrated under UV light conditions (Stubel 1911, Armstrong 1963, Alfano and Yao 1981). Measurable fluorescence from enamel is proportional to the amount of material present, therefore demineralised enamel emits a lower level than that of sound enamel. More specifically, the increased scattering coefficient of demineralised enamel reduces the chances of fluorophores of being emitted and therefore detected (de Josselin de Jong *et. al.* 1995, 2009). The QLF system is able to detect this difference and quantify it to allow numerical analysis. As this technique relies only on the detection of fluorescence, one of its main advantages over more classical techniques, such as TMR, is that it is non-destructive and can therefore be used to monitor progress over time, *in vivo* and can be combined with other, more destructive techniques. Further to this, it also is possible to use QLF clinically, with several units designed specifically for such use.

An example QLF system, the Inspektor Biluminator™ (Inspektor Research Systems, Netherlands), uses a digital SLR camera fitted with a biluminator tube containing 4 white and 12 high-power blue LED lights. The system uses associated software to capture an image using he blue light through a 520nm high pass yellow filter. A regular white light image is also captured as a reference. Visually, areas of demineralisation appear darker than adjacent sound enamel and the coupled analysis software is able to quantify this difference to produce a %fluorescence loss value (ΔF).

Whilst it is not considered a “gold standard” like TMR, the use of QLF-D for the assessment of demineralisation has been validated both alone and against TMR and results have been found to be reproducible (Pretty *et. al.* 2004). The system has been proved suitable for a range of both clinical and *in vitro* research applications.

8.1.3 MSI

With modern advances in fluorescence loss-based caries detection systems, a focus has been placed on the merit of multi-spectral imaging systems. Such systems follow a similar setup to previously described QLF-D, but instead of taking a single SLR image through a 520nm filter, images are taken through a range of different wavelengths using a specially designed camera to create a composite “cube” which can then be analysed and different wavelengths extracted and the resulting spectra compared. In addition, extracted images can be analysed through the QLF-D analysis software allowing it to be used in a comparable manner to assess mineral loss. The main drawback of using such novel techniques is the lack of research comparing and validating them against the accepted standards and as such they can often need to be conducted in conjunction with more traditional techniques.

8.2 Aims

The present work aimed to compare the ability of a newly-developed MSI system to assess fluorescence loss due to demineralisation, against an established QLF-D system. In addition, it aimed to compare the demineralisation detection capability of fluorescence loss-based technologies to the current “gold standard” for assessing changes in mineral (TMR).

8.3 Methods

8.3.1 Block Preparation

Bovine enamel was sourced, stored and prepared as previously described being mounted onto a ceramic anvil using Green-Stick impression compound (Kerr Corporation, California, USA) and cut using a water-cooled precision diamond wire saw (Model 3241; Well Diamantdrahtsagen GmbH, Mannheim, Germany) to produce 18 blocks approximately 10x10mm in size (Figure 8.1). In addition to the experimental block, a 10mmx5mm block was cut from each tooth to provide a baseline for TMR analysis.

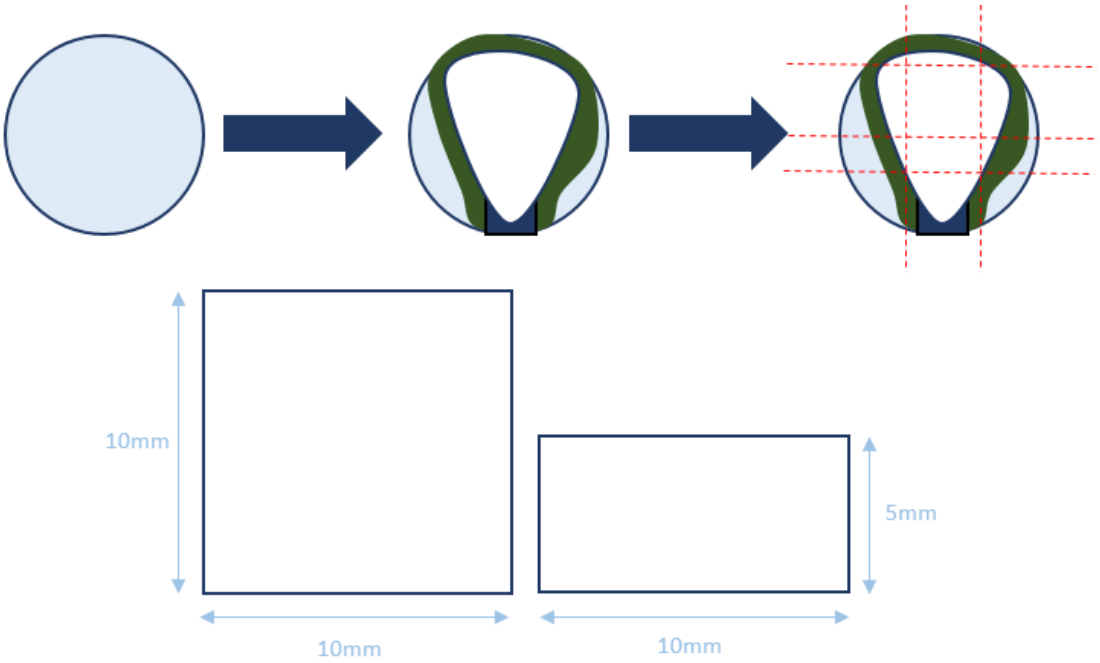

Figure 8.1: Illustration of Block Creation Process. *Schematic of mounting and cutting process to produce 10x10mm bovine enamel blocks in addition to 5x10mm baseline controls.*

Blocks were coated in clear acid resistant nail varnish (MaxFactor Nailfinity, Procter and Gamble, Weybridge, UK) with the exception of a 9x9mm experimental window on the polished enamel surface. Following air-drying, blocks were mounted individually with Green-Stick impression compound into 50ml disposable Sterilin containers

(Sterilin Ltd. Newport, UK) using a glass rod placed through the lid. This process is illustrated below (Figure 8.2).

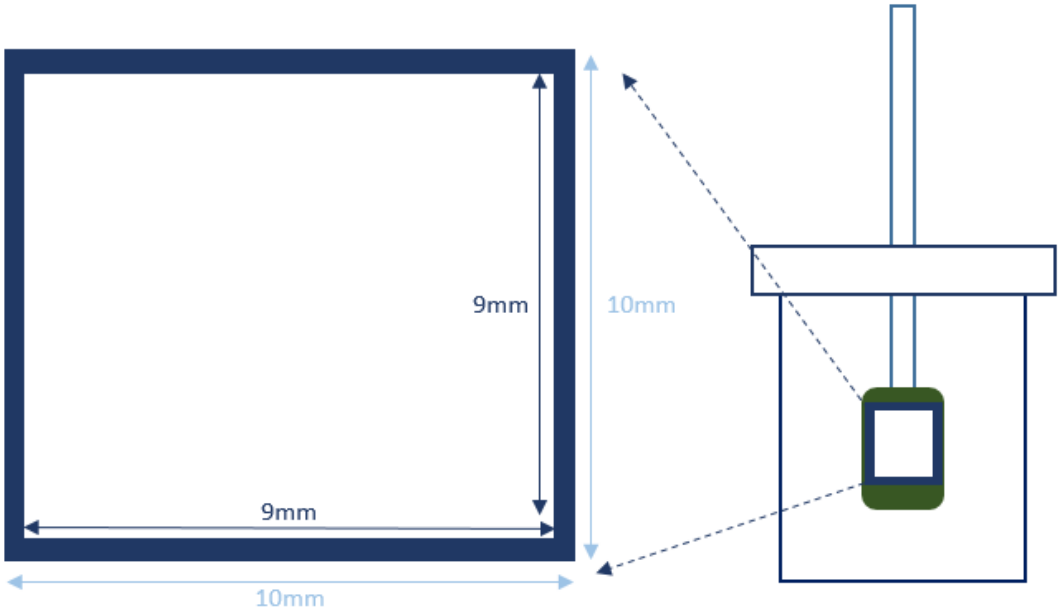

Figure 8.2: Illustration of block Preparation and Mounting. *Schematic of varnished block with a 9x9mm experimental window, mounted within a Sterilin container with green stick.*

8.3.2 Lesion Creation

Blocks were subjected to the standard acetic acid demineralisation challenge outlined previously (Section 2.6). At the 12h, 24h and 48h time points, blocks were removed from the solution, rinsed in de-ionised water. Blocks were then imaged using the QLF-D and MSI systems and a quarter of each block removed for TMR analysis. Before being placed back into the solution the exposed area of the block was sealed using acid resistant nail varnish (Figure 8.3).

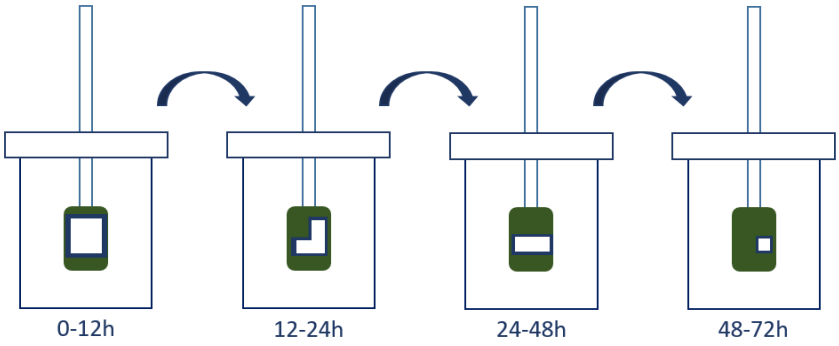

Figure 8.3: Schematic of Demineralisation Protocol. *Illustration on demineralisation process showing removal of lesion area of analysis at 12, 24 and 48h time points.*

8.3.3 TMR

TMR was mostly conducted as previously described (Section 2.10). Baseline and quarter blocks were mounted onto ceramic anvils with Green-Stick Impression Compound and cut into transverse sections approximately 1.2mm in width using a precision diamond wire saw. Three sections from each were then mounted onto brass anvils using nail varnish and polished down to approximately 80µm in thickness using a diamond impregnated disc.

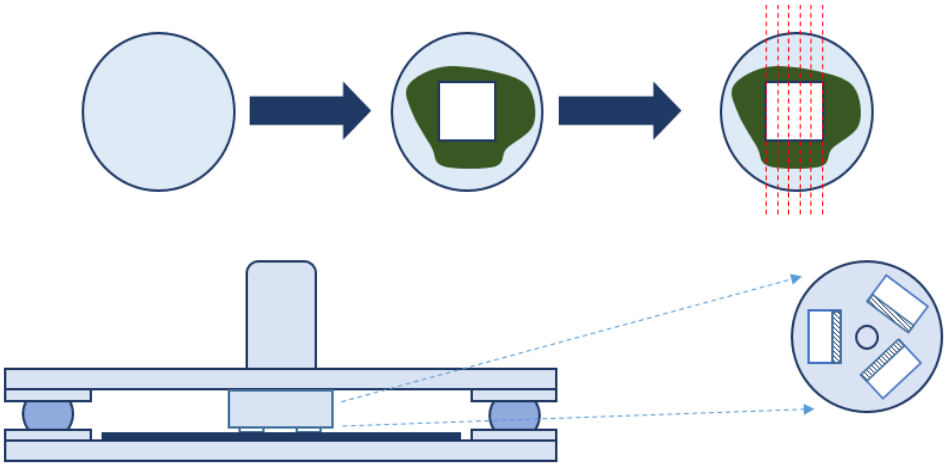

Figure 8.4: Illustration of TMR Section Preparation. *Schematic of mounting and cutting of blocks to produce 1.2mm transverse sections. Sections are mounted onto brass anvils in threes and ground using a custom-built diamond disc and ball-bearing system to produce sections 80µm in thickness.*

8.4 Results

8.4.1 Comment on the Ease of Operation of Each Technique.

When the process involved for each analysis technique is considered, fluorescence-based detection methods were relatively quicker and less labour intensive than TMR to carry-out. In terms of preparation, QLF-D and MSI only required air-drying samples, whereas the TMR preparation process takes several days to complete. Image capture for QLF-D is almost instant, whereas MSI takes around 30 seconds to construct an image cube. TMR requires a radiograph exposure time of 12 minutes followed by a 50-minute development process. A similar pattern is observed for analysis, with QLF-D having a relatively quick process in comparison to TMR, which requires manual calibration of the step wedge and capture of each area of interest. MSI analysis is conducted in the same manner as QLF-D, but requires extra steps to extract the 520nm image and convert it into a compatible file format. In terms of the ability for an individual to use each method, QLF-D and MSI are relatively accessible to new users, particularly QLF-D, as the process is fairly automatic and only requires placement of the sample and a few mouse clicks. MSI follows a similar process, but requires manual operation of the bioluminator and knowledge of the correct settings to select when capturing an image. On the other hand, the TMR process is less accessible to new users, as it requires learning the use of several pieces of equipment, practice of the preparation and image capture techniques and training in using the radiographic equipment. Information is presented in Table 8.1.

	QLF-D	MSI	TMR
Preparation Time	1h	1h	Several Days
Preparation Process	Air-Drying	Air-Drying	Sectioning, grinding and mounting
Image Capture Time	<10 seconds	2mins	>1h
Image Capture Process	Place Sample, Focus, Select Capture	Place Sample, Focus, Set Light, Set Exposure, Select Capture	Mount samples with stepwedge and plate, Exposure to X-rays, Develop, Fix, Wash
Analysis Process	Open analysis software, Select area of interest, select ok	Extract 520nm image, convert to BMP, Open analysis software, select area of interest, select ok	Calibrate stepwedge, Capture areas of interest as images, Open analysis software, select area of interest, select ok

Table 8.1: Comparison of Methods. *Table comparing the user-friendliness of the three demineralisation detection techniques*.

8.4.2 Images Produced by Each Approach

When placed together, visual data collected using QLF-D and MSI appears similar, with the area of demineralisation appearing as a darker square that increases in intensity at longer demineralisation times (Figure 8.5). For both techniques, the area of demineralisation is first visible following 3h exposure to acid, however the area is more pronounced in the images obtained via MSI. This trend extends to all time-points, with the demineralisation appearing darker and more apparent in MSI images than QLF-D counterparts.

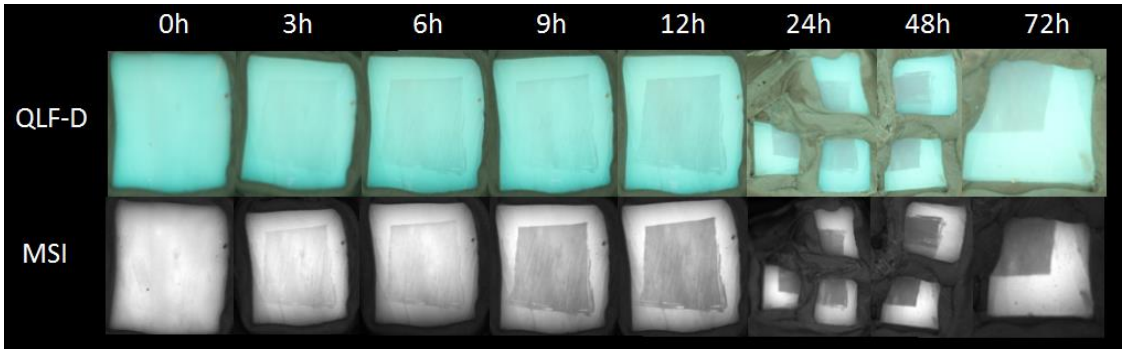

Figure 8.5: QLF-D and MSI Images During 72h Demineralisation. *Visual comparison between images obtained via QLF-D and MSI at 0, 3, 6, 9, 12, 24, 48 and 72h exposure to acetic acid demineralisation.*

In contrast to fluorescence-based methods, radiographs produced using TMR were only taken after 12 hours exposure, as the ability to detect lesions prior to this is limited, as is the amount of material that can be removed to create each time point. TMR images demonstrate the lesion as a dark area below an intact surface region that continues along the length of the section. In a similar manner to the previous techniques, the lesion area appears darker and more pronounced at longer acid exposure times (Figure 8.6).

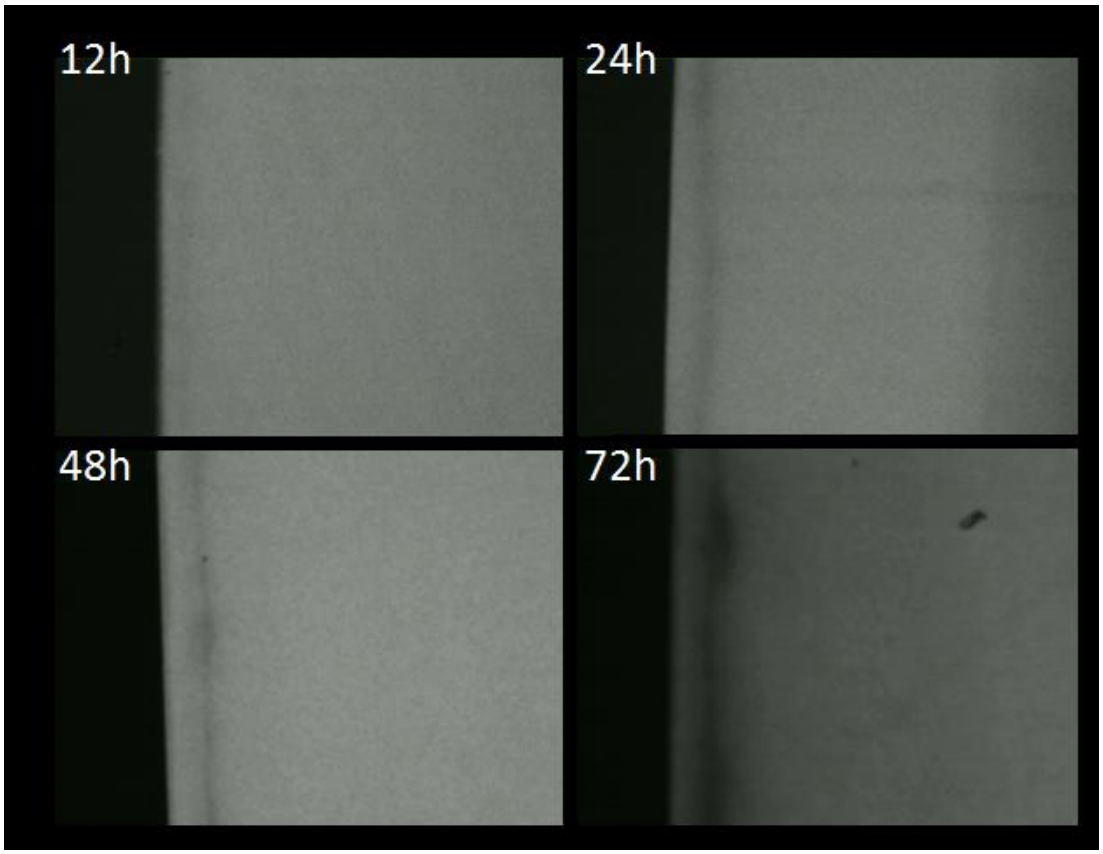

***Figure 8.6: Radiographic images during exposure to acid**. Radiographic images of transverse sections of enamel captured using TMR at 12, 24, 48 and 72h exposure to demineralisation.*

8.4.3 Comparison between Quantitative Data Collected

When the numerical data obtained via the two fluorescence-based techniques is considered (Figure 8.7), the same difference in intensity observed visually is reflected. Whilst both methods detected an average change in fluorescence at the 3h time point, this change was only observed in 3/18 blocks for QLF-D as opposed to 17/18 for MSI. Additionally, all 18 blocks demonstrated a change in fluorescence by 6h for MSI as opposed to QLF-D which did not detect loss in all blocks until 24h exposure to acid. Recorded fluorescence loss values are consistently higher for MSI than QLF-D at comparable time-points. When TMR data is considered, reported mineral loss values increased with demineralisation time and followed a pattern that was more comparable to MSI than QLF-D.

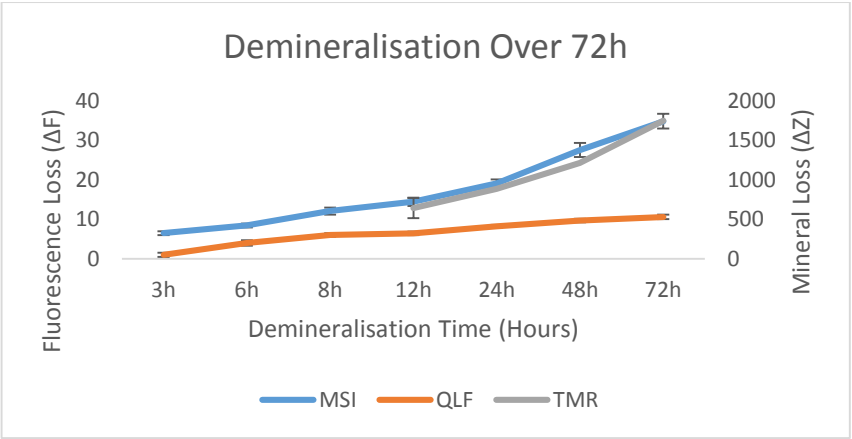

Figure 8.7: Graphical Representation of Data Collected Using Different Approaches. *Graph comparing mean changes in mineral as recorded by QLF-D and MSI (ΔF) and TMR (ΔZ).*

When the spread of the data recorded by comparable methods is considered, a large amount of variation is observed, particularly at higher levels of demineralisation (Figure 8.8).

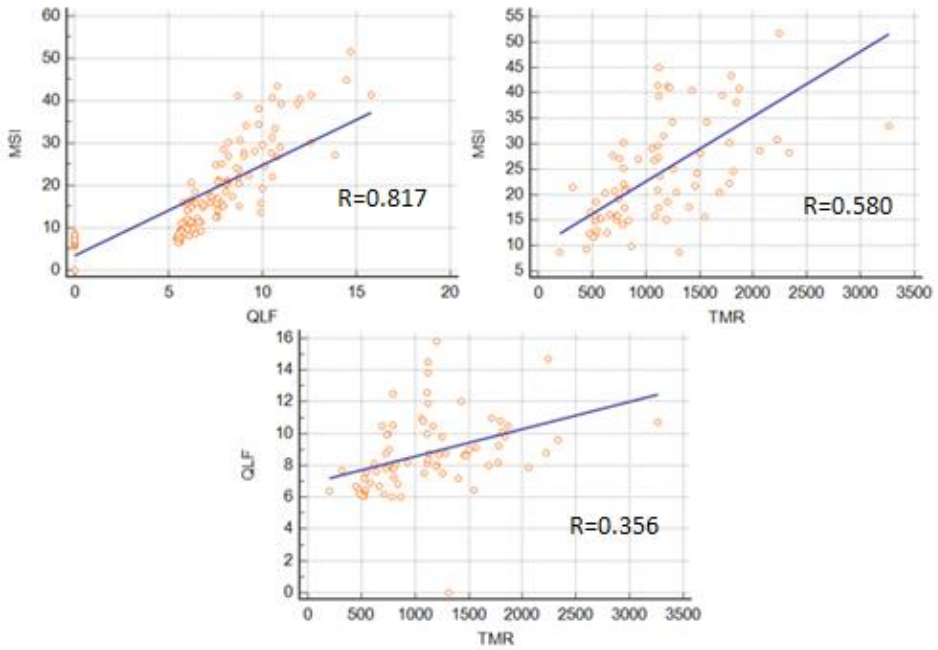

Figure 8.8: Scatter Plots Comparing Agreement Between Analysis Techniques*. Scatter plots fitted with regression (R) lines to demonstrate the agreement between measurements taken of the same lesion.*

8.4.4 Additional Features – MSI

Unlike the QLF-D system, which takes a single image, the MSI system scans through a wavelength range whilst capturing the image to produce a composite “cube”. Therefore, in addition to extracting an image at a single wavelength for analysis, the entire spectral cube can be analysed. When an area of interest is identified, a colour can be assigned and the spectral profile for that area is displayed. This can be repeated for multiple areas of interest, such as the experimental window and surrounding sound enamel as illustrated below. The software can then be used to “Unmix” the desired areas and produce a composite image of where the spectral profile of the image matches the areas selected. For baseline enamel and early demineralisation, the height difference between the spectra of the two areas is small and as such no clear definition between the two was observed, although it is worth noting that a slight difference was recorded even at baseline. In more heavily demineralised enamel the height difference between the spectra was more defined and as a result the unmixed images displayed two distinct areas of colour. In this case the recorded changes are only in the height of the same spectral profile as opposed to areas exhibiting different spectral features. An example of this feature is presented in Figure 8.9.

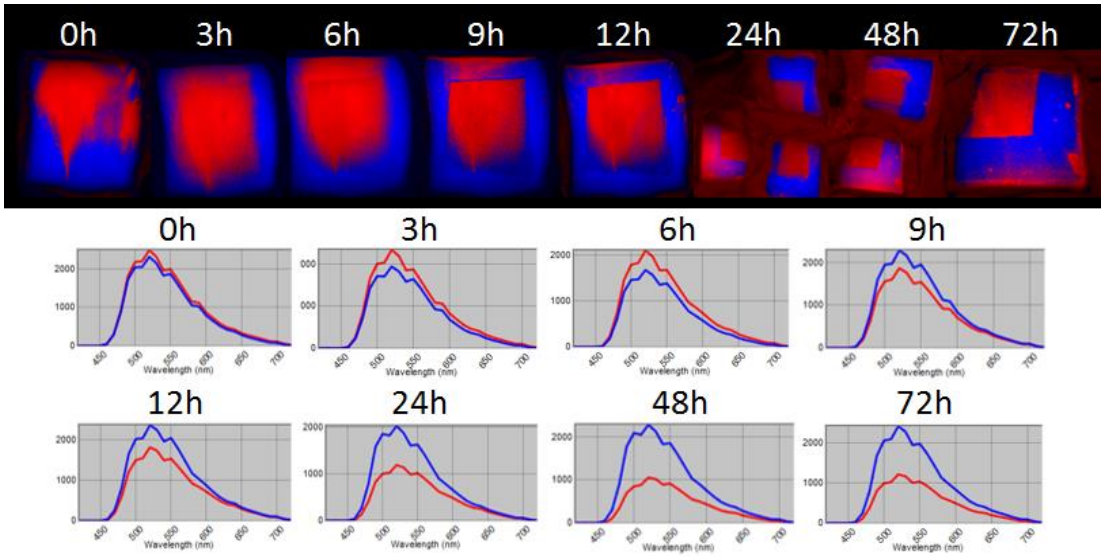

Figure 8.9: Spectral Analysis Using MSI. *Graphs following the changes in spectral profiled of the lesion and surrounding enamel during demineralisation. A visual representation of the different areas represented is also provided (Top).*

8.4.5 Additional Features – TMR

In addition to recording mineral loss, the images above also highlight the additional ability of TMR to identify the surface zone of the lesion. The TMR analysis software is capable of producing a profile on the lesion by plotting %Vol mineral as a function of depth allowing the characteristics of the lesion, particularly the surface area, to be visualised (Figure 8.10). This also affords the ability to distinguish between erosive and subsurface lesions. In addition to the profile and mineral loss values, the TMR analysis software can also give information on the depth and ratio of the lesion.

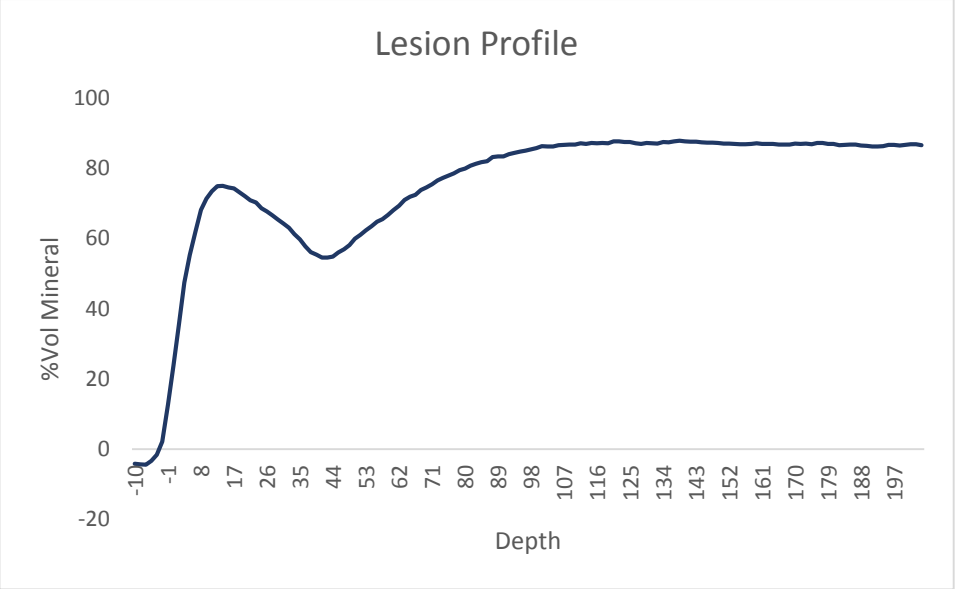

***Figure 8.10: Profile of lesion following 72h demineralisation**. Lesion profile obtained via TMR expressing the %vol mineral as a function of depth for enamel subjected to a 72h acetic acid demineralisation challenge.*

8.5 Discussion

In terms of usability, the fluorescence-based techniques were easier to both learn and conduct in comparison with TMR. This provides support for previous authors who have expressed concern over the destructive nature of the TMR preparation process and the loss of samples incurred as a result (Anderson *et. al.* 1998). This may serve in part to explain the variability observed from the presented scatter plots, when comparing TMR with the other methods. Another explanation for the variability observed is the differing capability of the different methods to detect demineralisation, which is particularly evident when the images produced by the two fluorescence-based techniques are considered visually. The difference, combined with the different measurement scale used for TMR made statistical comparisons to determine the agreement of the methods challenging, as traditional approaches, such as Bland-Altman plots are designed to compare two methods using the same scale and assume that the same value is desired by both methods at each measurement point (Myles 2007).

Whilst the agreement between TMR and QLF-D observed here was less than that reported previously (Angmar-Mansson and ten Bosch 2001, Pretty *et. al.* 2004), the MSI data showed higher comparability. This may be due to its apparent increased ability to detect demineralisation. The difference between the two fluorescence-based techniques appears to be due to the camera used within the MSI system being more sensitive, as the rest of the equipment and process behind the two methods is the same.

When the information obtained by each method is considered, it is understandable that TMR is considered the "gold standard", as it was the only method able to provide information on the characteristics of the lesion beyond mineral loss. This is important when considering *in vitro* use, as the surface area is a defining feature of caries lesions over other types of mineral loss such as erosion (Silverstone 1968, Larsen 1991), and can give valuable information, particularly in studies where fluoride and other therapeutic agents are used.

The ability for the MSI system to produce spectra that can be mapped onto the image is a really interesting feature, although its use within the type of work presented here is limited, as it does not provide any information not already available through visual examination and fluorescence loss data. It does however, have a range of applications within the dental field, as in cases where the spectral profiles of areas of interest differ, such as distinguishing between enamel, plaque and calculus, it would provide information not available through other methods.

To summarise, both fluorescence-based and microradiography techniques were able to demonstrate increasing mineral loss over a 72h demineralisation period, however the levels of agreement between methods previously observed in the literature were not recorded in this study. The MSI technique is particularly interesting, as it is able to detect demineralisation at an earlier time point than the other methods.

Chapter Nine: General Discussion

9.1 Selection of an *in vitro* PEM Model

Whilst several approaches widely used within the dental field would serve as a basis of an *in vitro* model of PEM, the main two considered for the work presented here were the use of a biological caries model, such as a constant-depth film fermenter (CDFF) or a chemical-based pH-cycling model, both of which are discussed previously (Section 1.8). After considering the suitability of both approaches, a pH-cycling method was chosen. It is widely accepted that, whilst the exact mechanism by which PEM occurs is not known, it is believed to be the result of exposure to the cyclic nature of the oral environment, causing intermittent periods of conditions favouring de- and remineralisation (Lynch 2013). pH-cycling provides a way to re-create alternating periods of acidic and remineralising conditions *in vitro*, whilst also affording the ability to have control over the parameters by which these periods occur and their frequency. The use of such a technique as the basis allows the development of a model within which the conditions can theoretically be easily varied to allow a range of investigations to be conducted. This ability to control the chemical components of the test solutions used, should serve to reduce variability from one experiment to another and is one of the main reasons for the choice of a chemical-based model as opposed to a biological one. The aim being development of a model which, once established, could be adapted to and tested within a more variable biological model.

9.2 Effect of pH-cycling on Enamel

Throughout the chapters presented in this thesis, exposure to plaque-fluid relevant pH-cycling conditions has shown an ability to confer changes to the outer layers of the enamel, as demonstrated by a decrease in susceptibility to an acid challenge when

compared with non-cycled enamel. This is in keeping with the literature, where a previously remineralised enamel, particularly in the case of arrested caries, has been shown to be similar, if not less susceptible than sound enamel to a repeated acidic challenge (ten Cate and Duijsters 1982, Lagerweij and ten Cate 2006). Additionally, the incorporation of fluoride, a known factor in acid resistance, is known to occur more effectively during periods of demineralisation as opposed to when applied to sound enamel (Fejerskov *et. al.* 1994, Featherstone 1999, Lynch and Smith 2012, Lynch 2013). This is also an important outcome of this work when the overall aims are taken into consideration, as it provides previously lacking, evidence for the proposed mechanism of PEM being the cyclic conditions of the mouth leading he observed chemical and physical changes.

9.3 Evaluation of Proposed Model

When addressing the main aims of this project it is important to assess the ability of the end result to meet the goals set out. When considering the ability of the model to allow the future detailed study of the PEM process, it is first required to assess whether the model can be classed as creating “matured” enamel. Whilst little has been done to chemically categorise mature human enamel, the ability of matured human enamel to present decreased susceptibility to acid challenges when compared with “immature” counterparts has been widely reported (Carlos and Gittelsohn 1965, Francis and Briner 1966). If considering the model against this requirement, it can be argued that, yes, it is effective at re-creating the observed effects of PEM, as reported mineral loss values for cycled enamel when matched with non-cycled controls has been repeatedly presented throughout this work.

The second parameter by which PEM is often defined within the literature is an increase in surface hardness observed following exposure to the oral environment and PEM occurring (Brudevold *et. al.* 1982, Palti *et. al.* 2008, Cardoso *et. al.* 2009). Whilst

the model has demonstrated an ability to incorporate this as a parameter, the ability for it to produce “mature” enamel by this condition is less well demonstrated, as only enamel in certain conditions within the model (Zn/F and Sr-containing) was reported to have increased surface microhardness following pH-cycling. However, it can be argued that these elements have been shown to be present in the enamel following eruption, that these conditions within the model may therefore be the most representative of the *in vivo* PEM process in terms of ion availability. This seems particularly relevant for the Zn/F treatment condition, as both Zn and F have been shown to accumulate in the surface layers of enamel shortly after eruption before being gradually lost (Brudevold *et. al.* 1963, Weatherell *et. al.* 1972), suggesting a role in the PEM process.

The third reported measure of PEM is the one that this model has not yet demonstrated an ability to address. Newly-erupted enamel has been shown to become less porous following exposure to the oral environment (Brudevold *et. al.* 1982, Schulte *et. al.* 1999, Kataoka *et. al.* 2007), probably due to the loss of HPA impurities such as Carbonate and magnesium in addition to more soluble organic material (Marshall and Lawless 1981, Robinson *et. al.* 2000). To this point, the effect of the proposed pH-cycling model on enamel porosity has not been demonstrated, and therefore, in terms of this criteria, it cannot claim to have fully reproduced the reported effects of PEM. There would, however, be an easy additional outcome measure to incorporate within the current design and would feature highly on a list of future steps that need to be taken to continue the work started here.

9.4 Role of Ions

In addition to assessing the ability of the model to re-create the PEM process *in vitro*, the work within this thesis also provides the material to discuss the interactions between ions such as F, Zn and Sr with dental enamel and their possible roles within the PEM process. The ability of fluoride to reduce susceptibility of enamel to acid

challenges is widely established (Bratthall *et. al.* 1996), therefore, in that regard the results reported within this work are not surprising, as they support this observation. It is, however, more interesting to consider the interactions of F with the other ions used in the PEM model. It has been suggested that zinc is capable of both inhibiting and facilitating remineralisation of enamel (Brudevold *et. al.* 1963, Dedhiya *et. al.* 1973, LeGeros 1997, Abdullah *et. al.* 2006). This is supported by the findings from the model where in some cases zinc treatments produced smaller amounts of mineral loss than controls, whilst in others it appeared to cause more demineralisation as opposed to inferring any sort of protection. When then considered in conjunction with fluoride, the Zn/F treatment group consistently demonstrated reduced mineral loss than controls when administered both with and without pH-cycling. One explanation that has been proposed for this is the surface-softening characteristic of zinc allowing better penetration of F into the lesion, as it commonly congregates in the outer layers otherwise (Lynch 2013). When the lesion profiles recorded using TMR in chapter six are considered, this appears to a reasonable suggestion, as profiles for the F treatment group displayed a more defined surface area when compared the relatively flat, shallow lesions created in blocks from the combined Zn/F group. Even more interestingly, profiles for the combined Sr/F group presented in chapter seven also demonstrate this shallow lesion-effect, which may be an indication that strontium and fluoride are also able to interact in a similar manner.

When the limited EPMA results from chapter 2 are also considered, they appear to provide support for the ability of the pH-cycling process to aid the incorporation of fluoride into the surface enamel, however, as discussed previously, the samples may not be fully representative and, as such, further work is needed to use such techniques within the refined version of the model and with a more appropriate sample size.

9.5 Clinical Relevance

It is important when conducting any dental-based research to consider the findings and how they apply to the wider clinical situation. When the incredibly high prevalence and financial burden of dental caries is considered, any information that can aid the reduction of the disease is worth obtaining (Selwitz *et. al.* 2007, NHS Report 2008, Vos *et. al.* 2015). As PEM is a naturally occurring phenomenon that serves to decrease enamel susceptibility to acid dissolution, understanding more about how this process works is of clinical interest, particularly as the focus has shifted towards prevention as opposed to treatment after-the-fact (Carlos and Gittelsohn 1965, Woltgens *et. al.* 1981b, ten Cate and Duijsters 1982, Maltz *et. al.* 2006). The model that has been proposed within this work allows the PEM process to be re-created to a certain extent *in vitro*, allowing the mechanisms to be better understood. This would allow the construction of advice tailored to those at tooth eruption age to ensure that they do things to aid and even enhance the process and avoid potentially antagonistic practices. To this effect even just the act of conducting research to revive the subject is useful, as increased awareness of the existence of the process can serve to remind both clinicians and patients about the increased caries risk of newly erupted teeth. The importance of this is highlighted by the high caries prevalence in teenagers, which may in part be due to the eruption of “immature” teeth that are more susceptible (NHS 2013). Additionally, the model allows the investigation of the effect of different conditions and treatments on the process, providing the potential to devise product and treatments aimed at improving the ability of the enamel to resist acid dissolution.

9.6 Future Work

Whilst the work presented here forms a foundation for the study of PEM and serves to provide evidence for previously only hypothesised explanations regarding its mechanisms, much more work is needed. Initially, in order to make the model more

rounded in terms of what is understood about PEM, a method for assessing the porosity of the enamel pre-and post-cycling should be introduced. The model already addresses two of the three reported outcomes of the PEM process, introducing porosity would bring this up to all three.

In light of modern advances in technology and the wide range of chemical analysis techniques available, it would be of interest to investigate the effect of pH-cycling on the composition of the enamel. Whilst some EPMA was used within this work, it was conducted before the model was properly defined and unfortunately the sections selected were subject to damage It would therefore be interesting to see the composition over depth in the refined model, especially with the Zn and F treatments included.

With such adjustment, it would then be of interest to continue to substitute the parameters of the model in order to assess the effect of different ion concentrations and other agents on the “artificially matured” enamel and subsequent lesions. This would help further our understanding and help to achieve the clinical aims described above. One particular area of interest would be to investigate the effect of different F salts.

On area that has not been addressed in the previous literature that would be of interest to approach is the effect of the model when the demineralisation challenge is substituted for an erosive one. Given the established effects of ions such as fluoride to reduce erosion and the fact that erosion affects the outer enamel surface, it makes sense to speculate that the PEM process would serve to reduce the susceptibility of enamel to erosion to a certain extent. One of the advantages of the model proposed within this thesis is that such an investigation would be relatively simple to conduct, as the only change that would need to be made is to substitute the acid-gel demineralisation for exposure to an established erosive agent such as citric acid or

orange juice. Additionally, the previously excluded NCSP analysis could be re-introduced to provide further information on the resulting surface-loss.

Whilst the use of bovine enamel is well established within the cariology field, there are known differences in the structure and behaviour between bovine and human enamel when used *in vitro*. As such it important for both the validation of the model and our understanding of the PEM process to substitute the bovine enamel substrate used within the model for human enamel. Any differences in behaviour between the two can then be addresses and the model refined is necessary.

Along a similar vein, it would also be of interest to try and apply the parameters of this pH-cycling model within a more representative biological model such as a CDFF. This would allow the impact of the microbial biofilm to be assessed and would help inform subsequent advances towards clinical research.

Reference List

Abdullah, A. Z., Strafford, S. M., Brookes, S. J. and Duggal, M. S. (2006) The Effect of Copper on Demineralization of Dental Enamel. *Journal of Dental Research.* **85, 11.** 1011-1015.

Afseth, J., Opperman, R. V. and Rolla, G. (1983) Accumulation of Cu and Zn in Human Dental Plaque *in vivo*. *Caries Research.* **17,** 310-314.

Alfano, R.R. and Yao, S.S. (1981) Human Teeth with and without Dental Caries Studied by Visible Luminescent Spectroscopy. *Journal of Dental Research*. **60, 2**. 120-122.

Alves, K. M. R. P., Pessan, J. P., Brighenti, F. L., Franco, K. S., Oliveira, F. A. L., Buzalaf, M. A. R., Sassaki, K. T. and Delbem, A. C. B. (2007) *In vitro* Evaluation of the Effectiveness of Acidic Fluoride Dentifrices. *Caries Research.* **41, 4.** 263-267.

Amaechi, B. T., Higham, S. M. and Edgar, W. M. (1999) Factors Influencing the Development of Dental Erosion *in vitro*: Enamel Type, Temperature and Exposure Time. *Journal of Oral Rehabilitation.* **26,** 624-630.

Amaechi, B. T. and Higham, S. M. (2001) *In vitro* Remineralisation of Eroded Enamel Lesions by Saliva. *Journal of Dentistry.* **29,** 371-376.

Anderson, P., Levinkind, M. and Elliot, J. C. (1998) Scanning Microradiographic Studies of Rates of *in vitro* Demineralization in Human and Bovine Dental Enamel. *Archives of Oral Biology.* **43, 8.** 649-656.

Angmar, B., Carlstrom, D. and Glas, J. E. (1963) Studies on the Ultrastructure of Dental Enamel: IV, The Mineralization of Normal Human Enamel. *Journal of Ultrastructure Research.* **8, 1-2**, 12-23.

Angmar-Mansson, B. and ten Bosch, J. J. (2001) Quantitative light-induced Fluorescence (QLF): a method for assessment of incipient caries lesions. *Dentomaxilofacial Radiology.* **30,** 298-307.

Aoba, T., Shimazu, Y., Taya, Y., Soeno, Y., Sato, K. and Miake, Y. (2003) Fluoride and Apatite Formation *in vivo* and *in vitro*. *Journal of Electron Microscopy.* **52,** 615-625.

Aoba, T. (2004) Solubility Properties of Human Tooth Mineral and Pathogenesis of Dental Caries. *Oral Diseases.* **10,** 249-257.

Arends, J. and Jongebloed, W. L. (1978) Crystallites Dimensions of Enamel. *Journal de Biology Buccale.* **6, 3.** 161-171.

Arends, J., Christoffersen, J., Christoffersen, M.R. and Schuthof, J. (1983a). Influence of Fluoride Concentration on the Progress of Demineralization in Bovine Enamel at pH 4.5. *Caries Research*. **17, 5**. 455-457.

Arends, J., Gelhard, T., Lodding, A. and Odelius, H. (1983b) Fluoride Gradients in Enamel Lesions after in vivo Remineralization Period of 3 Months - a SIMS Study. *Caries Research*. **17, 2**. 169-170.

Arends, J., Christoffersen, J., Schuthof, J. and Smits, M. T. (1984) Influence of Xylitol on Demineralization of Enamel. *Caries Research.* **18, 4.** 296-301.

Arends, J. and Christoffersen, J. (1986) The Nature of Early Caries Lesions in Enamel. *Journal of Dental Research.* **65, 1.** 2-11.

Arends, J., Christoffersen, J., Ruben, J. and Jongebloed, W. L. (1989) Remineralization of Bovine Dentine *in vitro*. The Influence of the F Content in Solution on Mineral Distribution. *Caries Research.* **23, 5.** 309-314.

Arends, J. and Christoffersen, J. (1990) Nature and Role of Loosely Bound Fluoride in Dental Caries. *Journal of Dental Research*. **69,** 634-606.

Arends, J. (1995) The Application of *in vitro* Models to Research on Demineralization and Remineralization of the Teeth. *Advances in Dental Research.* **9,** 194-197.

Armstrong, W.G. (1963) Fluorescence Characteristics of Sound and Carious Human Dentine

Preparations. *Archives of Oral Biology*. **8, 2**. 79-90.

Attin, T., Wegehaupt, F., Gries, D. and Wiegand, A. (2007) The Potential of Deciduous and Permanent Bovine Enamel as a Substitute for Deciduous and Permanent Human enamel: Erosion-abrasion Experiments. *Journal of Dentistry.* **35,** 773-777.

Adeyemi, A. A., Desmons, S., Miles, E., Burnside, G., Valappil, S., Lynch, R., de Josselin de Jong, E. and Higham, S. M. (2013) The Visual Assessment of Early *in vitro* Chemical Demineralisation Using a Multispectral Imaging Method (Abstract). *In 60th Annual ORCA Congress. Liverpool, UK.*

Bachra, B. N. and Trautz, O. R. (1962) Carbonic Anhydrase and the Precipitation of Apatite. *Science.* **137,** 337-338.

Bahkt, K. (2014) Developing a Biological Caries Model & Studying Fluoride in Caries Control. *PhD Thesis, University of Liverpool, UK.*

Bardow, A., Lagerlof, B. N. and Tenovuo, J. (2008) The Role of Saliva. *Dental Caries: the Disease and its Clinical Management.* Fejerskov, O. and Kidd, E. A. M. Oxford, Wiley-Blackwell, 189-207.

Baumann, T., Carvalho, T. S. and Lussi, A. (2015) The Effect of Enamel Proteins on Erosion. *Scientific Reports.* **5, 15194.** 1-8.

Bechtle, S., Habelitz, S., Klocke, A., Fett, T. and Schneider, G. A. (2010) The Fracture Behaviour of Dental Enamel. *Biomaterials*. **31,** 375-384.

Bedi, R., Pitts, N. B., Horowitz, A. M., Phantumvaint, P., Blinkhorn, A., Evans, W., Allukian, M., Twetman, S., Niederman, R., Schulte, A., Ellwood, R. P., Kleinman, D., Evans, C., Douglas, C.: Stop caries now for a caries-free future. http://www.allianceforacavityfreefuture.org/Caries/Tools/en/us/imageslocale/ACFF_Declaration.pdf, **2016**.

Boskey, A. L. and Posner, A. S. (1974) Magnesium Stabilization of Amorphous Calcium Phosphate: a Kinetic Study. *Materials Research Bulletin.* **9,** 907-916.

Boyde, A. and Lester, K. S. (1967) Electron Microscopy of Resorbing Surfaces of Dental Hard Tissues. *Zeitschrift für Zellforschung und Mikroskopische Anatomie.* **83, 4.** 538-548.

Boyde, A. (1989) 'Enamel', in Oksche A, V. L.(ed), *Handbook of Microscopic Anatomy. Vol. 6 'Teeth*' Berlin: Springer-Verlag, 309-473.

Bratthall, D., Hansel-Petersson, G. and Sundberg, H. (1996) Reasons for the Caries Decline: What do the Experts Believe? *European Journal of Oral Sciences.* **104, 4.** 416-422.

Brennecke, J. and Radlanski, R. J. (1995) Is Vickers Hardness Test Applicable for Enamel Hardness Determination? A Scanning Electron Microscopic Evaluation (Abstract). *10th International Symposium on Dental Morphology.* Berlin. September 6-10, 1995.

Brighenti, F. L., Takeshita, E. M., Santana, C. O., Buzalaf, M. A. R. and Delbem, C. B. (2013) Effect of Low Fluoride Acidic Dentifrices on Dental Remineralization. *Brazilian Dental Journal.* **24, 1.** 35-39.

Brill, N., Tryde, G., Stoltze, K. and El Ghamrawy, E. (1977) Ecologic Changes in the Oral Cavity Caused by Removable Partial Dentures. *Journal of Prosthetic Dentistry.* **38,** 138-148.

Briner, W. W. and Rosen, S. (1967) Effect of Fluoride on Hypomineralized Areas in the Molars of Rats Fed a Cariogenic Diet. *Archives of Oral Biology.* **12,** 1077-1084.

Briner, W. W. and Rosen, S. (1968) Effect of Fluoride and Penicillin on Post-Eruptive Maturation of Rat Molars. *Calcified Tissue Research.* **2, 1.** 60-66.

Briner, W. W., Francis, M. D. and Widder, J. S. (1971) Factors Affecting the Rate of Post-Eruptive Maturation of Dental Enamel. *Calcified Tissue Research.* **7**, 249-256.

Brudevold, F. (1948) A Study on the Phosphate Solubility of the Human Enamel Surface. *Journal of Dental Research.* **27, 3.** 320-329.

Brudevold, F., Steadman, L. T., Spinelli, M. A., Amdur, B. H. and Gron, P. (1963) A Study of Zinc in Human Teeth. *Archives of Oral Biology.* **8**, 135-144.

Brudevold, F., Aasenden, R. and Bakhos, Y. (1982) A Preliminary Study of Posteruptive Maturation of Teeth *in situ*. *Caries Research.* **16,** 243-248.

Bruun, C. (1973) Uptake and Retention of Fluoride by In-tact Enamel *in vivo* After Application of Neutral Sodium Fluoride. *Scandinavian Journal of Dental Research.* **81,** 92-100.

Burguera-Pascu, M., Rodriguez-Archilla, A., Burguera, M., Rondon, C. and Carrero, P. (2007) Flow Injection On-Line Dilution for Zinc Determination in Human Saliva with Electrothermal Atomic Absorption Spectrometry Detection. *Analytica Chimica Acta.* **600, 1-2.** 214-220.

Burt, B. A. (1998) Prevention Policies in the Light of the Changed Distribution of Dental Caries. *Acta Odontologica Scandinavica*. **56,** 179-86.

Cai, F., Shen, P., Morgan, M. V. and Reynolds, E. C. (2003) Remineralization of Enamel Subsurface Lesions *in situ* by Sugar-Free Lozenges Containing Casein Phosphopeptideamorphous Calcium Phosphate. *Australian Dental Journal.* **48, 4.** 240-243.

Camargo, C. H., Bernardineli, N., Valera, M. C., de Carvalho, C. A., de Oliveria, L. D., Menezes, M. M., Afonso, S. E. and Mancini, M. N. (2006) Vehicle Influence on Calcium Hydroxide Pastes Diffusion in Human and Bovine Teeth. *Dental Traumatology.* **22, 6.** 302-306.

Cardoso, C. A. B., Magalhaes, A. C., Rios, D. and Lima, J. E. O. (2009) Cross-sectional Hardness of Enamel from Human Teeth at Different Posteruptive Ages. *Caries Research.* **43,** 491-494.

Carlos, J. P. and Gittelsohn, A. M. (1965) Longitudinal Studies of the Natural History of Caries. II. A Life-table Study of Caries Incidence in the Permanent Teeth. *Archives of Oral Biology.* **10, 5.** 739-751.

Christoffersen, J., Christoffersen, M. R., Arends, J. and Leonardsen, E. S. (1995) Formation of Phosphate-Containing Calcium Fluoride at the Expense of Enamel, Hydroxyapatite and Fluorapatite. *Caries Research*. **29,** 223-230.

Coombe, R.A., Tatevossian, A. and Wimpenny, J.W.T. (1982). An *in vitro* Model for Dental Plaque (Abstract). *30th Meeting, British Division of the International Association for Dental Research. University of Edinburgh, Scotland*.

Costa, A. M., Rossi, A. M. and Soares, G. A. (2003) Effect of Zinc Content on *in vitro* Dissolution of Non-Calcinated and Calcinated Zn-Containing Hydroxyapatite. *Acta Microscopica.* **12, Supp. C.** 49-50.

Costerton, J. W., Stewart, P. S. and Greenberg, E. P. (1999) Bacterial Biofilms: a Common Cause of Persistent Infections. *Science*. **284, 5418.** 1318-1322.

Crabb, H. S. (1976) The Porous Outer Enamel of Unerupted Human Premolars. *Caries Research.* **10,** 1-7.

Cummins, D. and Creeth, J. E. (1992) Delivery of Anti-plaque Agents from Dentifrices, Gels and Mouthwashes. *Journal of Dental Research.* **91,** 42-45.

Cuy, J. L., Mann, A. B., Livi, K. J., Teaford, M. F., and Weihs, T. P. (2002) Nanoindentation Mapping of the Mechanical Properties of Human Molar Tooth Enamel. *Archives of Oral Biology.* **47,** 281-291.

Daculsi, G., Menanteau, J., Kerebel, L. M. and Mitre, D. (1984) Length and Shape of Enamel Crystals. *Calcified Tissue International.* **36, 5.** 550-555.

Davidson, C. L., Boom, G. and Arends, J. (1973) Calcium Distribution in Human and Bovine Surface Enamel. *Caries Research.* **7,** 349-359.

Dawes, C. (2003) What is the Critical pH and Why Does a Tooth Dissolve in Acid? *Journal of the Canadian Dental Association.* **69, 11.** 722-724.

De Boever, J., Hirzel, H. C. and Muhlemann, H. R. (1969) The Effect of Concentrated Sucrose Solutions on pH of Interproximal Plaque. *Helvectica Odontologica Acta.* **13, 2,** 27-28.

Dedhiya, M. G., Young, F. and Higuchi, W. I. (1973) Mechanism for the Retardation of the Acid Dissolution Rate of Hydroxyapatite by Strontium. *Journal of Dental Research.* **52,** 1097-1109.

de Josselin de Jong, E., ten Bosch, J.J. and Noordmans, J. (1987) Optimised Microcomputer-Guided Quantitative Microradiography on Dental Mineralised Tissue Slices. *Physics in Medicine and Biology*. **32, 7.** 887-899.

de Josselin de Jong, E., Sundstrom, F., Westerling, H., Tranaeus, S., ten Bosch, J.J. and AngmarMansson, B. (1995) A New Method for *in vivo* Quantification of Changes in Initial Enamel Caries with Laser Fluorescence. *Caries Research*. **29, 1**. 2-7.

de Josselin de Jong, E.D., Higham, S.M., Smith, P.W., van Daelen, C.J. and van der Veen, M.H. (2009) Quantified Light-Induced Fluorescence, Review of a Diagnostic Tool in Prevention of Oral Disease. *Journal of Applied Physics*. **105, 10**. 7.

Demato, F. A., Strang, R. and Stephen, K. W. (1990) Effect of Fluoride Concentration on Remineralization of Carious Enamel an *in vitro* pH-Cycling Study. *Caries Research.* **24, 3.** 174-180.

DePaola, P. F. and Mellberg, J. R. (1973) Caries Experience and Fluoride Uptake in Children Receiving Semi-Annual Prophylaxis with an Acidulated Phosphate Fluoride Paste. *Journal of the American Dental Association.* **87,** 155-159.

Desmons, S., Adeyemi, A. A., Miles, E., Burnside, G., de Josselin de Jong, E., Valappil, S., Lynch, R. and Higham, S. M. (2013) Comparing Two Methods in the Early Detection of *in*

vitro Chemical Demineralisation: A Pilot Study (Abstract). *In 60th Annual ORCA Congress. Liverpool, UK*

Driessens, F. C., Heyligers, H. J., Woltgens, J. H. and Verbeeck, R. M. (1982) X-ray Diffraction of Enamel from Human Premolars Several Years After Eruption. *Journal de Biologie Buccale.* **10, 3.** 199-206.

Edgar, W. M. and Higham, S. M. (1995) Role of saliva in caries models. *Advances in Dental Research.* **9, 3.** 325-238.

Edmunds, D. H., Whittaker, D. K. and Green, R. M. (1988) Suitability of Human, Bovine, Equine, and Ovine Tooth Enamel for Studies of Artificial Bacterial Carious Lesions. *Caries Research.* **22. 6.** 327-336.

Elliot, J. C., Holcomb, D. W. and Young, R. A. (1985) Infared Determination of the Degree of Substitution of Hydroxyl by Carbonate Ions in Human Dental Enamel. *Calcified Tissue International.* **37, 4.** 372-375.

Elliot, J. C., Wong, F. S. L., Anderson, P., Davis, G. R. and Dowker, S. E. P. (1998) Determination of Mineral Concentration in Dental Enamel from X-Ray Attenuation Measurements. *Connective Tissue Research.* **38,** 61-72.

Epinosa, R., Valenica, R., Uribe, M., Ceja, I., Cruz, J. and Saadia, M. (2010) Resin Replica in Enamel Deproteinization and its Effect on Acid Etching. *Journal of Clinical Paediatric Dentistry.* **35, 1.** 47-51.

Ericsson, Y. (1962) Some Differences Between Human and Rodent Saliva of Probable Importance for the Different Specie Reactions to Cariogenic and Cariostatic Agents. *Archives of Oral Biology.* **7,** 327-226.

Fang, M. M., Lei, K. Y. and Kilgore L. T. (1980) Effects of Zinc Deficiency on Dental Caries in Rats. *Journal of Nutrition.* **110**, 1032-1036.

Feagin, F., Koulourides, T. and Pigman, W. (1969) The Characterization of Enamel Surface Demineralization, Remineralization, and Associated Hardness Changes in Human and Bovine Material. *Archives of Oral Biology.* **14, 12.** 1407-1417.

Featherstone, J. D. B. and Nelson, D. G. A. (1980) The Effect of Fluoride, Zinc, Strontium, Magnesium and Iron on the Crystal-Structural Disorder in Synthetic Carbonated Apatites. *Australian Journal of Chemistry.* **33,** 2363-2368.

Featherstone, J. D. B. and Mellberg, J. R. (1981) Relative Rates of Progress of Artificial Carious Lesions in Bovine, Ovine and Human Enamel. *Caries Research.* **15,** 109-114.

Featherstone, J. D., Mayer, I., Driessens, F. C., Verbeeck, R. M. and Heijligers, H. J. (1983) Synthetic Apatites Containing Na, Mg, and CO3 and their Comparison with Tooth Enamel Mineral. *Calcified Tissue International.* **35, 2.** 169-171.

Featherstone, J. D. B., Glena, R., Shariati, M. and Shields, C. P. (1990) Dependence of *in vitro* Demineralization of Apatite and Remineralization of Dental Enamel on Fluoride Concentration. *Journal of Dental Research.* **69,** 620-625.

Featherstone, J. D. B. (1999) Prevention and Reversal of Dental Caries: Role of Low Level Fluoride. *Community Dentistry and Oral Epidemiology.* **27,** 31-40.

Fejerskov O. and Manji F. (1990) Risk Assessment in Dental Caries. Bader JD, Risk Assessment in Dentistry. Chapel Hill, North Carolina Dental Ecology, 1990, pp 215 - 217.

Fejerskov, O., Larsen, M. J., Richards, A. and Baelum, V. (1994) Dental Tissue Effects of Fluoride. *Advances in Dental Research.* **8,** 15-31.

Fejerskov, O., Kidd, E. A. M., Nyvad, B and Baelum, V. (2008) Defining the Disease and its Diagnosis. *Dental Caries: the Disease and its Clinical Management.* Fejerskov, O. and Kidd, E. A. M. Oxford, Wiley-Blackwell, 3-6.

Ferrazzano, G. F., Cantile, T., Quarto, M., Ingenito, A., Chianese, L. and Addeo, F. (2008) Protective Effect of Yogurt Extract on Dental Enamel Demineralization *in vitro*. *Australian Dental Journal.* **53, 4.** 314-319.

Fincham, A. G., Belcourt, A. B. and Termine, J. D. (1982) Changing Patterns of Enamel Matrix Proteins in the Developing Bovine Tooth. *Caries Research.* **16,** 64-71.

Fonseca, R. B., Haiter-Neto, F., Carlo, H. L., Soares, C. J., Sinhoreti, M. A. C., Puppin-Rontani, R. M. and Correr-Sobrinho, L. (2008) Radiodensity and Hardness of Enamel and Dentin of Human and Bovine Teeth, Varying Bovine Teeth Age. *Archives of Oral Biology.* **53, 11.** 1023-1-29.

Fosdick, L. S. and Stark, A. C. (1939) Solubility of tooth enamel in saliva at various pH levels. *Journal of Dental Research.* **18,** 417-430.

Francis, M. D. (1965) Solubility Behaviour of Dental Enamel and Other Calcium Phosphates. *Annals of the New York Academy of Sciences.* **131,** 694-712.

Francis, M. D. and Briner W. W. (1966) The Development and Regression of Hypomineralized Areas of Rat Molars. *Archives of Oral Biology.* **11**, 349-354.

Frank, R. M., Sargentini-Maier, M. L., Turlot, J. C. and Leroy, M. J. (1989) Zinc and strontium Analyses by Energy Dispersive X-Ray Fluorescence in Human Permanent Teeth. *Archives of Oral Biology.* **34, 8.** 593-597.

Fulmer, A., Ban, A., Gaszner, B., Nagy, B., Sandor, B., Molnar, B., Nemes, B., Benke, B., Kerema, B., Nemeth, D., *et. al.* (2014) Digital Method and Content Development of the Hungarian Higher Education in Dentistry in Hungarian, German and English. University Of Pécs; Semmelweis University; Dialog Campus, Hungary.

Gao, X. J., Fan, Y., Kent, R. L., Van Houte, J. and Margolis, H.C. (2001) Association of Caries Activity with the Composition of Dental Plaque Fluid. *Journal of Dental Research*. **80,** 1834-1839.

Garcia-Godoy, F. and Hicks, M. J. (2008) Maintaining the Integrity of the Enamel Surface: The Role of Dental Biofilm, Saliva and Preventive Agents in Enamel Demineralization and Remineralization. *Journal of the American Dental Association.* **139, Suppl. 2.** 25-34.

Ge, J., Cui, F. Z., Wang, X. M. and Feng, H. L. (2005) Property Variations in the Prism and the Organic Sheath within Enamel by Nanoindentation. *Biomaterials.* **26,** 3333-3339.

Gerritsen, A., Allen, P. F., Witter, D., Bronkhorst, E. and Creugers, N. (2010) Tooth Loss and Oral Health-Related Quality of Life: A Systematic Review and Meta-Analysis. *Health and Quality of Life Outcomes.* **8,** 126.

Gilbert, R. J. and Ingram, G. S. (1988) The Oral Disposition of Zinc Following the Use of an Anti-calculus Toothpaste Containing 0.05% Zinc Citrate. *Journal of Pharmacy and Pharmacology.* **40,** 399-402.

Graf, H. and Muhlemann, H. R. (1966) Telemetry of Plaque pH from Interdental Area. *Helvectica Odontologica Acta.* **10, 2**, 94-101.

Groeneveld, A. and Arends, J. (1975). Influence of pH and Demineralization Time on Mineral Content, Thickness of Surface Layer and Depth of Artificial Caries Lesions. *Caries Research.* **9, 1**. 36-44.

Gruythuysen, R. J., van der Linden, L. W., Woltgens, J. H. and Geraets, W. G. (1991) Approximal Caries in Children. *Nederlands Tijdschrift voor Tandheelkunde.* **98,** 38-40.

Gustafson, G., Stelling, Em. and Brunius, E. (1968) The Pre- and Post-Eruptive Effect of Bone Meal on Dental Caries in Hamsters Fed an Ordinary Human Diet. *Caries Research*. **2**, 338-346.

Gutierrez-Salazar, M. D. P. and Reyes-Gasga, J. (2003) Microhardness and Chemical Composition of Human Tooth. *Materials Research.* **6, 3.** 367-373.

Gwinnett, A. J. (1967) The Ultrastructure of the “Prismless” Enamel of Permanent Human Teeth. *Archives of Oral Biology.* **12,** 381-387.

Gwinnett, A.J. (1992) Structure and composition of enamel. *Operative Dentistry.* **5,** 10–17.

Hagberg, C. (1987) Assesment of Bite Force: a Review. *Journal of Craniomandibular Disorders: Facial and Oral Pain.* **1, 3.** 162-169.

Hall, R. C., Embery, G. and Shellis, R. P. (2000) Biological and Structural Features of Enamel and Dentine: Current Concepts Relevant to Erosion and Dentine Hypersensitivity. *Tooth Wear and Sensitivity: Clinical Advances in Restorative Dentistry.* 1 ed. Addy M, E. G., Edgar W M, Orchardson R. Informa Healthcare. 3-18.

Hall, P. J., Green, A. K., Horay, C. P., de Brabander, S., Beasley, T. J., Cromwell, V. J., Holt, J. S. and Savage, D. J. (2003) Plaque Antibacterial Levels Following Controlled Food Intake and Use of a Toothpaste Containing 2% Zinc Citrate and 0.3% Triclosan. *International Dental Journal.* **53, 6 (Suppl 1).** 379-384.

Hallsworth, A. S., Robinson, C. and Weatherell, J. A. (1972) Mineral and Magnesium Distribution within the Approximal Carious Lesion of Dental Enamel. *Caries Research.* **6, 2.** 156-168.

Harrap, G. J., Best, J. S. and Saxton, C. A. (1984) Human Oral Retention of Zinc from Mouthwashes Containing Zinc Salts and its Relevance to Dental Plaque Control. *Archives of Oral Biology.* **59,** 279-281.

He, L. H. and Swain, M. V. (2007) Contact-Induced Deformation of Enamel. *Applied Physics Letters.* **90,** 1-3.

He, B., Huang, S., Jing, J. and Hao, Y. (2010) Measurement of Hydroxyapatite Density and Knoop Hardness in Sound Human Enamel and a Correlational Analysis Between them. *Archives of Oral Biology.* **55, 2.** 134-141.

He, B., Huang, S., Zhang, C., Jing, J., Hao, Y., Xiao, L. and Zhou, X. (2011) Mineral Densities and Elemental Content in Different Layers of Healthy Human Enamel with Varying Teeth Age. *Archives of Oral Biology.* **56**, 997-1004.

Hope, C.K., Bakht, K., Burnside, G., Martin, G. C., Burnett, G., de Josselin de Jong, E. and Higham, S. M. (2012) Reducing the Variability Between Constant-Depth Film Fermenter Experiments when Modelling Oral Biofilm. *Journal of Applied Microbiology.* **113,** 601-608.

Iijima, Y. and Takagi, O. (2000) *In situ* Acid Resistance of *in vivo* Formed White Spot Lesions. *Caries Research.* **34**, 388-394.

Ingram, G. S., Baker, A. G., Best, J. S. and Mellor-Chrimes, C. P. (1984) The Influence of Zinc Citrate in a Fluoride Dentifrice on Rat Caries and Fluoride Content of Molar Enamel *in vivo*. *Journal of Dental Research.* **63,** 497.

Ingram, G. S., Horay, C. P. and Stead, W. J. (1992) Interaction of Zinc with Dental Mineral. *Caries Research.* **26,** 248-253.

Johansen, E. (1965) Electron Microscopic and Chemical Studies of Carious Lesions with Reference to Organic Phase of Affected Tissues. *Annals of the New York Academy of Sciences.* **131, A2**, 776-785.

Kataoka, S., Sakuma, S., Wang, J., Yoshihara, A. and Miyazaki, H. (2007) Changes in Electrical Resistance of Sound Fissure Enamel in First Molars for 66 Months from Eruption. *Caries Research*. **41**, 161-164.

Kay, M. I., Young, R. A. and Posner, A. S. (1964) Crystal Structure of Hydroxyapatite. *Nature*. **204,** 1050-1052.

Kidd, E. A. M. and Joyston-Bechal, S. (1997) Essentials of dental caries: The disease and its management. 2nd ed. New York: Oxford University Press.

Kilkenny, C., Browne, W. J., Cuthill, I. C., Emerson, M. and Altman, D. G. (2010) The ARRIVE Guidelines: Animal Research: Reporting of *In Vivo* Experiments. *British Journal of Pharmacology.* **160,** 1577-1579.

Kinniment, S.L., Wimpenny, J.W., Adams, D. and Marsh, P.D. (1996). Development of a Steady-State Oral Microbial Biofilm Community Using the Constant-Depth Film Fermenter. *Microbiology*. **142, 3**. 631- 638.

Kirkham, J., Robinson, C., Strong, M. and Shore, R. C. (1994) Effects of Frequency and Duration of Acid Exposure on Demineralization/Remineralization Behaviour of Human Enamel *in vitro*. *Caries Research.* **28, 1.** 9-13.

Kodaka, T., Nakajima, F. and Higashi, S. (1989) Structure of the So-Called 'Prismless' Enamel in Human Deciduous Teeth. *Caries Research.* **23, 5.** 290-296.

Komarov, G. N., Cooper, L., Hope, C. K., Flannigan, N. L., Valappil, S. P., Smith, P. W. and Higham, S. M. (2016) Effect of Starch Based Snacks on Enamel Demineralisation *in situ* (Abstract). *In 94th General Session & Exhibition of the International Association for Dental Research. Seoul, Republic of Korea.*

Koulourides, T., Feagin, F. and Pigman, W. (1965) Remineralization of Dental Enamel by Saliva *in Vitro*. *Annals of the New York Academy of Sciences.* **131,** 751-757.

Lagerweij, M. D. and ten Cate, J. M. (2006) Acid Susceptibility at Various Depths of pH-Cycled Enamel and Dentine Specimens. *Caries Research.* **40**, 33-37.

Lambrechts, P., Debels, E., Van Landuyt, K., Peumans, M. and Van Meerbeek, B. (2006) How to Simulate Wear?: Overview of Existing Methods. *Dental Materials.* **22, 8.** 693-701.

Lane, D. W. and Peach, D. F. (1997) Some Observations on the Trace Element Concentrations in Human Dental Enamel. *Biological Trace Element Research.* **60, 1-2.** 1-11.

Larsen, M. J. and Bruun, C. (2008) Caries Chemistry and Fluoride- Mechanisms of Action. *Textbook of Clinical Cariology.* Thylstrup. A. and Fejerskov, O. Copenhagen, Munksgaard. 231-252.

Larsen, M. J. and Keyes, P. H. (1967) The Influence of Reduced Salivary flow on the Intensity of the Cariogenic Challenge. *Helvetica Odontologica Acta.* **11,** 36-43.

Larsen, M. J. (1974) Chemically Induced *in vitro* Lesions in Dental Enamel. *Scandinavian Journal of Dental Research.* **82, 7.** 496-509.

Larsen, M. J. (1991) Effect of Diffusion Layer on the Nature of Enamel Demineralization. *Caries Research.* **25,** 161-165.

Laucello, M., Noel, N., Ferro, R., Lynch, R. J. M. and Lipscombe, C. (2007) The Anti-Caries Efficacy of a Silica-Based Fluoride Toothpaste Containing Zinc Citrate, Triclosan, Vitamin E and Sunflower Oil. *International Dental Journal.* **57,** 145-149.

Leach, S. A., Lee, G. T. R. and Edgar, W. M. (1989) Remineralization of Artificial Caries-like Lesions in Human Enamel *in situ* by Chewing Sorbitol Gum. *Journal of Dental Research.* **68, 6.** 1064-1068.

LeGeros, R. Z., Trautz, O. R., LeGeros, J. P., Klein, E. and Shirra, W. P. (1967) Apatite Crystallites: Effects of Carbonate on Morphology. *Science.* **155, 3768.** 1409-1411.

LeGeros, R. (1981) Apatites in Biological Systems. *Progress in Crystal Growth and Characterisation*. **4,** 1-45.

LeGeros, R. Z. and Tung, M. S. (1983) Chemical Stability of Carbonate- and Fluoride-Containing Apatities. *Caries Research.* **17, 5.** 419-429.

LeGeros, R.Z. (1984) Incorporation of Magnesium in Synthetic and in Biological Apatites. in: R.W. Fearnhead, S. Suga (Eds.) *Tooth Enamel IV*. Elsevier Science, Amsterdam. 32–36.

LeGeros, R. Z. (1991) Calcium Phosphates in Oral Biology and Medicine. *Monographs in Oral Science.* **15,** 1-201.

LeGeros, R. Z., Sakae, T., Bautista, C., Retino, M. and LeGeros, J. P. (1996) Magnesium and Carbonate in Enamel and Synthetic Apatites. *Advances in Dental Research.* **10, 2.** 225-231.

LeGeros, R. Z. (1997) Effect of Zinc on the Formation of Calcium Phosphates *in vitro*. *Caries Research.* **31,** 434-440.

Lindh, U. and Tveit, A. (2007) Proton Microprobe Determination of Fluorine Depth Distributions and Surface Multielement Characterization in Dental Enamel. *Journal of Radioanalytical and Nuclear Chemistry.* **59, 1.**

Lippert, F., Butler, A., Lynch, R. J. M. and Hara, A. T. (2012) Effect of Fluoride, Lesion Baseline Severity and Mineral Distribution on Lesion Progression. *Caries Research.* **46,** 23-30.

Lippert, F. and Hara, A. T. (2013) Strontium and caries: a Long and Complicated Relationship. *Caries Research.* **47, 1.** 34-49.

Little, M. F. and Brudevold, F. (1958) A Study of the Inorganic Carbon Dioxide in Intact Human Enamel. *Journal of Dental Research.* **37,** 991-1000.

Locker, D. (1992) The Burden of Oral Disorders in a Population of Older Adults. *Community Dental Health.* **9,** 109-124.

Low, W., Tam, S. and Schwartz, S. (1999) The Effect of Severe Caries on the Quality of Life

in Young Children. *Paediatric Dentistry.* **21, 6.** 325-326.

Low, I. M., Duraman, N. Mahmood, U. (2008) Mapping the Structure, Composition and Mechanical Properties of Human Teeth. *Materials Science and Engineering: C.* **28, 2.** 243-247.

Lubarsky, G. V., D'Sa, R. A., Deb, S., Meenan, B. J. and Lemoine, P. (2012) The Role of Enamel Proteins in Protecting Mature Human Enamel Against Acidic Environments: a Double Layer Force Spectroscopy Study. *Biointerphases.* **7, 14.**

Lubarsky, G. V., Lemoine, P., Meenan, B. J., Deb, S., Mutreja, I., Carolan, P. and Petkov, N. (2014) Enamel Proteins Mitigate Mechanical and Structural Degradations in Mature Human Enamel During Acid Attack. *Materials Research Express.* **1, 2.** 2-20.

Lynch, R. J. M. (2011) Zinc in the Mouth, its Interactions with Dental Enamel and Possible Effects on Caries; a Review of the Literature. *International Dental Journal.* **61,** 46-54.

Lynch, R. J. M., Churchley, D., Butler, A., Kearns, S., Thomas, G. V., Badrock, T. C., Cooper, L. and Higham, S. M. (2011) Effects of Zinc and Fluoride on the Remineralisation of Artificial Carious Lesions Under Simulated Plaque Fluid Conditions. *Caries Research.* **45, 3.** 313-322.

Lynch, R. J. M. and Smith, S. R. (2012) Remineralization Agents - New and Effective or Just Marketing Hype? *Advances in Dental Research.* **24, 2.** 63-67.

Lynch, R. J. M. (2013) The Primary and Mixed Dentition, Post-Eruptive Enamel Maturation and Dental Caries: a Review. *International Dental Journal.* **63, Suppl 2**. 3-13.

Maltz. M., Scherer, S. C., Parolo, C. C. F. and Jardim, J. J. (2006) Acid Susceptibility of Arrested Enamel Lesions: *In situ* Study. *Caries Research.* **40**, 251-255.

Manly, R. S. and Harrington, D. P. (1959) Solution Rate of Tooth Enamel in an Acetate Buffer. *Journal of Dental Research.* **38,** 910-919.

Manning, R. H. and Edgar, W. M. (1992) Intra-oral Models for Studying De- and Remineralization in Man: Methodology and Measurement. *Journal of Dental Research.* **71, Spec. Issue**. 895-900.

Margolis, H. C. (1990) An Assessment of Recent Advances in the Study of the Chemistry and Biochemistry of Dental Plaque Fluid. *Journal of Dental Research*. **69, 6.** 1337-1342.

Margolis, H. C. and Moreno, E. C. (1992) Composition of Pooled Plaque Fluid from Caries-Free and Caries-Positive Individuals Following Sucrose Exposure. *Journal of Dental Research.* **71, 11.** 1776-1784.

Marsh, P. D. (1992) Microbiological Aspects of the Chemical Control of Plaque and Gingivitis. *Journal of Dental Research.* **68**, 1567-1575.

Marsh, P. D. and Bradshaw, D. J. (1995) Dental Plaque as a Biofilm. *Journal of Industrial Microbiology.* **15, 3.** 169-175.

Marsh, P. and Martin, M. V. (1999) *Oral Microbiology*, Oxford: Wright. P1-2.

Marsh, P. D. (2004) Dental Plaque as a Microbial Biofilm. *Caries Research.* **38,** 204-211.

Marshall, A. F. and Lawless, K. R. (1981) TEM Study of the Central Line in Enamel Crystallites. *Journal of Dental Research.* **60,** 1773-1783.

Matsunaga, T., Ishizaki, H., Tanabe, S. and Hayashi, Y. (2009) Synchrotron Radiation Microbeam X-Ray Fluorescence Analysis of Zinc Concentration in Remineralized Enamel *in situ*. *Archives in Oral Biology.* **54, 5.** 420-423.

Mayer, I., Apfelbaum, F. and Featherstone, J. D. B. (1994) Zinc Ions in Synthetic Carbonated Apatites. *Archives in Oral Biology.* **39,** 87-90.

Mayer, I. and Featherstone, J. D. B. (2000) Dissolution Studies of Zn-containing Carbonated Hydroxyapatites. *Journal of Crystal Growth.* **219,** 98-101.

McBride, J. W. and Maul, C. (2004) The 3D Measurement and Analysis of High Precision Surfaces using Con-focal Optical Methods. *IEICE Transactions on Electronics.* **E87, C.** 1261-1271.

McDowell, H., Gregory, T. M. and Brown, W. E. (1977) Solubility of $Ca_5(PO_4)3OH$ in system $Ca(OH)_2$- H_3PO_4-H_2O at 5 degrees C, 15 degrees C, 25 degrees C and 37 degrees C. *Journal of Research of the National Bureau of Standards Section A – Physics and Chemistry.* **81, 2-3.** 273-281.

Mejare, I. and Kidd, E. A. M. (2008) Radiography of Caries Diagnosis. *Dental Caries: the Disease and its Clinical Management.* Fejerskov, O. and Kidd, E. A. M. Oxford, Wiley-Blackwell, 69-88.

Mellberg, J. R. and Nicholson, C. R. (1968) *In vitro* Fluoride Uptake by Erupted and Unerupted Tooth Enamel. *Journal of Dental Research.* ***47,*** 176

Menegario, A. A., Packer, A. P. and Gine, M. F. (2001) Determination of Ba, Cd, Cu, Pb and Zn in Saliva by Isotope Dilution Direct Injection Inductively Coupled Plasma Mass Spectrometry. *Analyst.* **126,** 1363-1368.

Meredith, J. H., Sherriff, M., Setchell, D. J. and Swanson, S. A. (1996) Measurement of the Microhardness and Young's Modulus of Human Enamel and Dentine using an Indentation Technique. *Archives of Oral Biology.* **41, 6.** 539-545.

Miake, Y., Tsutsui, S. and Eshita, Y. (2016) Variation in the Colour of Japanese Teeth and Structural Changes in Enamel Rod Sheath Associated with Age. *Journal of Hard Tissue Biology.* **25, 2.** 131-136.

Moreno, E.C. and Zahradnik, R.T. (1974). Chemistry of Enamel Subsurface Demineralization *in vitro*. *Journal of Dental Research*. **53, 2**. 226-235.

Moreno, E. C. and Margolis, H. C. (1988) Composition of Human Plaque Fluid. *Journal of Dental Research.* **67, 9.** 1181-1189.

Murray, M. M. (1936) The Chemical Composition of Teeth: The Calcium, Magnesium and Phosphorus Contents of the Teeth of Different Animals. A Brief Consideration of the Mechanism of Calcification. *Biochemical Journal.* **30, 9.** 1567-1571.

Myles, P. S. (2007) Using the Bland–Altman Method to Measure Agreement with Repeated Measures. *British Journal of Anaesthesia.* **99, 3.** 309-311.

Myrberg, N. (1968) Proton Magnetic Resonance in Human Dental Enamel and Dentine. An Experimental Investigation Using Wide Line NMR. *Transactions of the Royal Schools of Dentistry, Stockholm and Umea.* Stockholm, Tandlakarhogskolan. **14, 4**, 1-62.

Nakajima, O., Miake, Y. and Takaaki, Y. (2003) The Influence of saliva on Post-Eruptive Maturation in Enamel. *Shikwa* Gakuho*.* **103, 4***.* 289-298.

NHS (2008) NHS Report: NHS Expenditure for General Dental Services and Personal Dental Services, England 1997/98 to 2005/06. *The NHS Information Centre for Health and Social Care, Dental Statistics.*

NHS (2013) Child Dental Health Survey 2013, England, Wales and Northern Ireland. *Health and Social Care Information Centre.*

NIH (2001) Diagnosis and Management of Dental Caries Throughout Life. *NIH Consensus Statement.***18,** 1-23.

Nyvad, B., Fejerskov, O. & Baelum, V. (2008) Visual-Tactile Caries Diagnosis. *Dental Caries: the Disease and its Clinical Management.* Fejerskov, O. and Kidd, E. A. M. Oxford, Wiley-Blackwell, 49-69.

Nyvad, B., Crielaard, W., Mira, A., Takahashi, N. and Beighton, D. (2013) Dental Caries from a Molecular Microbiological Perspective. *Caries Research*. **47,** 89-102.

Okazaki, M. and LeGeros, R. Z. (1996) Properties of Heterogeneous Apatites Containing Magnesium, Fluoride, and Carbonate. *Advances in Dental Research.* **10, 2.** 252-259.

Owens, G. J. (2013) *In vitro* caries: Dental Plaque Formation and Acidogenicity. *PhD Thesis, University of Liverpool, UK.*

Palti, D. G., Machado, M. A. A. M., Silva, S. M. B., Abdo, R. C. C. and Lima, J. E. O. (2008) Evaluation of Superficial Microhardness in Dental Enamel with Different Eruptive Ages. *Brazilian Journal of Oral Research.* **22,** 311-315.

Patel, P. R. and Brown, W. E. (1975) Thermodynamic Solubility Product of Human Tooth Enamel – Powdered Sample. *Journal of Dental Research.* **54, 4.** 728-736.

Peters, A.C. and Wimpenny, J.W.T. (1988). A Constant-Depth Laboratory Model Film Fermentor. *Biotechnology and Bioengineering.* **32, 3.** 263-270.

Pitts N. (2004) "ICDAS"—an International System for Caries Detection and Assessment being Developed to Facilitate Caries Epidemiology, Research and Appropriate Clinical Management. *Community Dental Health.* **21,** 193–208.

Posner, A. S. and Perloff, A. (1957) Apatites Deficient in Divalent Cations. *Journal of Research of the National Bureau of Standards.* **58, 5**. 279-286.

Pretty, I. A., Edgar, W. M. and Higham, S. M. (2004) The Validation of Quantitative Light-Induced Fluorescence to Quantify Acid Erosion of Human Enamel. *Archives of Oral Biology.* **49, 4.** 285-294.

Reeh, E. S., Douglas, W. H. and Levine, M. J. (1995) Lubrication of Human and Bovine Enamel Compared in an Artificial Mouth. *Archives of Oral Biology.* **40, 11.** 1063-1072.

Reynolds, E. C. (1997) Remineralization of Enamel Subsurface Lesions by Casein Phosphopeptide-stabilized Calcium Phosphate Solutions. *Journal of Dental Research.* **76, 9.** 1587-1595.

Rios, D., Honorio, H. M., Magalhaes, A. C., Buzalaf, M. A. R., Pamla-Dibb, R. G., Machado, M. A. and da Silva, S. M. B. (2006a) Influence of Toothbrushing on Enamel Softening and Abrasive Wear of Eroded Bovine Enamel: an *in situ* Study. *Brazilian Oral Research.* **20, 2.** 148-154.

Rios, D., Honorio, H. M., Magalhaes, A. C., Delbem, A. C., Machado, M. A., Silva, S. M. and Buzalaf, M. A. (2006b) Effect of Salivary Stimulation on Erosion of Human and Bovine Enamel Subjected or not to Subsequent Abrasion: an *in situ*/*ex vivo* Study. *Caries Research.* **40, 3.** 218-223.

Ripa, L. W., Leske, G. S., Triol, C. W. and Volpe, A. R. (1990) Clinical Study of the Anticaries Efficacy of Three Fluoride Dentifrices Containing Anticalculus Ingredients: Three-Year (Final) Results. *Journal of Clinical Dentistry.* **2, 2.** 29-33.

Ripa, L. W. (1991) A Critique of Topical Fluoride Methods (Dentifrices, Mouthrinses, Operator-, and Self-Applied Gels) in an Era of Decreased Caries and Increased Fluorosis Prevalence. *Journal of Public Health Dentistry*. **51**, 23-41.

Robinson, C., Weatherell, I. A. and Hallsworth, A. S. (1981) Distribution of Magnesium in Mature Human Enamel. *Caries Research.* **15, 1.** 70-77.

Robinson, C., Weatherell, I. A. and Hallsworth, A. S. (1983) Alterations in the Composition of Permanent Human Enamel During Carious Attack. *On the Demineralisation and Remineralisation of the Teeth.* Leach, S. A. and Edgar, W. M. Oxford, IRL Press, 209-223.

Robinson, C., Kirkham. J., Brookes. S, J. and Shore, R. (1995a) Chemistry of Mature Enamel. *Dental Enamel: Formation to Destruction.* Robinson, C., Kirkham, J. and Shore, R. Cc. Boca Raton (Fla), CRC P, 167 - 192.

Robinson, C., Kirkham, J., Brookes, S. J., Bonass, W. A. and Shore, R. C. (1995b) The Chemistry of Enamel Development. *International Journal of Developmental Biology.* **39, 1.** 145-152.

Robinson, C., Shore, R. C., Brookes, S. J., Strafford, S., Wood, S. R. and Kirkham, J. (2000) The Chemistry of Enamel Caries. *Critical Reviews in Oral Biology and Medicine.* **11, 4**. 481-495.

Robinson, C. (2009) Fluoride and the Caries Lesion: Interactions and Mechanism of Action. *European Archives of Paediatric Dentistry: Official Journal of the European Academy of Paediatric Dentistry.* **10,** 136-140.

Rodriguez, J. M., Curtis, R. V. and Bartlett, D. W. (2008) Surface Roughness of Impression Materials and Dental Stones Scanned by Non-contacting Laser Profilometry. *Dental Materials.* **25, 4.** 500-505.

Roy, S. and Basu, B. (2008) Mechanical and Tribiological Characterisation of Human Tooth. *Materials Characterization.* **59, 6.** 747-756.

Ruxton, C. H. S., Garceau, F. J. S. and Cottrell, R. C. (1999) Guidelines for Sugar Consumption in Europe: Is a Quantitative Approach Justified? *European Journal of Clinical Nutrition.* **53,** 503-513.

Sabel, N., Klinberg, G., Nietzsche, S., Robertson, A., Odelius, H. and Noren, J. G. (2009) Analysis of Some Elements in Primary Enamel During Postnatal Mineralization. *Swedish Dental Journal.* **33, 2.** 85-95.

Savory, A. and Brudevold, F. (1959) The Distribution of Nitrogen in Human Enamel. *Journal of Dental Research.* **38, 3.** 436-442.

Saxton, C. A., Harrap, G. J. and Lloyd, A. M. (1986) The Effect of Dentifrices Containing Zinc Citrate on Plaque Growth and Oral Zinc Levels. *Journal of Clinical Periodontology.* **13,** 301-306.

Schulte, A., Gente, M. and Pieper, K. (1999) Posteruptive Changes of Electrical Resistance Values in Fissure Enamel of Premolars. *Caries Research*. **33**, 242-247.

Segreto, V. A., Collins, E. M., D'Agostino, R., Cancro, L. P., Pfeifer, H. J. and Gilbert, R. J. (1991) Anticalculus Effect of a Dentifrice Containing 0.5% Zinc Citrate Trihydrate. *Community Dentistry and Oral Epidemiology.* **19, 1.** 29-31.

Selvig, K. A. and Halse, A. (1972) Crystal Growth in Rat Incisor Enamel. *Anatomical Record.* **173,** 453-468.

Selwitz, R. H., Ismail, A. I and Pitts, N. B. (2007) Dental Caries. *The Lancet.* **369**, 51-59.

Shellis, R. P. (1996) A Scanning Electron-Microscopic Study of Solubility Variations in Human Enamel and Dentine. *Archives of Oral Biology.* **41,** 473-484.

Silverstone, L. M. (1967) Surface Phenomena in Dental Caries. *Nature.* **214, 84.** 203-204.

Silverstone, L. M. (1968) The Surface Zone in Caries and Caries-like Lesions Produced *in vitro*. *British Dental Journal.* **125,** 145-157.

Silverstone, L.M. and Johnson, N.W. (1971). The Effect on Sound Human Enamel of Exposure to Calcifying Fluids *in vitro*. *Caries Research*. **5, 4**. 323-342.

Sissons, C. H. (1997) Artificial Dental Plaque Biofilm Model Systems. *Advances in Dental Research*. **11,** 110-126.

Sissons, C. H., Anderson, S. A., Wong, L., Coleman, M. J. and White, D. C. (2007) Microbiota of Plaque Microcosm Biofilms: Effect of Three Times Daily Sucrose pulses in Different Simulated Oral Environments. *Caries Research.* **41,** 413-422.

Sobel, A. E. (1962) Dietary Phosphate and Caries Susceptibility. *Dental Progress.* **2,** 48-52.

Sognnaes, R. F. (1975) Reflections on the Reactivity of Dental Enamel. *Journal of Dental Research.* **54,** 106-113.

Speirs, R. L. (1967) Factors Influencing “Maturation” of Developmental Hypomineralized Areas in the Enamel of Rat Molars. *Caries Research*. **1,** 15-31.

Stachowiak, G. and Batchelor, A. (2004) Characterization of Test Specimens. *Experimental Methods in Tribology, 1st Edition.* Elsevier Science. 115-149.

Stephan, R. M. (1940) Changes in Hydrogen Ion Concentration on Tooth Surfaces and in Carious Lesions. *Journal of the American Dental Association.* **27**, 718.

Stephan, R. M. and Miller, B. F. (1943) A Qualitative Method for Evaluation Physical and Chemical Agents which Modify Production of Acids in Bacterial Plaques on Human Teeth. *Journal of Dental Research.* **22,** 45-51.

Stookey, GT. K., Schemehorn, B. R., Cheetham, B. L., Wood, G. D. and Walton, G. V. (1985) *In situ* Fluoride Uptake from Fluoride Dentifrices by Carious Enamel. *Journal of Dental Research.* **64, 6.** 900-903.

Stubel, H. (1911). The Fluorescence of Animal Tissues in Ultraviolet Light. *Pflugers Archiv Fur Die Gesamte Physiologie Des Menschen Und Der Tiere*. **142, 1/2**. 1-14.

Tang, Y., Chappell, H. F., Dove, M. T., Reeder, R. J. and Lee, Y. J. (2009) Zinc Incorporation into Hydroxylapatite. *Biomaterials.* **30, 15.** 2864-2872.

Tantbirojn, D., Huang, A., Ericson, M. D. and Poolthong, S. (2008) Change in Surface Hardness of Enamel by a Cola Drink and CPP-ACP Paste. *Journal of Dentistry.* **38, 1.** 74-79.

Tarbet, W. J. and Fosdick, R. S. (1971) Permeability of Human Dental Enamel to Acriflavine and Potassium Fluoride. *Archives of Oral Biology.* **16,** 951-961.

Ten Bosch, J. J. and Angmar-Mansson, B. (1991) A Review of Quantitative Methods for Studies of Mineral Content of Intraoral Caries Lesions. *Journal of Dental Research.* **70,** 2-14.

ten Cate, A. R. (2007) Oral Histology: Development, Structure and Function. 7th Ed. Elsevier, Amsterdam, the Netherlands.

ten Cate, J.M. and Duijsters, P.P.E. (1982) Alternating Demineralization and Remineralization of Artificial Enamel Lesions. *Caries Research*. **16, 3.** 201-210.

ten Cate, J.M. and Duijsters, P.P.E. (1983) Influence of Fluoride in Solution on Tooth Demineralization: I. Chemical Data. *Caries Research.* **17, 3.** 193-199.

ten Cate, J. M., Timmer, K., Shariati, M. and Featehrstone, J. D. B. (1988) Effect of Timing of Fluoride Treatment on Enamel De- and Remineralization *in vitro*: A pH-Cycling Study. *Caries Research.* **22,** 20-26.

ten Cate, J. M. (1990) *In vitro* Studies on the Effects of Fluoride on De- and Remineralization. *Journal of Dental Research.* **69,** 614-619.

ten Cate, J. M. (1993) The Caries-Preventative Effect of a Fluoride Dentifrice Containing Triclosan and Zinc Citrate, a Compilation of *in vitro* and *in situ* Studies. *International Dental Journal.* **43,** 407-413.

ten Cate, J. M. (1994) *In situ* Models, Physico-Chemical Aspects. *Advances in Dental Research.* **8, 2.** 125-133.

ten Cate, J. M. (1997) Review on Fluoride, with Special Emphasis on Calcium Fluoride Mechanisms in Caries Prevention. *European Journal of Oral Sciences.* **105, 5.** 461-465.

Terra, J., Jiang, M. and Ellis, D. E. (2002) Characterization of Electronic Structure and Bonding in Hydroxyapatite: Zn Substitution for Ca. *Philosophical Magazine A.* **82,** 2357-2377.

Thiradilok, S. and Feagin, F. (1978) Effects of Magnesium and Fluoride on Acid Resistance of Remineralized Enamel. *Alabama Journal of Medical Sciences.***15, 2.** 144-148.

Thuy, T., Nakagaki, H., Kato, K., Hung, P., Inukai, J., Tsuboi, S., Nakagaki, H., Hirose, M., Igarashi. S. and Robinson, C. (2008) Effect of Strontium in Combination with Fluoride on Enamel Remineralization *in vitro*. *Archives of Oral Biology.* **53, 11.** 1017-1022.

Valappil, S. P., Owens, G. J., Miles, E. J., Farmer, N. L., Cooper, L., Miller, G., Clowes, R., Lynch, R. J. and Higham, S. M. (2014) Effect of Gallium on Growth of Streptococcus Mutans NCTC 10449 and Dental Tissues. *Caries Research.* **48, 2.** 137-146.

van Loveren, C. (1990) The Antimicrobial Action of Fluoride and its Role in Caries Inhibition. *Journal of Dental Research.* **69, Suppl. 2.** 676-681.

Vernois, V., Deschamps, N. and Revel, G. (1989) Characterization of Human Dental Enamel by Epithermal Neutron Activation Analysis. *Journal of Trace Elements and Electrolytes.* **3, 2.** 67-70.

Virtanen, J. I., Bloigu, R. S. and Larmas, M. A. (1996) Effect of Early or Late Eruption of Permanent Teeth on Caries Susceptibility. *Journal of Dentistry*. **24, 4**. 245-250.

Vogel, G. L., Zhang, Z., Chow, L. C., Carey, C. M., Schumacher, G. E. and Banting, D. W. (2000) Effect of *in vitro* Acidification on Plaque Fluid Composition With and Without a NaF or a Controlled-release Fluoride Rinse. *Journal of Dental Research.* **79, 4.** 983-990.

Vos, T., Barber, R. M., Bell, B., Bertozzi-Villa, A., Biryukov, S., Bolliger, I., Charlson, F., Davis, A., Degenhardt, L., Dicker, D. *et. al.* (2015) Global, Regional, and National Incidence, Prevalence, and Years Lived with Disability for 301 Acute and chronic Diseases and Injuries in 188 Countries, 1990-2013: a Systematic Analysis for the Global Burden of Disease Study 2013. *The Lancet.* **386, 9995.** 743-800.

Watson, J. E., Fremlin, J. H. and Stubbins, M. I. (1967) The Distribution of Carbon in Human Tooth Enamel Determined by Charged Particle Activation Analysis. *Caries Research.* **1**, 318-326.

Watson, P. S., Pontefract, H. A., Devine, D. A., Shore, R. C., Nattress, B. R., Kirkham, J. and Robinson, C. (2005) Penetration of Fluoride into Natural Plaque Biofilms. *Journal of Dental Research.* **84, 5.** 451-455.

Weatherell, J, A., Robinson, C. and Hiller, C. R. (1968) Distribution of Carbonate in Thin Sections of Dental Enamel. *Caries Research.* **2**, 1-9.

Weatherell, J. A., Robinson, C. and Hallsworth, A. S. (1972) Changes in the Fluoride Concentration of the Labial Enamel Surface with Age. *Caries Research.* **6,** 312-324.

Wellock, W. D., Maitland, A. and Brudevold, F. (1965) Caries Increments, Tooth Discoloration, and State of Oral hygiene in Children Given Simple Annual Applications of Acid Phosphate-Fluoride and Stannous Fluoride. *Archives of Oral Biology.* **10,** 453-460.

West, N. X., Hughes, J. A., Parker, D. M., Moohan, M. and Addy, M. (2003) Development of Low Erosive Carbonated Fruit Drinks 2. Evaluation of an Experimental

Carbonated Blackcurrant Drink Compared to a Conventional Carbonated Drink. *Journal of Dentistry.* **31, 5.** 361-365.

White, D.J. (1987). Reactivity of Fluoride Dentifrices with Artificial Caries. 1. Effects on Early Lesions – F-Uptake, Surface Hardening and Remineralization. *Caries Research*. **21, 2**. 126-140.

White, D. J. (1992) The Comparative Sensitivity of Intraoral *in vitro* and Animal Models in the Profile Evaluation of Topical Fluorides. *Journal of Dental Research.* **71,** 884-894.

White, D. J. (1995) The Application of *in vitro* Models to Research on Demineralization and Remineralisation of the Teeth. *Advances in Dental Research.* **9,** 175-193.

White, A. J., Yorath, C., ten Hengel, V., Leary, S. D., Huysmans, M. C. and Barbour, M. E. (2010) Human and Bovine Enamel Erosion Under “Single-drink” Conditions. *European Journal of Oral Sciences.* **118, 6.** 604-609.

WHO (2012) Who Factsheet 318: Oral Health. **2016**.

Winand, L., Dallemagne, M. J. and Duyckaerts, G. (1961) Hydrogen Bonding in Apatitic Calcium Phosphates. *Nature.* **190, 477**. 164-165.

Woltgens, J. H. M., Bervoets, Th. J. M., Witjes, F. and Driessens, F. C. M. (1981a) Changes in the Composition of the Enamel of Human Premolar Teeth Shortly After Eruption. *Archives of Oral Biology.* **26**, 717-719.

Woltgens, J. H. M., Bervoets, Th. J. M., Witjes, F. and Driessens, F. C. M. (1981b) Effect of Post-Eruptive Age on Ca and P Loss from Human Enamel During Demineralization *in vitro*. *Archives of Oral Biology.* **26**, 721-725.

Wright, T. C., Cant, J. P. and McBride, B. W. (2008) Use of Metabolic Control Analysis in Lactation Biology. *The Journal of Agricultural Science.* **146, 3.** 267-273.

Xie, Z. H., Mahoney, E. K., Kilpatrick, N. M., Swain, M. V. and Hoffman, M. (2007) On the Structure-Property Relationship of Sound and Hypomineralized Enamel. *Acta Biomaterialia.* **3,** 865-872.

Young, R. A. and Spooner, S. (1969) Neutron Diffraction Studies of Human Enamel. *Archives of Oral Biology.* **15,** 47-63.

Young, R. A. (1975) Some Aspects of Crystal Structural Modelling of Biological Apatites. *Colloques Internationaux.* **230,** 21-39.

Young, A., Jonski, G. and Rolla, G. (2003) Inhibition or Orally Produced Volatile Sulfur Compounds by Zinc, Chlorhexidine or Cetylpyridinium Chloride-effect of Concentration. *European Journal of Oral Science.* **111,** 400-404.

Zero, D. T. (1995) *In Situ* Caries Models. *Advances in Dental Research.* **9, 3.** 214-230.